Conveyance Estimation for Meandering Channels

C S James
J B Wark

Report SR 329
December 1992

HR Wallingford

Registered Office: HR Wallingford Ltd. Howbery Park, Wallingford, Oxfordshire OX10 8BA, UK
Telephone: 0491 35381 International + 44 491 35381 Telex: 848552 HRSWAL G.
Facsimile: 0491 32233 International + 44 491 32233 Registered in England No. 1622174

Contract

This report describes work carried out as an extension of an NRA R&D project. This report was funded by the Ministry of Agriculture, Fisheries and Food (MAFF) under the commission on River flood protection, nominated project officer B D Richardson. The HR job number was QPS/0013/J2.

This work was carried out by Prof C S James of The University of the Witwatersrand and Mr J B Wark of HR Wallingford. The project was managed by Dr Nigel Walmsley.

This report is published on behalf of the Ministry of Agriculture, Fisheries and Food, but any opinions expressed are not necessarily those of the Ministry.

Prepared by James B. Wark 26/3/93

Checked by James B. Wark 26/3/93

Approved by N. Walmsley 26/3/93.

Date 26/3/93

Summary

Conveyance Estimation for Meandering Channels

C S James
J B Wark

Report SR 329
December 1992

The work detailed below was carried out in the Computational Methods Group of the Research Department. For further information please contact Mr J B Wark or Dr N Walmsley.

The Science and Engineering Research Council Flood Channel Facility (SERC FCF) at HR Wallingford was constructed to provide the ability to carry out large scale physical model studies of river channel and flood plain interactions. Phase A investigated the behaviour of straight compound channels and experiments were carried out over a three year period, 1986-1989. It was felt to be important to disseminate the results of this research to the Civil Engineering profession and P. Ackers developed a design method for straight channels based on the SERC FCF data.

Phase B of the SERC FCF research programme was designed to investigate the behaviour of meandering channels during overbank flow. Experiments were carried out over a two year period, 1989-1991 and in 1991, HR Wallingford was commissioned by the National Rivers Authority (NRA) to produce a hydraulics manual for meandering compound channels. A second report was then commissioned by MAFF covering the technical details of the work.

This report details the results of the work carried out in producing this hydraulics manual. The behaviour of meandering channels during inbank and overbank conditions investigated.

A literature search was carried out to identify other laboratory data which could be used to supplement the SERC FCF data set. A limited number of laboratory studies have been carried out in small flumes and some of these data were useful in the analysis of flow in meandering channels.

Various methods were identified in the literature to account for the effects of meandering on both in and out of bank flow. The available laboratory data was used to evaluate the existing inbank methods. The SCS and LSCS methods were found to give adequate results for use in practice but Chang's (1984) method is more general and is potentially more useful.

The measured point velocities from the various experiments in the SERC FCF were analyzed to provide data on the distribution of discharge within meandering compound channels. The literature survey and the results of analyses carried out by the researchers involved in the SERC FCF work indicated that different loss mechanisms affect the discharge capacity of each zone of a meandering compound channel. A four way division into: main channel; inner flood plain and two outer flood plains was found to be the most

appropriate. The SERC FCF data was used to formulate procedures which describe the effects of the important mechanisms in each zone.

The discharge within the main channel was found to vary along the length of the channel, being maximum at the bend apices and minimum at some point in between. This variation in discharge was ignored in the analysis and the mean discharge in the main channel was used in all subsequent analysis and modelling.

An empirical procedure was developed to account for the effect of secondary currents on the main channel discharge. Two methods were investigated for modelling the inner floodplain discharges. The first (James and Wark) accounted for the effect of the expansion and contraction of flow as it passes over the main channel with a semi-empirical approach while the second method (James and Wark 2) was purely empirical.

These two methods developed by the authors were applied to the available laboratory data along with some of the methods proposed in the literature. The James and Wark method was found to give superior predictions of total discharge and the distribution of discharge for the available data. The James and Wark method was also applied to one set of field data and gave good predictions of the stage-discharges. Consequently the James and Wark method is recommended over the other methods.

The work uncovered some gaps in the existing data and knowledge and recommendations have been given for further research to improve the current understanding of the mechanics of flow in meandering channels.

List of symbols

A	cross-sectional area
A	unsubscripted, cross-sectional area of main channel
B	top width of main channel
C	Chezy bed friction parameter
C_{sl}	length coefficient for expansion and contraction losses, zone 2
C_{ssc}	side slope coefficient for contraction loss, zone 2
C_{sse}	side slope coefficient for expansion loss, zone 2
C_{wd}	shape coefficient for expansion and contraction losses, zone 2
c	coefficient in equation for zone 1 adjustment factor
D_{50}	median size of bed material
F_r	Froude number
F_1	factor for non-friction losses in zone 2 associated with main channel geometry
F_2	factor for additional non-friction losses in zone 2 associated with main channel sinuosity
f	Darcy-Weisbach friction factor due to bed friction only
f_l	Darcy-Weisbach friction factor due to channel bends
f'	Total Darcy-Weisbach friction factor due to bed friction and bends ($f + f_l$)
f'	ratio of flood plain and main channel Darcy-Weisbach friction factors
f^{*}_{R}	parameter in Ranga Ragu's resistance law
g	gravitational acceleration
h	hydraulic depth of main channel, = A/B
h_L	head loss through a bend
K	coefficient in equation for zone 1 adjustment factor
K_e	factor for expansion and contraction losses in zone 2
K_c	contraction coefficient
K_L	bend loss coefficient
l	length of bend
l_c	length of bend required for fully developed secondary currents
L	meander wavelength
L_{co}	length of straight cross over
m	coefficient in equation for zone 1 adjustment factor
N	parameter related to free vortex flow
n	Manning's friction parameter bed friction only
n'	Manning's friction parameter including bend losses
Q	zonal discharge
Q_{calc}	calculated discharge
Q_{meas}	measured discharge
Q_{bf}	main channel bankfull discharge
Q_T	total discharge
Q_1'	adjustment factor for zone 1 discharge
R	hydraulic radius
R_e	Reynolds number
r_c	mean radius of curvature
r_o	outer radius of curvature
r_i	inner radius of curvature
S_o	flood plain gradient

S_f	friction gradient
S_s	cotangent of main channel side slope
S_{sf}	cotangent of flood plain side slope
S''	gradient associated with transverse secondary currents
S''_{fd}	gradient associated with fully developed transverse secondary currents
s	channel sinuosity
T	temperature in degrees Centigrade
V	flow velocity
V_*	shear velocity
v_r	transverse velocity
v_{rc}	transverse velocity at the water surface in the centre of the channel
v_{rcfd}	fully developed v_{rc}
W_2	width of zone 2
W_T	width of flood plain
y	flow depth
y_m	average flow depth at position along bend where secondary currents become fully developed
y_2	flow depth on flood plain at main channel bank
y'	dimensionless flow depth on flood plain, $= y_2/(A/B)$
z	vertical distance
θ	angle between cross over length of main channel and flood plain centre line
θ_m	mean angle between flood plain centre line and main channel centre line
θ_{fd}	angle of bend required for fully developed secondary currents
ϕ	parameter related to bend angle
κ	von Karman constant
ξ	parameter in Ranga Ragu's resistance law
ρ	fluid density
υ	kinematic viscosity
τ	shear stress
τ_l	shear stress due to channel curvature
τ_s	shear stress due to friction onlySubscripts

1	zone 1
2	zone 2
bf	bankfull
ave	average
calc	predicted value
meas	measured value
m	measured value
p	predicted value

Contents

Contents continued

Tables

Contents continued

Figures

Contents continued

Contents continued

1 Introduction

The estimation of channel conveyance is probably the most commonly encountered problem in river engineering practice. It requires quantitative accounting for the energy dissipated or "lost" by the flow. Energy can be lost by a variety of different mechanisms, depending on the physical characteristics of the channel and the flow condition. In a straight, prismatic channel the energy loss can be ascribed wholly to friction. Bends in a channel induce secondary circulation in the flow, which effectively adds to the energy loss by reducing the energy available for the primary flow. For overbank flows in a straight channel, further energy is lost through the interaction between the main channel and flood plain flows. For overbank flow in a channel with bends, the mechanisms are yet more complex and the energy loss still greater.

The Science and Engineering Research Council (SERC) Flood Channel Facility (SERC FCF) was constructed at HR Wallingford (HR) in order to provide a national facility in which large scale experiments on flow in flood channels could be carried out. Thus the effects of the complex flow mechanisms could be studied and quantified.

A research programme is being carried out in three phases as follows:

- Phase A, straight and skewed channels
- Phase B, meandering channels and dispersion
- Phase C, sediment experiments (provisional)

The programme is sponsored principally by the SERC and HR with financial support from the National Rivers Authority (NRA). The experiments are carried out by a number of university research groups.

The Phase A experiments were completed in June 1989 and a design method for estimating flood discharges in straight compound channels has been produced (Ackers, 1991). This analysis stemmed from a need to make the results of the research being carried out on the SERC FCF available to practising engineers in a useful form. Ackers work was funded by the former Regional Water Authorities of England and Wales, later the National Rivers Authority (NRA), and HR Wallingford.

The Phase B experiments were completed in October 1991 and in September 1991 the NRA invited HR to tender for an R&D project to produce a procedure based on the results of the Phase B experiments. The objective of the project was to prepare an hydraulic manual to allow the NRA to utilise the results of the Phase B experiments carried out in the SERC FCF.

It was understood that the intention of the NRA in commissioning this project was that the end product should be of immediate applicability to the NRA regional offices and their field staff. This was borne in mind during the course of the project and significantly affected the forms of analyses chosen.

The project involved the following tasks:

1 Summarize the work done during the FCF programme straight compound channels, by the researchers who took the measurements and others who analysed the data.

2 Apply the Flood Channel Facility Phase A Method, (FCFAM) to field data and compare it with other straight channel methods.

3 Summarize the data available from the SERC FCF and other laboratory or field studies into meandering compound channels.

4 Develop procedures to describe the head loss in inbank meandering flows.

5 Develop procedures to describe the head loss in overbank meandering flows.

6 Develop guidelines to assist in determining boundary shear stresses in meandering overbank flow.

7 Devise guidelines to assist in application of the procedures to natural channels.

The NRA required only a short summary of the results of each of these tasks in the final report submitted to them. It was felt to be important that the full details of the development of the methods and the conduct of the research should be recorded as well. Consequently the Ministry of Agriculture, Fisheries and Food agreed to fund production of this more detailed report.

The work carried out on the Ackers method and straight compound channels is described in Chapter 2. Chapter 3 gives a summary of the available information on meandering compound channels. The analysis of inbank and overbank meandering flows are reported in Chapters 4 and 5 respectively.

The various methods for overbank meandering channels are applied to the available laboratory and field data in Chapter 6. Chapter 7 gives some recommendations for future research and the main conclusions of the study are sumarised in Chapter 8.

2 *Straight compound channel methods*

2.1 Background

The initial part of the NRA R&D project involved preparing a summary of previous work carried out on the conveyance capacity of straight compound channels, Ackers (1991). The method Ackers produced is based on an exhaustive analysis of the data collected on the SERC FCF during Phase A, by teams of researchers from various universities. The NRA also commissioned HR Wallingford to evaluate this method against other straight channel methods by application to a range of channel types and conditions; but the NRA requested that the SERC FCF Phase A data should not be analyzed further, since this has already been carried out by Ackers (1991). This work extends some earlier work, (Wark et al , 1991), carried out at HR for MAFF by including the new method developed by Ackers in the analysis. This method will be referred to as the Flood Channel Facility Phase A Method, FCFAM.

In addition, some of these methods for calculating discharge in straight compound channels were applied to a selection of the meandering channel data collected during Phase B of the SERC FCF work. The purpose of this was to confirm that straight channel methods are inappropriate for use when analysing meandering channels with overbank flow.

2.2 Straight channel methods

The methods detailed below were identified as appropriate for application to measured stage discharges in straight compound channels.

LDM	Lateral Distribution Method with NEV = 0.16
DCM	Divided Channel Method, using vertical division lines which are included in the wetted perimeter of the main channel but omitted from the wetted perimeter of the flood plains
SCM	Single Channel Method, applying the bankfull main channel Manning's n value to the whole compound channels
SCM2	Horton's Composite Roughness Method
SCM3	Lotter's Composite Roughness Method
SCM4	Einstein and Banks Composite Roughness Method
SCM5	Krishnamurthy and Christensen Composite Roughness Method
SSGM	Sum of Segments Method
DCM2	Divided Channel Method, using vertical division lines which are not included in the wetted perimeter of either the main channel or the flood plains
FCFAM	Method developed by Ackers, based on Flood Channel Facility Phase A data. Main channel slope used for main channel flow.

These methods for calculating discharge in straight compound channels fall into four broad categories:

- divided channel methods
- method of segments
- composite roughness methods
- more complex physically based methods

Two divided channel methods (DCM and DCM2) were considered. These are based on vertical division lines at the main channel-flood plain boundaries thereby dividing the flow between the main channel and the flood plains. In a review of some simple methods of estimating discharge in compound channels Ramsbottom (1989) concluded that the division lines should be included in the wetted perimeter of the main channel but not the flood plains. This approach is adopted in the DCM method whereas in DCM2 the division lines are not included in either the main channel or flood plain wetted perimeters.

The sum of segments method and the LDM allow variable roughness values to be assigned across the channel perimeter, whereas the divided channel methods by definition allow roughnesses to be designated for the whole of the main channel and the flood plains. The composite roughness methods considered here were identified through earlier work carried out at HR and are listed in HR Report EX 1799. They are all based on the assumption that a representative roughness value for the whole compound channel can be obtained by taking some weighted average of the roughness values associated with different regions across the channel. Appendix 1 repeats appendix F1 of EX 1799 and gives the details of the various methods. It is worth noting that Lotter's method (SCM3) and the sum of segments method (SSGM) are based on identical assumptions and give identical results. The sum of segments method is simple to apply and is popular in numerical models.

The Lateral Distribution Method (LDM) is based on the work of Wark et al (1990). The LDM was developed from an analysis of the results obtained from Phase A of the SERC FCF work. It is a fairly complex mathematical model of flow distributions in straight compound channels and is based on approximations to the physical processes rather than an empirical approach. The details of the method are given by Wark et al (1990) and are summarized in Appendix 2. The main problem with the LDM lies in the choice of an appropriate Non-dimensional Eddy Viscosity (NEV) value. The work reported here was carried out with a fixed value of 0.16. This value has been found to give acceptable results in a fairly wide range of situations (see Wark et al, 1990 and 1991 and Chapter 6 of Ackers, 1991). The quoted value of 0.16 gave reasonably good results over all when applied to the FCF Phase A data. However, when considering individual data points the optimum values obtained varied with flow depth and other geometric variables over the range 0.1 to 0.5.

The FCFAM procedures are based on a detailed analysis of stage discharge data collected from the FCF during Phase A. The FCF data is the most comprehensive and accurate laboratory data set that exists. Other laboratory data sets were also considered by Ackers (1991) and also a selection of field data. The FCFAM procedures allow prediction of stage-discharge relationships, division of total discharge into main channel and flood plain components and estimation of boundary shear stresses. This method for stage-discharge prediction is based on the divided channel approach (DCM2).

A basic discharge is calculated separately for each zone using a conventional resistance equation (such as Manning's) and these are then added together to give the total basic discharge. This is then adjusted to account for the effects of the interactions between the zonal flows. Four regions of flow behaviour were identified, (Ackers 1991), within which the variation of the interaction effect with flow depth was different. A different adjustment function is presented for each region. It is not possible to identify the appropriate region and function for a particular water level beforehand, but a procedure is given for selecting the correct result from those obtained using each adjustment function. An additional correction is also given to account for the effect of moderate angles of skewness of the main channel. The total discharge can be divided into main channel and flood plain components using intermediate results from the primary calculations.

The interaction between main channel and flood plain flows also affects the magnitude and distribution of boundary shear stress in a compound section. Procedures are given for making provisional estimates of the average boundary shear stress in the main channel and the average and local maximum values on the flood plains.

The FCFAM method for stage-discharge prediction, separation of main channel and flood plain flow and estimation of boundary shear stress has been summarised as a step by step design procedure in Appendix 3. This summary was used as the basis of an internal NRA document which is intended for distribution within the NRA, R&D Note 44.

2.3 Field and laboratory data on straight channels

River gauging data at sites with compound channels was supplied to HR by various NRA regions as part of a previous MAFF funded study into methods of improving flood discharge assessment (Ramsbottom 1989 and Wark et al 1991). Additional laboratory data was supplied by Dr WRC Myers of the University of Ulster, who also supplied details of the River Main study in Northern Ireland. The MAFF study involved the evaluation of various methods of estimating discharge in compound channels. The results reported in this section extend this earlier work to include the FCFAM method.

In total eight sets of field gauging data were obtained. The identified channels displayed a wide variation of geometric parameters, see Tables 1 and 2. The cross-sections are also shown in Figures 1 and 2. As is to be expected with data collected under field conditions none of the information is perfect and all of the sites show some deviation from the ideal cases studied in the laboratory. In particular not all the cases are truly straight prismatic channels with uniform flow. The various sites and the data collected from them are described in detail by Ramsbottom (1989), Wark et al (1991) and Ackers (1991). As can be observed for some of the sites it is difficult to define the bankfull level exactly in these cases each engineer must apply his own judgement. When applying the FCFAM procedures it may be difficult to define the geometric parameters used. It is not the purpose of this report to act as a detailed design guide and if the procedures given in Appendix 3 are found to be inadequate further guidance should be sought from the report by Ackers (1991).

Bed roughness values

As with the geometric properties of the channels, the variation of roughness values from the identified data sets is also notable. Table 2 gives the main channel and flood plain roughness values used in this analysis along with the bankfull and maximum stage values. The various methods were applied to the data using two basic estimates of the main channel and flood plain roughness values.

The Authors' estimates of main channel roughness values vary from about 0.025 to 0.046 and the flood plain roughnesses from 0.025 to about 0.100. The main channel roughness values were obtained by back calculation using the inbank measured flows. The bankfull value was used at all higher stages. The flood plain roughness for the Blackwater, Main, Severn and the Tees were estimated by comparing measured and calculated distributions of depth averaged velocity profiles across the flood plains. The LDM method with a NEV value of 0.16 was used to simulate the measured flood plain velocities and the values of Manning's n which gave the best fit between the calculated and measured velocity profiles was adopted. In the case of the Torridge an estimated value of n = 0.06 was assumed. In general the values adopted are similar to those obtained by Ramsbottom (1989) on the basis of the divided channel method (DCM).

Ackers (1991) applied the FCFAM method to some of the sites listed in Table 1, Main Sections 6 and 14, Severn, Torridge and the Trent. Table 5.3 of Ackers (1991) reports the mean discrepancies, defined as: $(1.0 - Q_{meas}/Q_{calc})$ obtained for each site with a range of roughness values for both main channel and floodplain. The second set of roughness values listed in Table 2 are the values which Ackers found to give the minimum mean discrepancy for each site, in effect optimum values of flood plain Manning n for the FCFAM.

The information on the River Main used by Ramsbottom (1989), Wark et al (1991) and Ackers (1991) has been found to contain an error arising from published information, Myers (1990) and Higginson et al (1990). In addition to providing a corrected cross-section geometry for Section 14, Myers (1992) also confirmed that the channel gradient is variable along the study reach and flow is non-uniform. As this reach of the Main also includes bends, Ackers (1991) concluded that it is not strictly an appropriate test case. As a result a correction was issued to SR 281 by Ackers, effectively withdrawing this site from his analysis.

However, the bends on this reach of the River Main are not particularly tight and straight channel techniques are regularly applied by engineers to rivers with this type of plan form. The stage discharge data from the two River Main sections is included in the analysis described here since the Authors considered that in practice engineers regularly deal with channels of this type. The application reported here was carried out using the corrected cross-section and the average hydraulic slope reported by Myers et al (1990). Hence the back calculated main channel Manning's n value for Section 14 is now 0.0278 rather than 0.0248. Flow in the study reach on the River Main is known to be non-uniform, the hydraulic slope varies along the reach. The roughness values derived using this average hydraulic slope are not valid for other hydraulic slopes.

The other sites used are gauging stations operated by the NRA and water surface slopes are not regularly measured when gauging flows at these sites. The implicit assumption is made that the gauging sites are situated where steady, uniform and normal flow conditions operate. No information exists to confirm or refute this assumption but it should be noted that natural flows are rarely steady, uniform or normal. Indeed a close inspection of the rating sheets from some of these sites shows that during the two or three hours required to measure the discharge by the point velocity method the water level could rise or fall by significant amounts. Other causes of uncertainty also exist for some of these sites and the various authors noted above have discounted some of these sites as unsuitable. For example, the River Blackwater section has flood banks at the main channel edges which may affect the degree of interaction. The River Ouse section has very small floodplains and may act more like a simple channel. Both the Rivers Tees and Torridge sections have irregular floodplains with flood banks. The analysis reported here has been carried out using all eight sites and only the Severn, Torridge and Trent sites.

Myers' laboratory data were obtained from a scale model of part of the River Main and the two channel geometries are shown in Figure 3. The series A channel had a total width of about 1.6m with a main channel top width of 0.67m. The series F case studied the effect of removing one flood plain to give an asymmetric channel. In this case the total channel was about 1.3m wide and the main channel was 0.78m wide. In both cases the flume was set to a longitudinal slope of 1.906×10^{-3}. The main channel and flood plains were kept smooth during these two tests and the Manning's n value was taken as 0.01.

2.4 Application of straight channel methods to straight channel data

In total, nine methods of estimating discharge were used to compare measured discharge against predicted discharge. The work reported by Wark et al (1991) was based on observed discharges derived from rating curves developed at each of the gauging sites, which were developed by Ramsbottom (1989) and Myers, rather than the individual observations. This procedure was said to average out measurement errors and seasonal changes in vegetation and cross-section. Between 5 and 12 points were selected on each stage-discharge curve. This procedure has been criticised and in the work reported here the actual observed pairs of stage and discharge were used. In the cases of the Severn and the Tees these data points were smoothed using running averages over three consecutive data points. Between five and thirty six data points were obtained for each site. All of the discharge estimation methods were applied with identical conditions, such as the cross-section geometry and roughness values.

The idealised cross-sections shown in Figure 3 are approximate and are included only for information. They are based on the estimated main channel side slopes. The main channel side slopes and corresponding idealised depth were estimated following the procedure described in Section 6.4 of the summary to Ackers (1991). These two parameters were only used in the FCFAM method and appear in the calculations for the correction factors. The basic flows were calculated with the actual channel and flood plain cross-sections as recommended by Ackers (1991). Ackers also recommends that the factor Q_{2^*c} should have a lower limit of 0.5 and this limit was used in this work.

The mean percentage errors for the various methods, averaged over various subsets of the data, are shown in Table 3. These averages and standard deviations were obtained from the individual results and not by averaging the mean values for each site. As mentioned above there was some debate over the usefulness of some of this data and the following discussion is limited to the three sets of data collected from the Severn, Torridge and Trent. The mean errors averaged over each river site are shown in Table 4.

Results with Authors' n values

The roughness values used for the flood plains in this work were derived, in the main, by adjusting them to give good agreement between the measured depth averaged velocity profiles and the velocity distribution predicted by the LDM. In general these values agreed reasonably closely with those obtained by Ramsbottom (1989), who integrated the velocity profiles to obtain the actual flood plain discharge and then estimated the flood plain roughness using a divided channel method

The two divided channel methods perform well over all the natural (Severn, Torridge and Trent, case D) data with mean errors in the range -0.3% to 0.3%. The LDM gave the next best accuracy with a mean error of 0.7%. The FCFAM method follows in fourth place with a mean error of -2.2%. The single channel methods all show much greater mean errors and standard deviations than the four best methods and will not be considered further. The mean errors over each individual river site in Table 4 tend to confirm these conclusions, although the ranking of the various methods varies from site to site. These differences are probably due, in part at least, to the wide range of channel cross section type, scale and shape. It is worth noting that the standard deviations reported are partly due to random errors in the measured data and partly due to systematic differences between the predictions and the measurements. For the four best methods the standard deviations are all in the range 4.4% to 6.7%.

Results with Ackers n values

Ackers (1991) reports broadly similar results with the Authors' n values. He also reported results obtained with roughness values adjusted to reduce these errors for the FCFAM method. However, Ackers did not compare his method with existing techniques, as this lay outwith the scope of his project. The analysis reported above has been repeated using these adjusted Manning's n values. The mean errors for the LDM and the two divided channel methods have increased from between -1% and +1% to between 2% and 5%. The mean error for the FCFAM method is actually slightly worse at -3.1%. The standard deviations are similar at approximately 4% to 5%. Figure 4 shows these errors and standard deviations. The errors reported by Ackers for his method with these data sets are slightly better and this is probably due, in part, to different approaches in applying the method to non-symmetric natural channels. The Authors have treated each flood plain separately in order to calculate velocities and basic discharges. This has the advantage of allowing different roughness values to be assigned to the two flood plains. Ackers, 1991, takes averaged floodplain widths and elevations to define an average floodplain geometry, which combined with an average floodplain roughness value is used to derive average floodplain velocity and basic discharge values. No further attempt has been made to identify causes of the differences between Ackers (1991) analysis and that reported here. The differences lie in the subjective interpretation of the geometry of natural cross-sections and the variation of order of a few percent indicates the likely computational tolerance in practice that may be obtained by river engineers in practice.

Comparisons with the FCF Phase A data

Although a comparison with this data set was specifically excluded from the analysis at the request of the NRA it is worth mentioning that such a comparison has been carried out by the second author, Wark (1993). The FCF data is the best data set available for the development and verification of methods for calculating conveyances in straight compound channels. The details confirm the work reported by Ackers (1991). The FCFAM method gave a mean error in predicted discharge for the Phase A data of -2% with a standard deviation of 3.8%, although over only the smooth flood plain cases this improved to -0.3% and 1.7%. These results are very similar to those reported by Ackers (1991): 0.001%, SD 0.8% and 0.08% and 1.46%. The slight differences in these results are not significant and are probably due to small differences in the computed bed friction factors.

Discussion

The above results from field data show that of the ten methods investigated four are worthy of further consideration, namely: The LDM, DCM, DCM2 and the FCFAM method. It is difficult to make definitive statements as to which is best on the basis of these results. The lack of independent calibration data means that the bed friction calibrations have been based on the obtained results. It has been shown that the bed roughness values for natural rivers and flood plains are not well defined, the choice of value is often influenced by the method used to compute the channel conveyance. Therefore these results are inconclusive and do not confirm (in the strict scientific definition) that any of the four methods gives more accurate results than the others. It has been demonstrated that all four methods can be calibrated to match field data.

The case of straight compound channels is misleading when considering meandering rivers. There are three main processes operating:

- bed friction locally,
- lateral shear between the co-flowing main channel and flood plains,
- the exchange of momentum through secondary currents, Knight and Shiono, (1991).

The relative strength of these processes is determined by the distribution of depths and roughness and the shear layers at the edges of the main channel can extend over the whole main channel.

The main channel and flood plain flows in the meandering case are known to vary in direction both through the depth of the flow and along the channel. The lateral shear layers which have such an important effect in the straight channels do not form and the effect of lateral shear on the flow structure and stage-discharge relationships is minor. Thus the important flow mechanisms in meandering channels are likely to be considerably more complex than in straight compound channels, this topic is covered more fully in Chapter 5. It is therefore unlikely that methods for calculating conveyance in straight compound channels will give accurate predictions if applied to meandering compound channels. Ackers, (1991), from a review of previous research also reached the conclusion that straight channel methods should not be applied to meandering compound channels. The work described in the following sections confirms that none of the straight channel methods considered above is able to represent the meandering channel data available from Phase B of the FCF programme.

2.5 Application of straight channel methods to meandering channel data

2.5.1 The methods

The methods used in this work are listed below. These are simple methods which are practical to apply by hand. The Lateral Distribution Method which was found to give the best results for straight channels has not been included in this assessment since it is a computational model and the NRA R&D project put a high priority on hand calculation methods. The various composite roughness methods have not been included here since their performance against straight channel data was poor.

DCM Divided Channel Method, using vertical division lines which are included in the wetted perimeter of the main channel but omitted from the wetted perimeter of the flood plains. Main channel slope used for main channel flow.

SCM Single Channel Method, using main channel slope.

SSGM Sum of Segments Method, using main channel slope for main channel segments.

DCM2 Divided Channel Method, using vertical division lines which are not included in the wetted perimeter of either the main channel or the flood plains.
Main channel slope used for main channel flow.

FCFAM Method developed by Ackers, based on Flood Channel Facility Phase A data. Main channel slope used for main channel flow.

HOR1 Divided Channel Method, using a horizontal division line at bankfull stage. Division line is included in flood plain wetted perimeter but not in main channel wetted perimeter. Flood plain slope used for main channel and flood plain flows

HOR2 Divided Channel Method, using a horizontal division line at bankfull stage. Division line is included in flood plain and main channel wetted perimeters.
Flood plain slope used for main channel and flood plain flows.

HOR3 Divided Channel Method, using a horizontal division line at bankfull stage. Division line is included in flood plain wetted perimeter but not in main channel wetted perimeter. Main channel slope used for main channel flow.

HOR4 Divided Channel Method, using a horizontal division line at bankfull stage. Division line is included in flood plain and main channel wetted perimeters. Main channel slope used for main channel flow.

The two divided channel methods (DCM and DCM2); the single channel method (SCM); the sum of segments method (SSGM) and the FCFAM method were all applied as described in Table 4.1. These are methods which could be applied by hand to calculate flows in compound channels. Ackers (1991) specifically advises that the FCFAM method should not be applied to meandering cases. However it has been included in the work reported below since, as a hand calculation technique, it came within the scope of the NRA project. The various horizontal division line methods (HOR1, HOR2, HOR3, HOR4) are simplifications of the methods proposed by Toebes and Sooky (1967) and Smith (1977). The main channel and flood plains are considered to be split by a horizontal line at bankfull level. The region above the dividing line is included in the flood plain area when calculating the flood plain flow. The sinuosity of a meandering channel is the ratio of the curvilinear distance along the channel to the straight distance between the two points.

2.5.2 The data set

The SERC FCF Phase B stage-discharge test programme is summarized in Table 5. Of this data series numbers B32, B33, B46 and B48 have been excluded from this analysis for the following reasons.

B32, B46 Flood plain roughened with rows of isolated breeze blocks, special methods must be used to account for the head losses due to these blocks.

B33 Flood plain only partially roughened. The roughness zones were limited to the 'meander belt', creating two distinct roughness regions on the flood plains. The methods described above are suitable for flood plains which are homogeneously roughened.

B48 Flood plains are totally blocked by breeze block walls which run from the inner bend apices to the outer edge of the flood plain. This simulates the case were development has occurred over the whole flood plain. Again the simple methods used here are not suitable for this geometry.

The series B21, B26, B31, B34, B39, B43 and B47 from Phase B of the FCF were all analyzed using the methods described above. In total 107 data points were used in this analysis. The full details of the experiments are given in Chapter 3. The bed friction terms for the various tests were calculated using a modified smooth law for the smooth cases and the Ackers rod roughness method for the roughened cases. The full details of these are given in Chapter 3.

2.5.3 Results

The mean errors and standard deviations in the mean errors for the various methods are listed in Table 6. The results differed considerably depending whether the flood plains were roughened or not and so mean errors are given over the smooth data, the roughened data and over all the smooth and rough data.

Table 4.3 shows that for the whole data set the mean errors for the various methods vary from 7.3% to 70.1%. All the methods over-predict discharge by significant amounts. The corresponding standard deviations vary between 16.8% and 56.7% showing that the errors vary by very large margins about the mean values.

It is worth looking more closely at the results averaged over the smooth and rough data sets. The mean error for the fourth horizontal division line method (HOR4) taken over all the data is 7.3% and so this method would appear to give the best results. However, when the mean error is calculated over the smooth and rough data sets the mean errors are 19.5% and -19.8% respectively. Thus the relatively low mean error achieved by considering the whole data set is actually the result of large positive errors for the smooth cases and large negative errors for the rough cases. This wide band of errors is highlighted by the large values of the standard deviations.

The results discussed above show that the simple methods developed for straight compound channels are likely to give rise to large errors in estimated discharges if applied to meandering compound channels.

The range of errors to be expected will vary with the following parameters:

1 sinuosity
2 flood plain width / main channel width
3 flood plain roughness / main channel roughness
4 flood plain depth / main channel depth

For cases similar to the Phase B geometries considered the errors in calculated discharges may be as large as 100%. Hence a different method is required to calculate the discharge in meandering compound channels.

The four methods based on a simple two way division with a horizontal line at bankfull stage appear to perform slightly better overall than the other methods. This suggests that horizontal divisions are most appropriate for meandering channels. In straight compound channels the best divisions are based on vertical divisions at the edges of the main channel.

2.6 Summary

This chapter reports the results obtained by applying various methods developed for discharge estimation in straight compound channels to field data collected on straight reaches and to meandering laboratory data. The application to straight field data was inconclusive, The LDM, DCM, DCM2 and FCFAM methods giving similar results, depending on the roughness values used. Applications of these methods to laboratory data, reported elsewhere, showed that the FCFAM method and the LDM methods can predict discharges in laboratory compound channels more accurately than the other methods. In practical design exercises the FCFAM method should be used since it is based on a careful analysis of the best available laboratory data. It will also give a slightly more conservative solution than the other four methods.

Of the simple methods applied to the meandering laboratory data the horizontal division methods gave marginally more accurate predictions. In general straight channel methods are not appropriate for the analysis of meandering compound channels. This confirmed that the development of a new procedure for discharge estimation in meandering compound channels is worthwhile and the next chapter lists the details of laboratory data which was available.

3 Laboratory investigations into meandering overbank flow

3.1 Background

In the previous chapter methods of calculating discharge in straight compound channels were applied to some of the data collected during phase B of the FCF work. The poor results obtained demonstrated that straight channel methods are not appropriate for use with meandering channels. The next task, therefore, was to develop a new procedure for the estimation of discharge in meandering channels. In order to carry out this work information on the behaviour of both inbank and out of bank meandering channels was required. The following laboratory and field experiments were identified from the literature. Both the SERC FCF data and the Aberdeen data were used in the development of the procedures, other sets of laboratory data were used to verify the methods. The development and verification of the procedures were carried out separately.

The main characteristics and findings of each of the laboratory investigations are detailed below.

3.2 Laboratory data

3.2.1 Phase B SERC FCF

The FCF at HR Wallingford provided the primary set of data used in this work. The details of the experiments and the data collected were made available to the authors by the various university researchers involved in the experiments. This project put a high priority on stage discharge and flow distribution data and most effort was put into obtaining details and data from these experiments.

The Phase B geometries were constructed from concrete with a smooth mortar finish. The basic surface roughness size was identical within the main channel and on the flood plains. In general the full flood plain width of 10m was used although tests with a reduced flood plain width were also undertaken. Two basic meander geometries with different sinuosities were constructed for the Phase B experiments. The first geometry had a sinuosity of 1.37 (60° meander) and included four complete meanders. The second geometry had a sinuosity of 2.04 (110° meander) and included four and a half meander wavelengths, see Figures 5, 6, 7 and 8 and Plates 1 and 2.

The design longitudinal slope of the flood plain was 1.0×10^{-3}. The actual longitudinal slope of the flood plain surface for the first channel geometry was 0.996×10^{-3} and 1.021×10^{-3} for the second.

Two main channel cross-section geometries were used with the 60° meander geometry. The first was a simple trapezium with a base width of 0.90m, side slopes of 45° and a depth of 0.15m see Figures 5 and 6 and Plate 1. The second was an approximation to a typical natural geometry, reproducing the relatively deep pools which form on the outsides of the bends and the symmetric geometry at the cross-over sections. Only the natural main channel cross-sectional geometry was used with the 110° meander geometry. See Figures 7 and 8 and Plates 2 and 3.

The full flood plain width of 10.0m was used for most experiments, but stage-discharges were also measured with the flood plain edges tangential to the meander bends. This was carried out for both the meander geometries with natural main channel cross sections. The flood plain sides were sloped at 45° (1:1) in these cases.

In general the experiments included no artificial roughening of the flood plains or main channel, the surfaces being left as trowelled mortar. However, a few experiments did include artificial roughening on the flood plains by utilising vertical dowel rods placed in differing geometric patterns. The rod roughened tests had the rods placed over the whole flood plain, while the partially roughened tests had only the inner flood plain or meander belt covered with rods, see Plates 4 and 5.

Additional tests were also carried out by introducing a blockage to the flood plain flow. Concrete blocks aligned in the flow direction were used to approximate the behaviour of bridge piers on the flood plain, Plate 6. In the case of the 110° geometry these block were also used to construct walls across the full widths of the flood plains to the inner bend apices. This simulated the effect of complete development on the flood plain, which would restrict the flow to the main channel. This data has not been used since no reliable method of calculating the flow resistance of the blocks or walls exists.

The smooth and rod roughened cases correspond to calibration tests carried out during Phase A of the FCF work into straight compound channels and Ackers (1991) provides accurate bed friction calibrations for these two conditions.

The test programme included investigation of in-bank and out of bank flows. Measurements of stage, velocity (magnitude and direction), boundary shear stress, turbulence and dispersion were all included in the programme.

The procedure followed when carrying out the stage discharge experiments was as follows. The pumps were set to give the required discharge, which was measured using orifice plates in the supply pipes. The tail gates were then adjusted to give a water surface slope approximately equal to the flood plain bed slope. Water surface slopes were measured using tapping points at intervals along the centreline of the flume. The water level at the tapping points was measured in stilling pots attached to the side of the flume with pointer gauges. A least squares procedure was then used to determine the slope of the measured water surface. In order to obtain stage-discharge data for uniform flow readings would be taken for several tail gate settings at the same flow. The stage and water surface slope values for each of these gate settings would be slightly different. Linear interpolation between these slope and stage values was then carried out to provide stage values 'corrected' to the actual bed slope. Considerable care was taken during the project to check the measured stage-discharges collected during phase B. The interpolated stages for each case were recalculated and a few minor errors and anomalies corrected.

For the other measurements the flow would be set and then the tail gate adjusted until the water surface slope was approximately equal to the bed slope (within ±2%). Point velocities were measured using a two stage method. Miniature propeller meters were used to measure point velocities. In order to give accurate results these instruments need to be aligned with the local velocity direction. First the local flow direction was measured using vanes mounted on rotary potentiometers. When positioned in the flow the vane aligned its self with the local horizontal velocity direction. The resulting voltage from the potentiometer was related to the angle between the assumed datum and the velocity vector. These angle readings were stored and used in a subsequent experiment to align the propeller with the flow direction. Thus for any flow condition two experiments were carried out, one to measure the directions of the velocities and a second to measure their magnitudes.

Separate measurements of angles and velocities were made in the main channel and flood plain areas. For the main channel measurements were taken on eleven cross sections along a quarter of a wave length of the 60° channel and on fourteen cross sections over half a wave length of the 110° channel. These main channel sections were taken perpendicular to the main channel centreline and extended 300mm on to the flood plains on either sides. Measurements were made on a grid with horizontal spacings of 150mm or 50mm and vertical spacing of 15mm. On the flood plain measurements were made at 13 (60°) or 11 (110°) traverses covering half a wave length. Readings were taken at spacings of 0.5m laterally and 10mm vertically. Only the main channel velocity data were used in this project.

Boundary shear stresses were measured in both geometries using a Preston tube on the smooth surfaces. The shear stress measurements were made at the same sections in the main channel and on the flood plain as the point velocity data. This information was not used directly during the project but the results and analysis reported by Knight et al (1992) were used.

A two component Laser Doppler Anemometer was used to measure turbulence data across the flood plain and main channel at one bend apex. Detailed water surface levels were measured using a Churchill probe both in the main channel and across the flood plain over one meander wave length. Dye dispersion tests were carried out at inbank flow conditions. These experiments involved injecting dye at various points across the channel and monitoring the concentrations at selected positions downstream. Flow visualisation experiments involved photographing the movements of either injected dye or floating bodies. The visualisation experiments provide qualitative indications of the complexity of the flow structures present. Because this project put a high priority on the estimation of both the total discharge and the distribution of discharge none of the turbulence, water surface level, dispersion or flow visualisation information was used in this project.

A full listing of the experiments undertaken in the Phase B tests is given in Table 7 and Table 5 lists the stage discharge experiments carried out. The test numbering system was devised by researchers from the University of Bristol. Tests one to nineteen were carried out during phase A of the FCF work into compound channels. To ease data handling the stage discharge data available from other sources were also assigned serial numbers. The Aberdeen stage discharge data were assigned numbers between 100 and 199. The Vicksburg data were assigned numbers between 200 and 299. Kiely's one set of stage discharge data was given the test number 301 and Sooky's data were assigned numbers 400 to 499.

3.2.2 Aberdeen

The Aberdeen flume, Willetts et al (1991) was constructed as a scale model of the SERC FCF. Although due to space limitations a smaller vertical scale was used leading to the model having distorted channel cross-sections when compared to the equivalent geometry on the SERC FCF. The meandering channels were formed in expanded polystyrene and painted. In all cases the flood plain width was 1.20 m and the flood plain and main channel roughnesses were identical. Experiments were conducted with four different channel sinuosities, viz. 1.00, 1.21, 1.40 and 2.04. An identical trapezoidal cross-section for the main channel was used for all sinuosities with a base width of 0.139m, a depth of 0.050m and side slopes of 70.7° (0.35:1).

Two additional experiments were conducted with 'natural' main channel cross sections. These were created by infilling the trapezoidal channels to a depth of 20 mm with bakelite powder. This moveable bed was subjected to bankfull flow until a stable bed topography had evolved, which was then fixed and painted. The water temperature was 14°C$\pm$1°C in all experiments.

The experimental conditions are summarized in Table 8. Stage-discharge measurements were taken for all conditions except for inbank flows in the 2.04 sinuosity channel with the natural cross-section. Figures 9 and 10 show the various plan and cross section geometries.

Willetts et al (1991) report some preliminary observations and conclusions. The study included measurement of stage discharges, point velocities within the main channel and water surface levels over a wavelength of the meander pattern. The objects of the investigation were:

1) To identify the flow structures associated with channel flood plain interaction.

2) To explore the dependency of these structures on channel cross section shape.

3) To determine whether main channel sinuosity and cross-section shape have significant influence on stage discharge relationships.

The stage discharge measurements show that the discharge capacity of the floodway reduces as the sinuosity of the main channel increases. For a given sinuosity the main channel cross section has a strong effect on the capacity. The 'natural' cases had larger total discharges than the equivalent trapezoidal channels at high stages, even though the trapezoidal channels had larger cross sectional areas. An explanation of this unexpected phenomenon was indicated by dye dispersion tests. The trapezoidal channels exhibited far stronger secondary currents and more interaction between main channel and flood plain flows than the natural cases. Thus channel cross section has a strong effect on the conveyance capacity of a floodway.

A complete set of stage-discharge data has been supplied by Willetts (1991). Only the data collected in the trapezoidal main channel and meandering cases have been used here however. The inbank stage discharges collected in the straight channel were used to calibrate a modified smooth friction law.

3.2.3 US Army Vicksburg

A series of stage-discharge experiments were conducted on compound meandering channels by the United States Army Corps of Engineers (1956) at the Waterways Experiment Station in Vicksburg, Mississippi, USA. The main purpose of these experiments was to determine the effects on floodway capacity of: radius of curvature of bends; sinuosity of main channel; depth of overbank flow; ratio of overbank area to main channel area and flood plain roughness. Two basic sizes of main channel cross section were constructed. The smaller channel was constructed with a trapezoidal cross section of base width one foot (0.305m) and was 0.5 feet (0.152m) deep. Stage discharges were measured for ten basic conditions. The results obtained with this one foot wide channel were inconclusive and a further set of tests were carried out with a larger main channel.

The main channel cross-section was trapezoidal in all cases, with side slopes of 63.4°. The bottom width was two feet (0.610m). The tests were conducted in a flume 30.5 m long and 9.2 m wide. Main channels with three planform geometries were moulded in sand and stabilized with a concrete veneer. The flood plain width was varied by installing temporary brick walls. The basic flood plain roughness was plain brushed concrete. Two additional roughnesses were obtained by covering the surface with expanded metal grating, laid with the openings oriented parallel and normal to the flow direction.

The three different meander planforms were constructed with this 2 ft wide channel, all with arcs of circles connected tangentially, with no straight reaches between them. The meander wave length was held constant at twenty four feet (7.315m). Three and a half full wave lengths were constructed for the three sinuosities. The valley slope was $1.0x10^{-3}$ in all cases. For each condition the discharge was measured at bankfull and three overbank stages. The main conclusions of the study were:

a) Where the main channel is narrow (and small) compared to the flood plain, the effect of channel sinuosity on the total discharge capacity is small.

b) The effect of increased main channel sinuosity is to reduce the total discharge capacity.

c) When the flood plain is more than three times the width of the meander belt the effect of channel sinuosity on the total discharge capacity is small.

d) The effect of increased flood plain roughness is to reduce the total discharge capacity.

In all stage-discharges were measured for eleven separate conditions with the 2 ft wide channel but it was found that the roughened flood plain cases could not be used since the quoted Manning's n values of 0.025 and 0.035 could not be verified. The smooth surface of the Vicksburg flume was similar to the SERC FCF and both facilities were constructed at similar scales. The Vicksburg flume had a quoted Manning's n of 0.012 but this could not be verified and it was decided to model bed friction using the modified smooth turbulent law developed for the SERC FCF. Thus only three of the measured stage-discharge curves could be used. The experimental conditions for the 2ft wide channel are listed in Table 9 and Figure 11.

3.2.4 Toebes and Sooky

Toebes and Sooky (1967) and Sooky (1964) carried out a laboratory study of overbank flow with a meandering channel, varying only the main channel depth. Measurements of stage-discharge as well as data on water surface and velocity variations across the channel and flood plains were recorded. The modelled geometry covered 5.5 meander wave lengths. The sinuous main channel was constructed with a sinusoidal plan form and a rectangular cross section in a flume 7.3m long and 1.18m wide, Figure 12. Two separate channel depths and seven longitudinal slopes were tested to give eleven individual stage-discharge cases. Calibration tests were also carried out in straight rectangular channels and this provided the necessary information to calibrate a modified smooth law for Sooky's flume.

Sooky analyzed these stage discharges based on division of the cross section into two zones by a horizontal line at bankfull. He assumed that flows in both regions are controlled by the longitudinal valley slope. Applying basic frictional losses and calculating the discharges in these two regions separately over-predicted discharge and so did not account for all energy losses. In order to account for these extra energy losses Sooky introduced an extra length of wetted perimeter (T) to both the main channel and flood plain calculations. He used his laboratory data to back calculate the values of T required to give zero error in the predicted discharges. T was found to be a complicated function of:

a) overbank flow depth
b) mean velocities in the two zones
c) longitudinal slope

On the basis of this analysis it was concluded that the additional energy losses (other than bed friction) introduced in overbank flow in meandering channels will depend on these parameters. In addition the following conclusions were also drawn:

1) The additional losses increase (from zero) with over bank stage up to some maximum. As depth increases beyond this point the extra losses then reduce.

2) The deeper and narrower the main channel the smaller are the extra energy losses.

3) For the purposes of calculating discharge in meandering compound channels, cross sections are best divided by a horizontal division at bankfull.

The measured velocities also provided useful information on the flow structure within the channel. It is well known that flow around channel bends induces spiral currents and superelevation. Inbank secondary currents are known to rotate with the surface currents directed towards the outside of the bend. During overbank flow Sooky observed that the secondary currents rotate in the opposite sense, ie the surface currents are directed towards the inside of the bend. This observation has been confirmed by other researchers (SERC FCF, Stein et al, 1988 and 1989). In addition the velocities were integrated to provide discharge values in the various regions of the channel.

3.2.5 Smith

Smith (1978) has published details of a laboratory investigation into overbank meandering flow. He carried out stage discharge experiments for three cases including a straight compound channel, a meandering compound channel and for the flood plain alone. The flume was set at a longitudinal slope of 1×10^{-3} and in both cases the main channel was trapezoidal with a top width of 0.27m and bankfull depth 0.076m. The model channel had 7 meander wave lengths and all three cases were constructed of trowelled mortar in a flume 24m long by 1.2m wide. The meandering planform was constructed with a sinuosity of 1.172 and filled the full width of the flume. Smith carried out some analyses of the meandering case using the straight channel divided channel method (DCM2). He concluded that straight channel methods are inappropriate for calculating the discharge in meandering compound channels. He carried out some dye injection tests to investigate flow patterns and found that the flow in the main channel varied along the wave length, spilling out of the channel onto the flood plain and back. The flow in the channel was observed to be lowest at the cross-over reach, half way between meander bends. At deep overbank stages the valley flow was observed to pass over the main channel. A separation zone occurred and a spiral eddy in the main channel was induced.

The main conclusions of Smith's work were:

1) Straight channel methods are inappropriate for calculating discharge in meandering compound channels.

2) For meandering overbank discharges the main channel and flood plain flows interact. This interaction has a strong effect on the discharge capacity and varies strongly with stage.

3) The flow in the main channel varies along a meander wavelength and is minimum at some point between bends.

Smith provided a bed friction calibration for Manning's n of about 0.01, although this did appear to vary for the various cases. During later work on verifying the authors method this data set was found to behave differently from the other data available. This was attributed to the poor bed friction calibration and it was decided that Smith's data is unreliable and so should not be used in any numerical work.

3.2.6 James and Brown

James and Brown (1977) carried out measurements to determine the geometric parameters which influence flood plain flow in a tilting flume 26.8m long by 1.5m wide. Out of fourteen tests they conducted nine with straight channels, three with single skewed crossovers, one with two cross-overs and one with three cross-overs. Only the last case even approaches a meandering geometry but is rather unrealistic when compared to typical natural planforms. The bend radius was too small and the length of straight cross-over too large. The straight and meandering channel stage-discharge data was analyzed in terms of Manning's n values. On the basis of this they concluded that 'The resistance factor increased as the crossover or meander length decreased'. This is equivalent to saying that the conveyance capacity was reduced as the sinuosity increased.

This data set was not used in any comparisons because of the relatively poor meandering geometry and the lack of adequate bed friction calibration data.

3.2.7 Kiely

Kiely et al (1989 and 1990) carried out experimental work into flows in straight and meandering compound channels. Discharges, point velocities and turbulence measurements were made in a 14.4m long by 1.2 m wide flume. A straight, single meander wave length and multiple meander (4.5 wave lengths) cases were investigated, see Figure 13. The flume was hydraulically smooth with a test section constructed of glass and perspex for use with a single component Laser Doppler system. The main channel was rectangular in all three cases and the flume was set at a valley slope of 1.0×10^{-3}. McKeogh and Kiely (1989) provide a modified smooth law which gives the bed friction in this flume. The laser system was used to investigate detailed flow structures in both the main channel and the flood plain. Kiely identified the following mechanisms in overbank meandering flow.

1) Secondary currents in the main channel during overbank flow were observed to rotate in the opposite direction to those seen during inbank flow. A detailed examination of the secondary current patterns suggests that the mechanisms producing these different patterns are both present during over bank flow but that the curvature induced currents are less

intense and become nullified. The energy losses due to secondary currents during overbank flow are greater than the losses during inbank flow.

2) Velocities within the main channel were generally observed to follow the direction of the main channel side walls. The direction of velocities at points over the main channel and above bankfull level were observed to vary with level. Above bank level the direction of flow changes from being parallel to the main channel at bankfull to being almost parallel to the flood plain, close to the water level. This change in the direction of local velocity through the water column indicates the presence of a horizontal shear layer between the main channel and flood plain flows.

3) At the crossover reaches the water on the flood plain it is observed to pass into and across the main channel. Thus fluid from the left hand flood plain crosses the main channel and ends up on the right hand flood plain. As the flow crosses into the channel the depth increases and as it passes out onto the flood plain the depth decreases. This expansion and contraction of the flow area is known to induce energy losses in analogous situations.

4) Velocities were seen to vary strongly across the flood plain. Outwith the meander zone the velocities were approximately uniform. Within the meander zone an area of reduced velocity was observed. It was felt that this was caused by the interaction of the main channel and flood plain flows, with relatively low velocity fluid leaving the channel at the cross over reaches and passing down the flood plain.

The multiple meander data has been used by the authors to test and verify various methods of calculating the conveyance capacity of meandering compound channels.

3.2.8 Stein and Rouve

Stein and Rouve (1988, 1989) have investigated the detailed flow structures present over one meander wave length for overbank flow conditions. Sophisticated laser doppler anemometry was used to measure all three point velocity components within the flow for one water level and discharge. The meandering channel was constructed in a flume 15.0m long by 3.0m wide. The main channel was rectangular with a width of 0.4m and a bankfull depth of 0.1m. The preliminary results presented allowed the following conclusions to be drawn.

1) Secondary currents in the main channel rotate in the opposite direction to those for inbank flow.

2) Fluid 'welling out of' the main channel slows the discharge on the flood plain.

3) A horizontal shear layer exists between the lower and upper parts of the main channel.

3.3 General Comments

Experimental work on flows in meandering channels during overbank conditions has been identified from the literature. The investigators and the main characteristics of their experiments are summarized below.

SERC FCF Phase B	Multiple meander, two sinuosities, two cross sections, two flood plain roughnesses, stage discharges, velocity, water surface and bed shear stresses.
Willetts et al	Multiple meander, three sinuosities, two cross sections, stage discharges, water surface levels and velocities.
US Army Vicksburg	Multiple meander, three sinuosities, three flood plain roughnesses, stage discharges.
Kiely	Single and multiple meander, one sinuosity, stage discharges, velocity, water surface and turbulence measurements.
Toebes and Sooky	Multiple meander, one sinuosity, two cross sections, seven slopes, stage discharges, water surface levels and velocities.
James and Brown	Multiple meander, stage discharges and velocities.
Smith	Multiple meander, stage discharges.
Stein and Rouve	Single meander, water surface levels, velocities and turbulence measurements.

The key physical dimensions of the test channels are given in Table 10. Table 11 shows the relationships between the key geometric parameters for the laboratory flume tests. Various authors have published details of empirical equations derived by regression analyses carried out on natural meander patterns. The exact equations vary from author to author but in general it is possible to say that in natural, fully developed, meander bends: the wave length is approximately ten times the channel width; the channel width is approximately ten times the channel bankfull depth and the radius of curvature of the bends is between two to three times the channel width.

A study of Table 11 shows that most laboratory studies have been carried out with main channel aspect ratios (B/h) which lie between 3.5 and 5.0. Only the SERC FCF geometries have channel cross sections which approximate to natural cross sections with an aspect ratio of 8.0. Toebes and Sooky (1967) and the work carried out at Vicksburg (1956) demonstrated that main channel cross section shape can have a strong effect on the discharge capacity of meandering channels during overbank flow. These observations have been confirmed by Willetts et al (1991).

Most of the investigations have used meanders with wavelength to channel width ratios which are close to the natural ratio of 10. Only the meander investigated by James and Brown (1977) with a value of about 33 is totally unrealistic in terms of this ratio. The final geometric ratio between the bend radius and channel width generally falls within the natural range of 2 to 3. Sooky, James and Brown and Smith all constructed channels with low sinuosity and this produced r_c/B ratios of about 4.0. However this is not a serious deviation since the relationships for natural channels were derived for fairly sinuous channels.

It has been demonstrated that all three of these geometric ratios effect the stage discharge capacity during overbank flow. Since only the large scale experiments carried out in the SERC FCF satisfied all three relationships it is likely that the flow patterns and stage discharge relationships for the FCF will be closer to those observed in nature than for the other experimental data collected in small scale models. Most investigators identified well-defined structures within the flow including: secondary currents within the main channel and bulk exchanges of flow between main channel and flood plain. Figure 14 shows the flow processes taking place during overbank flow in meandering channels.

3.4 Bed friction

In later chapters stage discharge data from these laboratory studies is used to develop and verify methods of estimating discharge in meandering channels. In order to carry out this work it is necessary to calculate energy losses due to bed friction. All of the laboratory models were constructed with hydraulically smooth surfaces. One of the conclusions arising from the earlier work by Ackers (1991) is that the bed friction in hydraulically smooth conditions should be obtained from a smooth turbulent expression. This expression correctly predicts the effect of viscosity on friction factor. In any given case it may be appropriate to derive a modified version of the smooth turbulent law which fits the data better than the general version quoted in the literature. This approach to determining bed friction has been followed and for each of the various data sets a modified smooth law has been obtained.

The original references either gave the appropriate modified smooth law or stage-discharge measurements in straight simple channels which could be used to calibrate the constant values in the smooth law. The general form of the modified smooth law is:

$$1/f^{1/2} = A \log (Re\ f^{1/2}) + B \qquad (1)$$

Where Re is the Reynolds number of the flow defined by:

$$Re = \frac{4RV}{\nu}$$

in which

V is the flow velocity,
R is the hydraulic radius, and
ν is the kinematic viscosity of the water.

The kinematic viscosity can be calculated from recorded temperatures by the equation

$$\nu = (1.741 - 0.0499\ T + 0.00066\ T^2) \times 10^{-6} \qquad (2)$$

in which T is the temperature in °C.

The values of the constants A and B derived for each of the data sources are listed below.

Data source	A	B	Comments
Vicksburg	2.02	-1.38	The SERC FCF smooth law was used
Toebes and Sooky	0.68	2.42	Values calibrated to given stage-discharges
Kiely	2.10	-1.56	Values provided by Kiely
Serc FCF	2.02	-1.38	Values provided by Ackers
Aberdeen	2.48	-2.91	Values calibrated to given stage-discharges

Some of the experiments carried out on the SERC FCF involved roughening the flood plains with vertical rods extending through the full depth of water. The pattern of rods consisted of a triangular distribution of angle 60°. This was designed to have a density of 12 rods per square metre. Under these conditions the resistance to flow is made up of drag of the rods and the shear force at the channel boundaries. Ackers has analyzed some calibration tests carried out during phase A of the SERC FCF work and developed a method of obtaining the total friction factor due to rod roughness.

He assumed that the rod drag and bed friction can be treated separately, accounting for the blockage effect of the rods on the mean velocity. The drag of the rods is related to the square of the mean flow velocity past the rods. Ackers calibrated an expression for the drag coefficient which depends on the ratio of rod diameter to flow depth. The expression is quite complex and in order to obtain friction factor values for a specific depth iteration is required. The equations and data for the method are given in Appendix 5.

3.5 Summary

This chapter presents the results of a literature search in to overbank flow in meandering compound channels. The main purposes of this review were:

a) To identify laboratory data to use in developing and verifying a new procedure for discharge estimation in overbank flow in meandering channels.

b) To summarize the current state of knowledge on the detailed flow structures present during overbank meandering flow and to gauge the effect these might have on the discharge capacity.

Eight laboratory investigations were identified, including the SERC FCF. The two most modern and extensive data sets (SERC FCF and Aberdeen) were considered to represent the best quality data available and it was decided to use these two sets in developing a new procedure. Three other investigations (Vicksburg, Kiely and Sooky) were deemed appropriate to use in verification of the new procedure.

The internal structure of currents during overbank flows has been found to be highly complex see Figure 14. The most important observations are:

1) The longitudinal velocities below bankfull tend to follow the main channel side walls while the floodplain velocities are generally in the valley direction. Thus the floodplain flows pass over the main channel and induce a horizontal shear layer.

2) The energy loss due to secondary currents in the main channel is greater than for an equivalent simple channel and the currents rotate in the opposite sense compared to inbank flows.

3) Fluid passes from the main channel onto the flood plain and back into the main channel in the following meander bend. Hence the proportion of discharge passed by the main channel and flood plain varies along a meander wavelength. These bulk exchanges of fluid between slow and fast moving regions of flow introduce extra flow resistance.

4) Flows on the flood plain outwith the meander belt are usually faster than those within the meander belt. It would appear that the extra flow resistance induced by the meandering main channel has a relatively small effect on the outer flood plain.

The following chapter examines the topic of energy losses during inbank flow in channel bends and meanders. Although the main thrust of the project was to deal with overbank flow it was felt that to be important to examine the inbank case as well. The transition from inbank to overbank flow is often the critical aspect of practical problems and it would be impossible to study it properly with out some knowledge of the characteristics of inbank flow.

4 Inbank meandering flow

4.1 Background

It has been recognised for many years that meandering can increase the effective resistance of channels significantly for inbank flows. Laboratory and theoretical investigations in to the characteristics of flow in channel bends have shown that complicated flow structures form and that these can have a large effect on the discharge capacity of the channel.

Secondary or spiral currents are induced by differences in centripetal accelerations acting on a vertical column. The longitudinal velocities are greater for particles close to the water surface. This implies that the lateral forces on the water column are not in equilibrium and so lateral movements of particles are induced. The currents move towards the outside of the bend at the water surface and towards the inside at the channel bed. These secondary currents also affect the water surface profile across the channel. In straight channels the water surface is uniform but in bends the surface is displaced and slopes down from the outside to the inside of the bend to balance the non-uniform lateral pressure distribution introduced by the secondary currents. These secondary currents affect the distribution of longitudinal flow within the channel cross section by advecting the faster moving fluid towards the outer bank. The flow distribution and associated longitudinal bed shear stresses becomes non-uniform across the channel. The secondary currents also induce a lateral component of bed shear stress which obviously increases the total shear stress acting on the bed.

The strength of these secondary currents is known to vary along a bend. In the case where a single bend has straight reaches both up and down stream then it has been observed that there are no secondary currents at the inlet to the bend. The strength of the currents increases along the bend until they become fully developed and are then uniform until the bend exit is reached. The secondary currents persist in the straight reach down stream, becoming less and less intense with distance from the bend exit. Where the straight reaches between bends are not long enough to fully dissipate the secondary currents then the residual currents at the bend entrance can have a strong effect on the flow in the bend. The growth and decay of secondary currents has a strong influence on the flow distribution within a channel bend.

It is known that the bend tightness (radius of curvature/width) has a strong influence on the secondary currents described above. The tighter the bend then the more pronounced the secondary currents. Tight bends also induce zones of flow separation particularly against the inner bank. The effect of this is to introduce a 'dead zone' close to the inner bank in which there is no significant longitudinal flow. A shear layer is induced and large horizontal vortices are induced within the zone. The effective width of the bend is reduced and the effect of secondary currents in displacing the longitudinal flow outwards is enhanced.

Natural channels are formed by the typical discharges they pass. The size and shape of the channel varies both with discharge and plan geometry. It is generally accepted that the important channel forming discharge for natural channels is close to the bankfull capacity of the channel. In straight channels the flow induces sediment movement which deepens and widens the channel until some equilibrium state is reached. The processes which induce the formation of river meanders are not well understood but it is likely that they are related to efficiency of the resulting geometry in terms of both discharge and sediment transport. That is to say the resulting geometry is the most efficient shape for passing the bankfull discharge and sediment load.

Given that a meander has developed then the secondary currents will develop up to some maximum strength and then decay away. These currents strongly affect the local bed shear stresses and form a channel cross section that varies strongly along the bend. At the entrance to the bend where the flow distribution and bed shear stresses are approximately uniform across the channel the cross section is approximately rectangular or trapezoidal. The secondary currents tend to deepen the channel on the outside and transport the material towards the inside of the bend where the lower velocities allow it to settle out. Thus many natural bends exhibit deep pools at the outside banks with shallow regions along the inner banks. The pools are deepest and the shallow area widest at about the apex of the bends. Although the shape of a channel varies along a meander it has been observed that the cross sectional area remains approximately constant throughout the bend.

4.2 Energy loss in channel bends

It is apparent that the presence of bends in a channel will affect the discharge capacity of the channel. In straight channels the only significant loss mechanism is bed friction but in curved channels other loss mechanisms may also be important. It was decided to investigate the relative effect of bends on stage-discharge relationships. The inbank stage-discharge data from phase B of the FCF work was available and was used in the following work.

4.2.1 Methods of evaluating non-friction losses

The available data was collected for uniform flow conditions. The rate or gradient of energy dissipation along the channels was constant and can be assumed to be represented by the bed slope (S_o).

The total energy loss is composed of friction loss, bend losses and all other losses. The rate of energy dissipation induced by these various mechanisms are all assumed to be constant and the total energy gradient is the sum of the individual gradients.

The friction gradient (S_f) can be calculated from the Darcy-Weisbach equation,

$$S_f = f V^2 / (8 g R) \qquad (3)$$

Subtracting the friction loss from the total loss gives the sum of all other losses. This can be represented by the difference between the total energy and friction gradients, $S_o - S_f$, or as a bend loss coefficient K_L, where

$$K_L = h_L / (V^2/2g) \qquad (4)$$

in which h_L is the head loss through the bend. This can be evaluated as

$$h_L = (S_o - S_f)\, l \qquad (5)$$

in which l is the length of the channel through the bend.

The losses associated with bends can also be accounted for in terms of a resistance coefficient, most commonly Manning's n. The ratio of the value including bend losses (n′) to the basic value (n) can be expressed in terms of the energy gradients through Manning's equation, i.e.

$$(n'/n) = (S_o/S_f)^{1/2} \qquad (6)$$

4.2.2 Data sets

The effect of meandering on flow resistance can be inferred from the stage-discharge data obtained from the inbank Phase B experiments in the SERC Flood Channel Facility. Three sets of data are available, one for each of the geometries tested, i.e.

the 60° meander geometry with trapezoidal cross-section,
the 60° meander geometry with the natural cross-section, and
the 110° meander geometry with the natural cross-section.

The measurements were all taken under uniform flow conditions (for the natural geometries the bed undulates considerably and uniformity is assumed to imply identical flow conditions at the same positions on successive bends).

4.2.3 Results and conclusions

For the 60° meander geometry with the trapezoidal cross-section the difference between total energy loss and friction loss can be wholly ascribed to effects associated with the meander planform. This loss has been calculated for each measured stage-discharge pair and expressed in each of the forms outlined above. The bed slope of the channel is given by

$$S_o = S_{of} / s \tag{7}$$

in which S_{of} is the slope of the flume, and s is the channel sinuosity.

For the 60° meander geometry the slope of the flume was 0.996×10^{-3} and the sinuosity was 1.374, giving a channel slope of 0.7248×10^{-3}. The length of the channel through the bend, L, was assumed to be measured through half a meander wavelength, i.e. 8.245 m. This distance includes the straight section of channel at the cross-over.

Estimation of bend losses for the 60° meander geometry with the natural cross-section is complicated by the variation of the cross-section shape along the channel. The flow distortions associated with this variation can be expected to cause additional energy losses, and so the difference between the average bed gradient and the friction gradient cannot be attributed to the effects of the meander planform alone. No experiments were performed with a straight channel with this natural geometry and the natural cross-section was about half the size of the trapezoidal one, so the losses associated with the meander planform and the cross-section variation cannot easily be separated.

Because the hydraulic radius varies along the channel the friction gradient, as calculated using Equations 1 and 3, will also vary. A value of S_f at each of the defined cross-sections was therefore computed and an average obtained, weighted by the relative distances represented by each cross-section. For the 60° meander geometry the weighted average is given by

$$S_{fav} = (1.25\, S_{f5} + 0.5745\, (S_{f4} + S_{f3} + S_{f2} + S_{f1} + S_{f0})) / 4.1225 \tag{8}$$

in which S_{f5} is the value calculated for the cross-section at the cross-over and S_{f0} to S_{f4} are the values calculated at the cross-sections defined at equal displacements through the bend.

The water level was measured at the cross-over section only. For calculating flow areas and wetted perimeters at the other sections it was assumed that the water surface was flat, with a slope equal to the average channel slope of 0.7248×10^{-3}. This assumption is reasonable because the cross-sections were designed with a constant cross-sectional area. An energy balance between the crossover and apex sections for one discharge confirmed that the change in water level associated with the cross-section variation was negligible.

Each natural cross-section was compound, with a deep section and a horizontal berm. It was assumed for these calculations that the discharge in the channel was the sum of the discharges in the deep and berm sections, with any interaction between the two regions unaccounted for. The friction gradient is then given by

$$S_f = \left(Q / \left(A_d\, (8\, g\, R_d / f_d)^{1/2} + A_b\, (8\, g\, R_b / f_b)^{1/2} \right) \right)^2 \tag{9}$$

in which Q is the total discharge, A is the flow area, and the subscripts d and b refer to the deep and berm sections respectively.

The friction factors were calculated using the appropriate modified smooth law, see Section 3.4. Equation 1 was modified slightly by expressing the velocity in the Reynolds number in terms of the friction gradient through equation 3, i.e.

$$1 / f^{1/2} = 2.02 \log \left(\left(4 (8 g)^{1/2} / \nu \right) R^{3/2} S_f^{1/2} \right) - 1.38 \qquad (10)$$

Equations 9 and 10 were solved iteratively to obtain the necessary values of S_f for each section and the average value then calculated by Equation 8.

The non-friction losses for the 60° meander geometry with the natural cross-section are presented in Table 12. The losses represent the sum of those associated with curvature and the varying cross-section.

The losses for the 110° meander geometry with the natural cross-section were evaluated in the same way as for the 60° meander geometry with the natural cross-section. In this case the slope of the flume was 1.021 x 10^{-3} and the channel sinuosity was 2.043, and hence the bed slope was 0.49972 x 10^{-3}, by Equation 7. The length of the channel through each bend, L, was 10.532 m. For this geometry there was no straight cross-over reach and the cross-sections were defined at equal displacements through the bend. The average friction slope was therefore calculated directly, without weighting.

The non-friction losses for the 110° meander geometry with the natural cross-section, which again include losses associated with channel curvature and varying cross-section, are presented in Table 13.

The mean values of S_o - S_f, K and n'/n for the three cases are listed below. The standard deviations are in brackets.

Channel	$S_o - S_f$ (x 10^{-3})	K	n'/n (= $(f'/f)^{1/2}$)
60° trapezoidal	0.107 (0.032)	0.081 (0.026)	1.078 (0.029)
60° natural	0.236 (0.012)	0.415 (0.113)	1.217 (0.013)
110° natural	0.186 (0.005)	0.954 (0.108)	1.262 (0.010)

It is interesting to note that the standard deviations on the energy gradients are much less in the case of the natural cross-sections. This implies that the rate of energy dissipation due to bend effects is more uniform with stage for natural channels than for trapezoidal channels. These sections were designed to mimic typical natural rivers and so in real channels the bend losses may not vary as strongly with depth as in the case of trapezoidal or rectangular channels. By comparing the results for the two 60° geometries we can see that channel cross-section shape strongly affects the non-friction losses and that these are approximately twice as large for the natural channel as for the trapezoidal channel. The differences between the results for the 60° and 110° are less conclusive but the non-friction losses appear to vary with channel sinuosity.

In order to assess the significance of these extra losses the mean gradients above have been normalised by the total energy gradients and are quoted below. These results show that non-friction losses can be very significant. In the cases examined the non-friction losses formed between 15% to 40% of the total energy losses. It is impossible to draw general conclusions from these data but they do indicate that further investigation of non-friction losses in channel bends is required.

Channel	$(S_o - S_f) / S_o$
60° trapezoidal	0.15
60° natural	0.32
110° natural	0.37

4.3 Energy loss mechanisms

The results presented above confirm that the presence of bends in open channel flows affect the energy loss compared to straight channels. The question which still remains to be answered is: How significant are these non-friction energy losses and what are the important parameters which affect them ? The following authors have tried to identify and quantify the mechanisms which induce this extra flow resistance.

Shukry (1950) carried out a set of experiments in rectangular channel bends. He constructed single bends which turned through angles (θ) of 90°, 135° and 180°. The experiments were conducted for depth to width ratios (y/B) of 0.6, 0.8, 1.0 and 1.2 and also for bend radius to width ratios (r_c/B) of 0.5, 1.0, 2.0 and 3.0. Shukry analyzed the extra energy loss induced by the presence of the bend using a bend loss coefficient (K_L), defined as:

$$h_L = K_L \, (V^2/2g) \tag{11}$$

in which h_L is the head loss due to bends only, and V is the overall mean velocity. He showed that the bend loss coefficient is a function of:

1) The Reynolds number
2) Depth ratio (y/B)
3) Radius of curvature (r_c/B)
4) The angle subtended by the bend (θ/180)

In addition he found that the proportion of these extra energy losses induced during development of the secondary currents were approximately constant at 40%.

Rozovskii (1957) published the seminal analytical work on flows in channel bends. He examines the theory of many of the mechanisms described above and compares predictions with both field and laboratory measurements. He identified the following sources of energy loss:

1) The redistribution of longitudinal flow across the channel
2) Energy lost in initiating secondary currents

3) Increased bed friction due to the secondary currents
4) Increased internal energy dissipation due to internal friction caused by the secondary currents
5) The redistribution of longitudinal flow in the vertical
6) Separation and the formation of eddy zones in sharp bends.

Rozovskii analyzed the energy dissipated by each of these mechanisms in a wide rectangular channel and concluded that the important mechanisms which significantly increase energy dissipation in bends are the increased bed and internal friction due to the secondary currents.

He provided the following expression for the extra energy losses:

$$h_L = (24\, g^{1/2}/C + 60\, g/C^2)\, (y/r_c)^2\, (l/y)\, (V^2/2g) \tag{12}$$

where h_L is the total extra energy loss in a bend of length l and radius r_c. y is the flow depth, g the acceleration due to gravity, V is the average flow velocity and C is the Chezy bed friction parameter. This equation was derived assuming a logarithmic distribution of the longitudinal velocities in the vertical and that the secondary currents are fully developed. In general this analysis shows that the energy losses due to a bend increase with channel roughness and the squares of flow velocity and depth to radius ratio. Hence the tighter a bend the larger the energy dissipated.

Much of Rozovskii's analysis was approximate: he was forced to make many assumptions and he concluded that further experimental and theoretical work is required.

Leopold et al (1960) explained the resistance behaviour of meandering channels by identifying three major types of resistance.

1) Skin resistance is associated with the surface roughness of the channel and varies with the square of the flow velocity.
2) Internal distortion resistance results from energy dissipation by eddies, secondary circulation and increased shear rate, wherever any boundary feature deflects part or all of the flow from its former direction. It will also vary with the square of the flow velocity.
3) Spill resistance is associated with local accelerations followed by sudden expansions in the flow and can be related to Froude number.

Leopold et al conducted experiments with inbank flows and moderately sinuous channels. They found that channel curvature could, by internal distortion, induce energy loss of the same order as that due to skin friction, and double that amount in tight curves. This type of loss could be related to radius of curvature of the bends and the ratio of channel width to radius.

Energy loss associated with spill resistance appears to be just as significant but only comes into effect at a critical value of Froude number (which is substantially less than 1.0). It appears that the Froude number at bankfull depth is generally less than this critical value in natural channels. This mechanism may be responsible for determining channel width by inducing bank erosion at its onset. It is unlikely to be a major loss mechanism for inbank flows in natural rivers and will be neglected.

Form resistance associated with flow around small-scale alluvial bed forms can be considered together with skin resistance by estimating a combined resistance coefficient. As noted by Onishi et al (1976), skin resistance is not independent of internal distortion and may be enhanced by the non-uniformity induced by secondary currents.

Internal distortion resistance results from energy dissipation by eddies, secondary circulation and increased shear rate wherever any boundary feature deflects part or all of the flow from its former direction. The secondary circulation induced by meandering is a major contributor to this type of resistance.

Onishi et al (1976) investigated inbank flows in meandering, alluvial channels. They attributed head loss to the following four categories of flow resistance.

1) Surface resistance or boundary stress, which may be enhanced by the nonuniform distribution induced by secondary currents.
2) Form drag, resulting from the unsymmetrical distribution of normal pressure around curves and deformations on the boundary. These losses are due primarily to separation but are also influenced by secondary currents. They depend on the Froude number, channel width, and the stream-wise and transverse non-uniformity of the channel geometry.
3) Superelevation, which causes additional asymmetry of the normal pressure distribution on walls and large scale bed forms, resulting in 'wave resistance'. These losses depend on the channel geometry and the Froude number.
4) Bed forms, in alluvial channels.

Onishi et al (1976) described the total loss due to bends using a bend loss coefficient, defined as:

$$h_L = K_L \, (V^2/2g) \qquad (13)$$

in which h_L is the head loss due to bends only, and V is the overall mean velocity. They showed that this could be expressed as:

$$K_L = L \,/\, 4R_b \, (f_{bc} - f_{bs}) \qquad (14)$$

in which L is the length of the bend, R_b is the bed hydraulic radius, f_{bc} is the bed friction factor for the meandering channel and f_{bs} is the bed friction factor for a similar but straight channel. The bed loss coefficient could be related to channel and flow characteristics by:

$$K_L = f\left(V \,/\, (g \, R_b)^{0.5} \,,\ R_b/D_{50} \,,\ B/r_c \right) \qquad (15)$$

In which D_{50} is the median size of the bed material, B is the channel width and r_c is the centre-line radius of curvature.

The results obtained by Onishi et al showed K_L to be strongly dependent on the Froude number. In some cases K_L was negative, implying an energy gradient less than for corresponding straight channels. This was attributed to a relative decrease in bedform drag and possible decreases in wave resistance and boundary shear.

Hayat (1965) obtained value of K_L (as defined above) for meandering channels with rectangular cross-sections and rigid beds. In contrast to the alluvial channel results of Onishi et al (1976), K_L was found to be approximately constant with Froude number.

The variation of cross-sectional geometry along a channel has also been identified as a source of energy loss (e.g. Chow, 1959). Kazemipour and Apelt (1979, 1983), however, have shown that such irregularity contributes no additional energy loss provided that no flow separation or broken surges occur.

From the above it is apparent that the main sources of energy loss in channel bends are:

1) Bed friction
2) Increased bed friction due to secondary currents
3) Internal energy dissipation due to increased turbulence induced by secondary currents.

The energy loss in a bend has been found to depend on the following parameters:

Bed roughness (f, C n etc)
Flow depth (y)
Bend radius (r_c)
Length of bend (l) or Angle of bend (θ, $l = r_c\,\theta$)
The cross-sectional shape of the channel.

Any general method for predicting flows in bends should account for these three processes and be formulated in terms of the five parameters above. Many methods have been identified in the literature. The majority of them have been derived empirically from laboratory data and may not include all of the important parameters. The following section describes methods which have been identified in the literature and in addition two methods have been modified to improve the predictions. The more promising of these methods are then applied to the available laboratory data.

4.4 Stage-discharge prediction methods

Although there is now better understanding of the mechanisms of energy loss, most hydraulics text books still recommend accounting for their effects together by a simple adjustment to the value of Manning's n for a similar but straight channel. Such adjustments have been proposed by Cowan (1956) and the Soil Conservation Service (1963). These methods are very similar and only the later one is covered below.

The Soil Conservation Service (SCS) (1963) Method

The Soil Conservation Service (1963) proposed accounting for meander losses by adjusting the basic value of Manning's n on the basis of sinuosity (s), as follows.

$n'/n = 1.0 \qquad \text{for } s \leq 1.2$

$n'/n = 1.15 \qquad \text{for } 1.2 \geq s < 1.5$

$n'/n = 1.30 \qquad \text{for } s \geq 1.5 \qquad (16)$

in which n' is the adjusted value and n is the basic value.

Because n is proportional to $f^{1/2}$, the adjustment should be squared when using the Darcy-Weisbach equation.

The Linearized SCS (LSCS) Method

The step nature of the SCS recommendation introduces discontinuities at the limits of the defined sinuosity ranges, with consequent ambiguity and uncertainty. To overcome this problem the relationship has been linearized and is expressed as:

$$n'/n = (f'/f)^{1/2} = 0.43\,s + 0.57 \qquad \text{for } s < 1.7$$

$$n'/n = (f'/f)^{1/2} = 1.30 \qquad \text{for } s \geq 1.7 \qquad (17)$$

in which f' is the adjusted Darcy-Weisbach friction factor.

The Method of Scobey (1933)

On the basis of flume tests Scobey suggested that the value of Manning's n should be increased by 0.001 for each 20 degrees of curvature in 100 ft of channel. These recommendations are not expressed in terms of dimensionless channel characteristics and are unlikely to have consistent accuracy at different scales.

The Method of Mockmore (1944)

Mockmore (1944) analyzed data from artificial channels and rivers for bend angles between 90° and 180° and proposed the relationship:

$$h_L = (2\,b/r_c)\,V^2 / 2g \qquad (18)$$

in which h_L is the energy lost through a bend, in excess of the friction loss. The friction loss is obtained from normal hydraulic calculations, eg the Darcy-Weisbach equation, i.e.

$$V = (\,8\,g\,R\,S_f\,/\,f\,)^{1/2} \qquad (19)$$

in which g is gravitational acceleration, R is the hydraulic radius of the cross-section, S_f is the energy gradient, and f is the friction factor. For uniform flow S_f can be equated to S_o, the bed gradient. The energy loss due to friction along a length of channel l is given by:

$$h_f = (\,f\,l\,/\,4\,R)\;V^2 / 2g \qquad (20)$$

Combining these gives the total head loss:

$$h_L + h_f = (\,(\,f\,l\,/\,4\,R) + 2B\,/\,r_c\,)\;V^2/\,2g \qquad (21)$$

on re-arranging this becomes :

$$h_L + h_f = (\,f + 8\,R\,B\,/\,l\,r_c\,)\,(l\,/\,4\,R)\;V^2 / 2g \qquad (22)$$

by comparing with Equation 20 it is apparent that the extra bend head losses can be considered as an adjustment to the straight channel friction factor with:

$$f' = f + 8 R B / l r_c \tag{23}$$

This form of the method is easier to apply to stage discharge data from meandering channels where a bed friction calibration for an equivalent straight channel is available.

The Method of Leopold et al (1960)

From a set of laboratory experiments carried out on meandering channels formed in sand Leopold et al presented a graphical relationship between the ratio of the additional boundary shear induced by channel curvature (τ_i) to the boundary shear associated with friction (τ_s) and the ratio of flow width (B) to mean radius of curvature (r_c). This can be expressed as:

$$\tau_i/\tau_s = 2.632 (B/r_c) - 0.526 \tag{24}$$

and applies below a critical value of Froude number (approximately 0.5). At higher Froude numbers the additional shear was a function of Froude number. By relating boundary shear stresses to velocity, Equation 24 can be interpreted as an adjustment to the friction factor as follows. The basic Darcy equation relates shear stress to the square of velocity with the coefficient f:

$$\tau = \rho f V^2 / 2g \tag{25}$$

Assuming that the total shear stress is composed of the two components defined and that each component has a corresponding friction factor then Equation 24 becomes:

$$f_i/f = 2.632 (B/r_c) - 0.526 \tag{26}$$

the total friction factor is given by

$$f' = f + f_i \tag{27}$$

rearranging and dividing by f gives

$$f_i / f = f' / f - 1 \tag{28}$$

substituting in Equation 26 gives

$$f' / f = 2.632 (B/r_c) + 0.474 \tag{29}$$

The Toebes and Sooky (1967) Method

From experimental results in a small laboratory channel with a sinuosity of 1.09, Toebes and Sooky (1967) proposed an adjustment to f. Below a critical value of the Froude number the adjustment depends solely on the hydraulic radius (in metres) according to:

$$f' / f = 1.0 + 6.89 R \tag{30}$$

They confirmed the conclusions of Leopold et al that above a critical Froude number the increase in losses due to channel curvature is a function of Froude number. The critical value of the Froude number was found to depend on hydraulic radius but was not exceeded in any of the applications reported here.

The Method of Agarwal et al (1984)

Agarwal et al (1984) performed a regression analysis on previously published data from alluvial channels to define a correction for bend losses. The actual flow velocity is determined by dividing the velocity calculated according to Ranga Raju's (1970) resistance law by ξ where:

$$\xi = 2.16\, f_{*R}^{-0.042} \tag{31}$$

with

$$f_{*R} = Re\, (\theta / 180°)^{-4.65}\, (B / y)^{1.11}\, (r_c / b)^{1.38}\, Fr^{9.29} \tag{32}$$

in which θ is the bend angle, y is the flow depth, Fr is the Froude number, in terms of the hydraulic radius, i.e. $V / (gR)^{1/2}$, and Re is the Reynolds number, $(4RV / \nu)$, where ν is the kinematic viscosity.

Ranga Raju's (1970) resistance law is intended for use in alluvial channels. The adjustment for bend losses is independent of the friction loss computation and it is assumed that it applies to rigid boundary channels as well, with any appropriate resistance law. It is unclear whether Re and Fr in Equation 32 are in terms of the actual velocity or that calculated from friction losses only, and the latter has been assumed.

The Method of Pacheco-Ceballos (1983)

Pacheco-Ceballos (1983) re-analyzed the results collected by Shukry (1950). He related the head loss due to the bend to the velocity at the bend entrance. Other authors express head loss in terms of the average velocity through the bend. By assuming that the lateral distribution of velocity within the bend follows the free vortex profile he produced the following equation for K_L:

$$K_L = (\, y_1 - y_m + V_1^2 / 2g - (\, N\, y^2\, V^2 / y_m^2\, 2g\,)\,)\, 5g / V^2 \tag{33}$$

Where y_1 and V_1 are the flow depth and velocity in an equivalent straight channel; y and V are the flow depth and velocity at the bend entrance and y_m is the average depth at the position along the bend where the secondary flow becomes fully developed. N is a parameter related to free vortex flow:

$$N = [\, (\, \ln r_o / r_1\,)^2\, r_o\, r_1 / B^2\,]^{-1} \tag{34}$$

where r_0 and r_1 are the radii of the outer and inner channel banks. The term $y_1 - y_m$ in Equation 33 is approximated by :

$$\log (y_1 - y_m) = 2.11\, V - (\, \phi + 0.7\, r_c/B - 0.06(r_c / B)^2 + y) \tag{35}$$

ϕ is a parameter which varies with the bend angle (θ). For Shukry's bends of 45°, 90° and 180° it has values 2.98, 2.70 and 2.64 respectively. Intermediate values can be obtained by interpolation.

The Method of Chang (1983)

Chang (1983) derived a general analytical model for the rate of energy expenditure per unit channel length associated with transverse flow. This model is based on the conceptual model developed by Rozovskii (1957) and assumes that the extra energy loss is due to increased bed friction and internal turbulence related to the secondary currents. Chang (1983) assumed a power law for the vertical distribution of longitudinal velocity. This gave a different expression for the secondary current compared to Rozovskii's.

For the case of a wide rectangular channel where super oneword elevation and the lateral variation of secondary currents are small he approximated the secondary currents with a linear distribution and produced a simplified expression for the energy loss in a bend where the secondary currents are fully developed.

$$S'' = \left(\frac{2.86\ f^{½} + 2.07\ f}{0.565\ + f^{½}}\right) \left(\frac{y}{r_c}\right)^2 Fr^2 \qquad (36)$$

in which S'' is the energy gradient associated with transverse flow (h_L/l). For uniform flow,

$$S_o - S_f = S''$$

or

$$1 - S_f / S_o = S'' / S_0 \qquad (37)$$

Since the rates of energy loss are linearly dependent on the friction factors,

$$1 - S_f/S_o = 1 - f / f' \qquad (38)$$

Rearranging and substituting it is possible to see that Chang's (1983) method can be interpreted as an adjustment to the basic straight channel friction factor.

$$f'/f = 1 / (1 - S''/ S_o) \qquad (39)$$

Chang (1988) reports a slightly different form of Equation 36:

$$S'' = \left(\frac{2.07\ f + 4.68\ f^{½} - 1.83\ f^{3/2}}{0.565\ + f^{½}}\right) \left(\frac{y}{r_c}\right)^2 Fr^2 \qquad (40)$$

However both forms were found to give very similar results in preliminary calculations and the simpler Equation 36 has been used throughout.

The Modified Chang Method

Chang's (1983) method was developed for wide, rectangular channels. Because most rivers and flood channels have large width to depth ratios this was not considered a major limitation, but the effect of shape warrants investigation at a later stage to confirm the method's validity.

Chang's (1983) method also assumes that secondary circulation is fully developed. In fact, the circulation takes considerable distance to develop through a bend and begins to decay once the channel straightens out. For meanders the circulation must reverse between successive bends and the associated energy gradient must drop to zero at two points over each wavelength. The average energy gradient associated with secondary circulation along the channel must therefore be substantially less than predicted assuming full development. Rozovskii (1957) studied this growth and decay of secondary currents analytically. He assumed that the distribution of the circulations remains constant during the process of decay. He showed that the angle of bend required for the secondary currents to become fully developed is:

$$\theta_{fd} = 2.3\ C\ y / (g^{1/2}\ r_c) \qquad (41)$$

where C is the Chezy coefficient. This can be written in terms of Darcy f:

$$\theta_{fd} = 6.5\, y / (f^{1/2}\, r_c) \qquad (42)$$

The corresponding length of channel required for fully developed secondary currents is

$$l_c = 6.5\, y / f^{1/2} \qquad (43)$$

Applying this criterion to the SERC channel geometry showed that under some flow conditions the circulation would never develop fully. Significantly, the degree of development varied greatly with stage in the same channel. For example, for the 60° trapezoidal channel, secondary circulation would be fully developed only after 152° of curvature at bankfull and after 54° for a flow depth of 0.06 m, which is approximately the lowest depth tested. The curvature of each bend in this geometry is 120°, so secondary circulation would probably be fully developed over a considerable proportion of the channel length at low stages, but not at all at relatively high stages.

Chang (1984) accounted for the effects of growth and decay of secondary circulation by applying his full secondary circulation loss model together with nonuniform flow calculations to predict the distribution of losses and boundary shear stresses, as well as water levels through bends. This requires integration of streamwise and transverse velocities at each computational section and would be impractical to use. As an alternative, his approach was simplified to apply to uniform flow through a sequence of identically repeated meanders. Because the energy gradient varies with the growth and decay of secondary circulation, flow can not actually be uniform. Also the bed slope is unlikely to be constant; it will vary over a meander wavelength even for idealized laboratory meanders. The assumption of uniformity is therefore a simplification, but the primary velocity and flow depth will not vary greatly. For determining the effective resistance in meandering channels average conditions are sufficient and minor departures from uniformity are unlikely to influence the conclusions. This approach enables a correction factor to be computed which can be applied to the energy gradient predicted by his wide-rectangular equation (44), to account for growth and decay of circulation.
Chang (1983) presented an Equation for the energy gradient associated with fully developed transverse circulation, S''_{fd}.

$$S''_{fd} = \left(\frac{2.86\, f^{1/2} + 2.07\, f}{0.565 + f^{1/2}}\right) \left(\frac{y}{r_c}\right)^2 Fr^2 \qquad (44)$$

in which Fr is the Froude number.

It is assumed (as by Chang, 1984) that the pattern of secondary circulation remains constant during growth and decay. The strength of the circulation, and its variation, can then be represented by the transverse velocity at one position on the profile, and particularly at the water surface at the centre of the channel. If it is further assumed that the local value of energy gradient associated with secondary circulation, S'', is proportional to transverse velocity (longitudinal velocity is constant by the uniformity assumption), then S'' can be related to the fully developed value by

$$S'' = S''_{fd}\, (v_{rc} / v_{rc\,fd}) \qquad (45)$$

in which v_{rc} is the transverse velocity at the water surface in the centre of the channel, and the subscript fd denotes the fully developed value. Similarly, the average value of S'' through a meander wavelength is given by

$$S''_{ave} = S''_{fd} \; (v_{rc\,ave} / v_{rc\,fd}) \tag{46}$$

In Equation 46 $v_{rc\,ave}$ is the average of absolute values because the sense of v_{rc} reverses between successive bends.

The total gradient of energy losses is the sum of friction gradient (S_f) and the secondary circulation loss gradient (it is assumed here that there are no other sources of energy loss, or that these are accounted for in the basic friction factor). Under uniform flow conditions the total gradient of losses is equal to the bed gradient S_o, and S'' can be represented by S''_{ave}. Therefore

$$S_f + S''_{ave} = S_o \tag{47}$$

S_f can be estimated using the Darcy-Weisbach Equation, i.e.

$$S_f = (f\,V^2)/(8\,g\,R) \tag{48}$$

in which V is the mean flow velocity and R is the hydraulic radius.

Substituting Equation 48 for S_f and Equation 46 for S''_{ave} in Equation 47 and rearranging gives

$$V = ((g\,S_o)/((f/(8R)) + K))^{1/2}$$

with

$$K = ((2.86\,f^{1/2} + 2.07\,f) / (0.565 + f^{1/2}))\,(y/r_c)^2\,(B/A)\,(v_{rc\,ave}/v_{rc\,fd}) \tag{49}$$

in which A is the cross-sectional area and B is the surface width of the flow.

Equation 49 can also be expressed as

$$V = ((8\,g\,R\,S_o)/f')^{1/2}$$

with

$$f' = f / (1 - S''_{ave}/S_o) \tag{50}$$

For evaluation of Equation 49 or 50, $v_{rc\,fd}$ can be calculated from the equation for the distribution of transverse velocity (v_r) under fully developed conditions given by Kikkewa et al (1976), i.e.

$$v_r/V = F^2\,(y/r)\,(1/\kappa)\,(\,F_1(z/y) - (1/\kappa)\,(V_*/V)\,F_2(z/y))$$

with

$$F = ((y/y_c)(r_c/r))^{1/2}$$

$$F_1(z/y) = -\,15(\,(z/y)^2 \ln(z/y) - 1/2\,(z/y)^2 + 15/24\,)$$

$$\begin{aligned} F_2(z/y) = {} & 15/2\,(\,(z/y)^2 \ln(z/y) - (z/y)^2 \ln(z/y) \\ & + 1/2\,(z/y)^2 - 19/54) \end{aligned} \tag{51}$$

in which κ is the von Karman constant, V_* is the shear velocity, y_c is the flow depth at the channel centre, z is the vertical direction, and r is the radial direction.

At the channel centre $y = y_c$ and at the water surface $z = y$, and so $F = 1$, $F_1 = 10/3$, and $F_2 = 10/9$. Substituting these values in Equation 51 gives the fully developed transverse velocity at the water surface at the channel centre,

$$v_{rc\,fd}/V = (y/r_c)(1/\kappa)(10/3 - (1/\kappa)(V_*/V)(10/9)) \tag{52}$$

The von Karman constant has a value of 0.4 and the shear velocity can be determined by

$$V_* = (g\ R\ S_f)^{1/2} \tag{53}$$

with $S_f = S_o$ for uniform flow.

The average surface transverse velocity, $v_{rc\,ave}$ is also required for evaluating Equation 49 or 50. Chang (1984) presented an equation for computing the transverse velocity at the water surface along the centre line through a bend. The velocity is computed at discrete cross sections along the channel, and the value at any section is related to that at the preceding section by

$$\begin{aligned}(v_{rc})_{j+1} = {} & ((v_{rc})_j + (f/2)^{1/2}\ (10/3 - (1/\kappa)(5/9)(f/2)^{1/2}) \\ & (V/r)\ \exp(\ (\kappa/y)(f/2)^{1/2}\ \Delta s)\Delta s))\ \exp(-(\kappa/y)(f/2)^{1/2}\ \Delta s\end{aligned} \tag{54}$$

in which the subscript j is the cross section index, and Δs is the distance between sections j and j + 1.

Equation 44 includes two terms, one describing the growth and the other the decay of secondary circulation. The full Equation applies to flow through a bend. Along a straight reach after a bend only the decay term applies and

$$(v_{rc})_{j+1} = (v_{rc})_j\ \exp(-(\kappa/y)(f/2)^{1/2}\ \Delta s \tag{55}$$

Calculation of $v_{rc\,ave}$ requires solution of Equations 44 and 45, with V given by Equation 49 or 50 and $v_{rc\,fd}$ is obtained from Equation 52. Because of the implicit nature of this set of equations the solution is iterative and is obtained as follows.

1) A first estimate of the mean velocity is calculated neglecting losses associated with secondary circulation, using the Darcy-Weisbach Equation and an appropriate formula for the friction factor.

2) This velocity and $(v_{rc})_1 = 0$ are used in Equations 54 and 55 to compute an initial distribution of v_{rc} through one complete meander wavelength.

3) The value of v_{rc} at the last section is substituted for $(v_{rc})_1$ and the distribution is recomputed iteratively until the value of v_{rc} at the first and last sections are identical, within a specified tolerance. This corresponds to uniform conditions through a series of identical meanders.

4) The average value of absolute v_{rc} through the wavelength is calculated as

$$(v_{rc})_{ave} = (\Sigma\ v_{rc}\ \Delta s)/(\Sigma\ \Delta s). \tag{56}$$

5) The mean flow velocity is recalculated, accounting for losses associated with secondary circulation, using Equation 49 or 50.

6) The recalculated mean velocity is then used in Equations 54 and 55 to compute a new distribution of v_{rc} through the wavelength.

7) This procedure is repeated until the recalculated mean velocity is the same as the previous one, within a specified tolerance.

This method is obviously not suitable for direct application in practice, but could be applied to different hypothetical situations to develop relationships between S''_{ave} and geometric and hydraulic parameters. This would provide a method for estimating head losses without the limitations of the LSCS method.

4.5 Application of prediction methods

Various methods have been identified for accounting for the additional resistance to flow induced by channel curvature. These are as proposed by:

Scobey (1933)
Cowan (1956)
Soil Conservation Service (SCS) (1967)
Toebes and Sooky (1967)
Leopold et al (1960)
Shukry (1950)
Mockmore (1944)
Onishi et al (1976)
Agarwal et al (1984)
Rozovskii (1957)
Chang (1983)
Chang (1988)
Pacheco-Ceballos (1983)

Some of these were not considered further for various reasons. Scobey's method gave unrealistic predictions for the data sets used, probably because it is not expressed in terms of dimensionless variables and suffers from scale effects. Cowan's approach is similar to the SCS method, which allows better quantitative description of channel characteristics. Shukry's method could not be applied to the data sets available because his curves for some parameters did not extend to their conditions. The method proposed by Onishi et al was intended for mobile bed channels and requires specification of sediment size; it is therefore not appropriate for the conditions under which the available data sets were obtained. Rozovskii's Equation is very similar to Chang's and it was not thought worth while to consider both. Chang's equation produced better results in preliminary applications and is also extended in subsequent publications; it was therefore selected in preference to Rozovskii's. Chang's 1983 and 1988 equations are virtually identical and the 1988 version was rejected as it performed slightly worse in the preliminary applications. The method of Pacheco-Ceballos is difficult to apply and has not been considered at this stage. Thus the following methods have been considered:

Soil Conservation Service (SCS) (1967)
Toebes and Sooky (1967)
Leopold et al (1960)
Mockmore (1944)
Agarwal et al (1984)
Chang (1983)
Modified Chang (1984)
Linearized Soil Conservation Service (LSCS)

To demonstrate the effect of meandering on channel conveyance and to provide a basis for comparison of the other methods, stage-discharge relationships were calculated ignoring non-friction losses.

Friction loss only

For a given stage the discharge is given by

$$Q = A V \tag{57}$$

in which A is the cross-sectional area and V is the flow velocity, given by the Darcy-Weisbach equation, i.e.

$$V = (8 g R S_f / f)^{1/2} \tag{58}$$

in which g is gravitational acceleration, R is the hydraulic radius of the cross-section, S_f is the energy gradient, and f is the friction factor. For uniform flow S_f can be equated to S_o, the bed gradient.

4.5.1 Data set

The selected prediction methods were applied to the following three sets of data, none of which were used in the development of any of the methods.

1. A full stage-discharge relationship for a trapezoidal channel constructed in the SERC Flood Facility at HR Wallingford, UK. This channel had a base width of 0.90 m, side slopes of 45°, a depth of 150 mm and a bed gradient of 0.00073. The sinuosity was 1.374 and four complete meanders were installed.

2. Full stage-discharge relationships for trapezoidal channels at the University of Aberdeen (Willetts, personal communication). These channels all had base widths of 139 mm, side slopes of 71°, and depths of 50 mm. Sinuosities were 1.21, 1.41 and 2.043 with bed slopes of 0.00083, 0.00071, and 0.00030 respectively.

3. Bankfull discharges for trapezoidal channels measured by the US Army Corps of Engineers at the Waterways Experiment Station, Vicksburg. The channels had side slopes of 63°, depths of 0.152 m and base widths of either 0.305 m or 0.610 m. For the wide channel sinuosities of 1.20, 1.40 and 1.57 were tested. For the narrow channel the sinuosities tested were 1.17, 1.22, 1.33, 1.49, 1.50, 1.75 and 2.54. In all cases the valley slope was 0.001. Full details of the channels and experiments are reported by the US Army Corps of Engineers (1956).

4.5.2 Results and conclusions

Each of the methods described above was applied to predict the discharge for every flow condition in these data sets. The friction factor for the SERC and Aberdeen channels varied with Reynolds number and were calculated by the appropriate modified smooth law, see Section 3.4. This required that the equations representing the different methods be solved iteratively. There were no data to establish variations of friction factor for the Vicksburg channels, and a constant value for each channel type was calculated from the bankfull flows in the corresponding straight channel.

The (per cent) error in each prediction was calculated as

$$\text{Error} = 100 (Q_p - Q_m) / Q_m$$

The average error and standard deviation of errors for each data set and for all the data together, are listed for each method in Table 14. Two values were computed for some of the Vicksburg data with the SCS Method. This was because the sinuosities fell on the thresholds of the correction factor defined by Equation 16. Values on either side of the thresholds were used and averages including both results presented. The first column gives the error obtained by ignoring bend losses and therefore gives an indication of the effect of meandering on resistance.

In terms of average error and the standard deviation of errors, the Modified Chang and SCS Methods appear to perform best with mean errors within the range -5% to +5% and standard deviations of less than 10%. Ignoring the energy loss induced by meandering gives unacceptably high errors in the prediction of discharge for inbank flows. Of the methods considered, those of Agarwal et al (1984), Mockmore (1944) and Chang (1983) appear to be unsatisfactory. The Chang methods are the only methods with a sound theoretical base, but the Modified Chang Method is not easy to apply in its present form. All the other methods are empirical and based largely on laboratory data; their generality is therefore not assured.

The overall performance of the SCS method is surprisingly good, and suggests that adjusting Manning's n by a factor related simply to sinuosity is reasonable. The relationship between the adjustment factor and sinuosity as recommended by SCS and as derived from the data used here is shown in Figure 15. (The values derived from the data are approximate. They were calculated from the discharges as measured and as calculated assuming friction loss only. The variation of friction coefficient with Reynolds number as bend losses are introduced are therefore not accounted for.)

One undesirable feature of the SCS recommendation is that it is a step function. The consequences of this are apparent in the prediction of the Vicksburg channel discharges. For the wide channel with a sinuosity of 1.2 the error is 30.71% or 13.66%, depending on which side of the step the sinuosity is assumed to lie. Similarly, for the narrow channel with sinuosity of 1.50 the error could be -8.10% or -18.71%. It would obviously be advisable to replace the SCS step function with a smooth curve. It is difficult to know where this curve should lie because the data are fairly spread out. One reason for the data spread is that bend losses are not caused by sinuosity per se, but rather by the degree of curvature. This is well demonstrated by the Vicksburg narrow channel data for sinuosities of 1.49 and 1.50. Although the sinuosities are almost identical, the bends in the 1.49 sinuosity channel are tighter, with longer straight reaches between bends. The tighter bends cause greater energy loss and the adjustment factor is 1.23, compared with 1.06 for the other, more gently curving channel. This effect is accounted for by the Modified Chang Method, as shown in Figure 16 where it was used to compute the adjustment factor for each data point. The spread of the predicted values is still considerable, confirming that it is associated with factors not accounted for by sinuosity alone, rather than experimental scatter. The range bars for the SERC and Aberdeen data points in Figures 15 and 16 show that the adjustment factor also varies considerably with stage, and that this is reproduced by the Modified Chang Method. It is therefore not entirely satisfactory to account for bend losses in meandering channels in terms of sinuosity alone. A more reliable adjustment function in terms of radius of curvature and bend angle could be determined using the Modified Chang Method in hypothetical applications.

Using the SCS method as it stands would not lead to major errors, however. To make it more satisfactory, the steps in the relationship could be eliminated by using the curve shown in Figure 16, although the inherent limitations remain. This has been done and the resulting method is referred to as the Linearized Soil Conservation Service method (LSCS). Prediction errors using this linearization are listed in Table 15 in the column headed LSCS Method, These reduced errors show that the linearized version is superior.

The following limitations remain with a relationship between an adjustment to Manning's n and sinuosity.

1) It cannot account for the variation of the adjustment with stage and radius of curvature.

2) It cannot account for the effects of cross-sectional shape. This can be significant, as shown by the SERC results : the ratio of total to friction losses in terms of Manning's n for the 1.37 sinuosity channel was 1.078 with a trapezoidal section and 1.22 with a pseudo-natural section.

3) An adjusted n value is useful for rivers and other channels with fairly uniform planforms which can be characterised by sinuosity. In many cases the planform is irregular and it would be preferable to account for losses in individual bends separately in non-uniform profile computations.

The relationship between bend radius and sinuosity is probably not highly variable in natural rivers, however, and this may not be cause for concern. The same comment applies to artificial channels designed in accordance with regime relationships.

Chang's theory could be applied to address these issues directly. The form used in this study already accounts for stage and bend radius effects. The complete form (Chang, 1984) would account for cross-sectional shape effects (but probably not for variations of cross-section along a reach). It would not be necessary to simulate the flow through each bend using the full theory. Rather, the theory could be used to generate general corrections to n, or preferably to the Darcy-Weisbach f, to account for these effects. It could also be used to develop a general relationship for the loss coefficient for single bends.

4.6 Summary

The effect of bends on flow resistance in open channels has been investigated. Laboratory data collected from meandering channels was analyzed to show that the meandering plan form increases the resistance to flow compared to equivalent straight channels.

A literature search was carried out to identify the important processes which induce this extra flow resistance. The main sources of flow resistance in a channel bend are: bed friction; increased bed friction due to secondary currents and internal energy dissipation due to increased turbulence induced by secondary currents. The flow resistance in a bend depends on bed roughness (f, C, n etc); flow depth (y); bend radius (r_c); length of bend (l) or angle of bend (θ, $l = r_c \theta$) and the cross-sectional shape of the channel. Flow resistance in a set of meander bends is likely to differ from the resistance induced by a single bend in an otherwise straight channel. This is due to the interaction (growth and decay) between the secondary currents induced in the individual bends.

Various methods which account for the extra flow resistance were identified in the literature and a selection of methods were applied to the available laboratory data. The methods were evaluated by comparing the mean errors in predicted discharge. The SCS method was found to give acceptable results for most practical purposes even though it does not account for the important mechanisms explicitly. An improved version of the SCS method was formulated to remove the undesirable step function (LSCS) and this linearized version gave better predictions. Although these methods, which adjust Manning's n based on the channel sinuosity, gave acceptable results they are empirical and their generality is not assured. Chang's approach in explicitly modelling the resistances due to secondary currents combined with backwater calculations along the channel is based on sound theoretical considerations. This approach is applicable to both single bends and series of meanders.

5 Formulation of the procedure for overbank meandering channels

The main objective of the study was to develop a procedure for calculating the conveyance of a meandering channel during overbank flow. The mechanisms which affect the conveyance capacity of meandering channels were identified in Chapter 3 and are summarized below. A further literature search was carried out to identify the means by which other authors have accounted for these mechanisms. Armed with this knowledge of physical processes and modelling techniques it was then possible to decide on an appropriate approach to be followed in developing a new procedure.

5.1 Important mechanisms

The internal structure of currents during overbank flows has been found to be highly complex. The available laboratory data has been reviewed in Chapter 3. The most important observations are:

1) The longitudinal velocities below bankfull tend to follow the main channel side walls while the floodplain velocities are generally in the valley direction. Thus the floodplain flows pass over the main channel and induce a horizontal shear layer.

2) The energy loss due to secondary currents in the main channel is greater than for an equivalent simple channel and the currents rotate in the opposite sense compared to inbank flows.

3) Fluid passes from the main channel onto the flood plain and back into the main channel in the following meander bend. Hence the proportion of discharge passed by the main channel and flood plain varies along a meander wavelength. These bulk exchanges of fluid between slow and fast moving regions of flow introduce extra flow resistance.

4) Flows on the flood plain outwith the meander belt are usually faster than those within the meander belt. It would appear that the extra flow resistance induced by the meandering main channel has a relatively small effect on the outer flood plain.

5.2 Methods available in the literature

Toebes and Sooky (1967) account for the interaction losses by separating the main channel and flood plain flows by a horizontal plane at bankfull level. The apparent shear on this plane is accounted for by adding a solid boundary equivalent to the wetted perimeters of both flow regions. The discharges in the two regions are then calculated separately and added. Experimental data were obtained from small-scale rectangular channels and these were used to evaluate the solid boundary addition. The addition was found to vary in a rather complex way with overbank flow depth, main channel depth, and channel gradient, but no general, practically usable relationship was proposed.

James and Brown (1977) proposed accounting for the interaction losses in straight and meandering compound channels by adjusting the value of Manning's n. From laboratory test results they developed an adjustment to the bankfull n value, dependent on relative flow depth and the ratio of floodplain width to main channel width. The adjusted n value is then applied to the cross-section considered as a single channel. Their experiments were conducted mainly with straight channels, however, and the data for meandering channels are very limited.

Yen and Yen (1983) also considered the compound section as a unit and treated the main channel as a resistance element. They proposed a Darcy-Weisbach type resistance coefficient which accounts for expansion and contraction losses induced by the main channel. This model does not account for flow in the main channel, and depends on empirical information obtained for closed conduits which is unverified for channels.

Ervine and Ellis (1987) also proposed division of the cross-section into three zones, viz. the main channel below bankfull level, the floodplain within the meander width, and the floodplain beyond the meander belt. They identified the main sources of energy losses in each of these zones. In the main channel these are :

1) friction on the wetted perimeter,

2) boundary resistance due to transverse shear and internal friction associated with secondary currents induced by the meander bends,

3) the turbulent shear stress generated by the velocity difference between the main channel and the co-linear component of the floodplain flow at the horizontal interface at bankfull level, and

4) form resistance associated with the undulating riffle-pool sequence.

Over the floodplain within the meander belt the main sources of energy loss are:

1) friction on the wetted perimeter,

2) expansion of the flow as it enters the main channel, and

3) contraction of the flow as it re-enters the floodplain.

The only loss over the floodplain beyond the meander belt is due to friction on the wetted perimeter.

Ervine and Ellis proposed a model for predicting stage-discharge relationships by quantifying the more important of these loss mechanisms. Friction losses are estimated using the Darcy-Weisbach equation with the friction factor given by the Colebrook-White equation. Losses associated with secondary currents in the main channel are estimated using the method proposed by Chang (1983) for fully developed circulation in wide, rectangular channels. Subsequent experimental observations have shown the secondary circulation to be generally opposite in sense for overbank flows compared with inbank flows. This is because it is driven by the horizontal shear at the bankfull level, rather than by centripetal acceleration. Chang's method was derived for the inbank mechanism, and is therefore inappropriate for overbank cases. Ervine and Ellis account for the growth and decay of secondary currents by applying only half of the head loss predicted by Chang's 1983 model.

Expansion losses for the floodplain flow are determined by application of the force-momentum principle, and contraction losses by using loss coefficient values presented by Rouse (1950) and used by Yen and Yen (1983). The losses in the main channel associated with the shear across the horizontal interface and with pool-riffle undulation were considered minor and not accounted for. They applied the model to the experimental conditions of the US Army Corps of Engineers, Waterways Experiment Station (1956) and Toebes and Sooky (1967) and produced fairly accurate predictions.

The method is summarized below.

Total discharge

$$Q_T = Q_1 + Q_2 + Q_3 + Q_4 \tag{59}$$

The zonal definitions are shown in Figure 17.

Main channel

$$Q_1 = A_1 V_1 \tag{60a}$$

$$V_1 = \left(\frac{2 \; g \; (S_o \; / \; s) \; R_1}{(f_1 / 4) \; + \; ((2.86 \; f_1^{½} + 2.07 \; f_1) \; / \; (5.565 + f_1^{½})) \; (R_1/r_c)^{½}} \right) \tag{60}$$

Where A_1 is the area of the main channel V_1 is the mean velocity in the main channel, r_c is the bend radius of curvature, S_o is the valley slope and s is the sinuosity.

Inner flood plain

$$Q_2 = A_2 V_2 \tag{61}$$

$$V_2 = \left(\frac{2 \; g \; (S_o \; / \; W_2)}{(f_2 / 4) + (W_2 - B \; s) / y_2 + s \; \sin^2(\theta_m) \; ((1 - y_2 / (y_2 + h))^2 + K_c)} \right) \tag{62}$$

Where W_2 is the width of the inner flood plain, B is the width of the main channel, y_2 is the depth of flow on the flood plain, h is the bankfull depth, θ_m is the mean angle between the main channel and the valley centre lines and K_c is the contraction coefficient. The values of contraction coefficient given by Rouse are listed in Table 16.

Outer flood plain

The flows (Q_3 and Q_4) are calculated assuming only bed friction with the division lines omitted from the definition of the wetted perimeters and the flood plain slope S_o is used in the calculation.

Greenhill (1992) has tried various different methods of calculating discharges for a selection of the SERC FCF data (tests 26, 31 and 39). No attempt was made to identify or model individual loss mechanisms and the methods are based on dividing the channel into the four zones and calculating the discharge in each zone assuming only bed friction. The two best methods Greenhill4 and Greenhill5) have been considered here.

The main channel discharge is calculated assuming that the horizontal division is included in the wetted perimeter of the main channel and the inner flood plain zone. Greenhill's method 4 applies vertical divisions at the meander belt edges and method 5 is based on division lines inclined outward at 45°. These division lines are included in the wetted perimeter of the inner flood plain zone but not the outer zones. The main channel hydraulic slope (S_o/s) is used when calculating the main channel and meander belt discharges while the flood plain gradient (S_o) is used in calculating the outer flood plain flows.

5.3 Approach to conveyance estimation

The possible forms of analysis were constrained by the time available for the study, the specific requirements of the NRA and the amount and type of data available.

The NRA required that the resulting methods should be applied by hand calculation. It must be recognised that flow in compound meandering channels is very complex and the development of methods to analyze it accurately will probably follow directions that are highly computational. A hand calculation method is unlikely to be compatible with this development and should not be viewed as a contribution to it. By disqualifying the most promising avenues for complete description of the processes involved, a hand method must compromise accuracy and be limited to first estimate applications. The NRA also required that the methods be design oriented. They should therefore be developed in terms of physical parameters which are meaningful in a design context. For example, the dependence of channel capacity on design variables, such as cross-section shape and size, should be fairly explicit.

The SERC Phase B tests were limited to just two different planform geometries, with sinuosities of 1.37 and 2.04. The Phase A tests, carried out in straight channels, represent the limiting case of sinuosity 1.0. This wide range of sinuosities is such that it would be unreasonable to expect to be able to interpolate flow characteristics between them. This makes a purely empirical, descriptive approach unrealistic, as it could be applied only to new situations which are very similar to the experimental ones.

To ensure generality of the design methods, it was decided to base them on conceptual models of the physical processes involved in dissipating energy and determining flow structure. The SERC data was used to quantify these processes, in terms of geometric and fluid state parameters. This involved theoretical and empirical formulations. The relative importance of the individual processes were expected to vary with the scale of the physical system, and also with the flow condition. Separation and individual treatment of the processes accounted for the effects of these variations on the required predictions (of stage-discharge relationships, for example) better than if these were made in terms of the geometries and fluid state parameters directly. The approach also has the advantage of being able to include data from different sources obtained under different conditions, and allowing incorporation of new results and analyses as they become available.

The division of the channel into four zones as proposed by Ervine and Ellis (1987) was adopted as the most flexible approach. The stage-discharge relationship for a compound meandering channel will be predicted by dividing the cross-section into zones and calculating the zonal discharges separately. The division will be by a horizontal line at bankfull level and a vertical line on either side of the meander belt. This approach also recognises the limited scope of the present investigation and allows for improved models to be substituted for the various zonal calculations in the future.

5.4 Formulation zone 1

The flow mechanisms in this zone are complex, and have been described by Willetts (1992), for example. The major mechanisms responsible for energy dissipation are:

1) friction,

2) secondary circulation driven by the shear imposed by the flood plain flow,

3) the apparent shear stress on the horizontal interface associated with the gradient of collinear velocity components across it,

4) the bulk exchange of water between the main channel and the flood plain.

Losses associated with variations in cross-section geometry and flow separation have been shown to be insignificant for the conditions likely to occur (Kazemipour and Apelt, 1979, 1982 and 1983).

It was originally intended to develop physically-based deterministic models to account for the effects of the various loss mechanisms on stage-discharge relationships. This has proved not to be possible, at least for the main channel zone, owing to the current lack of understanding of the mechanisms and their effects. An empirical approach has therefore been resorted to, based on the Phase B data and a rational selection of dimensionless variables. The procedure is to calculate the bankfull discharge (Q_{bf}) using an appropriate method for inbank flows, and then to adjust this to account for the effects of overbank flow. The bankfull discharge includes allowance for the effects of bend losses. This was used rather than an equivalent straight channel value to separate the inbank bend losses from the ultimate adjustment factor. This will allow future developments in inbank flow assessment to be incorporated. Also, it is likely that in some design applications inbank stage-discharge measurements will be available for the specific site, and these can then be used to evaluate Q_{bf} directly.

Discharges in this zone have been obtained by integration of the velocity magnitude and direction measurements taken in some of the Phase B experiments. The relevant experiments and integrated discharge values are listed in Table 17. The discharges were found to vary along the channel in a way consistent with the descriptive observations reported by Willets (1992), Figure 18.

A study of Figure 18 shows that for both the 60° and 110° geometries the discharges vary along a meander, being maximum at the bend apices (2 X / L = 0.0, 1.0) and minimum at some point in between. Figure 18A shows that cross-section shape does not affect the distribution strongly, with the trapezoidal and natural cases giving similar variations of discharge. Figures 18B and 18C show that while the roughness of the flood plain may affect the magnitudes of the main channel discharges it does not have a significant effect on the flow distribution. The effect of channel sinuosity is apparent from Figures 18B and 18C. The more sinuous channel was found to have a much wider variation in main channel discharge at similar depths compared to the less sinuous channel. For example at a flow depth of 200mm the 110° main channel discharge varied between about 0.4 and 1.3 of the mean while for the 60° main channel the variation is between 0.8 and 1.2 of the mean. The effect of depth is more pronounced for the more sinuous channel. The 60° main channel discharges vary between about 0.8 and 1.2 of the mean for all three depths while for the 110° main channel the variation was between 0.9 and 1.1 at low depth (165 mm) and 0.3 and 1.3 at high depth (200 mm).

These variations are ignored in this analysis as neither they nor their effects will be explicitly accounted for in the stage-discharge predictions; the values listed in Table 17 are averages of the integrations at all the measurement sections, weighted by the channel lengths represented by the sections.

The main channel bankfull discharges were not measured during the experiments, and have been determined indirectly. For the trapezoidal channel, the modified version of Chang's (1984) method for accounting for bend losses has previously been found to predict the stage-discharge relationship very accurately (-1.76% average error over all measured values). It was therefore used to predict the bankfull discharge. The stage-discharge relationship is shown in Figure 19. No method has yet been found which predicts the stage-discharge relationships sufficiently accurately for the pseudo-natural channels. The bankfull discharges were therefore determined for these cases by graphically extending the measured stage-discharge relationships, as shown in Figures 20 and 21. The bankfull discharges for each channel type are also listed in Table 17.

The ratios of main channel discharge to bankfull discharge ($Q/Q_{bf} = Q_1'$) are plotted against flood plain flow depth (y_2) on Figure 22. This shows that as the water level rises above the flood plain, the discharge initially decreases below the bankfull value and then gradually rises and may exceed the bankfull value at high stages. The relationship between main channel discharge and overbank flow depth is clearly affected by the channel cross-section geometry, the channel sinuosity (s) and the flood plain roughness. It is obviously desirable to express these characteristics in non-dimensional terms and appropriate measures have been selected. The flow depth is normalized by the hydraulic depth of the main channel at bankfull, i.e. A/B, where A is the cross-sectional area and B is the surface width. This has been chosen rather than a flow depth or hydraulic radius because it probably varies least along natural channels and will require the least field survey information. The data have been replotted in Figure 23 in terms of the dimensionless flow depth, $y_2/(A/B)$ ($= y'$). The cross-section geometry is characterized by the ratio of surface width to hydraulic depth. This is a physically meaningful parameter because it represents the ratio of the area on which the apparent shear stress on the horizontal interface is applied to a measure of the volume affected. Expressed as B^2/A it is also a shape factor, describing the deviation of the channel cross-section from square. The flood plain roughness is expressed as the ratio of flood plain and main channel Darcy-Weisbach friction factors, f_2/f_1 ($= f'$). For the main channel, both the basic straight channel value and the effective value accounting for bend resistance were considered, and the final results found to be indistinguishable. The basic value will be more meaningful to most engineers and has therefore been used.

Quantitative interpretation of the relationships between the channel discharge and the various physical characteristics is severely constrained by the amount of data available. In most cases effects are presented by only two data points. The exclusive use of linear functions to describe the relationships in this analysis is a consequence of the lack of data; it is unlikely that the processes are actually linear.

Figure 23 suggests that for any particular channel the relationship between Q_1' and y' can be represented by two straight lines. At low overbank stages the slope of the line is negative and not appreciably affected by channel geometry, sinuosity or flood plain roughness. At higher stages the slope is positive and both the slope and position of the line are affected by these characteristics.

The straight line describing the variation of Q_1' with y' at low overbank stages must obviously pass through the point (1.0, 0.0), which defines the constant in the relationship. The slope is defined by the four points at y' approximately equal to 0.2. These points are very close together although they represent widely different conditions, suggesting that the variation is not appreciably affected by these conditions. The effect of sinuosity appears to be similar to that for higher values of y', but there are insufficient data to distinguish the effect reliably and a common slope has been assumed. This was calculated as the average of the slopes for all four data points. The variation for low stages is then defined by

$$Q_1' = 1.0 - 1.69\, y' \tag{63}$$

For overbank stages higher than y' equal to approximately 0.2, the relationship between Q_1' and y' is more complex and is clearly affected by channel geometry, sinuosity and flood plain roughness. These characteristics had to be quantified for all data points. Both channel geometry (as represented by the ratio B^2/A) and sinuosity were constant in all experiments for each channel type, but the flood plain friction factor varied with flow depth for both smooth and rod-roughened experiments. As described before, flood plain roughness was accounted for in terms of the ratio (f') of the Darcy-Weisbach friction factor for the flood plain (f_2) and the equivalent straight channel value for the main channel at bankfull stage (f_c). The main channel and smooth flood plain values were calculated using the relationship for smooth channels derived by Ackers (1991) from straight channel data, Equation 1. For the rod-roughened flood plain, values were obtained from the procedure developed by Ackers (1991) and summarized in Appendix 5. The variable values are listed in Table 18.

The relationship between Q_1', y', B^2/A, s and f' for values of y' greater than about 0.2 was determined in seven different ways. These are discussed in the following paragraphs.

Method 1

As there are no more than two data points on the curve for each channel type on Figure 23, it is assumed that all relationships are linear. The basic relationship is

$$Q_1' = m\, y' + c \tag{64}$$

in which m is the slope of the line and c defines its position. Both m and c may be functions of B^2/A, s and f'. It is impossible to determine the effect of sinuosity on m because only two sinuosities were used (1.37 and 2.04), and only one flood plain flow depth was used for the 2.04 sinuosity channel in this range of y'. The accelerating effect of the apparent shear stress on the horizontal interface must decrease with sinuosity and the rate of increase of Q_1' with y' will be less, implying a smaller value of m. However, assigning a value of m to a sinuosity of 2.04 would be totally speculative without additional data, and it was assumed that it would be the same as for a sinuosity of 1.37. It was assumed, therefore, that m depends on B^2/A and f' only, i.e.

$$m = m\,(B^2/A, f') \tag{65}$$

Because no experiments were performed with the trapezoidal channel with rod-roughened flood plains, there is no evidence that the effects of B^2/A and f' on m are not independent, and they are assumed to be so.

The positions of the lines (and hence the values of c) are clearly dependent on B^2/A, s and f'. The dependence on B^2/A can be seen by comparing the points for the 60° trapezoidal and pseudo-natural channels with smooth flood plains. The dependence on sinuosity can be seen by comparing the points for the 60° and 110° pseudo-natural channels with smooth flood plains. The dependence on f' can be seen by comparing the points for the 60° pseudo-natural channels with smooth and rod-roughened flood plains. It was assumed, therefore, that

$$c = c\,(B^2/A,\ s,\ f')\tag{66}$$

As for m, there is no evidence that the effects of B^2/A and f' are not independent. No experiments were done with the trapezoidal channel with different sinuosities, so there is also no evidence that the effects of B^2/A and s are not independent. However, the effects of s and f' are clearly not independent, as can be seen by comparing the points for the smooth and rod-roughened flood plains for the 60° and 110° pseudo-natural channels : the effect of roughening the flood plain is much less if the sinuosity is greater. To account for this dependence, f' was initially omitted from the expression for c, i.e. it was assumed that

$$c = c\,(B^2/A,\ s) \tag{67}$$

The combined effect of s and f' was accounted for by a subsequent adjustment to Q_1'.

It can be seen in Table 18 that f' is substantially different at different flow depths, even when the flood plains are not roughened and the physical surface roughness are identical. For example, for the 60° pseudo-natural channel with smooth flood plains, f' varies by a factor of two over the range of y' tested. If the dependence on f' is being sought, it is therefore not correct to connect the points for each channel geometry, as done in Figure 23, because they have different f' values. This difficulty was addressed by adjusting the positions of the points so that points with identical f' values could be connected to define the relationships. Points with the same y', s and B^2/A were used to define the gradient of Q_1' with f' for that channel and y'. Assuming this gradient to be constant with Q_1', the position of a point could be adjusted to represent the same f' as another point with the same s and B^2/A but different y'. The line through these points would then represent the relationship between Q_1' and y' for a given channel with constant f'. As no data were obtained for the trapezoidal channel with roughened flood plains, the points for the trapezoidal channel were adjusted using the gradient of Q_1' with f' as calculated for the 60° pseudo-natural channel. The adjusted points and resulting linear relationships are shown in Figure 24 and Table 19. This diagram forms the basis of the discharge relationship for y' greater than about 0.2.

It was assumed that Equation 65 has the form

$$m = a_1\, B^2/A + a_2 f' + a_3 \tag{68}$$

One point and the line through it were selected to represent Equation 68 for each of the 60° trapezoidal, 60° pseudo-natural with smooth flood plain, and 60° pseudo-natural with roughened flood plain channels. The average value of f' for each channel was used. Three equations for m were therefore set up and these were solved simultaneously to determine values for a_1, a_2 and a_3. The resulting equation for m is

$$m = 0.0147\, B^2/A + 0.0320\, f' + 0.169 \tag{69}$$

The same approach was followed to evaluate c, with Equation 67 assumed to have the form

$$c = b_1\, B^2/A + b_2\, s + b_3 \tag{70}$$

The same points and lines as used to define m were again used to set up three equations for c, which were solved simultaneously to determine values for b_1, b_2, and b_3. The resulting equation for c is

$$c = 0.0132\ B^2/A - 0.302\ s + 0.851 \quad (71)$$

The initial adjustment to bankfull discharge is therefore given by

$$Q_1' = (0.0147\ B^2/A + 0.0320\ f' + 0.169)\ y' + 0.0132\ B^2/A - 0.302\ s + 0.851 \quad (72)$$

Equation 72 does not account for the joint effect of s and f' on c. A further adjustment was derived by calculating the ratios of measured Q_1' to the values calculated by equation (72), and relating them to s and f'. The predicted ($Q_{1\,p}'$) and measured (Q_1') values for those experiments in the appropriate range of y' are listed in Table 20.

The adjustment required to the discharge ratio predicted by Equation 72 is plotted in Figure 25. The data for high values of f' are too sparse to infer a variation with s. It was assumed that the adjustment varies linearly with f' and linear regression was used to obtain the relationship

$$Q_1'/Q_{1\,p}' = K = 1.07 - 0.0698\ f' \quad (73)$$

The adjustment factor for y' greater than about 0.2 is then given by

$$Q_1' = (m\,y' + c)\,K$$

with

$$m = 0.0147\ B^2/A + 0.032\ f' + 0.169$$

$$c = 0.0132\ B^2/A - 0.302\ s + 0.851$$

$$K = 1.07 - 0.0698\ f' \quad (74)$$

Method 2

The second adjustment in Method 1, represented by K, was intended to account for the interdependence of the effects of s and f' on Q_1'. As it turned out to be a function of f' only, which is accounted for in m, it need really only be applied to c. The adjustment to c (as predicted by Equation 71) was derived by calculating the ratios of the required values to these predicted values, and relating them to s and f'. The values of c required were calculated using Equation 64 with m given by Equation 69. The predicted (c_p) and required (c) values for those experiments in the appropriate range of y' are listed in Table 21.

The adjustment required to c as predicted by Equation 71 is plotted against f' in Figure 26. Again, the data are too sparse to infer a variation with s, and the following linear relationship with f' was obtained and is assumed to apply for all sinuosities.

$$c/c_p = 1.14 - 0.136\ f' \quad (75)$$

The adjustment factor for y' greater than about 0.2 is then given by

$$Q_1' = m\,y' + K\,c$$

with $m = 0.0147\,B^2/A + 0.032\,f' + 0.169$

$c = 0.0132\,B^2/A - 0.302\,s + 0.851$

$$K = 1.14 - 0.136\,f' \qquad (76)$$

Method 3

Methods 1 and 2 were derived by simultaneous solution of one equation for each of the channel types. Some of the data were therefore not used, and a more accurate formulation might be obtained from a regression analysis on all the data. In Method 3 a straight forward multiple linear regression analysis was performed, giving the following relationship.

$$Q_1' = 0.469\,y' + 0.0392\,B^2/A - 0.0645\,f' - 0.195\,s + 0.382 \qquad (77)$$

Method 4

Figure 24 presents a set of straight lines for y' greater than about 0.2, the slopes and positions of which appear to depend on B^2/A, f' and s. In this method multiple linear regression analyses were performed separately on the slopes and intercepts of the lines.

Because there is only one data point for the 110° crossover angle channel for each roughness condition, no slope could be determined. Slopes were therefore known for only one sinuosity and consequently no variation with sinuosity could be considered. It was therefore assumed that the slopes of the lines depend only on B^2/A and f'. Using the data for the channels with a 60° crossover angle, the following relationship for slope was found.

$$m = 0.0183\,B^2/A + 0.0128\,f' + 0.159 \qquad (78)$$

The intercepts (c) of the lines were assumed to depend on B^2/A, f' and s. Values of c for each line were calculated using Equation 64, with Q_1' as given in Table 18 and m measured on Figure 24. For the 110° crossover angle channels m was calculated using Equation 78. The resulting relationship for c is:

$$c = 0.00768\,B^2/A - 0.0708\,f' + 0.0672\,s + 0.435 \qquad (79)$$

The adjustment factor for y' greater than about 0.2 is then given by

$Q_1' = m\,y' + c$

with $m = 0.0183\,B^2/A + 0.0128\,f' + 0.159$

$$c = 0.00768\,B^2/A - 0.0708\,f' - 0.0672\,s + 0.435 \qquad (80)$$

Method 5

The slopes of the lines for y' greater than about 0.2 on Figure 24 do not vary greatly, and a simpler equation for Q_1' would result if the slope were assumed constant. It was assumed that the average slope (m = 0.433) applies to all lines and values of c were calculated using Equation 64 and this value. The relationship between c and the channel variables was reanalysed and the relationship for Q_1' is then given by

$$Q_1' = 0.433\,y' + 0.00715\,B^2/A - 0.0532\,f' + 0.0246\,s + 0.459 \qquad (81)$$

Method 6

There are only two data points for the 110° crossover channel for y' greater than 0.2. The point for the experiment with roughened flood plains suggests that sinuosity has no effect on Q_1', while the point for the experiment with smooth flood plains suggests a significant effect. Methods 1 to 5 attempted to reconcile this information.

In Method 6 it was assumed that Q_1' is independent of sinuosity, as suggested by the experiments with roughened flood plains. Although intuitively unappealing, there is some justification for this assumption. Sinuosity is accounted for in the estimate of Q_{bf}, and the implication is that the magnitude of main channel energy loss associated with meandering is similar for inbank and overbank flows, although it is recognised that the mechanisms are radically different. The validity of this assumption needs to be investigated using a data set with a wider range of sinuosities.

This method is therefore similar to Method 4, but the regression analysis for c excluded the data for the 110° crossover channel, resulting in a different formulation. The adjustment factor is given by

$$Q_1' = m\,y' + c$$

$$\text{with } m = 0.0183\,B^2/A + 0.0128\,f' + 0.159$$

$$c = 0.00888\,B^2/A - 0.0729\,f' + 0.402 \qquad (82)$$

Method 7

In this method it was assumed (as for Method 5) that m is constant, and that (as for Method 6) c is independent of sinuosity. Values of c were determined as in Method 5 and the regression analysis revised. The adjustment factor is then given by

$$Q_1' = 0.433\,y' + 0.0182\,B^2/A - 0.0614\,f' + 0.402 \qquad (83)$$

Evaluation of Methods

The errors in reproducing the data by each of the methods are listed in Table 22. The selection of the most appropriate method or methods was based on the magnitude, nature and distribution of errors, with some consideration of simplicity. Errors are most acceptable at high values of y' because the main channel contribution to total discharge becomes relatively less significant as stage increases. Errors are considered more acceptable at high sinuosities than at moderate sinuosities, as the latter are more common in design applications. Negative errors are preferable to positive errors because they would introduce conservative underestimation of main channel conveyance in design applications.

On the basis of the above criteria, Method 2 was selected, its worst performance is for high y' and high sinuosity with rough flood plains and the error for the latter condition is negative. It should be noted that the experimental flood plain roughness was extreme, and the error decreases for smoother flood plains.

Summary

The procedure is to calculate the bankfull discharge (Q_{bf}), and then to adjust this to account for the effects of overbank flow. The bankfull discharge can be estimated using inbank flow methods or obtained by measurement, if possible. The hydraulic slope which controls the flow in the main channel zone (S) is related to the flood plain or valley hydraulic slope by the channel sinuosity, (ie $S = S_o / s$). It should be noted that S_o can either be a ground slope if uniform flow is assumed or a water surface slope.

The adjustment factor was determined from the SERC FCF Phase B data. Actual discharges in this zone were obtained by integrating the velocity magnitude and direction measurements taken in some of the experiments. The ratio of actual to bankfull discharge defines the adjustment factor, Q_1'.

Q_1' was found to depend on:

1) the flood plain flow depth at the edge of the main channel (y_2);
2) the channel sinuosity (s);
3) the cross-section geometry and
4) flood plain roughness.

These characteristics are represented by dimensionless parameters which were chosen as being both meaningful and easy to measure. The flow depth is normalized by the hydraulic depth of the main channel at bankfull, Equation 84, where A is the cross-sectional area and B the surface width of the main channel at bankfull.

$$y' = y_2 / (A/B) \qquad (84)$$

The cross-section geometry is characterized by B^2/A. The flood plain roughness is expressed as the ratio of flood plain and main channel Darcy-Weisbach friction factors, i.e.

$$f' = f_2 / f_1 \qquad (85)$$

The Darcy-Weisbach friction factor can be calculated using the Colebrook-White equation. If Manning's n is used then f is related to n by

$$f = \frac{8\ g\ n^2}{R^{1/3}} \qquad (86)$$

The ratio f' can therefore also be expressed in terms of Manning's n

$$f' = (n_2/n_1)^2\ (R_1/R_2)^{1/3} \qquad (87)$$

The relationship between the adjustment factor and these variables is shown schematically in Figure 26b. This shows that the main channel discharge is initially reduced as stage rises above bankfull, and that this reduction is independent of channel characteristics. At higher stages the discharge increases with stage at a rate which depends strongly on B^2/A, s and f'. Various expressions for the relationship at high stages were derived by different methods. The relationship derived by method 2 above was chosen as the best.

Thus the variation in main channel discharge with overbank stage can be accounted for by choosing the adjustment factor to be the **greater** of

$$Q_1' = 1.0 - 1.69\, y' \qquad (88)$$

or

$$Q_1' = m\, y' + K c$$

with $m = 0.0147\ B^2/A + 0.032\ f' + 0.169$

$c = 0.0132\ B^2/A - 0.302\ s + 0.851$

$$K = 1.14 - 0.136\ f' \tag{89}$$

and the correct flow in zone 1 is given by

$$Q_1 = Q_{bf}\ Q_1' \tag{90}$$

5.5 Formulation zone 2

This section describes two alternative methods for predicting the discharge in the inner flood plain zone. The first method attempts to account for the principal loss mechanisms using physically-based deterministic formulations. The formulations are based on a very simple conceptual model of the loss mechanisms and require empirical adjustment to account for the additional complexities involved.

The second method is purely empirical and follows an approach similar to that used for the main channel zone. A basic discharge is calculated assuming friction losses only, and this is then adjusted to account for the effects of flow interaction with the main channel. The adjustment is based on data obtained from the SERC Phase B experiments and data provided by Professor B B Willetts (personal communication) obtained from experiments conducted under his supervision at the University of Aberdeen.

5.5.1 Expansion contraction model

The major energy loss mechanisms in the inner flood plain zone have been identified previously by other researchers (for example, Ervine and Ellis 1987, McKeogh and Kiely 1989) as

1) friction on the wetted perimeter,

2) expansion of the flow as it enters the main channel, and

3) contraction of the flow as it re-enters the floodplain.

The energy loss due to friction (h_f) over one meander wavelength (L) can be estimated using the Darcy-Weisbach equation,

$$h_f = \frac{f_2\ L\ V_2^2}{8\ g\ R_2} \tag{91}$$

in which f_2 is the Darcy-Weisbach friction factor for the inner flood plain,
g is the acceleration due to gravity,
V_2 is the flow velocity, and
R_2 is the hydraulic radius.

The hydraulic radius is defined as the ratio of the cross-sectional area to the wetted perimeter. The inner flood plain zone is rectangular and so the cross-sectional area is the product of the inner flood plain width (W_2) and the flow depth on the flood plain (y_2). The wetted perimeter includes the flood plain surface only, and not the horizontal plane dividing the inner flood plain and main channel zones. By considering the areas of the flood plain and division plane over a wavelength, it can be shown that the effective wetted perimeter is the width less the product of the sinuosity (s) and the main channel top width (B). The hydraulic radius for friction loss calculations is therefore given by:

$$R_2 = \frac{W_2 \ y_2}{W_2 - B \ s} \tag{92}$$

Expansion and contraction losses depend on the pattern of flow across the main channel, which is complex. The flow expansion is accompanied by deviation of the primary flow direction and entrainment of some of the flood plain flow into the main channel along the cross-over reach (Jasem, 1990). There are also bulk exchanges of water between the main channel and flood plain associated with the bend apex regions (Willetts, 1992). The model developed here assumes straight flow across a slot in which there is no transverse flow, and is therefore a very simplified representation of the real situation. A complete, quantitative description of the interactions between flood plain and channel flows would require detailed computational modelling. Appropriate models do not exist at present, nor do the understanding and quantitative information necessary for their development in the short term. For present purposes, however, only the energy loss associated with the flood plain - main channel interaction is to be predicted and the model does not need to be complete and accurate in all respects. It is assumed, therefore, that the magnitude of energy loss and its dependence on the main flow and geometric properties is similar for the simplified and real situations. In fact, insufficient information is available at present even to provide a good, general description of energy loss for the simple case and some broad assumptions are necessary.

The expansion loss over a simple downward step (as shown in Figure 27) can be estimated by application of energy and momentum equations between sections 1 and 2. This gives

$$h_e = \left(\frac{4 \ y_2 \ (y_2/y_1 - 1)}{y_2 + h + y_1} + (1 - (y_2/y_1)^2) \right) \frac{V_2^2}{2 \ g} \tag{93}$$

in which h_e is the energy lost in expansion of the flow,
y_1 is the flow depth in the main channel,
h is the step height,
V_2 is the velocity at Section 2, Figure 27

If it is assumed that the water surface is flat and unaffected by the step, then $y_1 = y_2 + h$ and Equation 93 reduces to

$$h_e = \left(1 - \frac{y_2}{y_1}\right)^2 \frac{V_2^2}{2g} \tag{94}$$

Equations 93 and 94 have both been applied to some data obtained by Jasem (1990) and the differences in their predictions found to be negligible. Equation 94 is therefore accepted as an adequate description. Note that this result is independent of θ, the inclination of the downward step to the direction of flow.

The flow pattern for contraction over an upward step is shown in Figure 28. The step induces a vena contracta a short distance downstream of the step, beyond which the flow expands to the normal flow conditions. The loss of energy associated with this pattern is concentrated in the expansion region, i.e. between Sections 3 and 4. The contraction loss (h_c) could therefore be described by an expansion loss equation similar to Equation 94, i.e.

$$h_c = (1 - y_3/y_2)^2 \frac{V_3^2}{2g} \tag{95}$$

Equation 95 cannot be used, however, without knowledge of the contraction coefficient necessary to define the flow conditions at Section 3. This cannot be determined analytically and has not been investigated experimentally. Yen and Yen (1983) recommended accounting for the contraction loss between a meandering channel and its flood plain with the relationship:

$$h_c = K_c \frac{V_2^2}{2g} \tag{96}$$

in which K_c is a contraction loss coefficient which varies with the ratio of flood plain to main channel flow depths, as given in Table 16. These values for K_c were given by Streeter in Rouse (1950) and are apparently based on data obtained from experiments in pipes conducted by Weisbach in 1855. Jasem's (1990) results for wide rectangular slots agree well with these values and they can therefore be accepted as reasonably accurate for free surface flows as well.

Both expansion and contraction losses can be expected to depend on the width of the main channel (B). The expansion develops over some distance from the downward step. If this development is incomplete before the upward step is encountered, then clearly the associated expansion loss will be proportionately reduced. Incomplete development will also mean that the flow contraction does not begin from the bed of the main channel, but some distance above it, and the associated loss will be less. Flow patterns for wide and narrow channels are illustrated in Figure 29.

Jasem (1990) measured expansion and contraction losses over slots with width to depth ratios ranging from 2 to 20. His results have been used to derive corrections to the expansion and contraction loss coefficients to account for width to depth ratio. The ratios of measured expansion loss coefficient to $(1 - y_2/y_1)^2$ are plotted against width to depth ratio (B/h) in Figure 30. The ratios of measured contraction loss coefficient to interpolated values from Table 16 are plotted against B/h in Figure 31. As the loss coefficients are additive a correction could be applied to both together, and the ratios of the sums of the measured values to the sums of $(1 - y_2/y_1)^2$ and values from Table 16 are plotted against B/h in Figure 32. In each case linear regression was used to obtain a relationship between the correction factor and width to depth ratio. These relationships are given on the figures. They are remarkably similar, and it would therefore be most practical to apply a single correction to the two coefficients together, i.e.

$$\text{Width to Depth Ratio Correction} = 0.02 (B / h) + 0.69 \tag{97}$$

For a channel angled across the flood plain the width presented to the flow would be greater than B and would vary with the angle. Attempts to refine Equation 97 to account for this are not worth while at the current state of knowledge of the processes.

Both expansion and contraction losses can also be expected to vary with the side slopes of the main channel. The effect on the contraction loss should be particularly significant because of the influence the bank slope must have on the contraction coefficient. These effects cannot be described analytically and no directly applicable experimental results can be found. Chow (1959), however, has presented results obtained by Formica (1955) for energy losses in lateral expansions and contractions in channels. These have been used to obtain first estimates of the effects of the transition geometries.

Formica measured energy losses across an abrupt contraction in width and a contraction with a straight taper of 30°. The energy loss varied considerably with discharge but on average the loss with the tapered contraction was about 0.3 times that with the abrupt contraction. If the contraction loss is assumed to decrease linearly with the cotangent of the side slope, a correction function can be written as

$$\text{Contraction Side Slope Correction} = 1 - (S_s / 2.5) \qquad (98)$$

in which S_s is the cotangent of the side slope. It would be realistic to set a minimum value above zero, say 0.1, to this correction.

Formica also conducted experiments with an abrupt expansion in width and expansions with straight tapers of 1:1, 1:2, 1:3 and 1:4. For the 1:4 taper the energy loss was about 0.3 times that for the abrupt expansion, and decreased quite uniformly over this range. Assuming a linear decrease of the expansion loss coefficient with side slope, the correction would be

$$\text{Expansion Side Slope Correction} = 1 - (S_s / 5.7) \qquad (99)$$

Again, it would be advisable to set a lower limit of, say, 0.1 to this correction.

Both downward and upward steps between the main channel and flood plain extend over a width of (W - B) over the inner flood plain between consecutive bend apices. Over a meander wavelength there will be two downward and two upward steps. If the losses are assumed proportional to the width over which expansion and contraction take place, then the losses should be further corrected by

$$\text{Step Length Correction} = 2 \ (W_2 - B) / W_2 \qquad (100)$$

The head loss over one wavelength associated with expansion and contraction, h_l, is therefore estimated as

$$h_L = h_e + h_c \qquad (101)$$

i.e.

$$h_L = K_e \ \frac{V^2}{2_g}$$

where

$$h_L = C_{sl} \, C_{wd} \, (C_{sse} \, (1 - y_2/y_1)^2 + C_{ssc} \, K_c) \, V_2^2 / 2 \, g \qquad (102)$$

in which C_{sl} is the step length correction $= 2 \, (W_2 - B) / W_2$,

C_{wd} is the width to depth ratio correction $= 0.02 \, B / h + 0.69$,

C_{sse} is the expansion side slope correction $= 1 - s / 5.7$,

C_{ssc} is the contraction side slope correction
$= 1 - s / 2.5$,

K_c is the basic contraction coefficient, as given in Table 16.

The total energy loss over one meander wavelength is the sum of the friction and expansion and contraction losses, i.e. $h_f + h_L$. Each of these major loss components can be expressed as a multiple of the velocity head, so that

$$h_f + h_L = (f_2 L / 4 R_2 + K_e) V_2^2 / 2 g \tag{103}$$

in which K_e is the total expansion-contraction loss coefficient, as defined by Equation (102). Under uniform flow conditions the total energy gradient is equal to the flood plain bed gradient, S_o, so that

$$h_f + h_L = S_o L \tag{104}$$

Equations (103) and (104) can be combined to give

$$V_2 = \left(\frac{2 \ g \ S_o \ L}{(f_2 \ L) \ / \ (4 \ R_2) \ + \ K_e} \right)^{1/2} \tag{105}$$

Considering the complexities of the flow mechanisms Equation 105 could not be expected to account for all the energy losses under all conditions. A comparison of the SERC Phase B and Aberdeen data showed the non-friction losses to be strongly influenced by the cross-sectional geometry of the main channel. The basic model, Equation 105, was found to predict stage-discharges reasonably well for the SERC 60° channels but to underpredict discharge quite badly (errors ~20%) for the Aberdeen channel with a similar sinuosity.

Apart from the scale the only significant difference between the two channels is the cross sectional shape. This has been described in the zone 1 model by the factor (B^2 / A) and was assumed to be an appropriate measure here as well.

It was assumed that the friction part of the model is adequate and that the non-friction term should be adjusted. Also it was assumed that the error in total discharge would most likely arise in the zone 2 model because its contribution is most significant at higher stages.

The correction is based on the SERC 60° trapezoidal channel ($B^2 / A = 9.14$) and the Aberdeen 1.4 sinuosity channel ($B^2 / A = 3.84$). It was found by trial that the shape effect observed in these two channels could be accounted for by multiplying the non-friction term in equation 105 (K_e) by a factor defined by

$$F_1 = 0.1 \ B^2/A \qquad \text{for } B^2/A < 10$$

$$F_1 = 1.0 \qquad \text{for } B^2/A > 10 \tag{106}$$

in which A is the cross-sectional area of the main channel below bankfull.
The SERC Phase B results suggest a further effect associated with main channel sinuosity (s). Application of the basic model (Equation 105) to this data showed that, for smooth flood plains, the predictions were reasonable for both the 60° trapezoidal and natural channels. The errors in calculated discharge over the whole range of stages are shown in Figures 33 and 34.

The cause of the high positive errors at low relative depth (y') is not known. They are not consistent, being clearly present for the 60° trapezoidal and 110° natural channels, but not for the 60° natural channel.

A correction for sinuosity was made based on the difference in errors for the different sinuosities at higher values of y'. The prediction for sinuosity 2.04 needs to be reduced by about 10%, while for sinuosity 1.37 no adjustment is required.

As for the shape correction factor it was assumed that the non-friction term should be adjusted and that the non-friction component of the zone 2 model. It was found by trial that this can be accounted for by multiplying K_e by another factor, defined by

$$F_2 = s / 1.4 \tag{107}$$

The discharge in the inner flood plain zone is therefore given by

$$Q_2 = W\, y_2\, V_2 \tag{108}$$

with V_2 given by

$$V_2 = \left(\frac{2\ g\ S_o\ L}{(f_2\ L) / (4\ R_2) + F_1\ F_2\ K_e} \right)^{1/2} \tag{109}$$

Preliminary applications of this model showed it to be quite insensitive to estimation of the step height, h. It is recommended that this be approximated by the hydraulic depth (= A/B).

5.5.2 *Empirical Model*

The physically-based model described above is unable to account adequately for the energy losses in the inner flood plain without empirical adjustment based on the SERC Phase B and Aberdeen data. Even then, the errors in predicting discharge over a range of overbank stages are inconsistent for some geometries and there is a case for considering further empirical adjustment. Because of the significant empirical content that would be required anyway, it would be practically expedient to apply empirical corrections to a basic discharge calculated in a simpler way than as required by the previous method.

The simplest empirical approach might be to disregard the horizontal division between the main channel and inner flood plain zones and consider the two together. This would be physically realistic considering the significant interaction and exchange of flows observed between the zones (e.g. Willetts, 1992); the separation of the zones is acknowledged to be rather artificial. However, knowledge of the zonal distribution of the discharge, albeit longitudinally averaged, would be most useful in design applications. The analysis for the main channel zone exposed significant variations of conveyance with stage which, although based on limited data, are significant. This information would be lost in a method which did not separate the zones. Subdivision of the cross-section into the previously defined zones has therefore been retained.

Empirical analysis of the inner flood plain zonal discharge is compromised by the lack of directly measured discharges. Velocity measurements were taken over the flood plains for only five conditions in the SERC Phase B experiments: at two flow depths for each of the 60° trapezoidal and pseudo-natural channels, and at one flow depth for the 110° pseudo-natural channel.

There were no measurements for the rod-roughened flood plains. Where velocities were measured, they could not easily be used to compute discharges over the defined zone. This was because the measuring sections above the plain surfaces and above the main channel did not fit together to provide single, continuous sections across the whole zone. There were therefore no practically usable velocity measurements for this zone. Inner flood plain discharges were estimated by subtracting calculated discharges for the main channel and outer flood plain zones from the total measured discharge. The main channel discharges were calculated using the method developed earlier. The outer flood plain discharges were calculated assuming friction losses only, using the Darcy-Weisbach equation. The friction factors were estimated using the appropriate modified smooth law for the particular experiments, see Section 3.4.

The use of calculated, rather than measured, discharges for analyzing the inner flood plain flows has obvious disadvantages. The method for calculating main channel discharges is based on very limited data from the SERC Phase B experiments only. As discussed in the section on the main channel analysis, only a limited range of stages and channel characteristics were included. There is, as yet, no evidence to confirm that the main channel model applies to the Aberdeen channels, as has been assumed in this analysis. On the other hand, obtaining discharges by calculation enables all the stage-discharge data to be incorporated in the analysis, rather than just the few conditions for which velocities were measured. This makes trends very much easier to detect and provides additional information for interpretation.

The Aberdeen data were included in this analysis because they represent some conditions (an extra sinuosity and different main channel geometry) which were not covered by the SERC Phase B experiments, and which were shown in the development of the physically-based model to be significant.

The basic discharge for the inner flood plain zone was calculated assuming friction to be the only loss mechanism. It was further assumed that the plane separating this zone from the main channel would offer the same resistance as the flood plain surface. An analysis was also done with the separating plane subtracted from the wetted perimeter. This did not reduce the final adjustment required and the simpler calculation was therefore adopted.

The flow in the inner flood plain zone can be expected to be affected by much the same characteristics as that in the main channel. This is supported by inspection of the variables appearing in the physically-based model. The same dimensionless parameters were therefore used. The flow depth was made nondimensional (y') by dividing by the hydraulic depth of the main channel at bankfull, and the cross-sectional shape of the main channel was accounted for by the value of B^2/A.

The data used in the analysis were the overbank stage discharge measurements for the SERC Phase B standard geometries with smooth and rod-roughened flood plains, and the overbank stage-discharge measurements for the Aberdeen trapezoidal channels. The geometric conditions for these sets are listed in Table 23.

For each measured stage the actual and basic inner flood plain discharges were calculated as described above. The ratio of these values (Q_2') defines the adjustment to be applied to the basic discharge. Q_2' is plotted against y' for the SERC Phase B data in Figure 35 and for the Aberdeen data in Figure 36. The numbered points on Figure 35 are calculated directly from the integrated main channel discharges used for deriving the prediction model; the numbers indicate the relevant experiments. These points provide checks on the accuracy of the main channel model for some conditions.

Both Figures 35 and 36 show a clear pattern. For small values of y' there is a rapid increase of Q_2' with y', in which no distinct variation with channel characteristics can be discerned. For larger values of y', Q_2' decreases with y' nonlinearly and at a rate dependent on B^2/A, s and roughness. The ranges of y' less than and greater than 0.2 were treated separately. It would have been difficult to establish relationships between the variables for the SERC data alone because only two sinuosities are represented and the two values of B^2/A are not greatly different. The inclusion of the Aberdeen data contributed considerable supplementary information.

The relationship between Q_2' and y' for y' less than about 0.2 is difficult to quantify because of the limited amount of data and their considerable scatter. Much of the scatter can be ascribed to the procedure used to determine the zonal discharge. At low overbank stages the inner flood plain contribution to total discharge is very small. As it was calculated as a small difference between relatively large quantities, errors can be expected to be significant. For the SERC Phase B data, shown on Figure 35, it is only for the 60° trapezoidal channel that there are sufficient values to define a trend. Data for the other channels suggest a decrease in Q_2' for low values of y' but there are insufficient points to establish the effects of the channel characteristics on the trend. The data for the Aberdeen experiments, shown on Figure 36, also show a distinct and similar trend, but again this is not sufficiently well-defined to quantify the effects of channel characteristics. The data for the 1.215 sinuosity channel are particularly widely scattered and some Q_2' values for very low y' are too high to appear on the graph. As it was not possible to establish multiple correlations, a single straight line was drawn through all the data, passing through the origin to ensure positive adjustment in all cases. This gave the relationship

$$Q_2' = 6.0\, y' \tag{110}$$

For values of y' greater than about 0.2 the relationship between Q_2' and y' is nonlinear and clearly dependent on B^2/A and s. The dependence on f' ($= f_2/f_1$) is questionable. The curves for the 60° crossover angle channels with smooth and rod-roughened flood plains coincide fairly closely, although the measured points suggest that roughness has some influence which is opposite at relatively low and high values of y'. The value of f' varies over the range of y' being considered from about 1.8 to 0.78 for the smooth flood plain cases, and from about 3.1 to 11.9 for the rod-roughened flood plain cases. Considering these variations and the close coincidence of the curves, it would appear that flood plain roughness has negligible effect. However, the curves for the 110° crossover angle channels with smooth and rod-roughened flood plains suggest that roughness has a very considerable effect. It would be extremely difficult to quantify this effect because no two points have the same value of f' and, if roughness is significant, each point actually lies on a different curve. A comparison of the SERC and Aberdeen data suggested that the curve for the rod-roughened case is consistent and that the curve for the smooth case is out of character.

The curves in Figures 35 and 36 can best be represented by an equation with the form

$$Q_2' = a\, y'^{\,b} \tag{111}$$

Values of a and b were determined for each case by plotting the data on logarithmic paper and fitting straight lines through them, as shown in Figures 37 and 38. The resulting values are listed in Table 24.

Visual assessment of Figures 37 and 38 suggests that a depends strongly on s, only slightly and not consistently on B^2/A, and on f' for high sinuosities. As discussed above, the dependence on f' is very difficult to establish. The parameter b depends strongly on B^2/A. The combined dependence of b on s and f' suggested by the data for the 110° channel with smooth flood plains is again problematic and cannot be accounted for without further information. The slope of the line representing this condition was assumed to be inconsistent and disregarded. It could then be assumed that a depends only on s, and b depends only on B^2/A.

The dependence of a on s was determined by calculating the average of the values of a in Table 24 for each sinuosity represented. These are plotted in Figure 39 and the relationship can be described by

$$a = 1.02\ s^{-0.915} \tag{112}$$

The dependence of b on B^2/A was determined in the same way, ignoring the value for Run B39. The average values of b are plotted against B^2/A in Figure 40. The relationship for b is given by

$$b = -0.81\ (B^2/A)^{-0.477} \tag{113}$$

The adjustment factor, as predicted by Equations (110) to (113), is plotted together with the SERC data in Figure 41 and with the Aberdeen data in Figure 42.

The discharge for the inner flood plain zone should therefore be obtained by first calculating a basic discharge using an appropriate resistance equation (e.g. Darcy-Weisbach, Chezy or Manning). For this calculation the wetted perimeter should be equal to the width of the meander belt and the friction factor should be appropriate for the inner flood plain surface. The basic discharge should then be adjusted by multiplying by the **lesser** of

$$Q_2' = 6.0\ y' \tag{114}$$

and

$$Q_2' = a\ y'^{\,b} \tag{115}$$

with

$$a = 1.02\ s^{-0.915} \tag{116}$$

$$b = -0.81\ (B^2/A)^{-0.477} \tag{117}$$

5.6 Formulation zones 3 and 4

The important mechanisms which affect discharge in the outer zones are

1) Friction
2) Shear on the interfaces with zone 2

Unfortunately there was not enough data to evaluate the relative importance of each of these mechanisms. However other authors work tends to indicate that shear on the division lines will be relatively unimportant. Hence flow in the outer flood plain zones is assumed to be solely controlled by friction. The zonal discharges are calculated using an appropriate friction equation with the division lines separating these zones from Zone 2 excluded from the wetted perimeter.

$$Q_3 = A_3 V_3$$

$$Q_4 = A_4 V_4 \tag{118}$$

where

$$V_3 = \left(\frac{8 \; g \; R_3 \; S_o}{f_3}\right)^{1/2}$$

$$V_4 = \left(\frac{8 \; g \; R_4 \; S_o}{f_4}\right)^{1/2} \tag{119}$$

5.7 Boundary shear stresses

Boundary shear stresses were also measured for some conditions during Phase B of the SERC FCF work. These data have been analyzed by Knight et al (1992) and Lorena (personal communication) and form the basis of the provisional recommendations presented here.

There is no simple, general method for predicting boundary shear for inbank flows in meandering channels, but several simulation models have been developed which can be used for this purpose (for example, by Bridge, 1992, and Nelson and Smith, 1989).

For overbank flows, Knight et al have shown that the sectional average boundary shear stress in the main channel is less than would occur at bankfull stage at all cross-sections through a meander wavelength. Sectional average values are insufficient for designing scour protection, however, because the distributions of boundary shear across the sections are not uniform and vary with flow condition. The measured distributions suggest that during overbank flows the shear stress on the main channel banks may be higher than for inbank flows at some locations through the meander. The shear stress on the bed, however, is less than for inbank flows. Design shear stresses for scour protection should therefore be based on inbank flows for the bed and on overbank flows for the banks.

Under overbank flow conditions the bank shear stress on the upstream bank does not exceed 1.6 $\gamma \, y_2 \, S_o$ in any of the measured distributions, where γ is the unit weight of water defined by ρg (9.81 x 10^3 N/m^3). On the downstream bank a high, localised stress concentration was observed downstream of each bend apex, associated with the expulsion of water from the main channel to the flood plain (see Figure 14). This concentration is shown in Figure 43, which presents Lorena's plot of contours of shear stress for the 2.04 sinuosity channel with a flow depth on the flood plain of 50 mm. The concentrations were centred at points between 60° and 70° downstream of the apex section for all the experimental conditions. The maximum observed shear stresses in the concentrations approached 5 $\gamma \, y_2 \, S_o$. The stress concentrations are very localised and decrease rapidly with distance but, because of the limited experimental conditions and consequent uncertainty regarding locations, they should be assumed to be more extensive when designing scour protection. The enhanced shear stresses also extend for some distance over the flood plain on the downstream side of the channel.

For the design of scour protection, it is recommended that boundary shear stresses be determined for the main channel bed and banks for the full range of inbank stages, using currently available methods. In addition, the banks should be able to resist stresses of

$$\tau = 1.6\,\gamma\, y_2\, S_o \tag{120}$$

on the upstream side, and

$$\tau = 5\,\gamma\, y_2\, S_o \tag{121}$$

on the downstream side.

The observed shear stress distributions suggest that the sediment transport capacity in the main channel will be lower for overbank flows than for inbank flows. Net deposition of sediment may therefore occur in the main channel during prolonged flood events. The shear concentrations on the downstream banks during overbank flows suggest enhancement of meander migration in the valley direction during prolonged flood flows, and also corroborate the mechanism of meander cutoff by opening chutes across point bars.

5.8 Summary

Experimental data from Phase B of the SERC FCF has been analyzed to produce two methods for the estimation of discharges in compound channels. The best approach was found to be based on dividing the cross-section into zones and calculating the discharge in each zone independently. The four zones chosen are:

1) The main channel below bankfull level.
2) The floodplain within the meander belt.
3) The floodplain beyond the meander belt on the left bank.
4) The floodplain beyond the meander belt on the right bank.

The zones are illustrated in Figure 44

For a given stage the total discharge will be calculated as the sum of the component discharges, i.e.

$$Q = Q_1 + Q_2 + Q_3 + Q_4 \tag{122}$$

The zonal discharges will be calculated independently, accounting for the appropriate energy loss mechanisms in each.

Zones 3 and 4

The discharges in zones 3 and 4 are assumed to be controlled by bed friction only and are given by Equations 118 and 119.

Zone 1

The loss mechanisms which affect the main channel discharge are complex. It was not possible to develop a physically based description of these mechanisms and an empirical procedure was developed. A correction factor is applied to the bankfull discharge to obtain the variation in the main channel discharge with over bank stage. The form of the correction factor is given by Equations 88, 89 and 90.

Zone 2

Two alternative methods for predicting the discharge in the inner flood plain zone were developed. The first method attempts to account for the principal loss mechanisms using physically-based deterministic formulations. The formulations are based on a very simple conceptual model of the loss mechanisms and required empirical adjustment to account for the additional complexities involved. The model explicitly accounts for bed friction and expansion / contraction over the main channel and is described by Equations 109, 108, 107, 106, and 102.

The second method is purely empirical and follows an approach similar to that used for the main channel zone. A basic discharge is calculated assuming friction losses only, and this is then adjusted to account for the effects of flow interaction with the main channel. The form of the correction factor is given by Equations 114, 115, 116 and 117.

These two approaches to computing the inner flood plain discharges give two separate methods of calculating discharges in meandering compound channels. For convenience the model incorporating the expansion contraction losses will be referred to as the James and Wark method while the empirical procedure for zone 2 will be referred to as the James and Wark 2 method.

Bed shear stresses

Bed shear stress data was measured under overbank conditions during Phase B of the FCF work. The analysis carried out by the investigators is summarised above. The main channel bed shear stresses are reduced during overbank flow compared to bank full conditions. The shear stresses on the floodplains adjacent to the main channel show peak values which are associated with the exchange of flow between the main channel and the flood plain. Equations 120 and 121 give a rough estimate of the likely peak bed shear stresses.

6 Verification of the procedure

6.1 Background

The previous chapter details the development of two new procedures for estimating the conveyance of meandering compound channels. One procedure (James and Wark) includes a semi-empirical model of the inner flood plain flows, while the other (James and Wark 2) is based on a purely empirical approach to the inner flood plain discharge. Other methods were also identified in the literature. The work reported in this chapter was carried out to compare the new and existing methods. A selection of the laboratory data available from various sources described in chapter 3 was obtained and the methods were applied to predict the stage discharge values. In some cases zonal discharges were also measured and these provide a check on the predicted distribution of flows in addition to total discharges.

6.2 Methods

Of the methods listed in chapter 5 the following have been used in this verification:

Bed friction only (BFO)
James and Wark (JW)
James and Wark 2 (JW2)
Ervine and Ellis (EE)

Greenhill 4 (GH4)
Greenhill 5 (GH5)

The James and Wark; Ervine and Ellis and the Greenhill methods are described in detail in chapter 5. The bed friction only method is based on the James and Wark channel subdivision. The discharges are calculated assuming only bed friction is acting and the areas, wetted perimeters and hydraulic slopes for each zone are as defined for the James and Wark method.

6.3 Application to laboratory data

6.3.1 Data

The available laboratory data is reviewed in Chapter 3. Five of the eight available data sets are considered to be of good enough quality for use in the development and verification processes. Two of these sets were used to develop the new procedures (SERC and Aberdeen). The data sets which have been used in this verification work are listed in Table 25 and 26. These are stage discharge data collected under overbank flow conditions. The test numbers have been assigned for ease of data handling. Tables 25 and 26 also list the values of parameters required for the various calculations, such as the width of zones 2 and the whole floodplain; the side slopes of the floodplain edges and radius of curvature of the channel centerline. These are shown on Figure 17. Table 27 lists the values of parameters required when calculating the main channel discharges. θ_m is the mean angle between the channel centerline and the flood plain centreline, averaged over a wave length. This mean angle is required for the Ervine and Ellis calculations. Because most of the geometries were constructed using a combination of straight reaches and circular arcs these parameters were easily calculated. In the case of Sooky's sinusoidal geometry a numerical integration was carried out to determine θ_m.

6.3.2 Total discharge and stage

Each of the above methods were applied to the available data as follows.

1) The predicted discharges were calculated for the measured stages. This allowed the error in the predicted discharges to be calculated according to:

   $\%\text{Error in predicted flow} = 100\,(Q_{calc} - Q_{meas}) / Q_{meas}$

2) The calculated stage discharge curves were then used to obtain calculated stage values by linear interpolation using the measured discharges. The error in the predicted stage was calculated in terms of the depth of flow in the main channel (H) according to:

   $\%\text{Error in predicted depth} = 100\,(H_{calc} - H_{meas}) / H_{meas}$

The mean values of these errors were calculated for each condition. In addition means were calculated over combinations of the data as follows:

1) All SERC data
2) Smooth flood plain SERC data
3) Rod roughened SERC data
4) Vicksburg data
5) Aberdeen data
6) Sooky data
7) All data

Errors in discharges

The mean errors in the predicted discharges for the SERC FCF data are shown in Table 28. The BFO method over predicts by considerable margins with mean errors of 44.8%, 12.3% and 32.5% for the smooth, rough and all the data. The JW method gives errors of less than 5% for all three subsets (-3.3%, -5.3% and -4.0%) although it is tending to under predict. JW2 gave good results for the smooth data, -5.2%, but gave poor results for the rod roughened data, -22.8%, which shows up in a larger error of -11.8% over all of the data. EE also gave reasonable results over both the smooth and rough data with errors of 4.9%, 8.2% and 6.1% respectively. GH4 tends to over predict for the smooth data and under predict for the rough data with errors of -22.5%, -0.2% and 13.9% over all the FCF data. GH5 does reduce these errors slightly to 12.7%, -7.5% and 5.1% overall.

Four of these methods (JW, JW2, GH4 and GH5) were developed based on the SERC FCF Phase B data. It is not surprising that these four methods give good accuracy when applied to this data set. The main conclusion is that the JW method is more accurate than the JW2 method for cases with roughened flood plains. None of the other data was collected with roughened flood plains and so it has been impossible to verify this conclusion against independent information. Future experimental work into conveyance of meandering overbank flow should cover conditions with rough flood plains.

Table 29 gives the mean errors for the various methods over the Aberdeen, Vicksburg and Kiely data sets. It is clear from the Aberdeen and Vicksburg results that the BFO method becomes less accurate for more sinuous channels. In general typical errors of about 30% to 40% were obtained with these data. Both the JW and JW2 methods give very similar results for the Aberdeen data with average errors of 0.6% and 0.8% respectively. This is not surprising since this data was used to develop both of the models for the inner flood plain flows. Again the EE method gave reasonable predictions with a mean error of -2.3%. GH4 and GH5 over predicted discharge by 16.9% and 12.7% respectively. There are too few data for each individual condition of the Vicksburg and Kiely data sets to make any detailed conclusions but it is possible to say that the JW, JW2 and the EE methods gave similar overall predictions.

The application to Sooky's data is summarized in Table 30. Again there are too few data for each individual condition to make any meaningful conclusions but over all 63 data points the BFO method gave a mean error in discharge of 20.8%. The JW and JW2 methods gave errors of -1.9% and 1.2% and the EE method an error of 14.6%. The GH4 and GH5 performed well on this data set with mean errors of -1.4% and 5.2% respectively.

Table 31 summarises the mean errors over the various sub sets and all the data. The BFO method over predicted discharge by 34.1% on average over all the laboratory data available. The JW and JW2 methods generally gave similar results for the smooth data and this is reflected in the mean errors of -2.1% and -4.3% respectively. The EE method gave a mean error of 5.3% and GH4 and GH5 gave mean errors of 11.5% and 8.0% respectively. Given these results Table 32 shows the six methods ranked in order of accuracy of predicted discharge for the various sub sets of the data. It is obvious that the bed friction only method is the worst of all six methods followed by Greenhill's methods 4 and 5 respectively. It is more difficult to distinguish between the best three methods.

The above discussion has concentrated on the mean errors and has ignored the standard deviations (SD) in these means. In general the JW and JW2 methods have SD's of between 5% and 10% for the various sub sets of the data. The Ervine and Ellis method although giving roughly equivalent mean errors shows SD's between 15% and 20%. These quite large standard deviations are not caused by random scatter about the means but are due to systematic trends in the errors with depth, this is discussed in detail below but it is possible to say that the JW and JW2 methods gave slightly more accurate predictions. Over all the data the JW method performed better with a mean error and standard deviation of -2.1% and 9.7% compared to -4.3% and 13.2% for the JW2 method. In addition it has been shown to be more accurate for the data with roughened flood plains, mean error and SD -4.0% and 8.4% compared to -11.8% and 14.4% for the JW2 method.

When considering only those data not used in the development of any of the methods slightly different results are obtained. The JW2 method turned out best with mean error and standard deviation of 1.8% and 10.8%, followed by GH4 (2.0% and 15.6%). The JW method gave slightly worse results at -2.6% and 11.7% respectively. The data from Vicksburg, Kiely and Sooky used here did not cover roughened flood plain conditions and this should be borne in mind when considering the relative merits of the various methods.

Errors in stage

The results shown in Tables 33 to 36 are the mean % errors in calculated depth for the various data sets. In general these results follow the discussion of the errors in discharges with two important exceptions.

1) Where a method over predicts discharge then it under predicts water level.

2) The values of errors in calculated stage are much less than the corresponding errors in discharge.

This can be demonstrated by comparing the values in Tables 31 and 36. The Bed Friction Only method over predicted discharge by 34.1% on average but under predicted the channel depth by 4.7%. Similar comparisons can be made for the other methods.

The variation of errors in predicted discharge and stage for the six methods with relative depth are shown in Figures 45 to 50. Ignoring all losses except bed friction gave errors in the predicted discharges which fall mainly in the range 10% to 50%, with corresponding errors in depth between -10% and -2%. It is apparent from Figure 45 that the errors depend on the geometry of the channel with the various cases displaying different distributions of errors with the depth of over bank flow. In general the errors show strong trends with stage.

The JW method gives a much smaller range of errors, Figure 46. Most of the data falls in the range -10% to 0% for discharge and -2% to 3% for the water depth. At low over bank stages (H-h/H < 0.15) the method tends to over predict discharges with the errors reducing at higher stages.

Figure 47 shows the error distributions for the JW2 method. The majority of the errors in predicted discharge fall in the range -20% to 10% with the corresponding errors in depth lying between 2% and 15%. There are more noticeable trends in the errors for this method compared to the JW method. The rod roughened data (33, 34 and 43) show a strong increase in the under prediction of discharge with depth.

The Ervine and Ellis method gave errors in predicted discharge in the range -30% to 50% with the corresponding errors in water depth lying in the range -8% to 10%, Figure 48. This method tends to over predict discharge (and under predict water level) at low relative depths and under predict discharge at high depths with an approximately linear graduation between. This agrees with the limited number of results quoted by Ervine and Ellis (1987). It is interesting to note from Table 29 that for the data collected from the Vicksburg flume the Ervine and Ellis method is the most accurate of all the methods. Ervine and Ellis only applied their method to the Vicksburg data and reported good agreement.

Figures 49 and 50 show the variation of errors for Greenhill's methods 4 and 5 respectively. Both these methods give variations of error for the various cases which are similar to those obtained with the bed friction only method but shifted towards the zero error line. Greenhill's method 4 shows errors in discharge which are shifted by approximately 20% - 22% while method 5 is gives errors in discharge shifted by about 25 - 27%. Both of these methods display quite wide ranges of errors.

The results above show that the semi-empirical expansion contraction model developed by the authors (JW) is more accurate than the other methods with a mean error that is well within experimental tolerances. The tendency of the method to under predict discharges is a conservative fault. In a design situation a channel is usually sized to have a required discharge capacity at a given water level. The authors method gives a slightly larger channel size than actually required hence water levels will be slightly lower than predicted. The Ervine and Ellis method, which is based on a similar conceptual model, gives a mean error which is probably acceptable in practice but the larger standard deviation indicates a wider and more systematic spread of errors about the mean. The alternative empirical model developed by the authors (JW2) was found to be less accurate when the flood plains are rougher than the main channel and is not recommended. By ignoring the effects of loss mechanisms other than bed friction the above results indicate that errors in total discharges in the order of 35% may be expected. The empirical attempts by Greenhill to reduce these errors do succeed to a limited extent but do not significantly reduce the spread of the errors. The James and Wark method has the additional advantage over the others that it is based on measured velocities and discharges for zone 1, and should give more reliable predictions of the zonal distribution of conveyance. There is limited independent information available on zonal distributions of flow and this is considered in Section 6.3.3.

Sensitivity analysis

The James and Wark method requires values of geometric parameters which are well defined in laboratory channels but usually poorly defined in natural channels. The values of meander wavelength and main channel side slopes (required for the zone 2 model) in particular are difficult to define exactly for natural channels. The following sensitivity analysis was carried out to determine the degree of precision required when estimating these parameters in practice.

The values of the wave length (L) and side slopes (S_s) for the available laboratory data are known exactly. Errors in the predicted discharges are not due to uncertainties in L or S_s but to other causes. The effects of uncertainties in L and S_s were investigated as follows.

The known values of L and S_s for all of the available data were factored up or down by fixed amounts. The JW method was applied using these factored values of L or S_s in the calculation. The mean errors in predicted discharge were calculated over all 279 data points. Thus the variation in errors could be related to the known errors in L or S_s.

The effect of uncertainties in wave length are summarized in Table 37. The mean error in the predicted discharges is reduced from -2.1% to -10.3% by the 50% reduction in wave length and increases to 2.3% for a 50% increase in wave length. Thus an error in wave length of ±50% results in a ±10% change in the mean error in predicted discharge. Similar results are shown in Table 38 for changes in side slope. The mean error is reduced from -2.1% to -5.3% by a 100% reduction in side slope and increases to 2.4% for a 100% increase in side slope. Thus changes of ±100% in side slope values results in a ±5% change in the mean error. These results, although not conclusive, indicate that predicted discharges are relatively insensitive to errors in wave length and main channel side slope and great accuracy in their estimation is not necessary. However similar sensitivity test should be carried out in any practical application to confirm these findings.

6.3.3 Discharge distributions

The results above demonstrate the overall accuracy of the various methods. The methods are based on similar channel subdivisions. The discharges in the various parts or zones of the channel are calculated separately and summed together to obtain the total discharge. Hence the methods give the distribution of flow between the zones in addition to the total discharge.

There is very little independent information available on the distribution of discharge in meandering overbank flow. Sooky (1966) carried out detailed velocity measurements in shallow (403, depth 0.0613 m) and deep (409, depth 0.080 m) meandering channels which were otherwise identical. These experiments were carried out in a channel which was built at a scale approximately 8-9 times smaller than the SERC FCF Phase B geometries. Sooky integrated these velocity measurements to obtain the proportion of the total discharge within each zone. Kiely (1989) gives similar information for two depths (Test 301, 0.060m and 0.080m). The measured discharges in all four zones for these four cases are given in Table 39. Table 40 gives the errors in the predicted discharges for these four cases. The BFO method over predicts by up to 50% while the JW method gave results accurate to within ±10%, the JW2 was accurate to ±17%, EE 30% and Greenhill's two methods to 30%. The JW method gave very good overall accuracy for Kiely's data while none of the methods were particularly accurate for Sooky's two conditions. The main reason was probably a poor definition of bed friction for Sooky's data.

Table 41 shows the measured and calculated distribution of flows between the various zones as percentages of the total discharge. The results obtained for Sooky's data show little difference between the various methods, they all give similar distribution of flows. This may be a function of the very low sinuosity of Sooky's channel. Kiely's results show more differences between the methods. The JW method gives excellent predictions of total discharge (within 4% and 1%). At the lower depth the JW method gives the distribution of flows almost exactly but under predicts the zone 1 discharge for the higher depth, this is coupled with a general over prediction for the other zones. The JW2 method gave similar results to the JW method for the flow distributions. It gave excellent results for the smaller depth case and under predicted the main channel discharge for the deeper case. In fact all the methods under predict the zone 1 discharges for the deeper case and this would indicate that the bed friction law is a better fit to the data at low stages. The EE and the two GH methods over predicted the zone 1 discharge and under predicted the zone 2 discharges.

These measured distributions of flow were derived from integrating point velocity measurements and the derived zonal flows are probably accurate to about 5%. The comparisons show that in general both the JW and JW2 methods give flow distributions which agree with the measured distributions. On the basis of this very limited data it can be concluded that the author's method (JW) gives superior predictions of both the total and zonal flows in meandering compound channels. It is hoped that future experimental work will concentrate on the collection of data giving the zonal distribution of discharges to confirm these conclusions.

6.4 Application to straight laboratory data

The SERC FCF work has been carried out in two phases. Phase A dealt with straight compound channels and Phase B dealt with meandering compound channels. The Phase A data has already been used to develop a method of calculating conveyance in straight compound channels, Ackers (1991). The work reported in Chapter 2 demonstrates that these straight channel methods cannot be used to predict discharges in meandering compound channels.

The James and Wark method was developed based on the Phase B data. The independent data available for verification included : the Vicksburg data with sinuosities of 1.57, 1.40 an 1.2; Kiely's data with sinuosity 1.22 and Sooky's data with sinuosity of 1.09. The authors method gave reasonable predictions for all of these data. Since the straight channel methods are known to give inaccurate predictions for meandering channels it is to be expected that the meandering channel methods will give poor predictions of discharge in straight compound channels.

The performance of the James and Wark method applied to data from straight compound channels has been investigated. The Phase A data set was available and was used in this evaluation along with the straight channel data available from the Aberdeen flume (100) and Kiely's results (300). The details of the various tests and results from Phase A are reported in full by Ackers (1991). Of the Phase A data tests 1, 2, 3, 5, 7, 8, 9, 10 were used in this evaluation, a total of 198 data points were available. The appropriate modified smooth law (section 2.3) or the Ackers rod roughness method were used to obtain the bed friction factors.

When applying the meandering channel methods to straight channel data the inner flood plain zone disappears. Zone 2 has the same width as the main channel and it was assumed that the zones 1 and 2 could be considered as a single unit. The channel division therefore has reduced to the straight channel division method (DCM2) described in Chapter 2.

The James and Wark method gave an average error in predicted discharge of -27.3% with a standard deviation of 17.0%. This general under prediction of discharges by up to 50% demonstrates that although the method can accurately predict discharges in channels with sinuosities as low as 1.09 it cannot be applied to straight compound channels. Obviously further work is required to investigate the conveyance of compound channels with sinuosity between 1.0 and 1.09.

6.5 Application to field data

The procedure presented above was developed and verified using laboratory model data. There is very little field information available regarding the performance of full scale meandering channels with flood plains. The only detailed field investigation known at present was carried out on the River Roding in Essex, see Sellin and Giles (1989) or Sellin et al (1990). One other site is also currently being investigated by Sellin. A physical model of a 250m long section of the River Blackwater in Hampshire has been constructed in the

SERC FCF at a scale of 1:5. Field measurements are scheduled to commence in early 1993 and are to run for three years. The results of this study were not available at the time of writing but should provide improved validation data.

The Roding study

The Roding is a relatively small river with a channel width and depth of about 7m and 1.5m respectively. Full details of the field and laboratory measurements carried out on this site are available in Sellin and Giles (1988) and Sellin et al (1990). The study reach lies downstream of Abridge and as part of a flood alleviation scheme a two stage channel was formed by excavating approximately 30m wide berms on either side of the main channel, Figures 51 and 52. The original channel was untouched and remained in the natural state with a bankfull capacity of approximately 3 cumecs. The resulting flood channel has a low flow channel which meanders within the berm limits with a sinuosity of 1.38 and a wave length of approximately 96m. Hence the channel does not possess outer floodplain zones. The berms were formed at a level below the surrounding floodplain and were intended to provide extra flood discharge capacity and so relieve flooding on the existing floodplain for flows with a return period of up to thirty years. Shortly after completion of the scheme it became clear that the actual capacity of the channel was less than the design value. This was partly assigned to the difference between the assumed berm vegetation (short grass) and the actual vegetation which was extremely dense. The design case assumed that the berm would be grazed by farm animals but in fact this did not happen and the National Rivers Authority (NRA) were forced to cut the growth mechanically at considerable cost.

The field and laboratory projects investigated the effects of different maintenance policies on the channel capacity. Most of the conditions investigated were with the flood berms covered, totally or partially, with extremely dense vegetation and verification of calibrated bed roughness values was not possible. The roughness values varied strongly both with stage and during the growing season. The data recorded after a full cut on the berm showed much less variation in berm roughness values and so were felt to provide the best information for validation of the author's procedure. The method was applied to the stage-discharge data from the following two cases.

P2 The berm growth was cut immediately after the summer growing season and so the berms were covered in short grass.

M2 The laboratory model data corresponding to the smooth berm case (P2 on the prototype).

In order to apply the procedure to these measurements the seven available surveyed sections were used to provided reach averaged areas, widths etc for both flow zones at stages up to 1.0m above the berm level and these are given in Table 42. The information provided by Sellin and Giles (1988) and Sellin et al (1990) combined with widely accepted guidelines, Chow (1959) and Henderson (1966) allowed the berm Manning's n values for the two cases, P2 and M2 to be estimated as 0.050 and the main channel Manning's n was estimated as 0.044. The longitudinal slope of the berm was 1.405×10^{-3}.

The mean errors in the predicted discharges given by the BFO, JW and JW2 methods are shown in Table 43. It is apparent that the recommended method (JW) improves the overall accuracy of the predicted discharges to about -2% and that by ignoring the non-friction head losses discharge will be over-predicted by about 10% on average. The empirical JW2 method gave very poor predictions resulting in a mean error of approximately -30%. These results are confirmed by Figure 53, the JW and BFO methods give stage discharge curves which follow the general trend of the data. The JW method tends to under predict discharge at low flood plain depths and over predict at high flood plain depth, while the BFO method over predicts for all stages.

Some sensitivity tests were carried out to investigate the effect of berm roughness on the total channel capacity. Table 44 shows the variation of mean errors in predicted discharges, for the BFO and JW methods, with berm roughness for case P2. Both methods over-predict discharges with low berm roughness and under-predict with high berm roughness. The author's method always gives smaller discharges because the non-friction energy losses in the two zones are explicitly accounted for. The difference between the mean errors for the two methods reduces from >100% at very low roughness to about 10% at the calibrated roughness. At higher roughnesses the difference between the two methods remains approximately constant at about 10%.

These results show that as the floodplain becomes smoother the two methods diverge more. Thus the effect of increased flood plain roughness is to make the non-friction head losses less important. Bed friction is likely to be the most important single source of energy loss in natural rivers and remains a potential source of significant error in conveyance predictions. The estimation of bed friction factors is largely subjective even given the comprehensive guidelines presented in standard texts such as Chow (1959) and Henderson (1966). Thus it is not possible to give general guidelines on the choice of bed friction value as site specific aspects are likely to govern the relative importance of the various loss mechanisms. Tests should be carried out for each application to gauge the sensitivity of the solution to variations in roughness values.

6.6 Summary and conclusions

The two methods developed by the authors and four other methods have been used to predict discharges and stages for the available laboratory data. The author's semi-empirical method (JW) was found to give the most accurate predictions of total discharge and acceptable predictions of the distribution of discharges.

The available data used in this verification covered a limited range of conditions. Further experimental work is required to look at both total discharges and the distribution of discharges for:

a) Meandering channels with low sinuosities (<1.09).

b) Meandering compound channels with rough flood plains.

c) Low over bank depths (y'< 0.2).

The sensitivity of the James and Wark method to variations in the values of both meander wave length and main channel side slope has been investigated. The results indicate that in great precision in estimating these values is not required.

The procedure has been applied to the best field data available and has been shown to give improved predictions compared to current practice. The sensitivity of the results to variations in bed roughness value has been investigated. The non-friction energy losses are shown to be less important as the floodplain is roughened. Bed friction remains the most significant source of energy loss in rivers with overbank flow.

7 Future research needs

The future research which still remains to be carried out falls into three main categories:

1) The collection of independent information to use in verifying the work presented in this report. This includes laboratory studies and field measurement programmes.

2) The development of two and three dimensional numerical models and their application to the available laboratory data.

3) The use of the procedures developed in this report within one dimensional river models has not been fully considered. The procedures were developed to model steady state stage discharges and the type of work required to confirm that the methods are appropriate for use in 1-D models is described below.

7.1 Stage-discharge prediction for inbank flows

The current project has put a low priority on inbank flows. It is clear, Chapter 4, that the effect of meandering on inbank channel conveyance is considerable, and the importance of main channel capacity in a two-stage channel design or analysis is obvious.

The SCS and LSCS methods of adjusting the friction factor to account for meander effects has been shown to be reasonable. They have no theoretical basis, however, and suffer from the main limitation of relating bend energy losses to only one parameter. In order to circumvent these limitations it is recommended that Chang's (1984) approach be further developed to provide simple guidelines for estimating losses that account for a wide range of all the relevant parameters, Chapter 4. The guidelines should allow losses to be evaluated for individual bends as well as for a meander train. The effect of variation of cross-section along the channel should also be investigated, but this would require a more complete description of flow in bends.

7.2 Laboratory studies

7.2.1 Extension of existing data sets

Existing laboratory studies cover a relatively narrow range of conditions. Further laboratory work would be required either to verify or extend the present method for conditions other than those covered by the existing data. In particular the following list of experiments would fill gaps in the available laboratory data. It should be noted that this list is not in any particular order or importance.

1) Undertake experiments to measure stage-discharge, velocity and bed shear stresses for meandering channels with sinuosities between 1.0 and 1.09. This is important because there is a need to establish at what sinuosity a compound channel analysis treatment should switch from straight to meandering.

2) Undertake experiments to measure stage-discharge, velocity and bed shear stresses for low overbank stages, ie (y_2/h) values between 0.0 and 0.1. There are few data points in this region and it is probably the most common range of overbank flow conditions which occur in nature.

3) Undertake experiments to measure stage-discharge, velocity and bed shear stresses for flood plains with transverse slope away from the main channel. There are few laboratory data for this condition and natural flood plains tend to slope laterally in this manner. There is some conjecture that it may be more realistic to analyze overbank flow in these geometries using straight channel techniques, as the flow will be constrained parallel to the main channel.

4) Undertake experiments to measure stage-discharge, velocity and bed shear stresses for sinuosities between 1.09 and 1.20; 1.20 and 1.40; 1.40 and 2.01 and for sinuosities greater than 2.01. All known laboratory experiments have been carried out at or very close to sinuosities of 1.09, 1.20, 1.40 and 2.01 and this is obviously leaves gaps in the available information.

5) Undertake experiments to measure stage-discharge, velocity and bed shear stresses in meandering channels for a range of channel to flood plain widths and for cases with asymmetric flood plains on either side of the main channel. All existing data have been collected for a limited range of channel to flood plain width ratios and with symmetric flood plains.

6) In order to confirm the SERC Phase B data it would be useful to conduct experiments in small scale flumes with geometries which are exact scale models of the phase B tests. If such experiments were carried out and proved to be positive then the gaps in the Phase B results could be filled using data collected in much smaller laboratory facilities.

7) Undertake experiments to measure stage-discharge, velocity and bed shear stresses in meandering channels with roughened flood plains. The only information currently available was obtained from the SERC FCF for only two channel sinuosities. The method of using vertical dowel rods to roughen the flood plain also produced extreme flood plain roughnesses. Independent information is required to confirm the SERC FCF data.

8) Undertake experiments to measure stage-discharge, velocity and bed shear stresses in meandering channels with different cross-sections. The SERC FCF phase B investigation covered trapezoidal and pseudo natural cross-sections. Other studies have been conducted either with rectangular or trapezoidal main channel cross-sections. Further information on the effects of varying channel side slopes in trapezoidal channels and the effects of changes in cross-section shape along a meander would be useful.

Laboratory work intended to extend existing information should be carried out in channels with idealized geometries similar to those from which the existing laboratory data were obtained. For example the flood plains should be uniform in width along the length of the channel and the meandering main channel plan geometry should be a simple repeating geometric shape.

7.2.2 Laboratory studies of loss mechanisms

The formulation of models of loss mechanisms has exposed some surprising gaps in experimental results. Some useful information could be obtained from relatively simple and inexpensive laboratory studies. The following studies would contribute to the descriptions of losses in the identified flow zones :

1) A quantification of contraction loss over an upward step.

2) A study of the effect of slot alignment on expansion and contraction losses.

7.3 Field data collection

The lack of adequate and reliable field data has been a major constraint in the verification of analysis methods for meandering compound channels. The method presented is based on results from laboratory experiments and while this is appropriate because of the high degree of control of the relevant variables required, the correspondence between laboratory and field conditions is not firmly established. The relative importance of different energy loss mechanisms may change with scale. Some information was available from the River Roding study (Sellin and Giles, 1988) and provided good initial verification of the findings reported above. However further field data should be sought to fully verify methods of estimating conveyance in meandering channels.

The River Blackwater study which combines laboratory and detailed field measurements will provide a useful data set to compare many of the details of the method. It is proposed to make measurements of stage discharge and point velocity distributions, both in the laboratory and the field. This research programme is planned to take place over three to four years and will provide a good deal of detailed information on flow distributions between the various zones in particular cases.

7.3.1 Strategy for field data collection

It is apparent that the analysis method has not yet been fully verified against field data because very few relevant field measurements have been made. Given that it is desirable to collect more field data it is important that the correct types of information are obtained in order to make the most efficient use of resources.

In general there are two levels of validation possible and these differ in the amount of hydraulic information to be measured at each site.

1) Collect only stage-discharge information at each site.

2) Collect stage-discharges, point velocities, and water levels both along and across the study reach.

Obviously it will be possible to carry out measurements at a larger number of sites if only total discharges are to be measured. This would provide a wide range of data for the validation of the overall method but would not provide information to validate the calculated flow distributions. If the more detailed validation is required then it is likely that fewer sites would be considered due to the increased costs.

It will either be possible to partially validate the overall method on a relatively large number of sites, or carry out more detailed validation on a limited number of sites. The detailed validation would require that at least three or four other projects similar to the Blackwater project be set up and the costs of running these projects over three of four years are likely to be considerable.

Partial validation of the method using stage-discharge data from a wider set of sites would probably be sufficient in the short term combined with the long term aim of collecting sufficient information to carry out full validation over a number of sites.

7.3.2 Suitable sites

Since this document is concerned with meandering compound channels any field data should also relate to meandering channels. The type of reach to be considered for field data collection should conform to the following guidelines.

1) Sites should have significant meanders or bends. The meander zone should form a significant part of the floodplain and the meanders should be distinct and well developed.

2) Sites should preferably have a fairly regular meander pattern. The meander wave length and amplitude should not vary significantly within each site.

3) Land usage, (vegetation etc) on each floodplain should be reasonably uniform.

4) The presence of buildings or other obstructions on the floodplain should not disqualify a site provided that the obstruction has a minor effect of the flow pattern through the site.

In order to carry out any hydraulic calculations relating to a chosen site certain information is required detailing both the plan and cross section geometries.

5) Enough survey data should be available from maps and channel cross sections to estimate both the main channel and floodplain longitudinal slopes. Where the local bed slopes at the site differ from the overall reach slopes both should be given.

7.3.3 Hydraulic data

In order to provide enough validation data for either a partial or a full validation then the following hydraulic data should be measured.

1) Water surface slopes. The important hydraulic slope which controls flow in open channels is the water surface slope. In uniform flow this slope will be equal to the valley or floodplain slope. Water surface slopes should be measured over the reaches of interest. It may be possible to do this relatively easily and cheaply using maximum water level recorders set at intervals along the reach.

2) Pairs of measured stage and corresponding discharge. These should be provided at both inbank and out of bank stages. It may be possible to identify suitable sites which are close to existing inbank gauging stations. Maximum water level recorders would provide stage values with discharges being obtained from the nearby gauging sites. This would probably be the most efficient method of collecting stage discharge data in meandering overbank reaches. In suitable reaches not close to existing gauging stations special arrangements would be required to measure discharge.

3) Velocity profiles. These may be either just in the main channel regions or across the whole channel and floodplain. This would require a cableway to be set up at selected sites in the reach.

To provide information for a partial validation items 1 and 2 above should be measured at as many sites as possible. If a more complete validation is required then item 3 above should also be measured at each site. In the immediate future it is recommended that suitable sites should be identified and, if possible, a partial validation carried out. In the longer term detailed measurements should be sought to add to the data set provided by the Blackwater project.

7.4 Computational modelling

7.4.1 Turbulence modelling

Three dimensional turbulence modelling is the most promising approach for developing methods to describe the complex mechanics of flow in meandering compound channels. It is not envisaged that turbulence models will be used directly for routine design applications, but rather that they could be used in parametric studies to generate general results for incorporation in standard design methods. By following such an approach the results of experimental work (such as the SERC FCF Phase A and B studies) and field studies could be extended and generalized. The procedure would be to calibrate the model on the existing laboratory data and then to use the computational model rather than the laboratory to generate information about a wider range of conditions. Turbulence modelling should be used to complement laboratory studies rather than replace them.

In design applications use of a 3-D flow and turbulence model is unlikely to be practical for the foreseeable future. However useful information may be obtained from a two dimensional, depth integrated model. This type of approach has proved to be useful in the simpler straight channel case, for example the Lateral Distribution Method (LDM), Appendix 2. Development of suitable 2-D models should be encouraged.

7.4.2 One dimensional modelling

Many one dimensional models of river flows exist which are based on the St Venant equations of 1-D flow. They generally use the computational technique of finite differences to solve the St Venant equations and so provide the variation of water level and discharge along a reach of channel. Typically these models are based on the use of pre-computed tables of conveyance which are accessed during the calculations.

Existing methods used to calculate conveyance

One dimensional models require channel cross-sections to be supplied at locations along the river. These cross-sections and other data describing the bed roughness of the channel are then used to calculate the conveyance of each cross-section within the model. Conveyance is a convenient measure of a river's capacity to pass discharge. Typically the methods used to compute conveyance are based on variants of the divided channel or sum of segment methods. These methods are appropriate for straight compound channels but have been found to give poor results when applied to meandering compound channels (Chapter 2). In the case of meandering compound channels the existing conveyance calculation could be replaced with the new procedure reported above.

Inclusion of the new procedure in 1-D models

The new method for calculating stage-discharges in meandering compound channels has a number of implications regarding its use in 1-D river models. Primarily these are changes in the data specification for the cross-sectional data (ie additional data items) and changes to the conveyance calculation procedures.

Data requirements

The data requirements for the new method are slightly greater than those that would currently be specified in existing packages. Modifications to the cross-sectional data inputs would be required to account for additional items such as :

1) sinuosity of the channel
2) meander wavelength
3) main channel side slope
4) pointers to indicate the limits of the inner flood plain meander belt

Where possible reach average values, based on sub-reaches of the model, should be used to specify these additional data items. The sub-reaches are likely to cover a number of cross-section locations in the model and should be selected such that the geometric parameters (main channel side slope, sinuosity and width of meander belt) remain approximately constant throughout the sub-reach. These data items are readily available from a combination of cross-section and plan surveys of the river reach and would not require any additional resources when undertaking a model study.

In unsteady flood modelling, storage on the flood plains can play an important role in the attenuation of flood peaks. In a highly meandering river specifying the flood plain length equivalent to the river length between adjacent cross-section locations may have a tendency to over-estimate the storage area available on the flood plains. This may then lead to errors in the attenuation of a flood wave. It is important therefore to specify the river length and flood plain lengths separately.

Implications for 1-D river models

There are a number of other issues to be considered when using a package with the new method of calculating conveyances. The usual procedure when modelling compound channels is to calibrate firstly for the inbank roughness and then proceed to calibrate the overbank roughness. Analysis of the Phase B data has shown that the inbank discharge falls as the water level moves from inbank to overbank conditions. In existing methods this may lead to large errors in the flood plain roughness as the calibration procedure implicitly assumes that the main channel discharge remains constant at overbank stages. This implies that the calculated main channel flows and velocities will be too high at overbank stages and those on the flood plain will be too low.

This results in incorrect values for the energy and momentum coefficients, which in turn leads to errors in:

1) afflux calculations at structures,
2) shear stress and sediment transport properties and
3) the effective flood wave speed.

A major factor to be considered, should the new hydraulic method for meandering compound channels be incorporated in existing modelling packages, is that the calibration coefficients obtained from earlier model studies may no longer be applicable in the revised versions of the modelling software. The calibrated roughness coefficients (Manning's n, Colebrook-White k_s or Chezy C) would be effectively compound roughness coefficients which take account of surface and form roughness, vegetation, and resistance losses due to meandering. The latter of these is included explicitly in the new hydraulic method and should therefore not be included in the roughness estimates for the channel or flood plain in any revised model. Considerable effort may therefore be required in re-calibrating existing models if further studies were to be undertaken using a revised modelling package.

Recommendations

Due to the lack of field data for meandering compound channels it has been impossible to verify fully the new hydraulic method and it is suggested that the method only be included in 1-D modelling packages for development purposes at this point in time.

The most appropriate development path to follow would be to include the method in a single 'trial' package so that an assessment and evaluation of the method could be made. For ease of application and interpretation of results, it would be desirable for this to be a steady-state backwater package (or steady-state module of an unsteady modelling package) with a switch to enable the method of conveyance calculation to be selected using a number of alternative calculation procedures including the newly proposed hydraulic method. Tests could then be carried out to find the most appropriate method of specifying the data requirements and to make comparisons with measured field data over river reaches with known or observed stage and discharge information.

8 Conclusions

1) A need to disseminate the results of recent high quality laboratory research into straight and meandering compound channels has been identified and HR Wallingford was commissioned to present this research in a form accessible to practising engineers.

2) This report presents work carried out on meandering compound channels and extends earlier work, Ackers 1991, on straight compound channels.

3) Various straight channel methods were applied to field data from straight compound channels. The Ackers method was verified as suitable for use in designing straight compound channels, Section 2.4.

4) Various straight channel methods were applied to meandering overbank data. The performance of these methods was found to be poor with typical mean errors in the range -50% to 50%. These straight channel methods should not be used to estimate flow in meandering compound channels. This confirmed that the development of a new procedure for discharge estimation in meandering compound channels is worthwhile, Section 2.5.

5) A literature search was carried out to identify laboratory and field data collected in meandering compound channels, Chapter 3. The following sets have proved to be of sufficient quality and quantity to be useful in this project.

   Laboratory data: SERC Phase B data; Aberdeen data; Vicksburg data; Kiely data; Sooky data.

   Field data: Roding study

   This study was carried out by Prof Sellin of the University of Bristol for the NRA. Recently he has carried out a laboratory study of the River Blackwater in Hampshire, using the SERC FCF. A three year programme of field measurements is due to commence in early 1993.

These data were not available for the work reported here but will provide good validation in the future.

6) The available laboratory data collected from inbank meandering channels were analyzed and the non-friction losses were found to form between 15% to 40% of the total energy losses. This confirmed that bends can significantly affect the discharge capacity of channels.

7) A literature search was carried out to identify possible sources of energy loss in inbank meandering channels, Chapter 4.

8) The main sources of flow resistance in a channel bend are: bed friction; increased bed friction due to secondary currents and internal energy dissipation due to increased turbulence induced by secondary currents. The flow resistance in a bend depends on bed roughness (f, C n etc); flow depth (y); bend radius (r_c); length of bend (l) or angle of bend (θ, $l = r_c\ \theta$) and the cross-sectional shape of the channel, Section 4.2.

9) Flow resistance in a set of meander bends is likely to differ from the resistance induced by a single bend in an otherwise straight channel. This is due to the interaction (growth and decay) between the secondary currents induced in the individual bends, Section 4.3.

10) Various methods which account for the extra flow resistance were identified in the literature and a selection of methods were applied to the available laboratory data. The methods were evaluated by comparing the mean errors in predicted discharge, Sections 4.4 and 4.5.

11) The SCS method was found to give acceptable results for most practical purposes even though it does not account for the important mechanisms explicitly. An improved version of the SCS method was formulated to remove the undesirable step function (LSCS) and this linearized version gave better predictions, Section 4.5.

12) Although these methods, which adjust Manning's n based on the channel sinuosity, gave acceptable results they are empirical and their generality is not assured. Chang's approach in explicitly modelling the resistances due to secondary currents combined with backwater calculations along the channel is based on sound theoretical considerations and is applicable to both single bends and series of meanders.

13) A literature search was carried out to summarize the current state of knowledge on the detailed flow structures present during overbank meandering flow and to gauge the effect these might have on the discharge capacity, Section 5.1.

14) The internal structure of currents during overbank flows has been found to be highly complex, Figure 14. The most important observations are:

    A) The longitudinal velocities below bankfull tend to follow the main channel side walls while the floodplain velocities are generally in the valley direction. Thus the floodplain flows pass over the main channel and induce a horizontal shear layer.

    B) The energy loss due to secondary currents in the main channel is greater than for an equivalent simple channel and the currents rotate in the opposite sense compared to inbank flows.

C) Fluid passes from the main channel onto the flood plain and back into the main channel in the following meander bend. Hence the proportion of discharge passed by the main channel and flood plain varies along a meander wavelength. These bulk exchanges of fluid between slow and fast moving regions of flow introduce extra flow resistance.

D) Flows on the flood plain outwith the meander belt are usually faster than those within the meander belt. It would appear that the extra flow resistance induced by the meandering main channel has a relatively small effect on the outer flood plain.

15) Various methods were identified in the literature for estimating conveyance in meandering compound channels. The most promising ones were proposed by: Ervine and Ellis (1987) and Greenhill (1992). The most appropriate channel sub division is based on a horizontal plane at bankfull level, Section 5.2, Figure 17.

16) The detailed data available from Phase B of the SERC FCF were used to develop procedures which describe the flow resistance in each of the zones.

17) The discharge within the main channel zone was found to vary along a meander wave length. The maximum discharge is found at the bend apices and reaches a minimum at some point in between. The corresponding discharge in the inner flood plain zone will also vary, being minimum at bend apices. The pattern of the variation varies with plan geometry and flood plain depth, Section 5.4.

18) These variations in discharge along the channel have been ignored in the analysis and the mean discharge in the main channel was used in all subsequent analysis and modelling, Section 5.4.

19) The discharge in the main channel was found to vary with flood plain depth compared to the bankfull flow. For low overbank depths ($y'<0.2$) the main channel discharge reduces, the rate of reduction appeared to be independent of the channel geometry. For higher overbank depths ($y'>0.2$) the main channel discharge starts to increase. The capacity of zone 1 was found to depend on sinuosity (s); channel shape (B^2/A) and the relative roughness of the flood plains (f'), Section 5.4.

20) An empirical description of the main channel discharge capacity was developed. The discharge in the main channel (zone 1) is calculated by adjusting the bankfull discharge as calculated using standard methods. The adjustment factor is the greater of the values given by Equations (88) and (89), Section 5.4.

21) The discharge capacity of the inner flood plain was considered in two ways. One procedure is based on a semi-empirical model of expansion and contraction losses. The other method is based on an empirical analysis of the SERC phase B and Aberdeen data sets, Section 5.5.

22) Independent data on expansion-contraction losses over slots (Jasem, 1990) were used to derive corrections to the standard model, for expansion-contraction losses, to take account of channel width to depth ratio and side slope, Section 5.5.1.

23) Main channel cross-section shape and sinuosity were also found to affect the magnitude of the expansion-contraction losses in the inner flood

plains. The Aberdeen data was used to develop correction factors for these parameters, Section 5.5.1.

24) The expansion-contraction (James and Wark) model for the inner flood plain flow is given by Equations (109, 108, 107, 106, 102), Section 5.5.1.

26) Empirical analysis of the inner flood plain discharges shows that at low overbank stages ($y'<0.2$) the inner flood plain discharge increases with depth. At higher overbank depths ($y'>0.2$) the discharge reduces, Section 5.5.2.

27) The empirical description (James and Wark 2) for the inner flood plain flow is given by Equations 114, 115, 116 and 117, Section 5.5.2.

28) The discharges in the outer flood plain zones (3 and 4) are controlled by bed friction only, Section 5.6.

29) The bed shear stress data collected on the SERC FCF has been analyzed in order to provide general guidelines. Bed shear stresses in the main channel during over bank flow are lower than those which occur at bankfull conditions. On the flood plain during overbank flow high concentrations of bed shear stresses have been observed. Equations 120 and 121 give the peak values on up and down stream banks, Section 5.7.

30) The two methods developed by the authors (JW and JW2) and four other methods have been used to predict discharges and stages for the available laboratory data. The authors semi-empirical method (JW) was found to give marginally more accurate predictions of total discharge and acceptable predictions of the distribution of discharges, Section 6.3.

31) The sensitivity of the James and Wark method to variations in the values of both meander wave length (L) and main channel side slope (S_s) has been investigated. The results indicate that great precision in estimating these values is not required, Section 6.3.3.

32) The two models (JW and JW2) have been applied to the best field data available, the river Roding study. The JW method was found to give better predictions of total discharge and is recommended for use in practice, Section 6.5.

33) The sensitivity of the results to variations in bed roughness value has been investigated. The non-friction energy losses are shown to be less important as the floodplain is roughened. Bed friction remains the most significant source of energy loss in rivers with overbank flow, Section 6.5.

34) The James and Wark method was applied to laboratory data collected in straight compound channels. The discharge was underpredicted by 27% on average. This confirmed that the methods developed for meandering compound channels should not be applied to straight compound channels, Section 6.4.

35) It is recommended that the JW method should be used for compound channels with sinuosities greater than 1.02. For sinuosities less than or equal to 1.02 it is recommended that a suitable straight channel method should be used with an appropriate correction for sinuosity, eg Ackers (1991), Section 6.6.

36) The available data used to verify the James and Wark method covered a limited range of conditions. Further experimental work is required to look at both total discharges and the distribution of discharges for :

A) Meandering channels with low sinuosities (<1.09).

B) Meandering compound channels with rough flood plains.

C) Low over bank depths (y'< 0.2)

37) With the currently available data, no further significant improvements of the new method could be achieved. New information must be obtained before any substantial further development of the method is undertaken.

38) The work uncovered some gaps in the existing knowledge and recommendations have been given for further research to improve the current understanding of the mechanics of flow in meandering channels, Chapter 7. The future research which still remains to be carried out falls into three main categories:

A) The collection of independent information to use in verifying the work presented in this report. This includes laboratory studies and field measurement programmes.

B) The development of two and three dimensional numerical models and their application to the available laboratory data.

C) The use of the procedures developed in this report within one dimensional river models has not been fully considered. The procedures were developed to model steady state stage discharges and the type of work required to confirm that the methods are appropriate for use in 1-D models is described below in Section 7.4.

39) Computational modelling including 3-D turbulence and 2-D modelling techniques have been identified as promising methods to use in further development of the understanding of the complex mechanics of flow in meandering compound channels.

40) Before including the new method in general 1-D river models it is recommended that the method is incorporated in a 'trial' modelling package so that a full assessment and evaluation of its performance can be made.

9 Acknowledgements

The work was done during the first author's sabbatical visit to HR Wallingford, for which additional financial support was provided by the Foundation for Research Development and the Murray and Roberts Charles Skeen Fellowship.

The contributions made by Dr Paul Samuels and Dr Nigel Walmsley to the conduct of the project are greatly appreciated. The assistance of Mrs M Johnstone, in collating the Phase B Data sets is gratefully acknowledged. The assistance of The NRA members of the Steering Group is gratefully acknowledged.

The academics and research assistants who carried out the Phase B investigation on the SERC FCF also gave invaluable assistance in collating the available data and provided the project with some results of their own analysis. The assistance of the following is gratefully acknowledged: Prof B B Willetts and Dr R Hardwick (The University of Aberdeen); Prof R H J Sellin and Dr R Greenhill (The University of Bristol); Dr D A Ervine and Dr M L Lorena (The University of Glasgow) and Dr D W Knight (The University of Birmingham).

10 References

Ackers P (1991) The hydraulic design of straight compound channels, Report SR 281, HR Wallingford, October.

Agarwal V C, Garde R J and Ranga Raju K G (1984) Resistance to flow and sediment transport in curved alluvial channels, Fourth Congress, Asian and Pacific Division, IAHR, Thailand, 11-13 September, pp 207-218.

Bridge J S (1992) A revised model for water flow, sediment transport, bed topography and grain size sorting in natural river bends, Water Resources Research, Vol 28, No 4, pp 999-1013.

Corps of Engineers US Army, Waterways Experiment Station, Vicksburg, Mississippi (1956) Hydraulic capacity of meandering channels in straight floodways.

Carling P A (1992) Personal communication.

Chow V T (1959) Open channel hydraulics, McGraw Hill, ISBN 0-07-Y85906-X.

Chang H H (1983) Energy expenditure in curved open channels, Journal of Hydraulic Engineering, Vol 109, No 7, pp 1012-1022.

* Chang H H (1984) Variation of flow resistance through curved channels, Journal of Hydraulic Engineering, Vol 110, No 12, pp 1772-1782.

Chang H H (1988) Fluvial processes in river engineering, John Wiley & Sons, ISBN 0-471-631396-6.

Cowan W L (1956) Estimating hydraulic roughness, Agricultural Engineering, Vol 37, No 7, pp 474-475.

Einstein H A and Banks R B, (1950). "Fluid resistance of composite roughness, Transactions, American Geophysical Union, Vol 31, No 4, pp 606-610.

Ervine D A and Ellis J (1987) Experimental and computational aspects of overbank floodplain flow, Transactions of the Royal Society of Edinburgh: Earth Sciences, Vol 78, pp 315-475.

Ervine D A and Jasem H K (1991) P/ersonal communication

Greenhill R (1992) An investigation into compound meandering channel flow, PhD thesis, Department of Civil Engineering, University of Bristol.

Hayat S (1965) The variation of loss coefficient with Froude number in an open channel bend. Thesis presented to the University of Iowa in partial fulfilment of the requirements for the degree of Master of Science.

Henderson F M (1966) Open Channel Flow, Macmillan.

Holden A P and James C S (1988) Discharge computation for compound channels, The Civil Engineer in South Africa, Vol 30, No 8, pp 371-376.

Horton R E, (1933). "Separate roughness coefficients for channel bottom and sides". Engineering News-Record, Vol 111, No 22, pp 652-653.

HR Wallingford (1988) Assessing the hydraulic performance of environmentally acceptable channels, Report EX 1799, HR Wallingford, September.

HR Wallingford (1991) Phase A & B Flood Channel Facility Manual, Inception Report, HR Wallingford, Report EX 2485 (November)

HR Wallingford (1992) Phase A & B Flood Channel Facility Manual, Interim Report, HR Wallingford, Report EX 2548 (March)

James M and Brown B J (1977) Geometric parameters that influence floodplain flow, Corps of Engineers US Army, Waterways Experiment Station, Vicksburg, Mississippi.

Jasem H K (1990) Flow in two stage channels with the main channel skewed to the flood plain direction, PhD thesis, University of Glasgow.

Kazemipour A K and Apelt C J (1979) Shape effects on resistance to uniform flow in open channels, Journal of Hydraulic Research, Vol 17, No 2, pp 129-148.

Kazemipour A K and Apelt C J (1983) Energy losses in irregular channels, Journal of Hydraulic Engineering, Vol 109, No 10, pp 1374-1379.

Kiely G, Javan M and McKeogh E J (1989) A comparison of turbulence measurements in straight, single meander and multiple meander channels, Int'l. Confr. on Channel Flow and Catchment Runoff, Centennial of Manning's and Kuichling's Rational Formula, University of Virginia, May.

Kiely G (1989) Experimental study of the mechanisms of flood flow in meandering channels, Proc. of the 23rd IAHR Congress, Ottawa, Canada, August.

Kiely G (1990) Overbank flow in meandering channels the important mechanisms, Proc of Intl Conf on River Flood Hydraulics, Wallingford, 17-20 September.

Kikkewa H, Ikeda S and Kitagawa A (1976) Flow and bed topography in curved open channels, Journal of the Hydraulics Division, ASCE, Vol 102, No HY9, pp 1327-1342.

Knight D W and Sellin R H J (1987) The SERC Flood Channel Facility, Journal of the Institution of Water and Environmental management, Vol 1, No 2, pp 198-204.

Knight D W, Yuan Y M and Fares Y R (1992) Boundary shear in meandering channels, Proc. Int. Symp. on Hydraulic Research in Nature and Laboratory, Wuhan, China, November, 1992.

Krisnamurthy M and Christensen B A, (1972). "Equivalent roughness for shallow channels". Journal of Hydraulics Div, ASCE, Vol 98, HY12, pp 2257-2262

Leopold L B, Bagnold R A, Wolman M G and Brush L M (1960) Flow resistance in sinuous or irregular channels, USGS Professional Paper 282-D, Washington, DC, pp111-134.

Lorena M L (1991) Personal Communication

Lotter G K, (1933). "Considerations on hydraulic design of channels with different roughness of walls", Transations, All-Union Scientific Research Institute, Leningrad, Vol 9, pp 238-241.

McKeogh E J and Kiely G (1989) A comparison of velocity measurements in straight, single meander and multiple meander channels, Int'l. Confr. on Channel Flow and Catchment Runoff, Centennial of Manning's and Kuichling's Rational Formula, University of Virginia, May.

Mockmore C A (1944) Flow around bends in stable channels, Transactions, ASCE, Vol 109, pp 593-618.

Myers W R C (1991) Personal communication

National Rivers Authority (1991) Design Method for Straight Compound Channels, R&D Note 44, NRA.

Nelson J M and Smith J D (1989) Flow in meandering channels with natural topography, in River Meandering, Ikeda S and Parker G (Eds), American Geophysical Union, Water Resources Monograph 12, pp 69-102.

Onishi Y, Jain S C and Kennedy J F (1976) Effects of meandering in alluvial streams, Journal of the Hydraulics Division, ASCE, Vol 102, No HY7, pp 899-917.

Posey C J (1976) Computation of discharge including over-bank flow, Civil Engineering, ASCE, pp 62-63.

Prinos P and Townsend R D (1983) Estimating discharge in compound open channels, in Proceedings of the 6th Canadian Hydrotechnical Conference, Ottawa, Canada. R D Townsend (Ed), vol 1, pp 129-146.

Ranga Raju, K. G. (1970). Resistance relations for alluvial streams, La Houille Blanche, No 1.

Ramsbottom D M (1989) Flood discharge assessment, interim report, Report SR 195, HR Wallingford, March.

Rouse H (Ed) (1950) Engineering Hydraulics, John Wiley and Sons, New York.

Rozovskii I L (1957) Flow of water in bends of open channels, The Academy of Science of the Ukraine SSR, translated from the Russian by the Israel Program for Scientific Translations, Jerusalem, Israel, 1961.

Scobey F C (1983) The flow of water in flumes, US Department of Agriculture, Tech Bull No 393.

Sellin R H J and Giles A (1988) Two stage channel flow, Final Report for Thames Water Authority, Department of Civil Engineering, University of Bristol.

Sellin R H J and Giles A (1989) Flow mechanisms in spilling meander channels, Proceedings, 23rd Congress, 1AHR, Ottawa, August 1989.

Sellin R H J, Giles A and Beesten D P (1990) Post-implementation appraisal of a two stage channel in the river Roding, Essex, Jrnl IWEM, 1990, 4, April.

Smith C D (1978) Effect of channel meanders on flood stage in valley, Jrnl Hydr Div, ASCE, Vol 104, HY1, pp 49-58.

Soil Conservation Service (1963) Guide for selecting roughness coefficient 'n' values for channels, US Department of Agriculture, Soil Conservation Services, Washington.

Sooky A (1964) The flow through a meander floodplain geometry, Ph D Thesis, Purdue University, (65-2647), University microfilms Inc, Ann Arbor, Michigan.

Stein C J and Rouve G (1988) 2D-LDV-Technique for measuring flow in a meandering channel with wetted flood plains - a new application and first results, Proc Intl Conf on fluvial hydr, Budapest, June 1988.

Stein C J and Rouve G (1989) 2D depth-averaged numerical predictions of the flow in a meandering channel with compound cross section, Hydrosoft, 1989, Vol 2, no. 1.

Toebes G H and Sooky A (1967) Hydraulics of meandering rivers with floodplains, Jrnl WW and Har Div, ASCE, Vol 93, WW2, pp 213-236.

Wark J B, Samuels P G and Ervine D A (1990) A practical method of estimating velocity and discharge in compound channels, Proc of Intl Conf on River Flood Hydraulics, Wallingford, 17-20 September.

Wark J B, Ramsbottom D M and Slade J E (1991) Flood discharge assessment by the lateral distribution method, Report SR 277, HR Wallingford.

Wark J B (1993) Overbank flow in straight and meandering compound channels, ph.d Thesis, The University of Glasgow, Under preparation.

Willetts B B, Hardwick R I and MacLean A G (1990) Model studies of overbank flow from a meandering channel, Proc of Intl Conf on River Flood Hydraulics, Wallingford, 17-20 September.

Willetts B B and Hardwick R I (1991) Personal Communication

Willetts B B (1992) The hydraulics of overbank flow in meandering rivers, Seminar on Multiple Stage Channels, HR Wallingford Ltd., Wallingford, UK.

Wormleaton P R, Allen J and Hadjipanos P (1982) Discharge assessment in compound channel flow, Journal of the Hydraulics Division, ASCE, Vol 108, No HY9, pp975-994.

Wormleaton P R and Merrett D J (1990) An improved method of calculation for steady uniform flow in prismatic main channel/flood sections, Journal of Hydraulic Research, Vol 28, No 2, pp157-174.

Yen B C and Yen C L (1983) Flood flow over meandering channels, Proceedings, Rivers '83, River Meandering, ASCE, pp 554-561.

Tables

Table 1 River channel and floodplain widths

Rivers	Site	BT	Bmc	Bfp	Slope	Qb
Blackwater	Blackford	72.0	6.0	66.0	1.60×10^{-3}	8.50
Main 6	Section 6	27.5	13.7	13.8	1.906×10^{-3}	12.75
Main 14	Section 14	26.3	12.8	13.5	1.906×10^{-3}	16.06
Ouse	Skelton	68.5	54.0	14.5	1.46×10^{-4}	250.20
Severn	Montford	125.0	35.0	90.0	1.95×10^{-4}	183.30
Tees	Low Moor	186.0	56.0	130.0	8.00×10^{-4}	266.20
Torridge	Torrington	120.0	30.0	90.0	1.45×10^{-3}	190.00
Trent	N. Muskham	180.0	72.0	36.0	3.20×10^{-4}	389.60

Notes

1 All dimensions in metres
2 B total width of channel and floodplains
3 Bmc total width of channel at bankfull
4 Bfp total width of floodplains (Bt - Bmc)
5 Qb bankfull discharge

Table 2 River channel depths and roughness values

River	BFSTGE	h	Hmax	Authors Estimate nb	Authors Estimate nfl	nfr	Ackers Estimate nb	Ackers Estimate nfl	nf
Blackwater	1.70	1.70	3.58	0.046	0.094	0.099	-	-	-
Main 6	0.90	0.90	2.20	0.032	0.040	0.040	0.030	0.050	0.050
Main 14	0.92	0.92	2.00	0.0278	0.040	0.040	-	0.02	0.020
Ouse	4.30	8.85	9.94	0.0448	-	0.060	-	-	-
Severn	4.09	5.75	7.75	0.031	0.025	0.045	0.0307	0.0338	0.0338
Tees	8.50	4.36	6.67	0.056	0.100	0.100	-	-	-
Torridge	17.20	2.78	5.29	0.027	0.060	-	0.024	0.026	0.026
Trent	7.60	5.70	8.21	0.032	-	0.032	0.032	-	0.032

Notes

1 BFSTGE Bankfull stage
2 Channel depth at bankfull stage
3 Hmax Channel depth at stage corresponding to the highest surveyed level on the cross-section
4 nb Main channel bankfull Manning's n
5 nfl, nfr Left and riight flood plain Manning's n

Table 3   Mean errors for straight field data

Data Set	A		B		C		D	
NOP	127		118		77		68	
	M	SD	M	SD	M	SD	M	SD
Authors' n values								
LDM	1.2	6.7	1.2	6.8	0.7	5.2	0.7	5.2
DCM	-1.0	6.6	-1.0	6.7	-0.4	4.5	-0.3	4.4
SCM	-11.9	15.6	-12.6	15.9	-10.9	17.5	-12.1	18.2
SCM2	-17.6	20.3	-18.7	20.6	-12.8	19.8	-14.1	20.6
SCM3	8.1	11.9	8.0	12.2	6.1	9.6	5.8	9.9
SCM4	-18.2	20.6	-19.3	20.9	-13.3	20.4	-14.7	21.2
SCM5	-12.9	16.2	-13.8	16.5	-10.8	17.5	-12.0	18.2
SSGM	8.1	11.9	8.0	12.2	6.1	9.6	5.8	9.9
DCM2	1.0	7.4	1.1	7.5	0.1	6.6	0.3	6.7
FCFAM	-4.4	8.4	-4.2	8.0	-2.8	6.8	-2.2	5.5
Ackers' n values								
LDM	5.0	6.9	4.5	6.6	5.5	4.9	4.6	3.9
DCM	2.2	7.4	1.5	7.0	3.5	5.0	2.5	3.8
SCM	-15.0	13.1	-16.9	11.4	-17.2	12.5	-20.9	7.4
SCM2	-20.5	16.9	-22.8	15.0	-19.4	13.9	-23.3	8.9
SCM3	14.0	9.6	13.4	9.5	14.4	5.4	13.3	4.3
SCM4	-20.7	17.0	-23.1	15.0	-19.4	13.9	-23.3	9.0
SCM5	-16.3	13.4	-18.4	11.4	-17.8	12.8	-21.5	7.8
SSGM	14.0	9.6	13.4	9.5	14.4	5.4	13.3	4.3
DCM2	5.0	6.8	4.6	6.6	5.3	4.9	4.6	4.1
FCFAM	-2.8	7.6	-3.4	6.8	-2.0	6.3	-3.1	4.5

Notes:

1 NEV = 0.16 in LDM 2M - mean SD - Standard deviation in mean

3 Error = $100^*(Q_{Calc} - Q_{meas})/Q_{meas}$

4 The data for the Severn and Trent has been smoothed using running averages of three consecutive data points

5 Means taken over following subsets of available stage discharge data:

A Blackwater, Main 6, Main 14, Ouse, Severn, Tees, Torridge, Trent

B As A with Ackers estimate of Bankfull Stage for Torridge

C Severn, Torridge and Trent only

D As C with Ackers estimate of Bankfull Stage for Torridge

Table 3a Mean errors for Myers lab data

	M	SD
LDM	0.2	7.2
DCM	-1.0	6.8
SCM	-13.2	6.3
SCM2	-13.2	6.3
SCM3	5.7	7.2
SCM4	-13.2	6.3
SCM5	-13.2	6.3
SSGM	5.7	7.2
DCM2	1.7	7.7
FCFAM	-5.2	5.2

Notes

1. NEV = 0.16 in LDM
2. M - mean SD - Standard deviation in mean
3. Error = $100^*(Q_{Calc} - Q_{meas})/Q_{meas}$
4. This Data was obtained from series A and F of Myers lab data nb =0.01, nf = 0.01, slope = 1.906×10^{-3}, number of observations = 20.

Table 4 Mean errors for each straight field site

SITE	Blackwater		Main 6		Main 14		Ouse	Severn	Tees		Torridge				Torridge[3]		Trent	
METHOD	ACC	SD	ACC	SD	ACC	SD	ACC	SD	ACC	SD	ACC	SD	ACC	SD	ACC	SD	ACC	SD
Authors n values																		
LDM	2.1	6.0	5.0	11.0	3.0	4.7	-3.5	7.9	4.5	3.1	4.9	6.7	-2.2	6.9	-7.1	5.9	5.6	8.4
DCM	3.6	6.1	1.0	9.5	0.6	4.9	-10.9	7.4	2.0	3.0	-0.8	6.3	-4.3	6.7	-8.7	5.7	3.0	8.2
SCM	-29.7	5.3	-8.5	14.8	-9.6	8.5	-12.5	7.5	-26.0	5.8	-14.2	11.4	-10.8	13.1	-24.2	8.2	-16.4	7.0
SCM2	-61.9	3.0	-15.7	12.4	-20.9	12.5	-18.0	7.8	-25.8	5.2	-27.6	18.4	-21.1	24.2	-48.2	10.6	-16.4	7.0
SCM3	39.3	8.5	7.4	12.0	6.8	4.8	5.0	8.4	14.4	3.4	7.0	6.8	-5.9	6.9	1.6	6.4	11.3	8.8
SCM4	-62.6	2.9	-15.9	12.4	-21.4	12.6	-18.2	7.6	-26.6	5.2	-28.6	18.6	-22.0	25.0	-50.0	10.3	-16.4	7.0
SCM5	-39.6	4.9	-10.3	12.3	-11.7	9.7	-13.4	7.6	-25.4	5.8	-15.4	12.8	-12.1	14.7	-27.4	8.7	-16.4	7.0
SSGM	39.3	8.5	7.4	12.0	6.8	4.8	5.0	8.4	14.4	3.4	7.0	6.9	5.9	6.9	1.6	6.3	11.3	8.8
DCM2	3.6	6.1	4.1	12.1	3.2	4.6	-0.2	7.8	5.5	4.1	0.4	6.4	-3.9	6.5	-7.9	5.7	3.4	8.2
FCFAM	-11.4	10.3	-6.9	9.9	-11.0	10.8	-0.4	7.8	-3.1	3.0	-8.9	8.0	-9.3	10.6	-14.1	5.6	-2.2	8.4
Ackers n values																		
LDM	2.1	6.0	10.0	9.6	7.5	6.7	-3.5	7.9	3.8	2.7	4.9	6.7	9.5	7.4	4.5	6.6	5.6	8.4
DCM	3.6	6.1	6.4	8.6	4.0	5.6	-10.9	7.4	1.8	2.7	-0.8	6.3	8.0	7.3	3.5	6.4	3.0	8.2
SCM	-29.7	5.3	-2.4	15.7	-9.6	8.5	-12.5	7.5	-25.4	5.8	-14.2	11.4	0.4	14.7	-14.7	9.2	-16.4	7.0
S1CM2	-61.9	3.0	-20.8	11.7	-1.0	8.0	-18.0	7.8	-29.5	6.5	-27.6	18.4	-0.6	15.8	-17.1	9.5	-16.4	7.0
SCM3	39.3	8.5	13.1	10.9	10.2	6.5	5.0	8.4	14.3	3.1	7.0	6.8	19.5	7.5	15.1	7.2	11.3	8.8
SCM4	-62.6	2.9	-21.9	11.6	-1.5	8.0	-18.2	7.6	-29.5	6.5	-28.6	18.6	-0.7	15.8	-17.1	9.5	-16.4	7.0
SCM5	-39.6	4.9	-6.7	10.7	-7.6	8.6	-13.4	7.6	-26.4	6.0	-15.4	12.8	0.2	14.9	-15.1	9.2	-16.4	7.0
SSGM	39.3	8.5	13.1	10.9	10.2	6.5	5.0	8.4	14.3	3.1	7.0	6.9	19.5	7.5	15.1	7.2	11.3	8.8
DCM2	3.6	6.1	9.7	11.1	6.5	6.7	-0.2	7.8	5.4	3.5	0.4	6.4	8.4	7.1	4.4	6.5	3.4	8.2
FCFAM	-11.4	10.3	-5.6	8.1	1.1	7.6	-0.4	7.8	-4.1	3.3	-8.9	8.0	3.2	10.0	-1.1	6.0	-2.2	8.4
	NOP		7.		14.		11.		13.		36.		5.		15.		6.	26.

Notes

1 NOP Number of data points at each site

2 ACC = 100*(Qcalc-Qmeas)/Qmeas, SD = Standard Deviation

3 Results using Ackers estimate of bankfull stage

Table 5 Summary of SERC Phase B stage discharge tests

Run No	Angle	Flow Type	X-Sn	FP	FP Config	No of Data Points
B20	60	Inbank	T	S	N/A	17
B21	60	Overbank	T	S	St	16
B25	60	Inbank	N	S	St	10
B26	60	Overbank	N	S	St	16
B31	60	Overbank	N	S	Na	14
B32	60	Overbank	N	R-BB	St	13
B33	60	Overbank	N	R-PD	St	12
B34	60	Overbank	N	R-D	St	18
B38	110	Inbank	N	S	N/A	11
B39	110	Overbank	N	S	St	14
B43	110	Overbank	N	R-D	St	15
B46	110	Overbank	N	R-BB	St	14
B47	110	Overbank	N	S	Na	14
B48	110	Overbank	N	S	W	8

Notes

1 T = Trapezoidal
2 N = Natural
3 S = Smooth
4 R-D = Roughend dowel rods
5 R-PD = Partially roughened dowel rods
6 R-BB = Roughened with breeze blocks
7 St = Standard
8 Na = Narrow
9 W = Walled
10 N/A = Not Applicable

Table 6 Mean errors straight methods meandering data

Method	All Data		Smooth Data		Rough Data	
	Mean Error %	SD	Mean Error %	SD	Mean Error %	SD
DCM	38.5	17.8	44.8	16.2	24.4	12.5
SCM	37.6	56.7	7.7	10.0	104.6	61.0
SSGM	70.1	30.6	69.4	29.9	71.6	32.5
DCM2	41.6	16.8	47.0	15.9	29.3	11.7
FCFAM	24.8	26.0	39.9	14.2	-9.1	8.2
HOR1	30.8	29.0	42.4	21.5	4.6	26.6
HOR2	13.8	23.5	25.5	16.8	-12.3	12.7
HOR3	20.6	23.3	32.9	14.2	-7.0	14.4
HOR4	7.3	23.2	19.5	16.6	-19.8	6.6

Notes

1 % Error = 100*(Qcalc-Qmeas)/Qmeas
2 SD = Standard Deviation in Mean % Error
3 All Data - B21, B26, B31, B34, B39, B43, B47
4 Smooth Data - B21, B26, B31, B39, B47
5 Rough Data - B34, B43

Table 7 Summary of SERC Phase B tests

Run No	Angle	Flow	X-Sn	FP Type	FP Config	S/D	UΘ Chan	UΘ FP	Lev	BS	Turb	Vis	Disp
B20	60	Inbank	T	S	N/A	*							*
B21	60	Overbank	T	S	St	*							
B22	60	D=100mm	T	S	St	N/A	*	N/A	*	*	*		*
B23	60	D=200mm	T	S	St	N/A	*	*	*	*	*	*	*
B24	60	D=250mm	T	S	St	N/A	*	*	*	*		*	
B25	60	Inbank	N	S	St	*							*
B26	60	Overbank	N	S	St	*							
B27	60	D=140mm	N	S	St	N/A	*	N/A	*	*	*		
B28	60	D=165mm	N	S	St	N/A	*	N/A	*	*	*	*	
B29	60	D=200mm	N	S	St	N/A	*	*	*	*	*	*	
B30	60	D=250mm	N	S	St	N/A	*	*	*			*	
B31	60	Overbank	N	S	Na	*							
B32	60	Overbank	N	R-BB	St	*							
B33	60	Overbank	N	R-PD	St	*							
B34	60	Overbank	N	R-D	St	*							
B35	60	D=165mm	N	R-D	St	N/A	*	N/A	*		*		
B36	60	D=200mm	N	R-D	St	N/A	*		*		*		
B37	60	D=250mm	N	R-D	St	N/A	*						

Notes:

1 S/D = Stage-discharge data
2 UΘ = Magnitudes and directions of velocities over test sections
3 Lev = Water surface levels
4 BS = Boundary shear stress
5 Turb = Turbulence data
6 Vis = Flow visualisation tests
7 Disp = Dispersion tests
8 T = Trapezoidal
9 N = Natural
10 S = Smooth
11 R-D = Roughend dowel rods
12 R-PD = Partially roughend dowel rods
13 R-BB = Roughened with breeze blocks
14 St = Standard
15 Na = Narrow
16 W = Walled
17 N/A = Not Applicable
18 In = In main channel only

Table 7 (cont) Summary of SERC Phase B tests

Run No	Angle	Flow	X-Sn	FP Type	FP Config	S/D	UΘ Chan	UΘ FP	Lev	BS	Turb	Vis	Disp
B38	110	Inbank	N	S	N/A	*							*
B39	110	Overbank	N	S	St	*							
B40	110	D=140mm	N	S	St	N/A	*	N/A	*	*	*	*	
B41	110	D=165mm	N	S	St	N/A	*	N/A	*	*	*	*	
B42	110	D=200mm	N	S	St	N/A	*	*	*	*	*	*	
B43	110	Overbank	N	R-D	St	*							
B44	110	D=165mm	N	R-D	St	N/A	*		In				
B45	110	D=200mm	N	R-D	St	N/A	*		In				
B46	110	Overbank	N	R-BB	St	*							
B47	110	Overbank	N	S	Na	*							
B48	110	Overbank	N	S	W	*							

Notes

1	S/D	=	Stage-discharge data	11	R-D	=	Roughened dowel rods
2	UΘ	=	Magnitudes and directions of velocities over test sections	12	R-PD	=	Partially roughened dowel rods
				13	R-BB	=	Roughened with breeze blocks
3	Lev	=	Water surface levels	14	St	=	Standard
4	BS	=	Boundary shear stress	15	Na	=	Narrow
5	Turb	=	Turbulence data	16	W	=	Walled
6	Vis	=	Flow visualisation tests	17	N/A	=	Not Applicable
7	Disp	=	Dispersion tests	18	In	=	In main channel only
8	T	=	Trapezoidal				
9	N	=	Natural				
10	S	=	Smooth				

Table 8 Summary of Aberdeen experiments

Sinuosity	Cross-section	Valley Slope	Test No
1.00	Trapezoidal	0.00100	AB100
1.00	Trapezoidal	0.00071	AB100A
1.21	Trapezoidal	0.00100	AB101
1.40	Trapezoidal	0.00100	AB102
1.40	Natural	0.00100	AB103
2.06	Trapezoidal	0.00062	AB104
2.06	Natural	0.00062	AB105

Table 9 Summary of Vicksburg experiments 2ft wide channel

Test No	Floodway Width (m)	Sinuosity	Meander Belt	Radius of	Assigned Test No
			Width (m)	Curvature (m)	
XII	4.877	1.570	4.420	1.829	201 202 203
XIII	4.877	1.400	3.761	1.865	204 205 206
XIV	4.877	1.200	2.822	2.137	207 208 209
XV	9.144	1.200	2.822	2.137	210
XVI	9.144	1.570	4.420	1.829	211

Table 10 Geometric parameters lab studies meandering channels

Source	L Wave Length (m)	B Channel Width (m)	h Channel Depth (m)	r_c Radius of Curvature (m)	s Sinuosity
SERC FCF	12.000	1.200	0.150	2.743	1.374
	10.310	0.174	0.150	2.743	2.043
Aberdeen	2.570	0.174	0.050	0.413	1.215
	1.909	0.174	0.050	0.413	1.406
	1.154	0.174	0.050	0.307	2.043
Vicksburg	7.315	0.762	0.152	1.829	1.571
	7.315	0.762	0.152	1.865	1.400
	7.315	0.762	0.152	2.136	1.200
Kiely	1.803	0.200	0.050	0.400	1.224
Toebes & Sooky	1.280	0.209	0.038	1.392	1.090
Smith	3.352	0.274	0.076	1.097	1.172
James & Brown	9.144	0.279	0.051	1.143	1.068
Stein & Rouve	6.500	0.400	0.100	1.800	-1.200

Table 11 Non-dimensional geometric parameters meandering channels

Source	L/B	B/h	τ_c/B
Natural Rivers	10.0	10.0	2-3.0
SERC FCF	10.0	8.0	2.3
	8.6	8.0	2.3
Aberdeen	14.8	3.5	2.4
	11.0	3.5	2.4
	6.6	5.0	1.8
Vicksburg	9.6	5.0	2.4
	9.6	5.0	2.5
	9.6	5.0	2.8
Kiely	9.0	4.0	2.0
Toebes & Sooky	6.1	5.5	6.7
Smith	12.2	3.6	4.0
James & Brown	32.8	5.5	4.1
Stein & Rouve	16.2	4.0	4.5

Table 12 Bend losses for 60° meander geometry, trapezoidal cross-section

*Flow Depth (m)	Discharge (m^3/s)	T (°C)	S_o-S_f ($x10^{-3}$)	K	n'/n
0.05932	0.01975	11.4	0.0634	0.0851	1.0477
0.06726	0.02512	11.0	0.0228	0.0312	1.0201
0.07198	0.02654	12.4	0.1039	0.1168	1.0805
0.07714	0.03056	10.8	0.0701	0.0690	1.0524
0.08263	0.03308	12.4	0.1176	0.1146	1.0920
0.08608	0.03630	11.6	0.0882	0.0780	1.0673
0.09170	0.04015	11.5	0.0947	0.0786	1.0279
0.09765	0.04425	11.6	0.1050	0.0824	1.0806
0.10192	0.04708	12.7	0.1203	0.0916	1.0943
0.10302	0.04782	11.5	0.1185	0.0894	1.0930
0.10593	0.05015	11.7	0.1188	0.0868	1.0931
0.10596	0.04974	10.9	0.1252	0.0930	1.0995
0.10680	0.04953	12.4	0.1489	0.1136	1.1219
0.11150	0.05467	13.7	0.1261	0.0869	1.0995
0.11394	0.05702	12.7	0.1163	0.0772	1.0916
0.11900	0.06035	13.6	0.1377	0.0899	1.1110
0.13150	0.07073	12.9	0.1457	0.0867	1.0576
Average:			0.1073	0.0809	1.0782
Standard Deviation			0.0320	0.0262	0.0285

* At cross-over section

Table 13 Non-friction losses for 60° meander geometry, natural cross-section

*Flow Depth (m)	Discharge (m^3/s)	T (°C)	S_o-S_f ($x10^{-3}$)	K	n'/n
0.09957	0.01019	16.1	0.2569	0.6762	1.2329
0.10359	0.01207	16.1	0.2284	0.5202	1.2084
0.10860	0.01442	16.1	0.2130	0.4228	1.1900
0.11225	0.01612	16.0	0.2248	0.4209	1.2040
0.11648	0.01806	16.1	0.2351	0.4146	1.2166
0.12316	0.02150	16.0	0.2407	0.3807	1.2237
0.12566	0.02288	16.0	0.2417	0.3669	1.2249
0.12923	0.02498	16.2	0.2413	0.3445	1.2244
0.13165	0.02646	16.0	0.2398	0.3287	1.2225
0.14235	0.03341	17.1	0.2398	0.2789	1.2227
Average:			0.2362	0.4154	1.2170
Standard Deviation:			0.0118	0.1125	0.0127

* At cross-over section

Table 14 Non-friction losses for 110° meander geometry, natural cross-section

*Flow Depth (m)	Discharge (m^3/s)	T (°C)	S_o-S_f ($x10^{-3}$)	K	n'/n
0.11006	0.01135	10.4	0.1805	0.7819	1.2512
0.11516	0.01322	15.0	0.1920	0.7558	1.2743
0.12030	0.01533	10.5	0.1857	0.6464	1.2615
0.12073	0.01560	14.4	0.1881	0.6228	1.2664
0.12420	0.01699	14.1	0.1881	0.6228	1.2664
0.12791	0.01873	10.3	0.1774	0.5459	1.2452
0.13072	0.02006	15.9	0.1878	0.5502	1.2657
0.13566	0.02206	14.9	0.1950	0.5473	1.2806
0.13854	0.02342	10.3	0.1872	0.5057	1.2646
0.14027	0.02432	10.5	0.1868	0.4908	1.2638
0.14672	0.02778	10.4	0.1844	0.4397	1.2589
Average:			0.1860	0.5935	1.2622
Standard Deviation:			0.0051	0.1077	0.0103

* At cross-over section

Table 15 Summary of Average Errors in Bend Loss Predictions

Data Set	Friction only	SCS (1963)	Toebes & Sooky (1967)	Leopold et al (1960)	Agarwal et al (1984)	Mockmore (1944)	Chang Rect. (1983)	Modified Chang	LSCS
SERC	9.54	-6.38	-14.60	-13.15	-15.97	-33.69	-5.31	0.85	-7.36
s = 1.37	2.88	2.51	1.62	1.42	3.30	4.36	3.03	1.34	2.49
Aberdeen	19.80	1.50	8.75	-6.74	-16.29	-51.73	-23.84	1.97	8.13
s = 1.21	9.43	8.12	7.08	6.22	8.29	3.65	6.37	4.50	8.60
Aberdeen	11.90	-5.24	1.70	-12.84	-30.57	-46.12	-27.71	-8.66	-7.36
s = 1.4	3.59	3.11	2.94	2.48	3.34	6.73	10.29	4.32	3.05
Aberdeen	28.66	-6.18	16.07	-12.68	-43.63	-37.42	-34.27	-10.78	-6.18
s = 2.06	3.26	2.52	2.13	1.63	2.15	3.95	7.14	2.78	2.52
Vicksburg	37.30	14.53	3.56	11.70	-4.79	-30.13	-6.19	16.29	17.68
wide	6.01	2.27 20.21* 7.88*	4.53	2.98	2.34	4.35	2.11	2.19	1.92
Vicksburg	10.61	-6.40	-13.09	10.32	-25.81	-20.59	-16.17	-2.00	0.37
narrow	7.27	11.34 -4.89* 10.25*	5.72	5.54	8.21	5.43	5.43	5.46	11.44
All Data	16.14	-3.46	-1.02	-7.68	-22.80	-39.43	-19.03	-1.76	-1.45
(62 points)	9.86	7.74 -2.76* 8.48*	12.06	9.36	11.48	11.12	12.33	7.35	9.84

Note

- Upper value is average error in %; lower value is standard deviation
- * lower adjustment where there is an option, otherwise higher value

Table 16 Contraction loss coefficients (Rouse, 1950)

$(y_2/(y_2 + h)$	0.00	0.10	0.20	0.30	0.40	0.50	0.60	0.70	0.80	0.90	1.00
K_c	0.50	0.48	0.45	0.41	0.36	0.29	0.21	0.13	0.07	0.01	0.00

Table 17 Main channel integrated discharges

Run	Channel Type	Flow Depth on Flood Plain (mm)	Main Channel Discharge (m^3/s)	Bankfull Discharge (m^3/s)
B23	60° Trap. smooth	50.5	0.0580	0.0865
B24		100.9	0.0710	0.0865
B28	60° Nat smooth	15.2	0.0270	0.0385
B29		50.0	0.0334	0.0385
B30		99.7	0.0437	0.0385
B35	60° Nat rough	15.3	0.0271	0.0385
B36		50.1	0.0223	0.0385
B37		101.0	0.0243	0.0385
B41	110° Nat smooth	15.0	0.0190	0.0297
B42		50.8	0.0204	0.0297
B44	110° Nat rough	15.6	0.0208	0.0297
B45		50.3	0.0173	0.0297

Table 18 Variables for defining main channel flow

Run	Q'_1	y'	B^2/A	s	f_2	f_1	f'
B23	0.671	0.385	9.142	1.37	0.02221	0.01682	1.320
B24	0.821	0.769	9.142	1.37	0.01708	0.01664	1.026
B28	0.701	0.185	14.60	1.37	0.03691	0.01936	1.907
B29	0.868	0.607	14.60	1.37	0.02158	0.01900	1.136
B30	1.135	1.211	14.60	1.37	0.01670	0.01883	0.887
B35	0.704	0.186	14.60	1.37	0.05150	0.01956	2.633
B36	0.579	0.609	14.60	1.37	0.10850	0.01945	5.578
B37	0.631	1.227	14.60	1.37	0.18050	0.01938	9.314
B41	0.640	0.183	14.60	2.04	0.03776	0.02050	1.842
B42	0.687	0.620	14.60	2.04	0.02906	0.02066	1.407
B44	0.700	0.190	14.60	2.04	0.05200	0.01996	2.605
B45	0.583	0.614	14.60	2.04	0.10850	0.01993	5.444

Table 19 Adjusted variables for defining main channel flow

Test	Q'_1	y'	B^2A	s	f'
B23'	0.690	0.385	9.142	1.37	1.026
B24'	0.802	0.769	9.142	1.37	1.320
B29'	0.884	0.607	14.60	1.37	0.887
B30'	1.113	1.211	14.60	1.37	1.136
B36'	0.336	0.609	14.60	1.37	9.314
B37'	0.963	1.227	14.60	1.37	5.578

Table 20 Roughness and sinuosity adjustment to Q'_1

Test	Q'_{1p}	Q'_1	Q'_1/Q'_{1p}
B23	0.691	0.671	0.971
B24	0.816	0.821	1.006
B29	0.885	0.868	0.981
B30	1.129	1.136	1.005
B36	0.693	0.687	0.991
B37	0.770	1.583	0.757

Table 21 Roughness and sinuosity adjustment to c

Test	c_p	c	c/c_p
B23	0.558	0.537	0.962
B24	0.558	0.562	1.007
B29	0.630	0.613	0.973
B30	0.630	1.636	1.010
B36	0.630	0.237	0.376
B37	0.630	-0.205	-0.325
B42	0.428	0.427	0.999
B45	0.428	0.240	0.561

Table 22 Errors (%) in reproducing Q'_1 for high values of y'

Run No	Method 1	2	3	4	5	6	7
B23	0.70	-0.40	-15.33	0.85	-2.47	-0.06	-2.57
B24	-0.71	-0.52	-6.55	0.49	1.87	-0.03	2.08
B29	1.00	0.90	3.47	-1.62	-7.91	-0.04	-0.09
B30	-3.03	-2.73	5.51	-0.22	-5.36	1.13	0.20
B36	14.30	0.62	5.78	2.59	-2.58	0.05	1.63
B37	-2.42	19.90	4.81	12.74	0.32	6.63	-0.71
B42	-0.53	-0.41	13.16	11.61	20.06	24.56	23.65
B45	-8.85	11.94	-15.51	-12.91	1.17	1.29	2.72
Ave	5.75	0.68	-0.58	1.69	0.64	4.19	3.27
S D	6.13	8.25	9.92	7.51	7.97	7.98	7.88

Table 23 Data sets for inner flood plain analysis

Run	Channel Type	B^2/A	s
B21	SERC 60° trapezoidal	9.142	1.374
B26	SERC 60° natural, smooth	14.600	1.374
B34	SERC 60° natural, rough	14.600	1.374
B39	SERC 60° natural, smooth	14.600	2.041
B43	SERC 110° natural, rough	14.600	2.041
AB101	Aberdeen, trapezoidal	3.837	1.215
AB102	Aberdeen, trapezoidal	3.837	1.406
AB104	Aberdeen, trapezoidal	3.837	2.041

Table 24 Equation parameters for y/ greater than 0.2

Run	a	b
B21	0.675	-0.2846
B26	0.792	-0.2051
B34	0.760	-0.2051
B39	0.660	-0.0356
B43	0.490	-0.2468
AB101	0.910	-0.3912
AB102	0.710	-0.3741
AB104	0.510	-0.4743

Table 25 Geometric data overbank laboratory studies

Test	θ (°)	L_{co} (m)	r_c (m)	B (m)	S_o x10-3	L (m)	s	W_2 (m)	W_T (m)	S_{sf}
SERC FCF Phase B										
21	60	2.500	2.743	1.200	0.996	12.000	1.374	6.107	10.000	0.00
26	60	2.500	2.743	1.200	0.996	12.000	1.374	6.107	10.000	0.00
31	60	2.500	2.743	1.200	0.996	12.000	1.374	6.107	6.107	1.00
33	60	2.500	2.743	1.200	0.996	12.000	1.374	6.107	10.000	0.00
34	60	2.500	2.743	1.200	0.996	12.000	1.374	6.107	10.000	0.00
39	110	0.000	2.743	1.200	1.021	10.310	2.043	8.560	10.000	0.00
43	110	0.000	2.743	1.200	1.021	10.310	2.043	8.560	10.000	0.00
47	110	0.000	2.743	1.200	1.021	10.310	2.043	8.560	8.560	1.00
Aberdeen										
101	40	0.984	0.413	0.174	1.000	2.570	1.215	1.000	1.200	0.00
102	60	0.477	0.413	0.174	1.000	1.909	1.406	1.000	1.200	0.00
104	110	0.000	0.307	0.174	0.621	1.154	2.043	1.000	1.200	0.00
Vicksburg										
201	90	0.000	1.829	0.762	1.000	7.315	1.571	4.420	4.877	0.00
204	78.7	0.000	1.865	0.762	1.000	7.315	1.400	3.761	4.877	0.00
207	58.8	0.000	2.136	0.762	1.000	7.315	1.200	2.822	4.877	0.00
Kiely										
301	45	0.475	0.4000	0.200	1.000	1.803	1.224	0.770	1.200	0.00

Table 26 Geometric data Sooky's laboratory study

Test	NOP	r_c (m)	B (m)	S_o x10-3	L (m)	s	W_2 (m)	W_t (m)	S_{sf}
Geometry 4									
401	5	1.392	0.209	0.675	1.280	1.090	0.462	1.184	0.00
402	6	1.392	0.209	8.700	1.280	1.090	0.462	1.184	0.00
403	6	1.392	0.209	1.600	1.280	1.090	0.462	1.184	0.00
404	6	1.392	0.209	3.670	1.280	1.090	0.462	1.184	0.00
Geometry 5									
405	5	1.392	0.209	0.300	1.280	1.090	0.462	1.184	0.00
406	7	1.392	0.209	0.675	1.280	1.090	0.462	1.184	0.00
407	7	1.392	0.209	0.870	1.280	1.090	0.462	1.184	0.00
408	5	1.392	0.209	1.000	1.280	1.090	0.462	1.184	0.00
409	6	1.392	0.209	1.600	1.280	1.090	0.462	1.184	0.00
410	5	1.392	0.209	3.000	1.280	1.090	0.462	1.184	0.00
411	5	1.392	0.209	3.670	1.280	1.090	0.462	1.184	0.00

Note : 1 NOP = number of data points

Table 27 Main channel geometric data

Test	Type of xs	h (m)	A_1 (m^2)	P_1 (m^1)	Q_b (l/s)	S_s	θ_m (°)
21	Trapezoidal	0.150	0.1575	1.324	86.50	1.00	39.10
26	Natural	0.150	0.0988	1.288	38.50	1.00	39.10
31	Natural	0.150	0.0988	1.288	38.50	1.00	39.10
33	Natural	0.150	0.0988	1.288	38.50	1.00	39.10
34	Natural	0.150	0.0988	1.288	38.50	1.00	39.10
39	Natural	0.150	0.0983	1.281	29.70	1.00	55.00
43	Natural	0.150	0.0983	1.281	29.70	1.00	55.00
47	Natural	0.150	0.0983	1.281	29.70	1.00	55.00
101	Trapezoidal	0.050	0.0078	0.245	1.76	0.35	32.61
102	Trapezoidal	0.050	0.0078	0.245	1.72	0.35	40.66
104	Trapezoidal	0.050	0.0078	0.245	0.94	0.35	55.00
201	Trapezoidal	0.152	0.1045	0.950	34.60	2.00	45.00
204	Trapezoidal	0.152	0.1045	0.950	39.08	2.00	39.35
207	Trapezoidal	0.152	0.1045	0.950	43.90	2.00	29.41
301	Rectangular	0.050	0.0100	0.300	2.32	0.00	32.19
401	Rectangular	0.038	0.0080	0.286	1.30	0.00	11.73
402	Rectangular	0.038	0.0080	0.286	1.50	0.00	11.73
403	Rectangular	0.038	0.0080	0.286	2.18	0.00	11.73
404	Rectangular	0.038	0.0080	0.286	2.90	0.00	11.73
405	Rectangular	0.076	0.0160	0.362	3.55	0.00	11.73
406	Rectangular	0.076	0.0160	0.362	3.55	0.00	11.73
407	Rectangular	0.076	0.0160	0.362	4.20	0.00	11.73
408	Rectangular	0.076	0.0160	0.362	4.65	0.00	11.73
409	Rectangular	0.076	0.0160	0.362	5.98	0.00	11.73
410	Rectangular	0.076	0.0160	0.362	7.62	0.00	11.73
411	Rectangular	0.076	0.0160	0.362	7.99	0.00	11.73

Table 28 Mean % errors in discharge FCF data

TEST	NOP	BFO	JW	JW2	EE	GH4	GH5
21	16	38.7	3.9	7.1	12.2	16.3	15.4
		8.4	6.1	1.3	15.1	3.3	3.5
26	16	29.2	-2.7	-1.3	4.2	9.8	8.7
		5.4	2.9	2.6	14.1	6.0	5.5
31	14	37.0	-7.5	-5.5	0.8	10.0	9.6
		5.4	5.3	22.8	19.1	5.2	4.9
33	12	8.9	-6.4	-13.7	6.0	-3.2	-6.0
		12.5	4.9	3.9	11.0	5.1	5.9
34	18	9.3	-6.9	-20.2	5.8	-5.3	-7.8
		15.1	3.7	8.5	13.8	9.1	9.7
39	14	59.1	-3.8	-11.7	3.2	39.0	15.1
		6.9	12.5	8.6	24.3	6.4	9.8
43	15	18.5	-2.4	-33.3	12.8	8.3	-8.2
		24.6	8.1	17.1	23.1	21.6	23.7
47	14	63.0	-7.3	-16.7	3.0	40.2	14.9
		6.0	13.3	9.2	27.5	5.7	9.9
smooth	74	44.8	-3.3	-5.2	4.9	22.5	12.7
		14.7	9.6	10.1	20.2	14.6	7.5
rough	45	12.3	-5.3	-22.8	8.2	-0.2	-7.5
		18.4	6.0	13.7	16.9	15.0	15.0
All	119	32.5	-4.0	-11.8	6.1	13.9	5.1
		22.6	8.4	14.4	19.0	18.4	14.6

Note : The lower values are standard deviations in the means
NOP - Number of data points
Smooth - 21 26 31 39 47
Rough - 33 34 43

Table 29 Mean % errors in discharge Aberdeen, Vicksburg and Kiely data

TEST	NOP	BFO	JW	JW2	EE	GH4	GH5
Aberdeen							
101	33	28.2	-6.1	-3.4	-4.0	0.5	2.5
		11.8	5.5	7.4	16.7	7.4	7.6
102	30	41.6	1.5	3.4	-2.0	14.2	11.9
		7.9	4.5	4.7	14.4	6.5	5.2
104	20	77.0	10.4	3.6	0.1	47.8	30.8
		22.4	8.3	7.1	15.7	14.6	11.7
All	83	44.8	0.6	0.8	-2.3	16.9	12.7
		23.7	8.7	7.2	15.5	20.7	13.6
Vicksburg							
201	3	59.3	-2.5	6.0	1.1	34.6	26.0
		7.6	6.1	3.8	13.4	6.3	4.2
204	3	45.3	-5.3	5.3	6.8	21.1	19.2
		9.9	11.2	10.0	2.5	9.6	8.4
207	3	32.9	-8.0	1.3	1.8	8.1	12.6
		5.8	11.3	12.6	4.9	7.0	7.8
All	9	45.8	-5.3	4.2	3.2	21.3	19.3
		13.3	8.9	8.6	7.7	13.3	8.4
Kiely							
301	5	39.2	-0.8	6.3	-1.9	11.1	14.9
		8.0	3.1	8.2	11.1	5.6	6.0

Note : The lower values are standard deviations in the means

Table 30 Mean % errors in discharge Sooky data

TEST	NOP	BFO	JW	JW2	EE	GH4	GH5
401	5	22.8	3.2	2.7	15.8	0.1	8.6
		5.0	4.3	4.7	4.8	4.2	4.7
402	6	23.5	3.7	3.8	16.6	0.8	9.4
		6.3	5.2	6.4	6.5	5.3	5.9
403	6	24.8	5.0	7.3	18.6	2.0	10.9
		7.7	6.1	7.5	8.1	6.2	6.8
404	6	40.2	12.8	17.9	34.4	14.4	24.2
		17.7	12.9	14.5	17.8	14.2	15.2
405	5	-13.9	-18.4	-14.9	-18.7	-29.8	-25.5
		4.9	7.9	6.0	6.0	4.0	3.7
406	7	7.5	-15.0	-7.9	1.1	-12.1	-6.5
		10.8	7.0	7.2	11.4	8.7	8.7
407	7	12.0	-10.8	-4.3	5.7	-8.5	-2.9
		11.4	8.5	6.3	12.1	9.1	8.9
408	5	17.9	-2.4	-0.7	12.4	-4.1	0.4
		9.2	11.0	5.1	10.2	6.9	5.7
409	6	20.7	-4.3	1.4	14.6	-1.3	4.4
		13.1	10.9	5.0	13.4	10.4	10.2
410	5	37.0	6.2	6.3	30.8	11.6	16.7
		8.1	9.6	3.7	8.8	6.0	4.6
411	5	39.7	3.0	1.7	33.4	13.9	19.4
		11.1	10.4	5.4	11.3	8.6	8.0
All	63	20.8	-1.9	1.2	14.6	-1.4	5.2
		17.5	12.4	10.6	17.6	14.2	15.1

Note : The lower values are standard deviations in the means
NOP - Number of data points

Table 31 Mean % errors in discharge all data

TEST	NOP	BFO	JW	JW2	EE	GH4	GH5
1	74	44.8	-3.3	-5.2	4.9	22.5	12.7
		14.7	9.6	10.1	20.2	14.6	7.5
2	45	12.3	-5.3	-22.8	8.2	-0.2	-7.5
		18.4	6.0	13.7	16.9	15.0	15.0
3	119	32.5	-4.0	-11.8	6.1	13.9	5.1
		22.6	8.4	14.4	19.0	18.4	14.6
4	83	44.8	0.6	0.8	-2.3	16.9	12.7
		23.7	8.7	7.2	15.5	20.7	13.6
5	9	45.8	-5.3	4.2	3.2	21.3	19.3
		13.3	8.9	8.6	7.7	13.3	8.4
6	63	20.8	-1.9	1.2	14.6	-1.4	5.2
		17.5	12.4	10.6	17.6	14.2	15.1
7	279	34.1	-2.1	-4.3	5.3	11.5	8.0
		23.2	9.7	13.2	18.3	19.3	14.7
8	77	24.9	-2.6	1.8	11.9	2.0	7.4
		18.8	11.7	10.2	17.2	15.6	14.8

Notes: The lower values are standard deviations in the means
1 - SERC PHASE B SMOOTH 21 26 31 39 47
2 - SERC PHASE B ROD ROUGHEND 33 34 43
3 - ALL SERC
4 - ALL ABERDEEN 101 102 104
5 - VICKSBURG 201 204 207
6 - ALL SOOKY 401 - 411
7 - ALL DATA
8 - VICKSBURG, KIELY AND SOOKY data only

Table 32 Ranking of methods

TEST	1st	2nd	3rd	4th	5th	6th
1	JW	EE	JW2	GH5	GH4	BFO
2	GH4	GH5	JW	EE	BFO	JW2
3	JW	GH5	EE	JW2	GH4	BFO
4	JW	JW2	EE	GH5	GH4	BFO
5	EE	JW2	JW	GH5	GH4	BFO
6	JW2	GH4	JW	GH5	EE	BFO
7	JW	JW2	EE	GH5	GH4	BFO

Table 33 Mean % errors in stage FCF data

TEST	NOP	BFO	JW	JW2	EE	GH4	GH5
21	16	-5.3	-0.6	-1.2	-1.0	-2.5	-2.4
		1.6	0.9	0.4	2.3	1.2	1.1
26	16	-4.0	0.8	0.5	0.5	-1.7	-1.5
		2.0	1.3	1.1	2.4	1.5	1.3
31	14	-4.9	2.4	1.6	2.5	-1.7	-1.6
		2.2	3.4	2.7	5.9	1.5	1.4
33	12	-0.8	0.9	3.2	-0.4	1.3	2.1
		1.0	0.9	2.2	1.0	1.6	2.2
34	18	-0.6	2.2	8.5	0.2	3.1	4.1
		2.2	1.4	5.8	2.4	3.5	4.0
39	14	-7.2	2.3	3.8	1.9	-5.3	-2.1
		3.5	3.1	3.5	4.0	2.6	0.7
43	15	-1.3	1.5	19.7	-0.2	1.2	7.7
		2.9	2.1	15.5	3.2	4.4	9.3
47	14	-7.1	3.3	5.1	2.7	-5.1	-2.0
		3.5	4.3	4.9	5.5	2.5	0.7
smooth	74	-5.6	1.6	1.9	1.2	-3.2	-1.9
		2.9	3.1	3.6	4.3	2.4	1.1
rough	45	-0.9	1.6	10.8	-0.1	2.0	4.8
		2.2	1.6	11.6	2.4	3.5	6.3
All	119	-3.8	1.6	5.2	0.7	-1.2	0.6
		3.5	2.6	8.8	3.8	3.8	5.1

Note : The lower values are standard deviations in the means
NOP - Number of data points
Smooth - 21 26 31 39 47
Rough - 33 34 43

Table 34 Mean % errors in stage Aberdeen, Vicksburg and Kiely data

TEST	NOP	BFO	JW	JW2	EE	GH4	GH5
Aberdeen							
101	33	-4.8	1.4	0.9	2.6	0.0	-0.3
		2.2	1.2	1.5	4.7	1.3	1.3
102	30	-5.7	-0.4	-0.7	2.2	-2.5	-2.1
		3.0	0.8	0.7	4.2	2.1	1.7
104	20	-8.7	-1.8	-0.7	1.7	-6.5	-4.7
		5.3	1.6	1.1	3.5	4.1	2.7
All	83	-6.1	0.0	0.0	2.2	-2.5	-2.0
		3.7	1.7	1.4	4.2	3.5	2.5
Vicksburg							
201	3	-8.5	0.1	-1.5	4.9	-5.9	-4.8
		3.9	1.2	1.4	10.0	3.0	2.3
204	3	-7.3	0.5	-1.6	-1.5	-4.2	-4.0
		3.8	1.8	2.3	0.2	3.0	2.7
207	3	-5.9	1.0	-1.0	4.0	-1.9	-2.8
		2.9	1.7	2.4	7.5	2.0	2.4
All	9	-7.2	0.5	-1.3	2.4	-4.0	-3.9
		3.3	1.4	1.8	6.9	2.9	2.3
Kiely							
301	5	-6.6	2.3	-1.6	3.3	-2.3	-3.0
		1.8	5.0	1.7	7.3	1.1	1.3

Note: The lower values are standard deviations in the means
NOP - Number of data points

Table 35 Mean % errors in stage Sooky data

TEST	NOP	BFO	JW	JW2	EE	GH4	GH5
401	5	-6.1	-0.2	0.0	-4.5	0.8	-2.6
		1.4	2.5	2.9	1.3	2.7	1.2
402	6	-5.9	-0.9	0.1	-4.4	0.9	-2.5
		1.1	1.4	3.5	1.2	3.3	1.4
403	6	-5.7	-1.1	-1.7	-4.5	0.5	-2.6
		0.8	1.3	1.5	1.1	2.8	1.1
404	6	-7.8	-2.5	-3.7	-7.0	-3.0	-4.9
		1.3	1.9	1.9	1.7	2.2	1.7
405	5	5.0	8.4	5.6	8.1	11.8	9.9
		5.0	6.7	5.8	6.7	7.4	6.6
406	7	-1.2	4.7	2.5	0.6	4.3	2.5
		2.8	3.5	3.1	3.8	4.1	3.5
407	7	-2.1	3.4	1.5	-0.5	3.1	1.4
		2.6	3.3	2.5	3.4	3.6	3.1
408	5	-3.6	1.2	0.9	-1.5	2.2	1.1
		1.6	5.3	3.3	4.2	4.3	3.7
409	6	-4.0	1.2	-0.1	-2.8	0.8	-0.6
		2.0	3.1	1.3	2.6	2.9	2.4
410	5	-7.0	-1.6	-1.6	-6.1	-2.5	-3.3
		0.8	3.3	1.2	1.0	1.1	0.6
411	5	-7.3	-0.5	-0.2	-6.5	-2.9	-3.7
		1.1	3.1	1.6	1.3	1.5	1.1
All	63	-4.1	1.2	0.3	-2.6	1.5	-0.5
		4.0	4.4	3.5	4.9	5.1	4.7

Note: The lower values are standard deviations in the means
NOP - Number of data points

Table 36 Mean % errors in stage all data

TEST	NOP	BFO	JW	JW2	EE	GH4	GH5
1	74	-5.6	1.6	1.9	1.2	-3.2	-1.9
		2.9	3.1	3.6	4.3	2.4	1.1
2	45	-0.9	1.6	10.8	-0.1	2.0	4.8
		2.2	1.6	11.6	2.4	3.5	6.3
3	119	-3.8	1.6	5.2	0.7	-1.2	0.6
		3.5	2.6	8.8	3.8	3.8	5.1
4	83	-6.1	0.0	0.0	2.2	-2.5	-2.0
		3.7	1.7	1.4	4.2	3.5	2.5
5	9	-7.2	0.5	-1.3	2.4	-4.0	-3.9
		3.3	1.4	1.8	6.9	2.9	2.3
6	63	-4.1	1.2	0.3	-2.6	1.5	-0.5
		4.0	4.4	3.5	4.9	5.1	4.7
7	279	-4.7	1.0	2.2	0.5	-1.1	-0.6
		3.8	3.0	6.6	4.7	4.3	4.4
8	77	-4.6	1.8	0.0	-1.4	0.6	-1.0
		4.0	4.7	3.3	5.9	5.1	4.5

Notes: The lower values are standard deviations in the means
1 - SERC PHASE B SMOOTH 21 26 31 39 47
2 - SERC PHASE B ROD ROUGHEND 33 34 43
3 - ALL SERC
4 - ALL ABERDEEN 101 102 104
5 - VICKSBURG 201 204 207
6 - ALL SOOKY 401 - 411
7 - ALL DATA
8 - VICKSBURG, KIELY AND SOOKY data only

Table 37 Sensitivity tests : effect of errors in wave length

Factor	% Error in L	mean % Error in discharge
0.50	-50.0	-10.3
0.75	-25.0	-5.5
1.00	0.0	-2.1
1.25	25.0	0.4
1.50	50.0	2.3

Table 38 Sensitivity tests : effect of errors in channel side slope

Factor	% Error in S_s	mean % Error in discharge
0.00	-100.0	-5.3
0.50	-50.0	-3.9
1.00	0.0	-2.1
1.50	50.0	-0.1
2.00	100.0	2.4

Table 39 Measured zonal discharges, Sooky and Kiely data

			Discharge (l/s)				
Test	source	Depth (mm)	Total	zone 1	zone 2	zone 3	zone 4
403	Sooky	61.3	7.89	2.09	2.58	1.54	1.68
409	Sooky	99.4	12.62	4.82	3.33	2.11	2.36
301	Kiely	60.0	3.10	1.49	1.11	0.40	0.40
301	Kiely	80.0	11.10	3.10	5.48	1.26	1.26

Table 40 Errors (%) in calculated total flows, Sooky and Kiely data

				Method			
Test	Depth	BFO	JW	JW2	EE	GH4	GH5
403	61.3	33.9	12.6	16.0	27.8	9.5	19.1
409	99.4	12.4	-10.3	2.2	5.8	-7.8	-1.8
301	60.0	52.9	3.8	6.8	14.8	20.6	24.6
301	80.0	36.0	-0.9	12.6	9.0	10.5	15.3

Table 41 Measured and calculated flow distributions

Zone	Measured		BFO	JW	JW2	EE	GH4	GH5
			%(Zonal flow / Total flow)					
	Test	403	Sooky depth = 61.3mm					
1	26.5		21.3	19.1	19.1	21.9	19.6	18.0
2	32.7		38.2	32.9	32.9	35.7	31.0	38.8
3	19.5		20.2	24.0	24.0	21.2	24.7	21.6
4	21.3		20.2	24.0	24.0	21.1	24.0	21.6
	Test	409	Sooky depth = 99.4mm					
1	38.2		41.1	33.5	29.4	42.2	40.4	37.8
2	26.4		28.5	28.7	37.6	25.8	23.0	29.6
3	16.7		15.0	18.9	16.5	16.0	18.3	16.3
4	16.7		15.0	18.9	16.5	16.0	18.3	16.3
	Test	301	Kiely depth = 60.0mm					
1	48.1		61.2	47.7	46.7	59.5	59.4	57.4
2	35.9		27.2	35.1	36.9	25.1	26.2	29.0
3	8.0		5.8	8.6	8.2	7.7	7.2	6.8
4	8.0		5.8	8.6	8.2	7.7	7.2	6.8
	Test	301	Kiely depth = 80.0mm					
1	27.8		19.2	14.8	13.0	21.0	18.0	17.3
2	49.4		57.2	53.0	58.6	43.8	53.0	58.3
3	11.4		11.8	16.1	14.2	17.6	14.5	12.2
4	11.4		11.8	16.1	14.2	17.6	14.5	12.2

Table 42 Reach averaged geometric parameters Roding study

y_2 (m)	Area (m^2)	Width (m)	Wetted perimeter (m)
Main channel at bankfull			
0.0	5.3	7.1	7.7
Zone 2			
0.1	2.1	20.5	10.8
0.2	4.4	25.3	15.7
0.3	7.1	27.9	18.4
0.4	10.0	29.0	19.5
0.5	12.9	29.9	20.4
0.6	15.9	30.4	20.9
0.7	19.0	30.9	21.4
0.8	22.1	31.3	21.9
0.9	25.3	31.8	22.5
1.0	28.5	32.4	23.1

Table 43 Errors in predicting overbank discharges

Case	P2		M2	
Method	Mean Error (%)	Standard Deviation (%)	Mean Error (%)	Standard Deviation (%)
Bed Friction Only	9.5	9.0	7.3	8.6
James and Wark	-2.0	1.7	-2.2	3.2
James and Wark 2	-27.1	10.0	-30.5	10.9

Note: %Error = $100^*(Q_{calc} - Q_{meas})/Q_{meas}$

Table 44 Sensitivity tests on the effect of floodplain roughness

Zone 2 Manning n	Mean BFO	%Errors JW	Difference in Means (BFO - JW)
0.01	305	142	163
0.02	122	78	44
0.03	61	40	21
0.04	31	16	15
0.05	10	-2	12
0.06	1	-10	11
0.08	-14	-25	11
0.10	-24	-33	9
0.18	-40	-47	7
0.30	-48	-58	10

Note: %Error = $100^{*}(Q_{calc} - Q_{meas})/Q_{meas}$

Figures

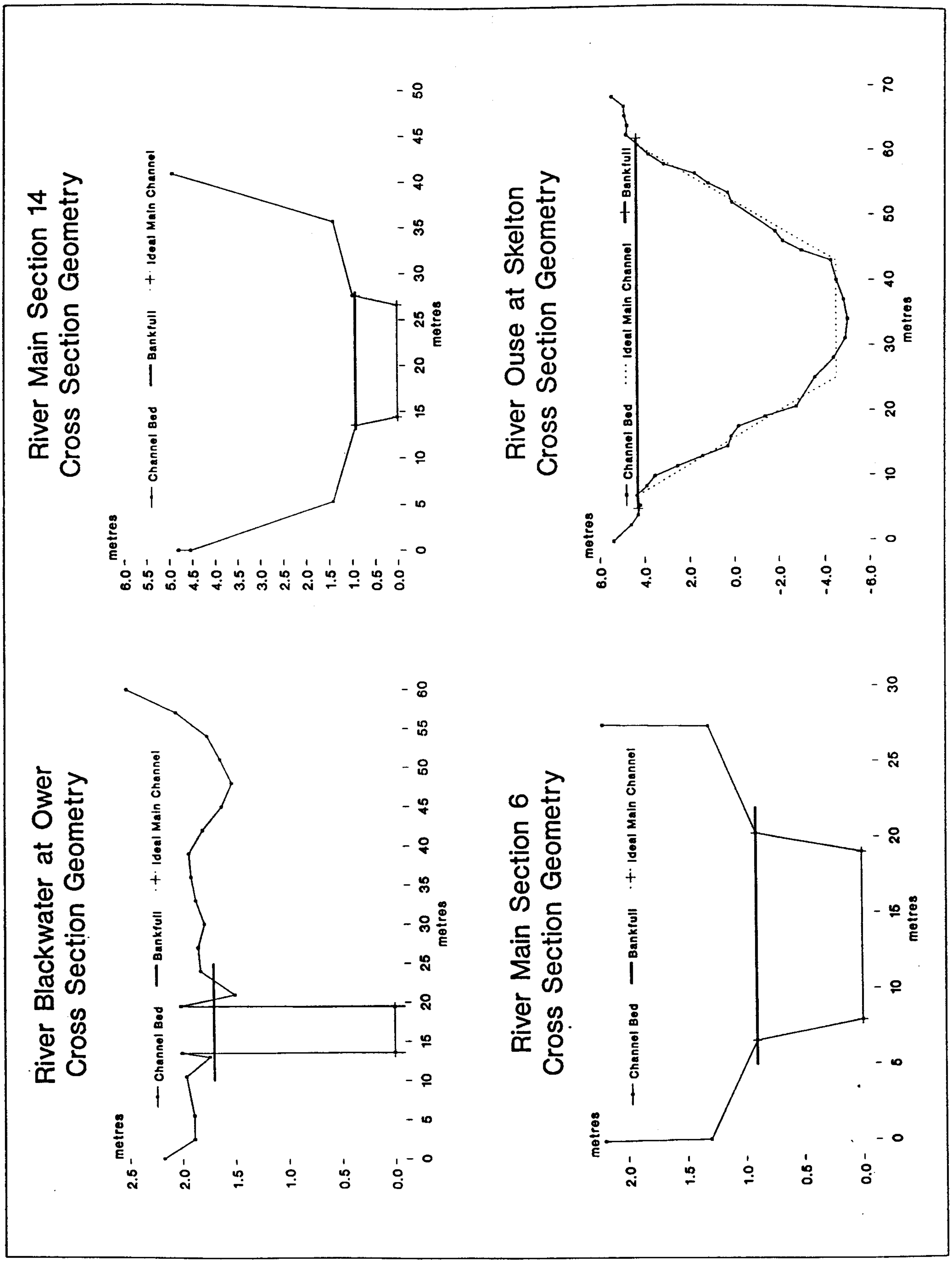

Figure 1 River channels cross-sections

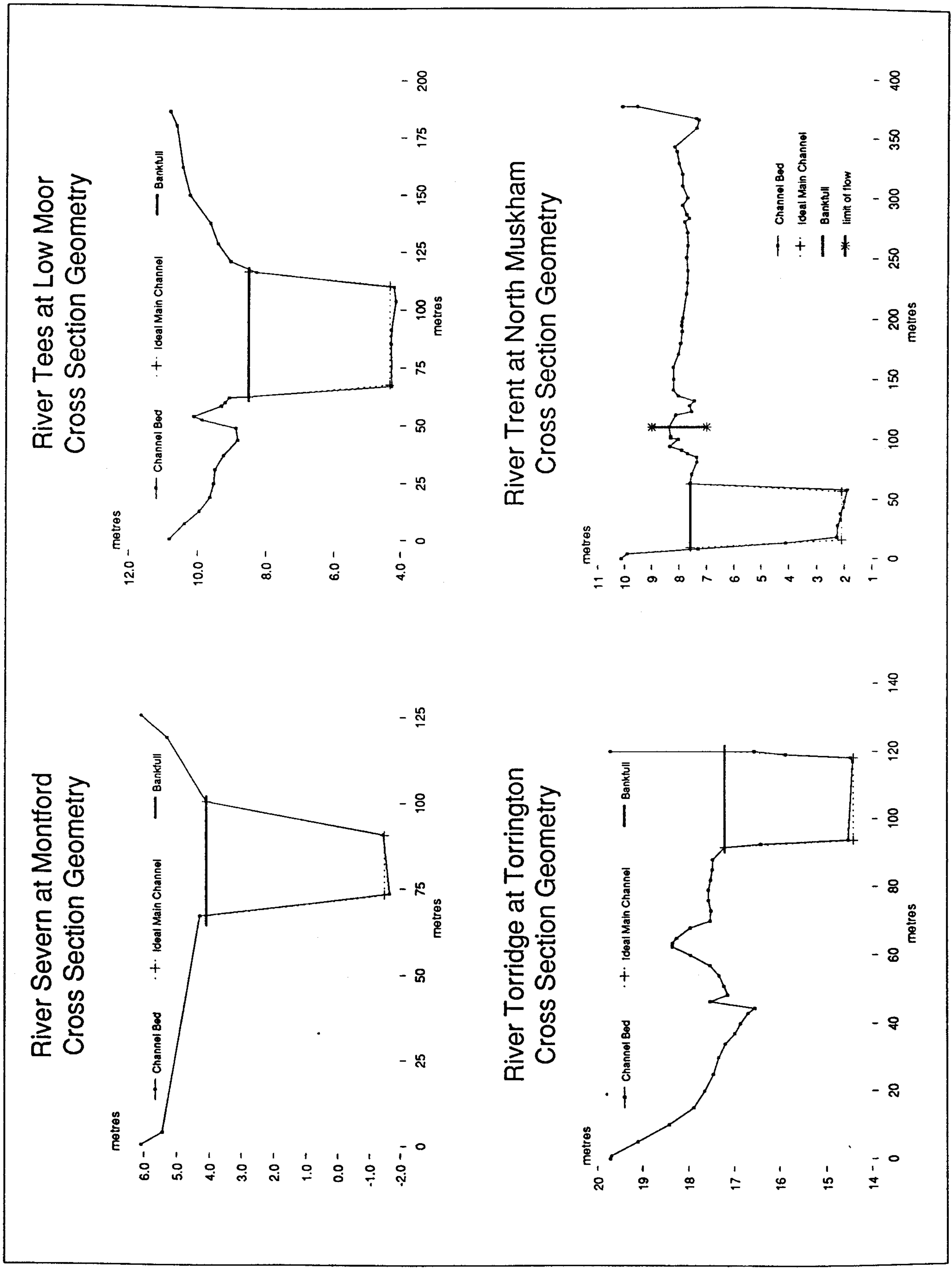

Figure 2 River channels cross-sections

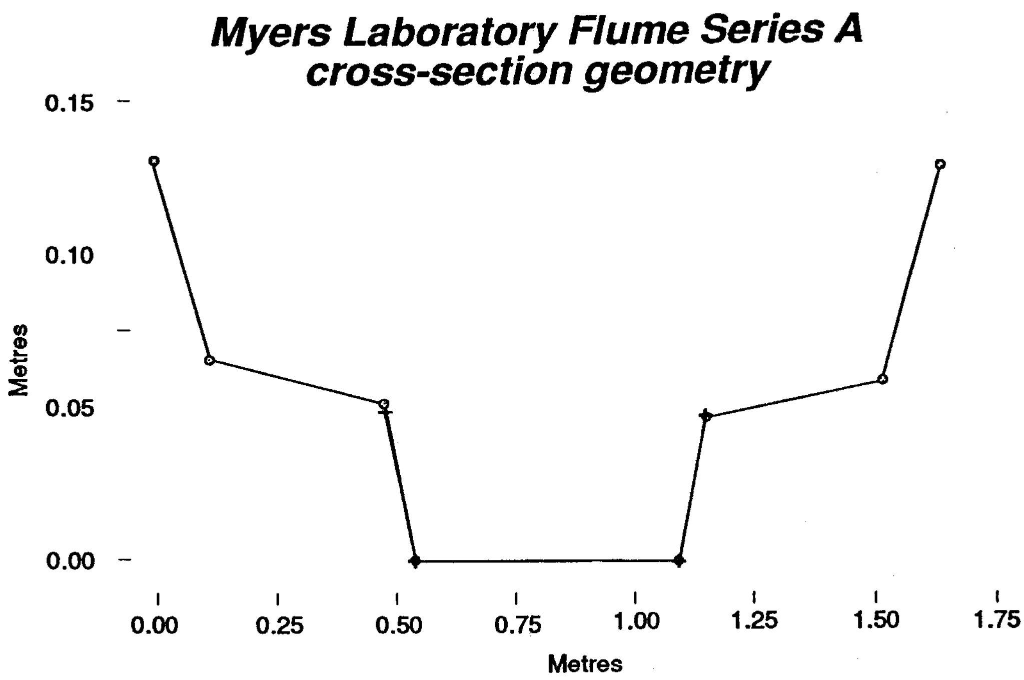

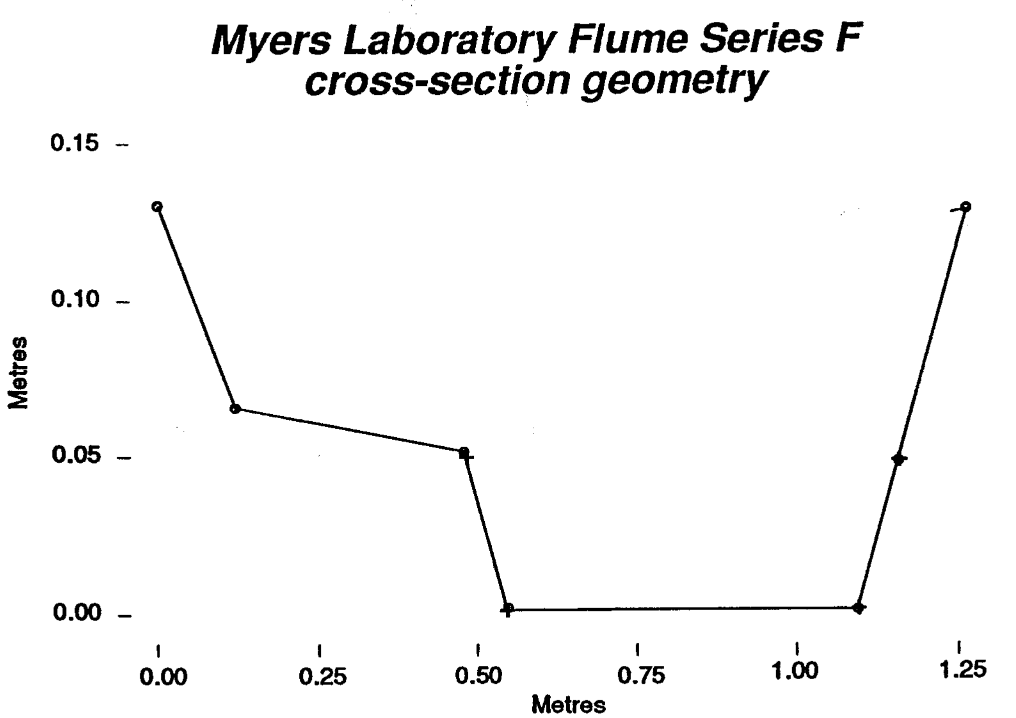

JBW/3/12-92/3D

Figure 3 Myers laboratory channel cross-sections

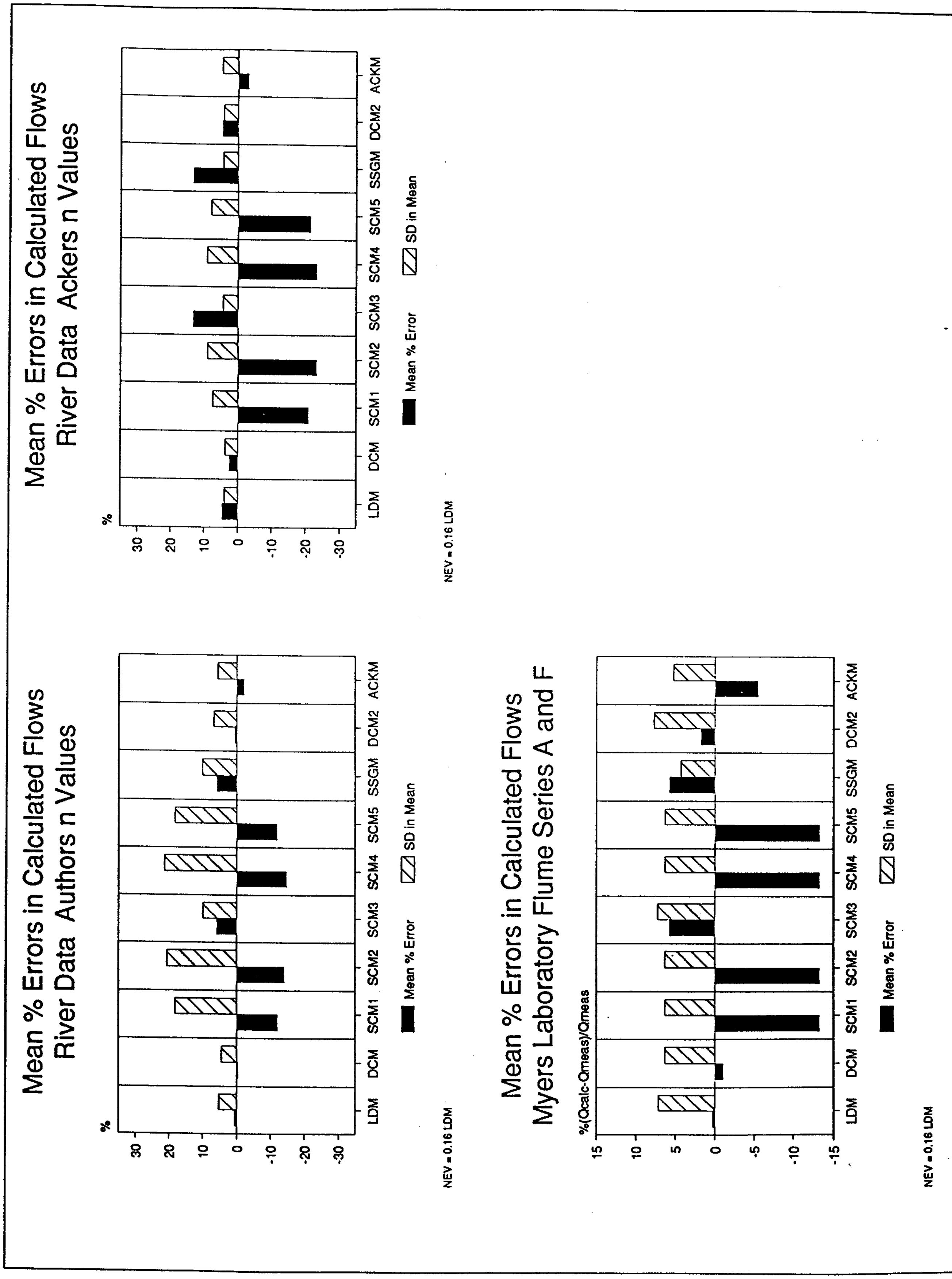

Figure 4 Mean errors, straight channel data

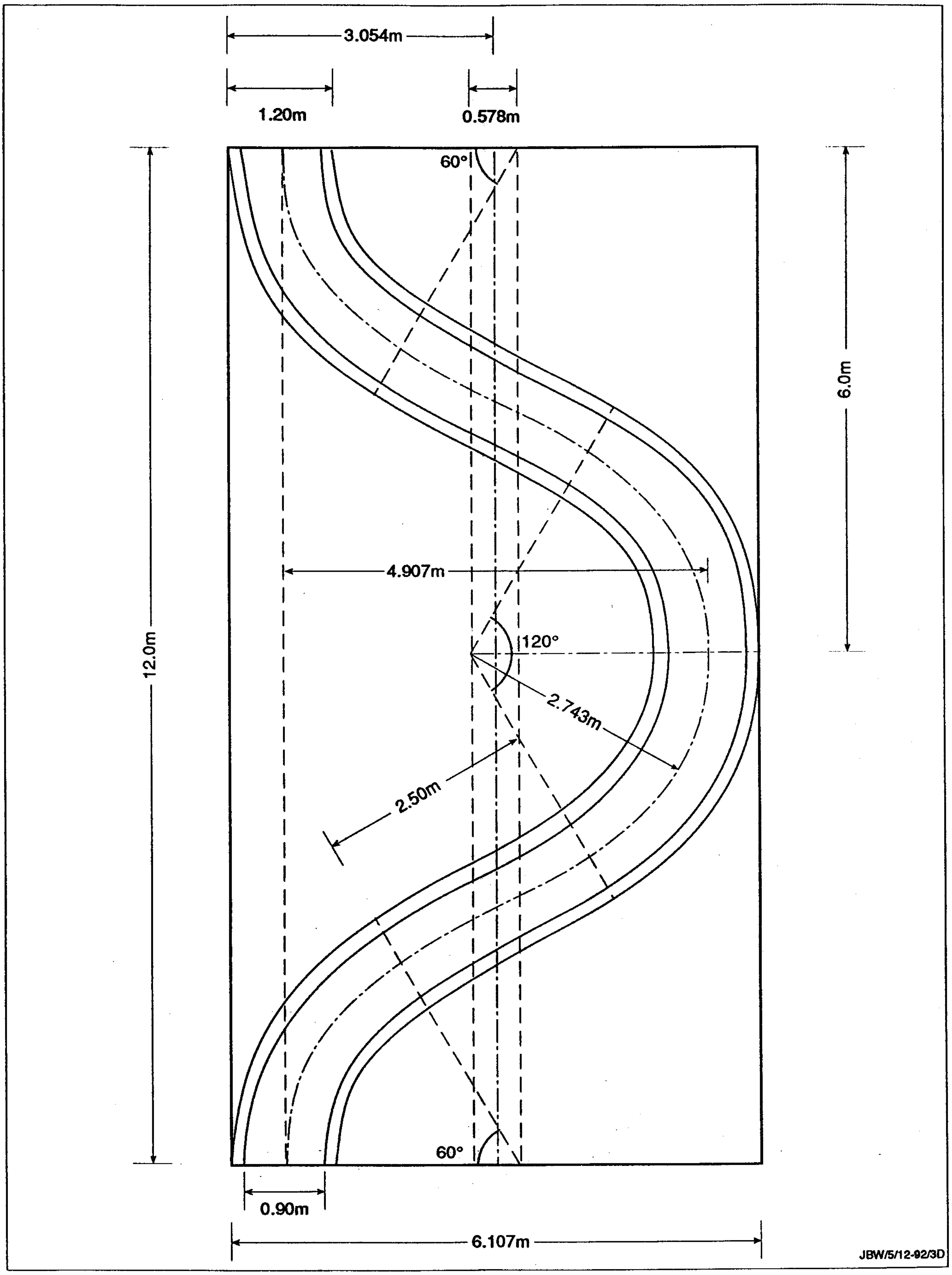

Figure 5   Detailed plan geometry of FCF 60° meander

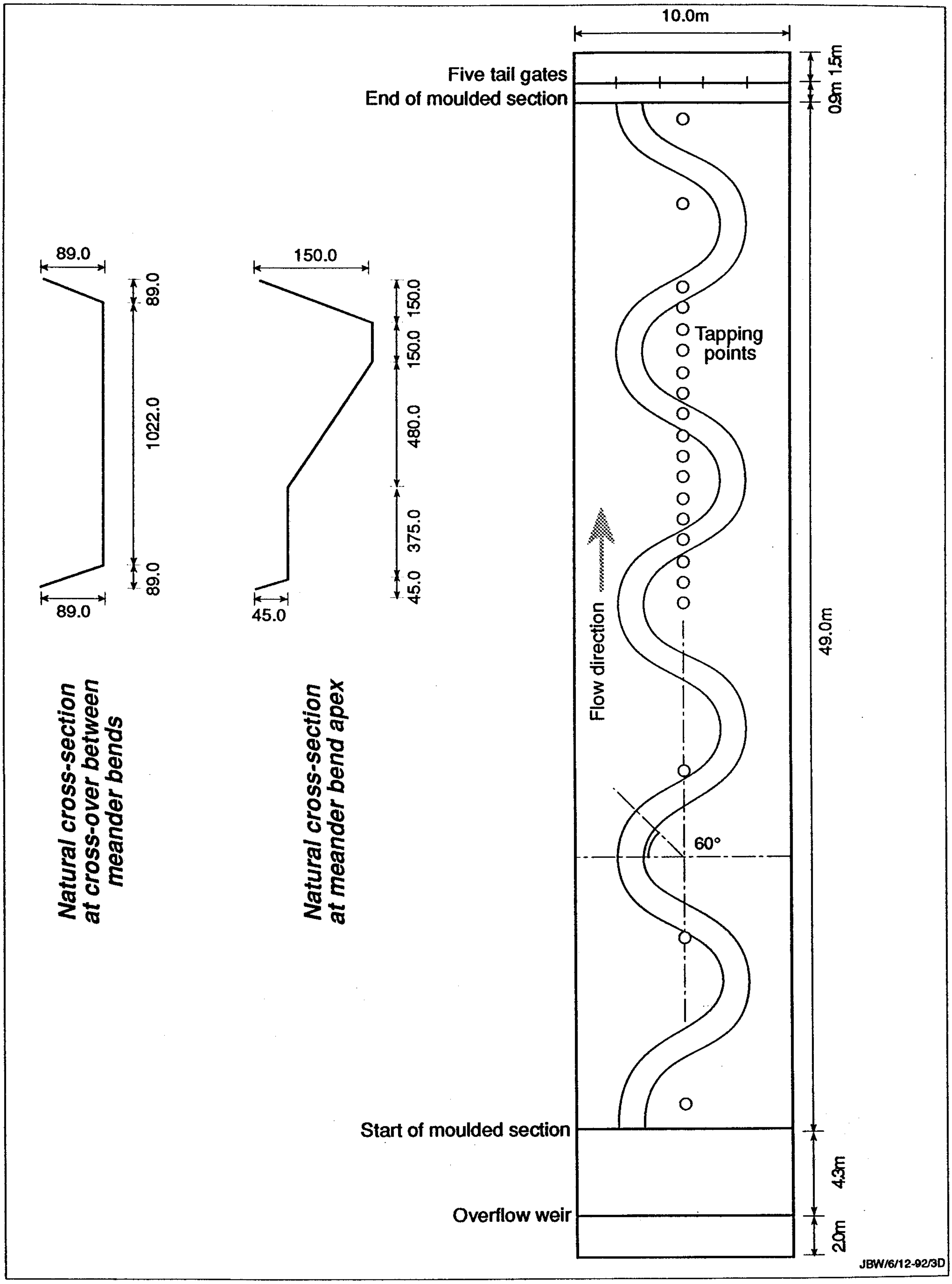

Figure 6 Plan of flume and natural cross-section geometry for 60° meander

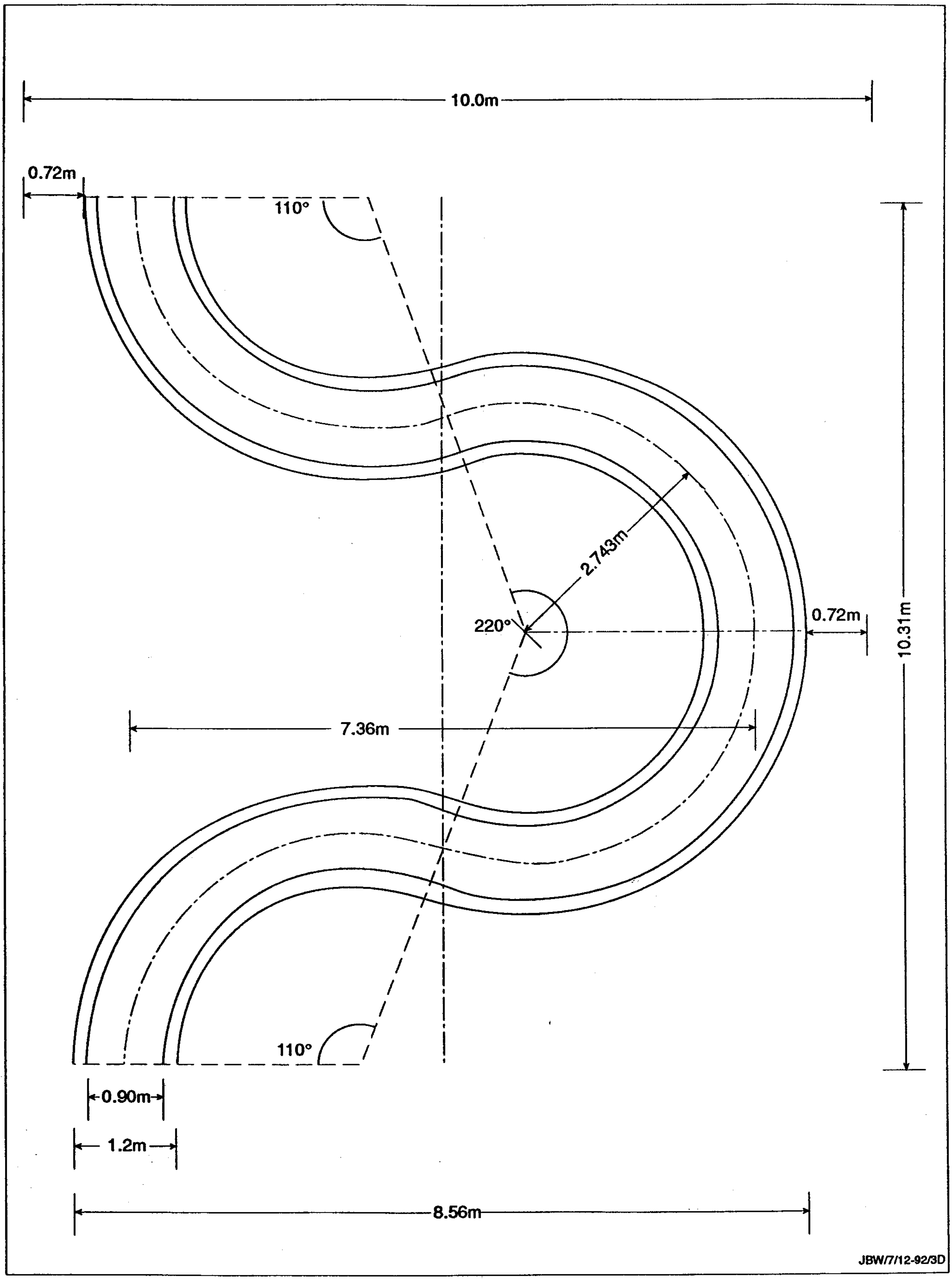

Figure 7 Detailed plan of geometry for FCF 110° meander

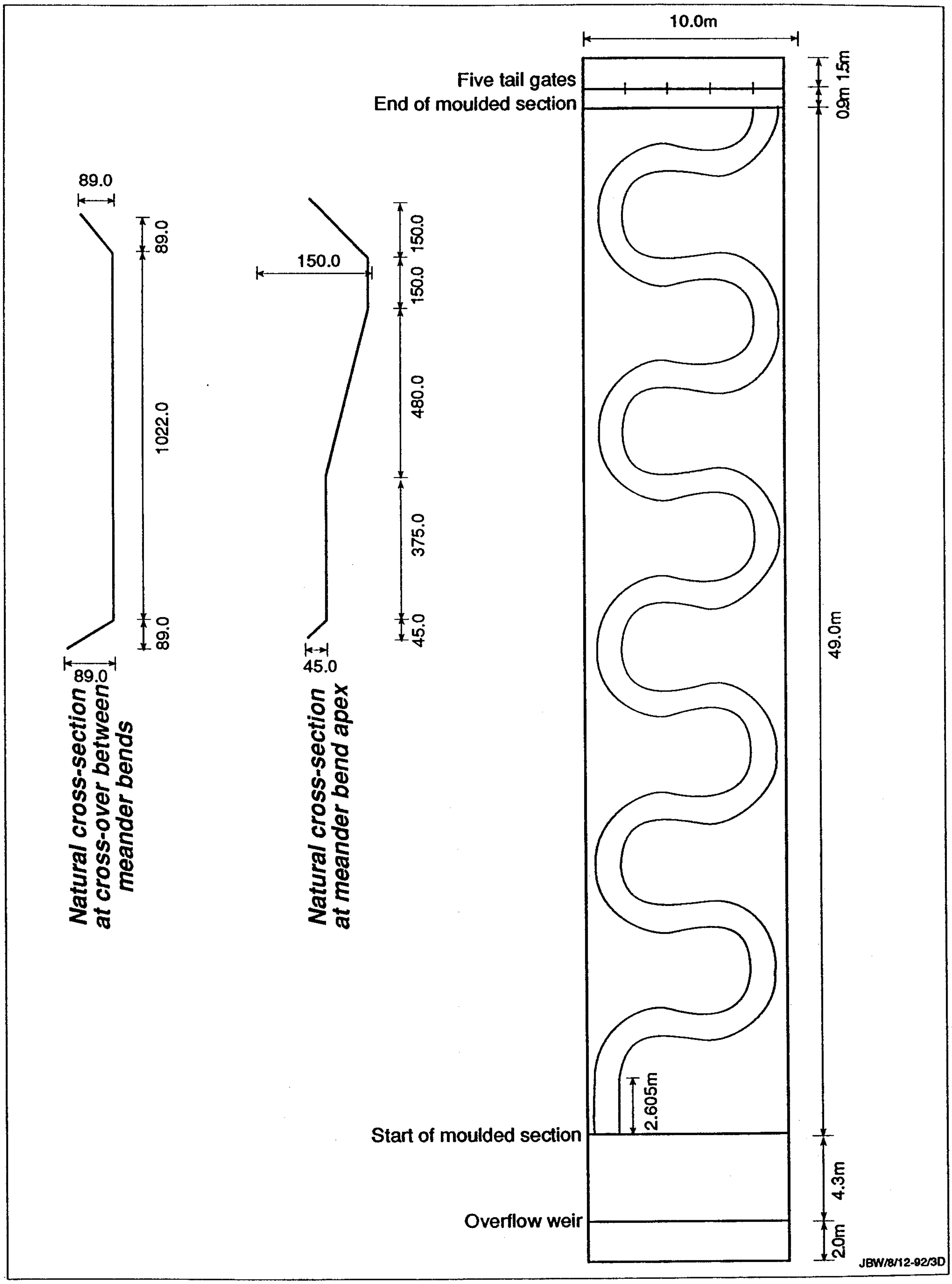

Figure 8 Plan of flume and natural cross-section geometry for 110° meander

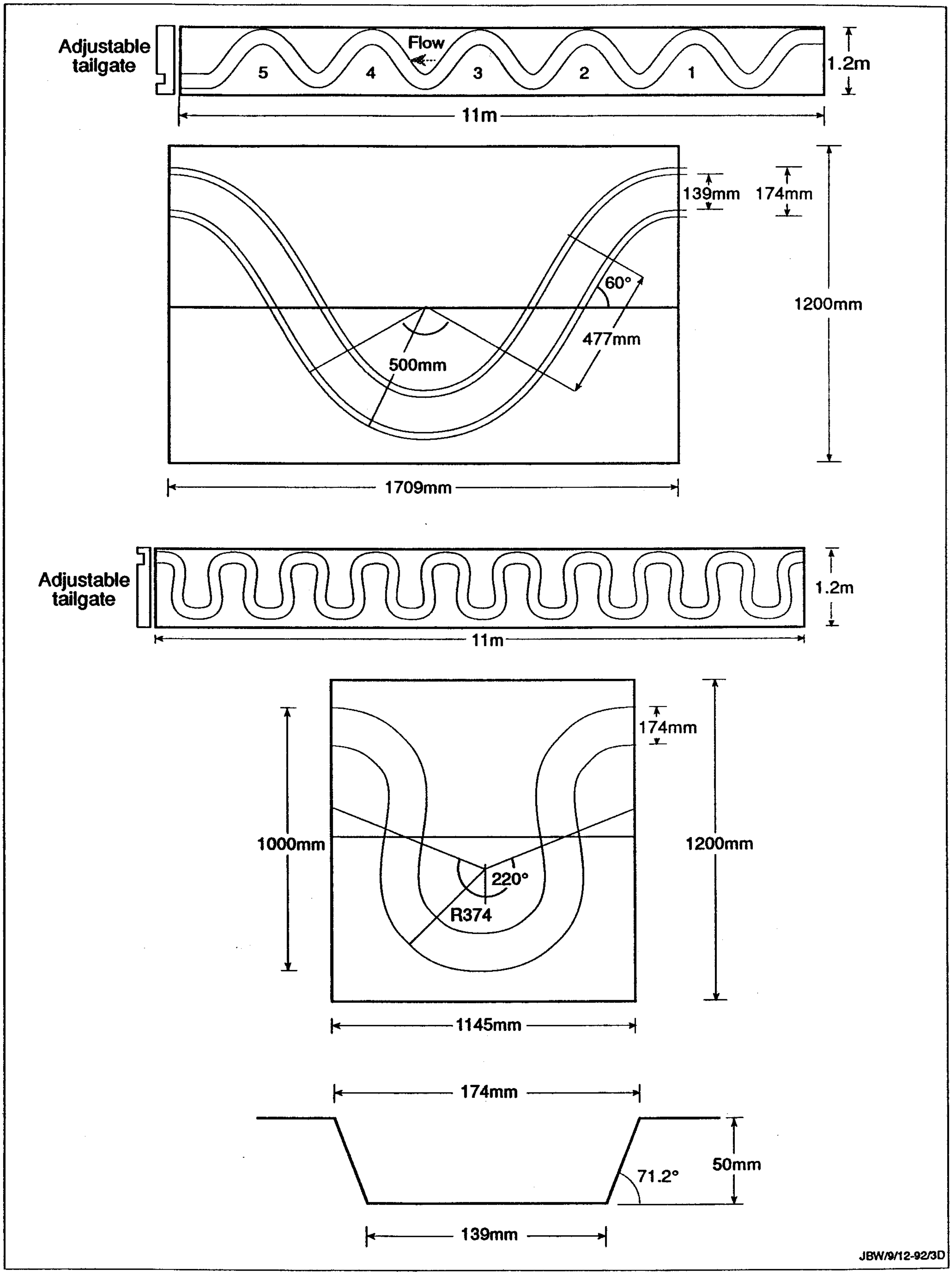

Figure 9 Plan geometries of the Aberdeen flume with channel sinuosities of 1.40 and 2.06 (after Willetts 1992)

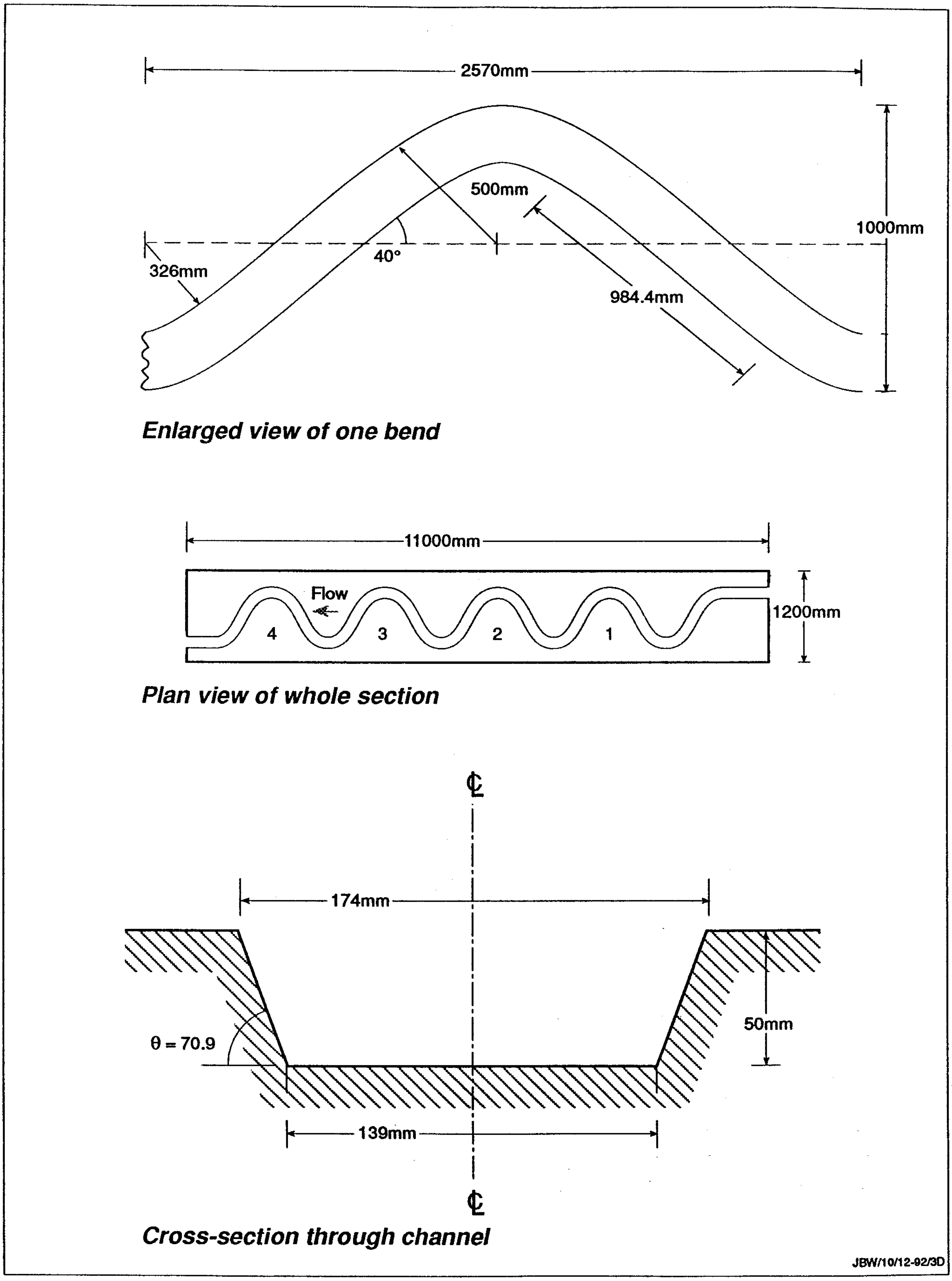

Figure 10 Plan geometry of the Aberdeen flume with channel sinuosity of 1.21 (after Willetts 1992)

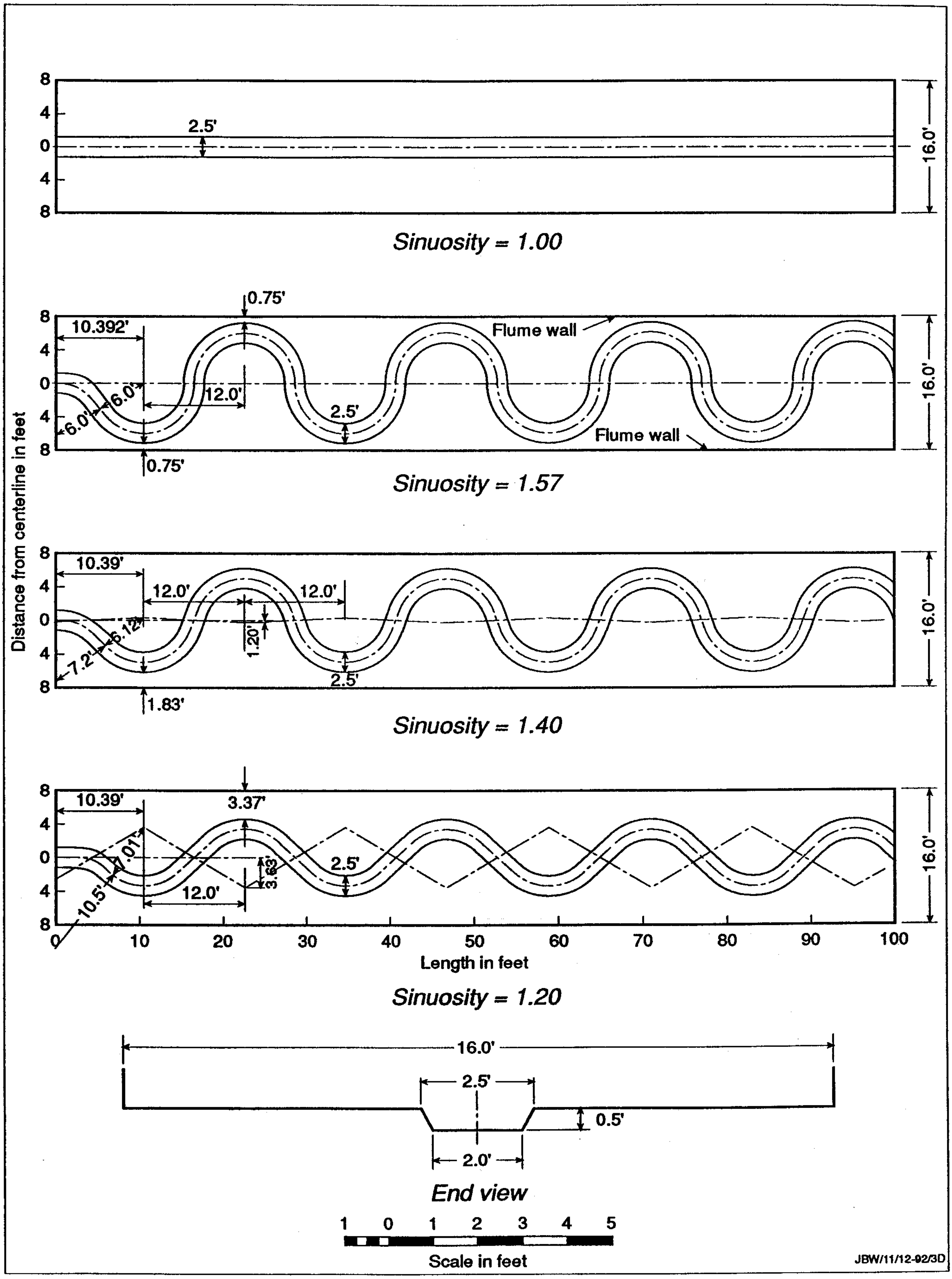

Figure 11 Plan and cross-sections for Vicksburg flume (after US Army 1956)

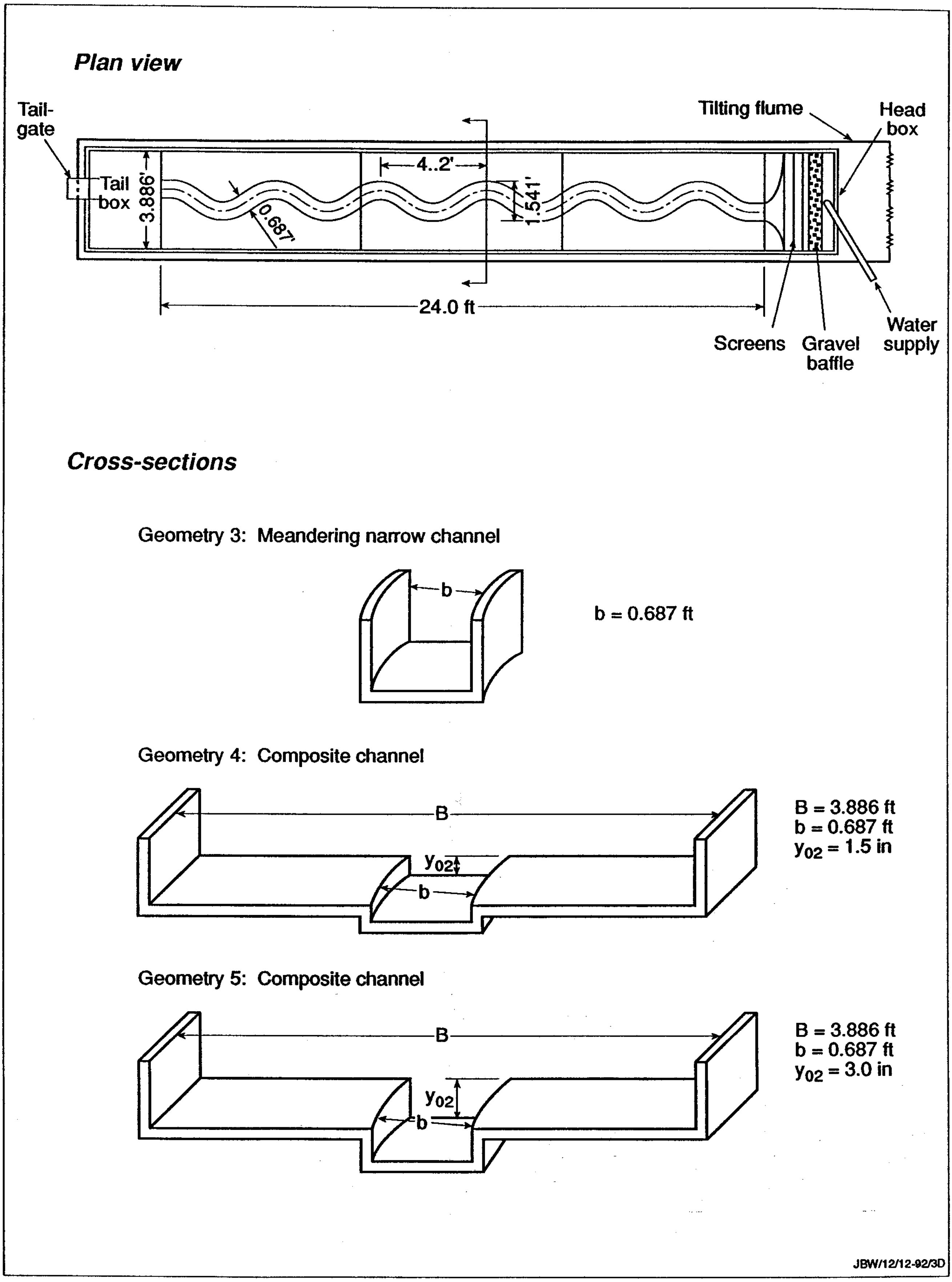

Figure 12 Plan and cross-sections for Sooky's flume (after Sooky 1964)

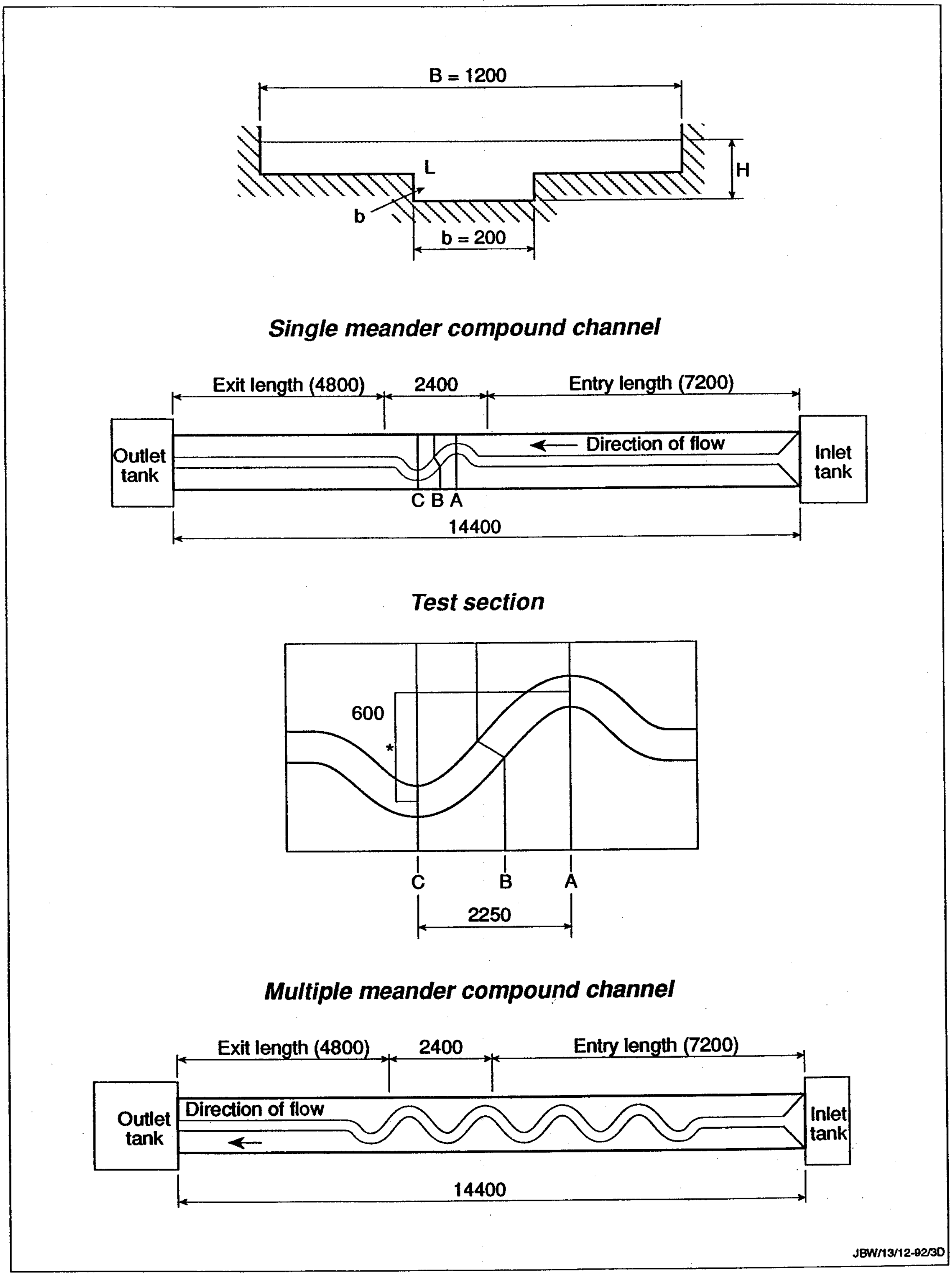

Figure 13 Plan and cross-sections for Kiely's flume (after Kiely 1990)

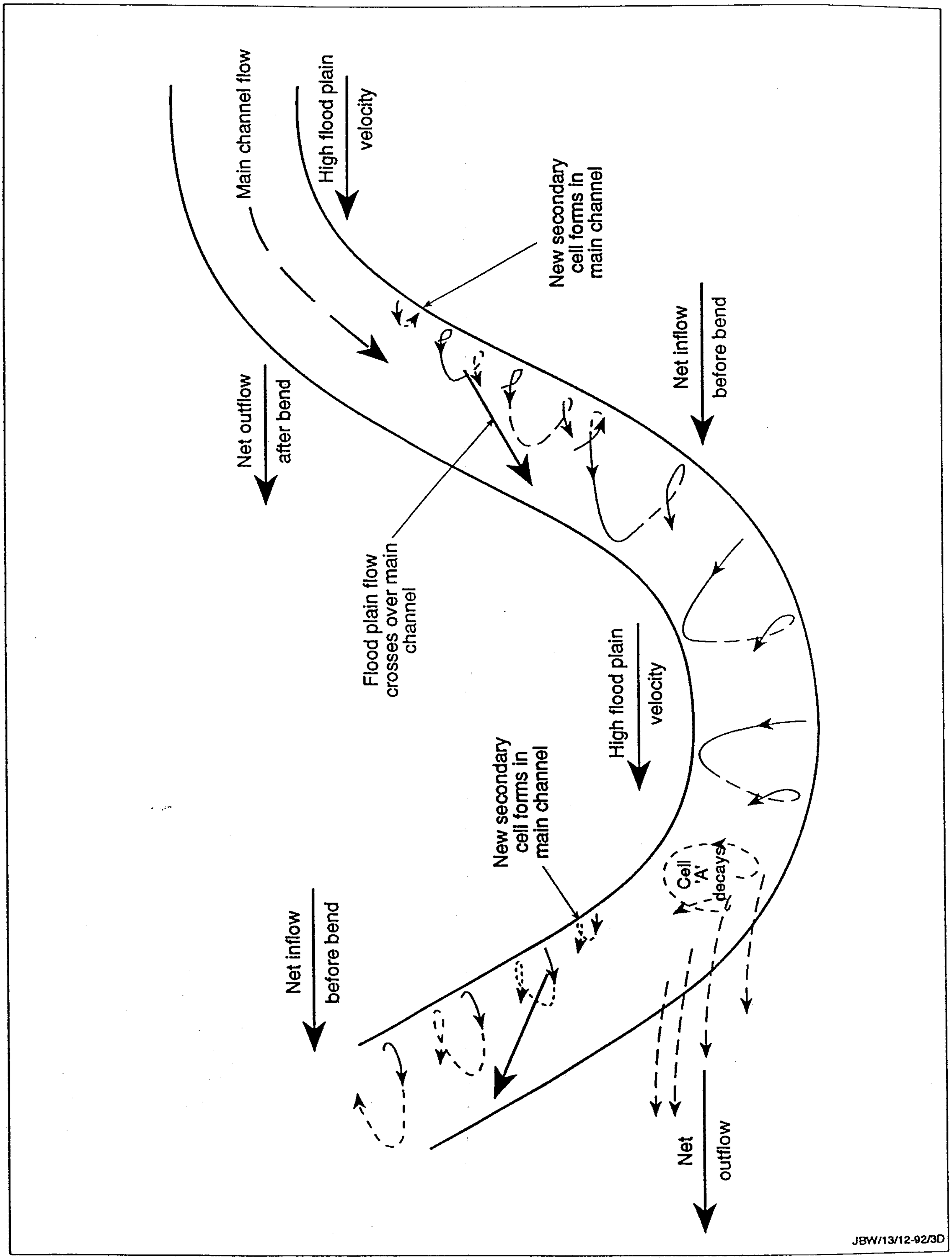

Figure 14 Flow processes in a meandering compound channel (after Ervine and Jasem, 1991)

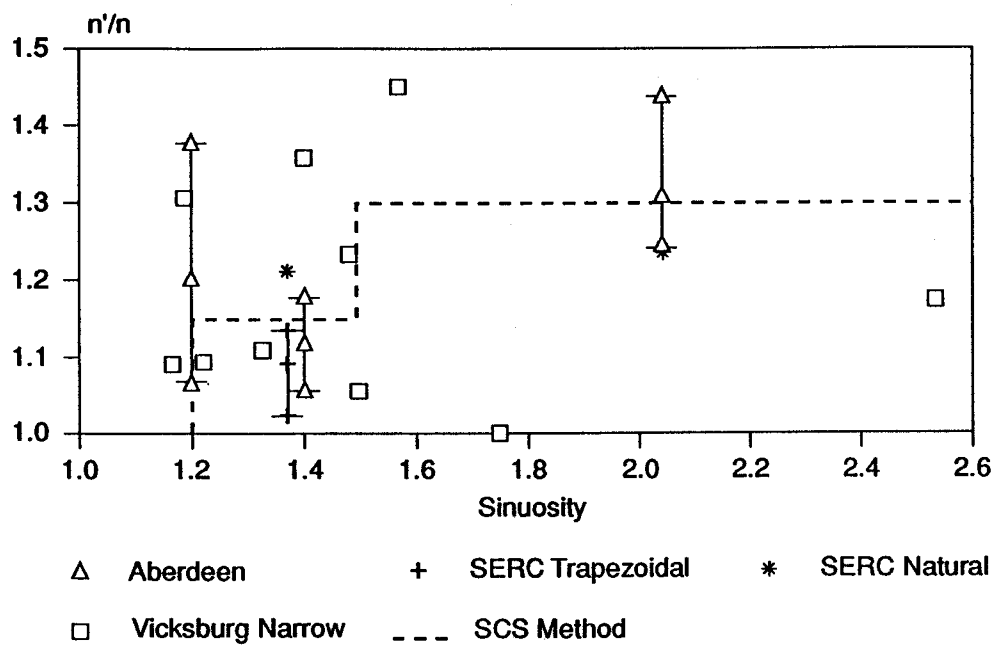

Figure 15 Adjustment to Manning's n for bend losses: measured and predicted

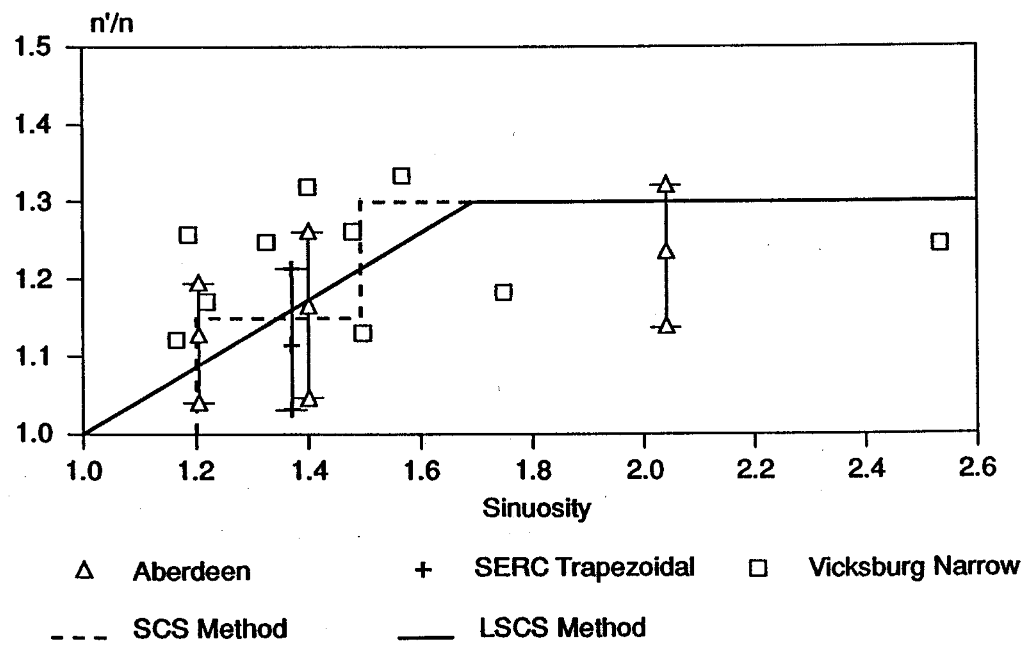

JBW/15,16/12-92/3D

Figure 16 Predicted adjustments to n for bend losses: Modified Chang method

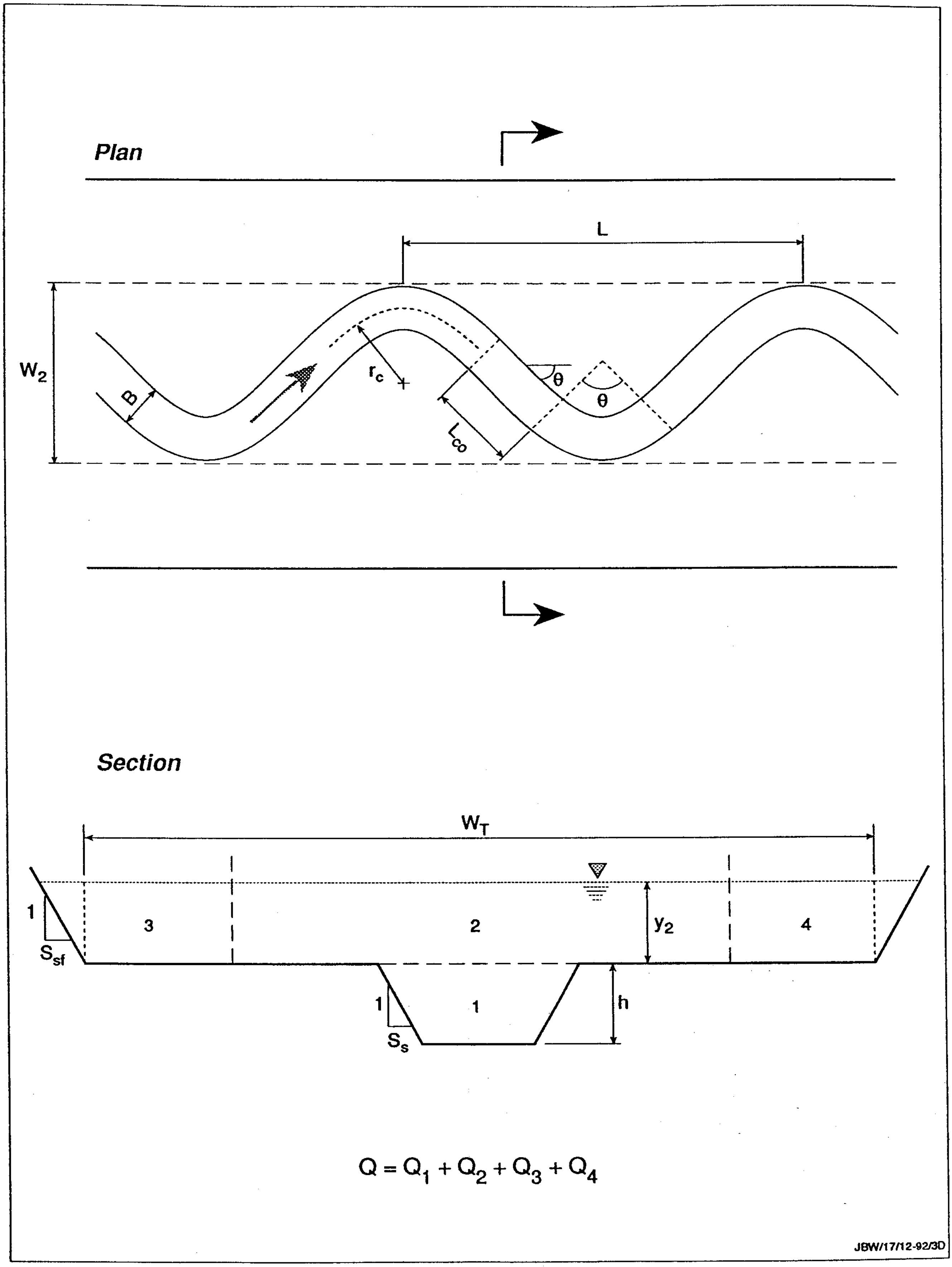

Figure 17 **Cross-section subdivision for overbank flows, Evine and Ellis (1987)**

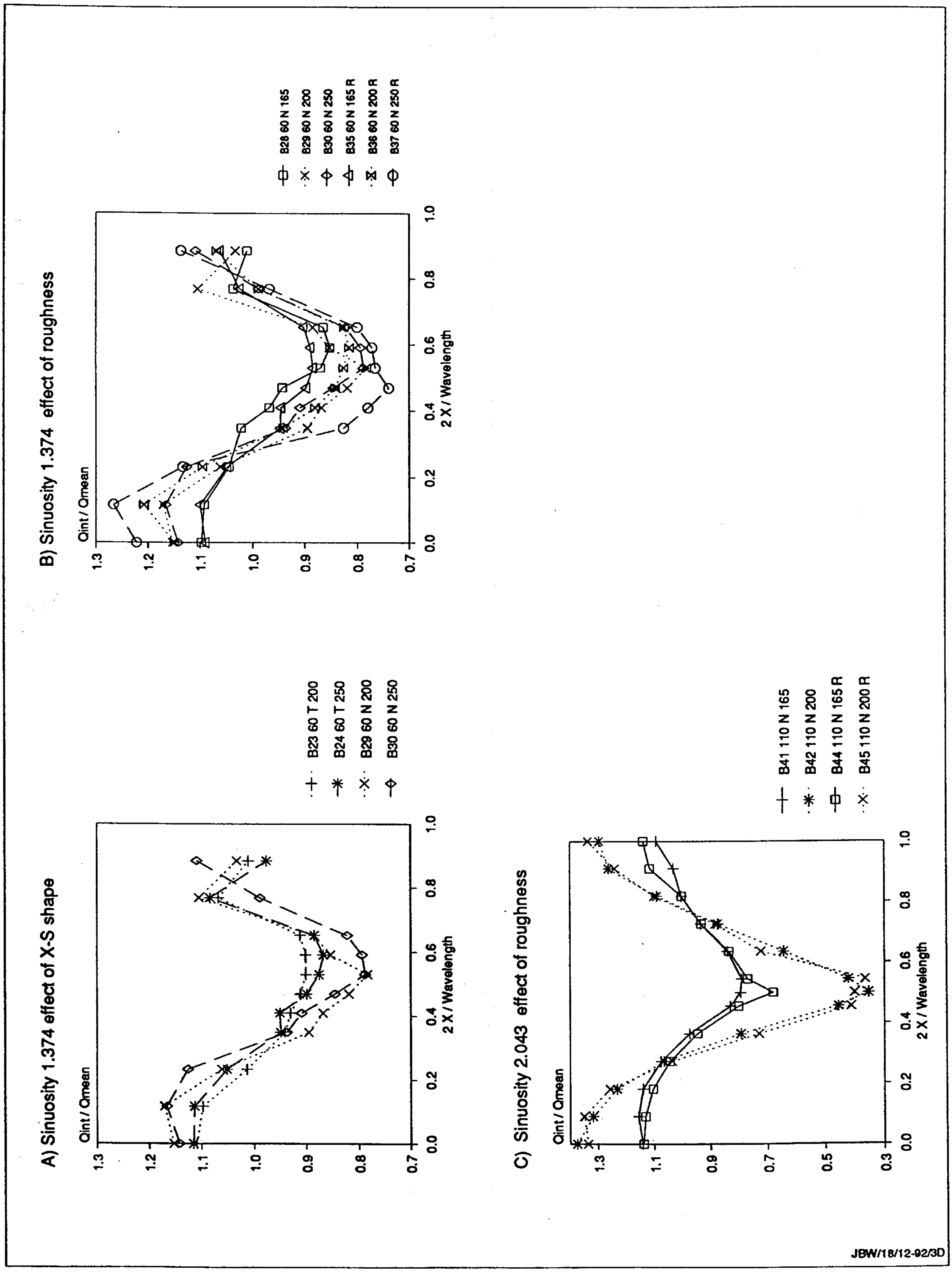

Figure 18 Variation of main channel discharge along a meander during overbank flow (FCF Phase B)

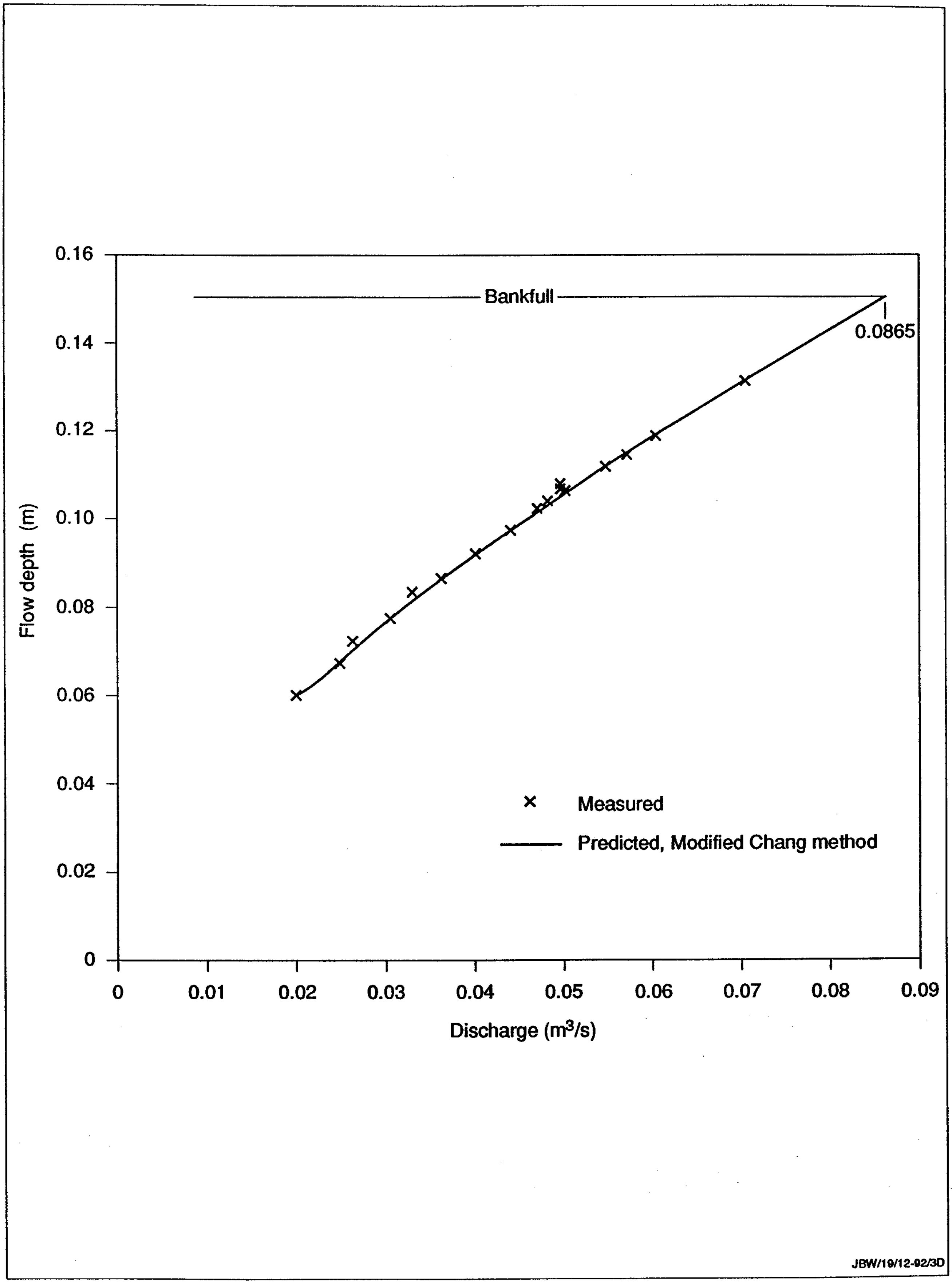

Figure 19 Stage-discharge relationship for 60° trapezoidal channel, inbank flows

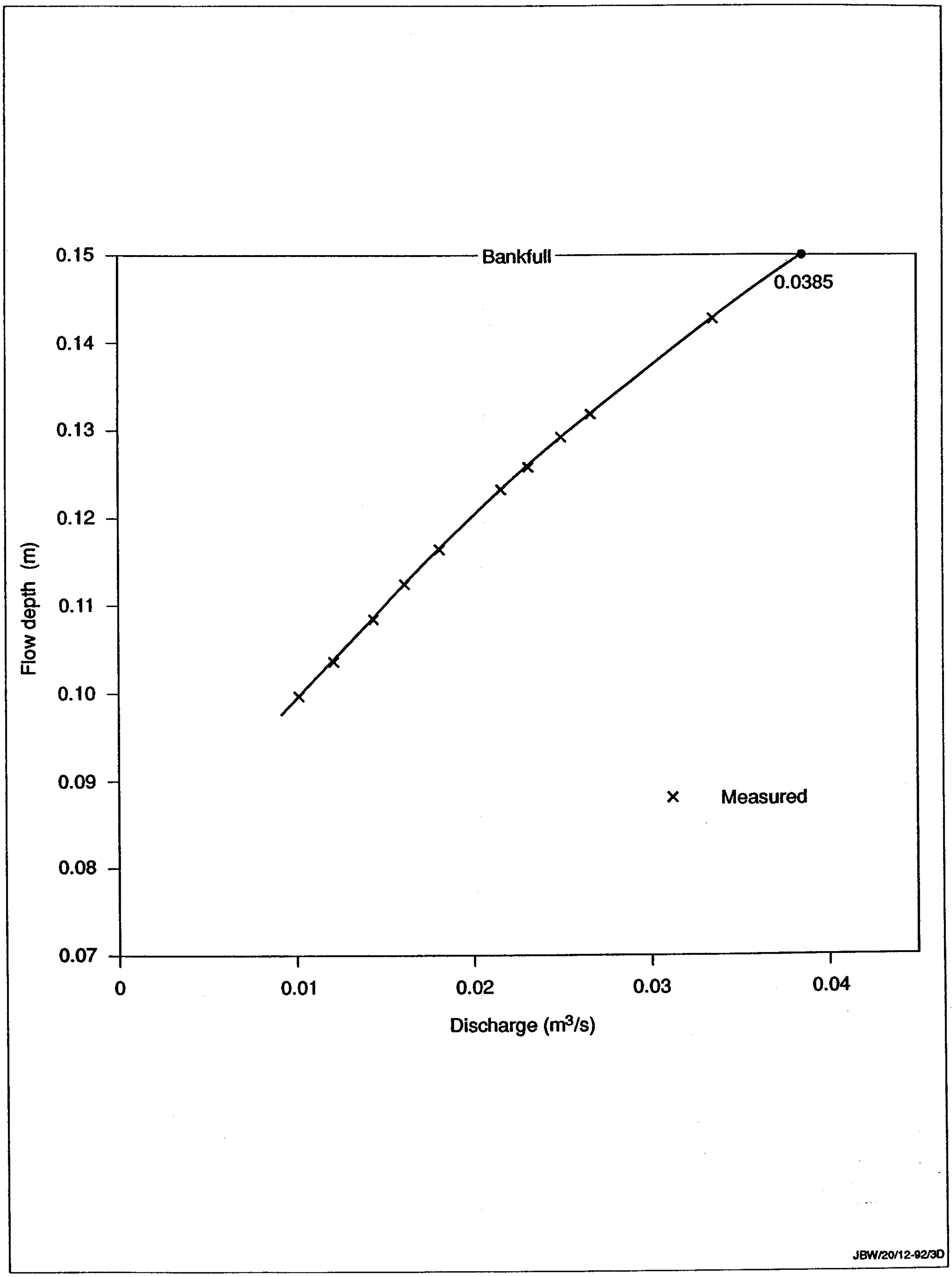

Figure 20 Stage-discharge relationship for 60° pseudo-natural channel, inbank flows

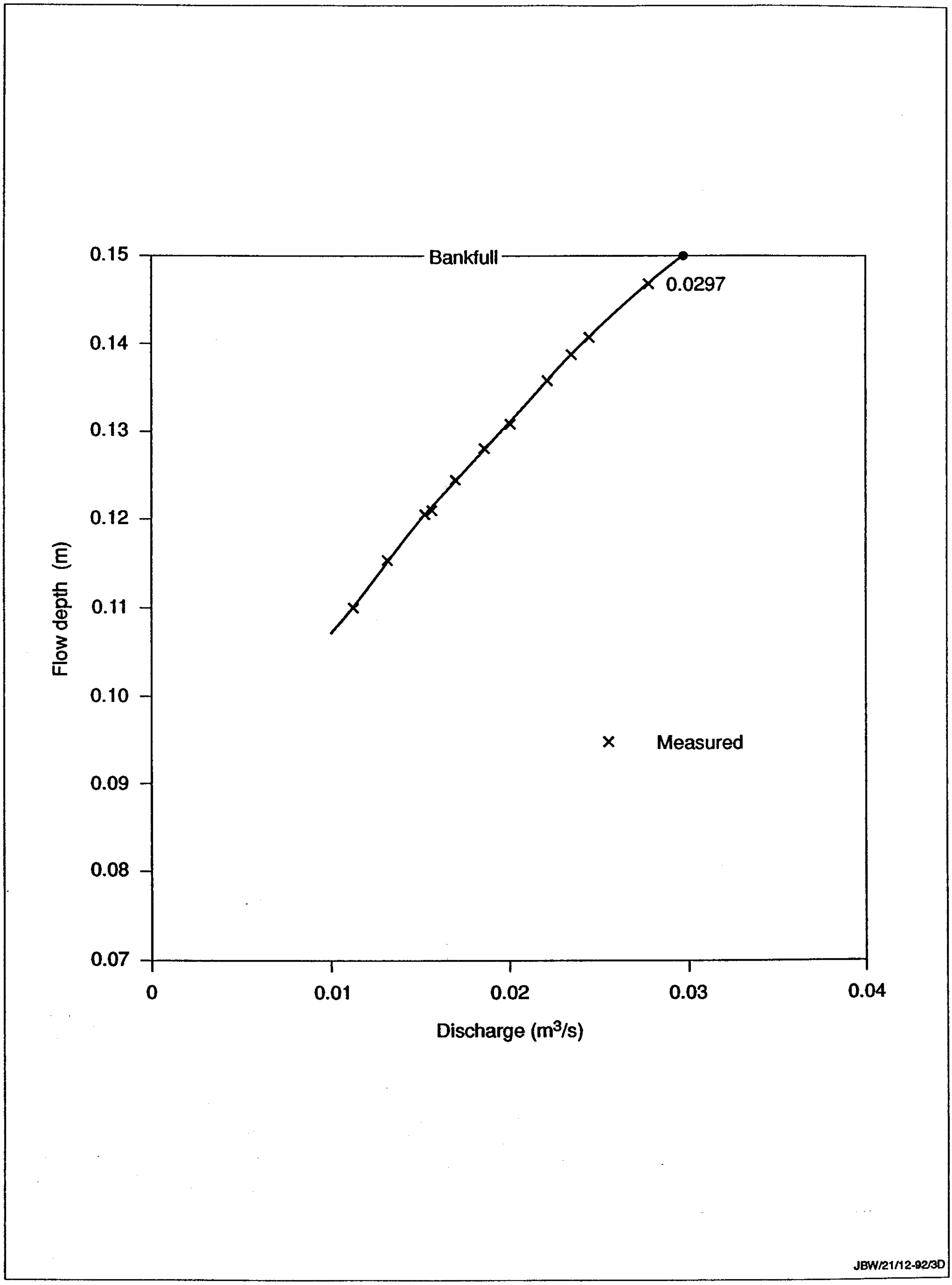

Figure 21 Stage-discharge relationship for 110° pseudo-natural channel, inbank flows

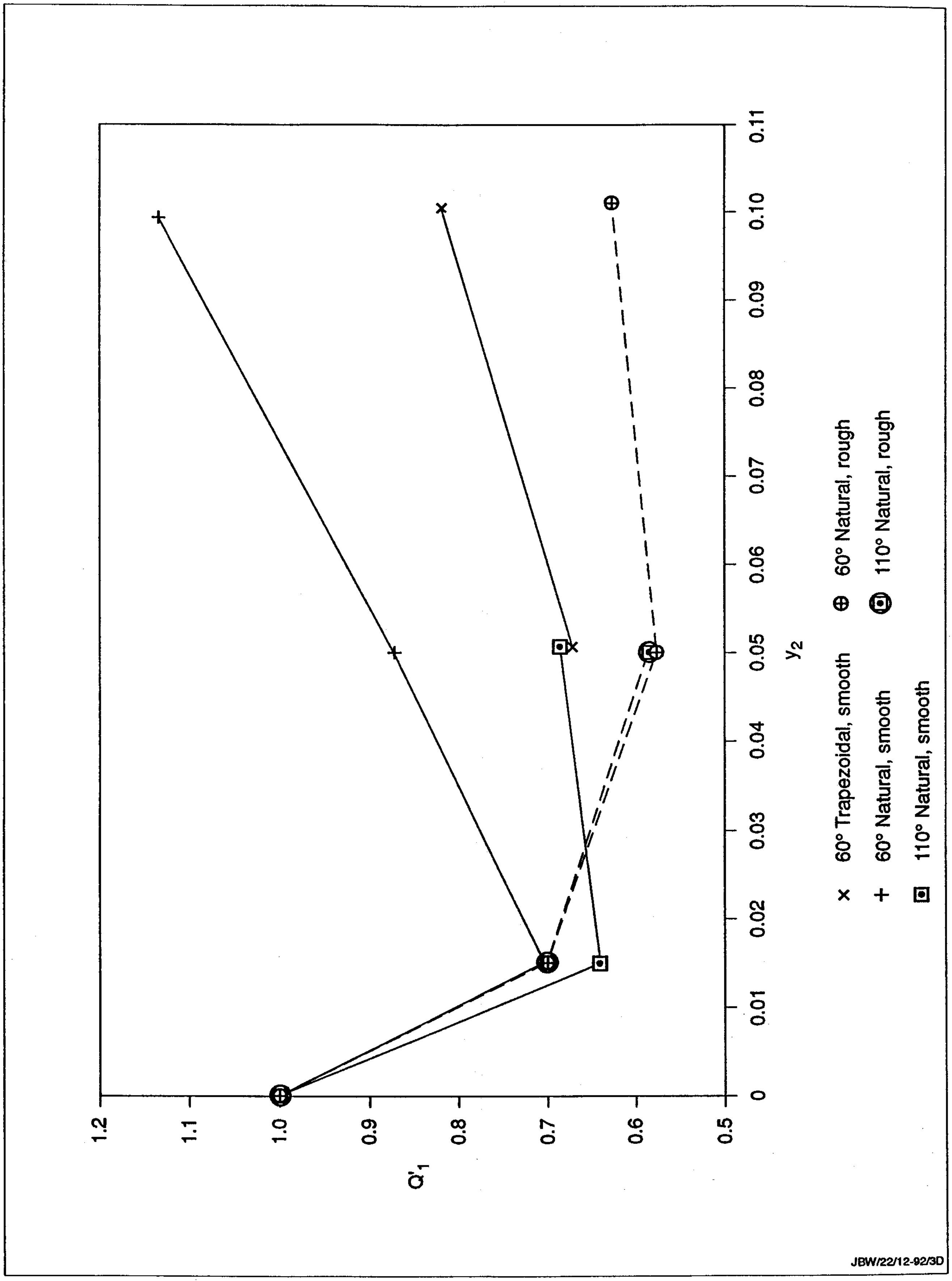

Figure 22 Variation of dimensionless main channel discharge with flow depth on flood plain

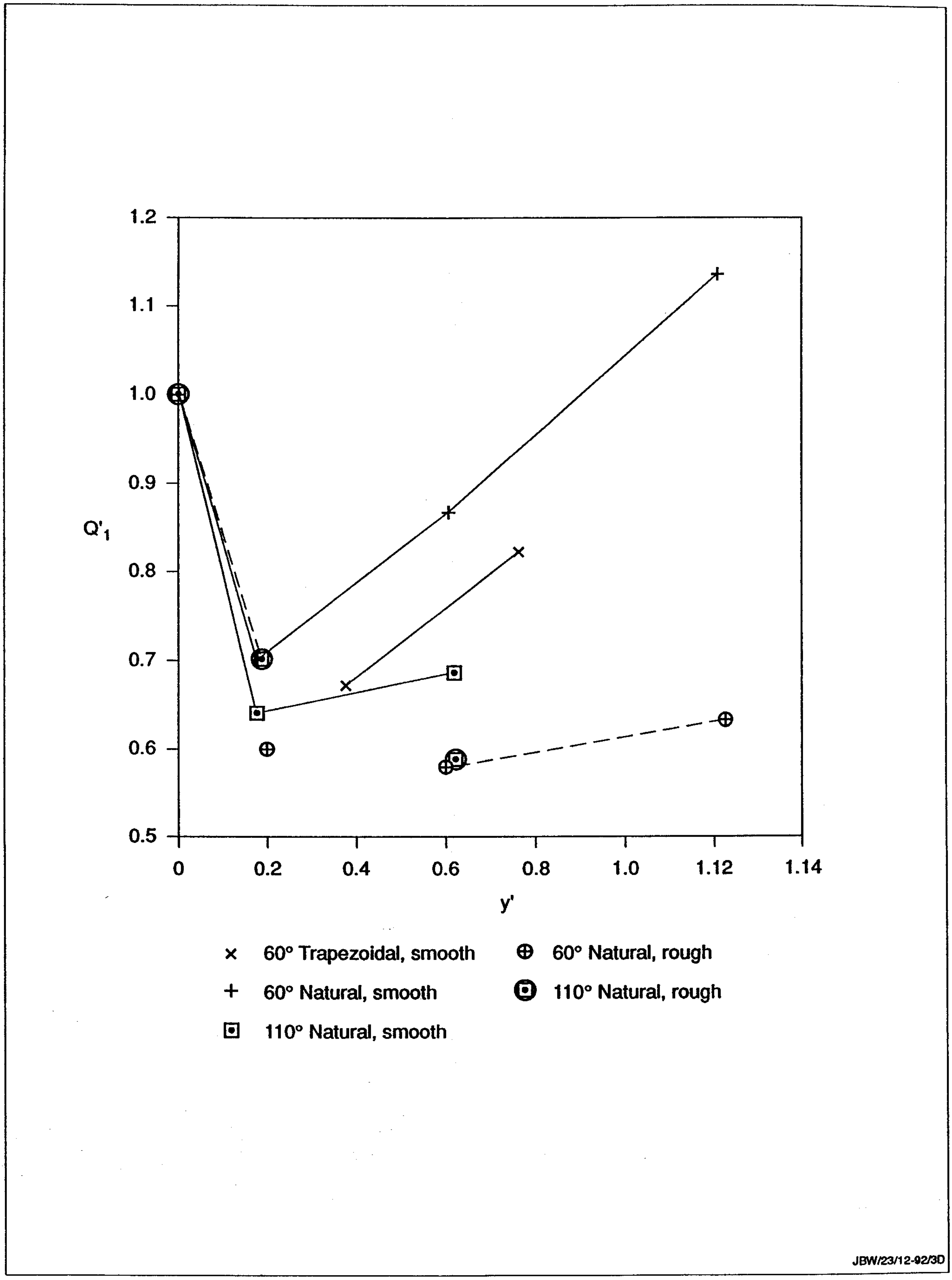

Figure 23 Variation of dimensionless main channel discharge with dimensionless flood plain flow depth

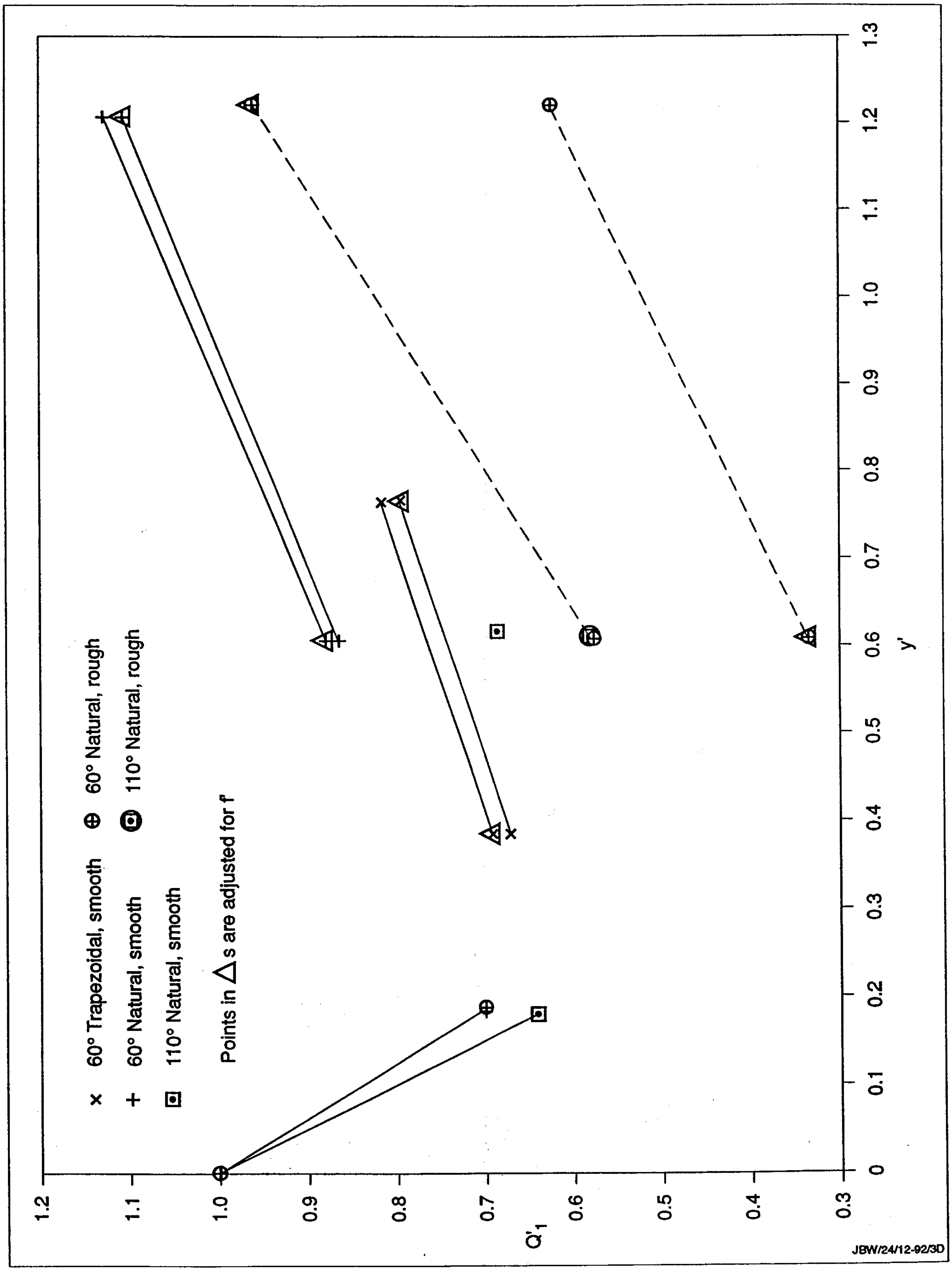

Figure 24 **Variation of dimensionless main channel discharge with dimensionless flow depth with points adjusted for friction factor ratio**

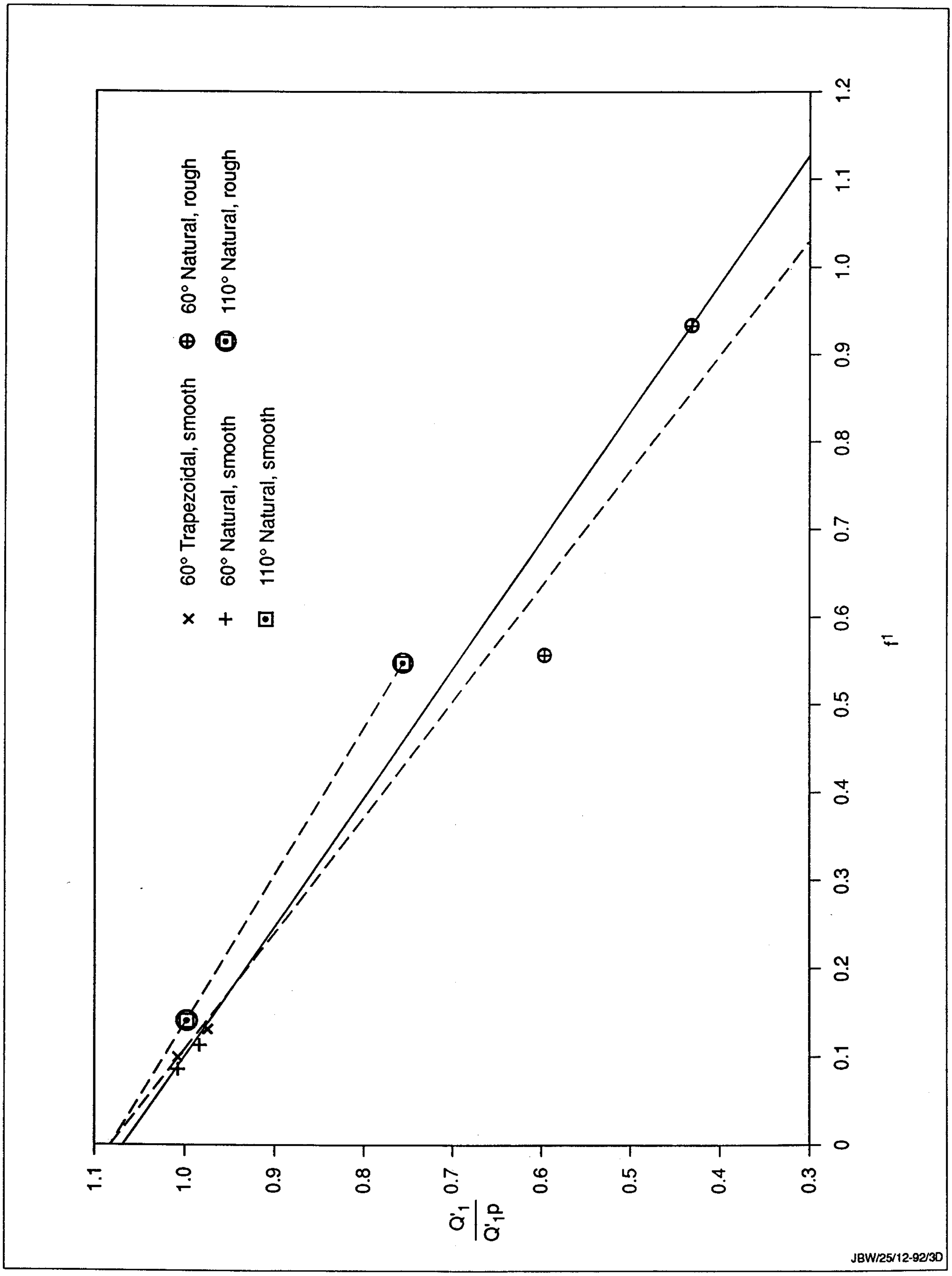

Figure 25 Additional adjustment to discharge for relative roughness

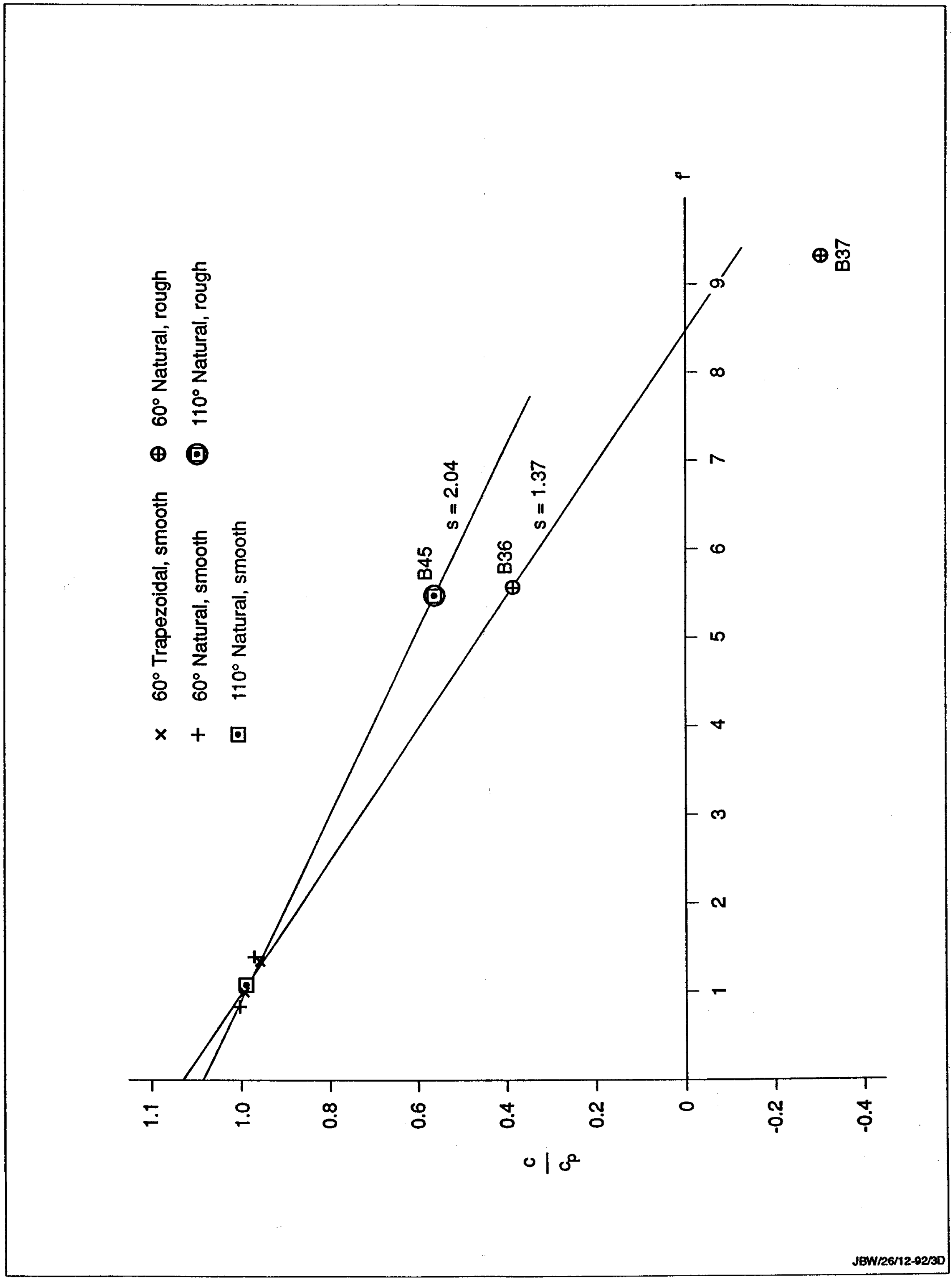

Figure 26 Adjustment to c for relative roughness

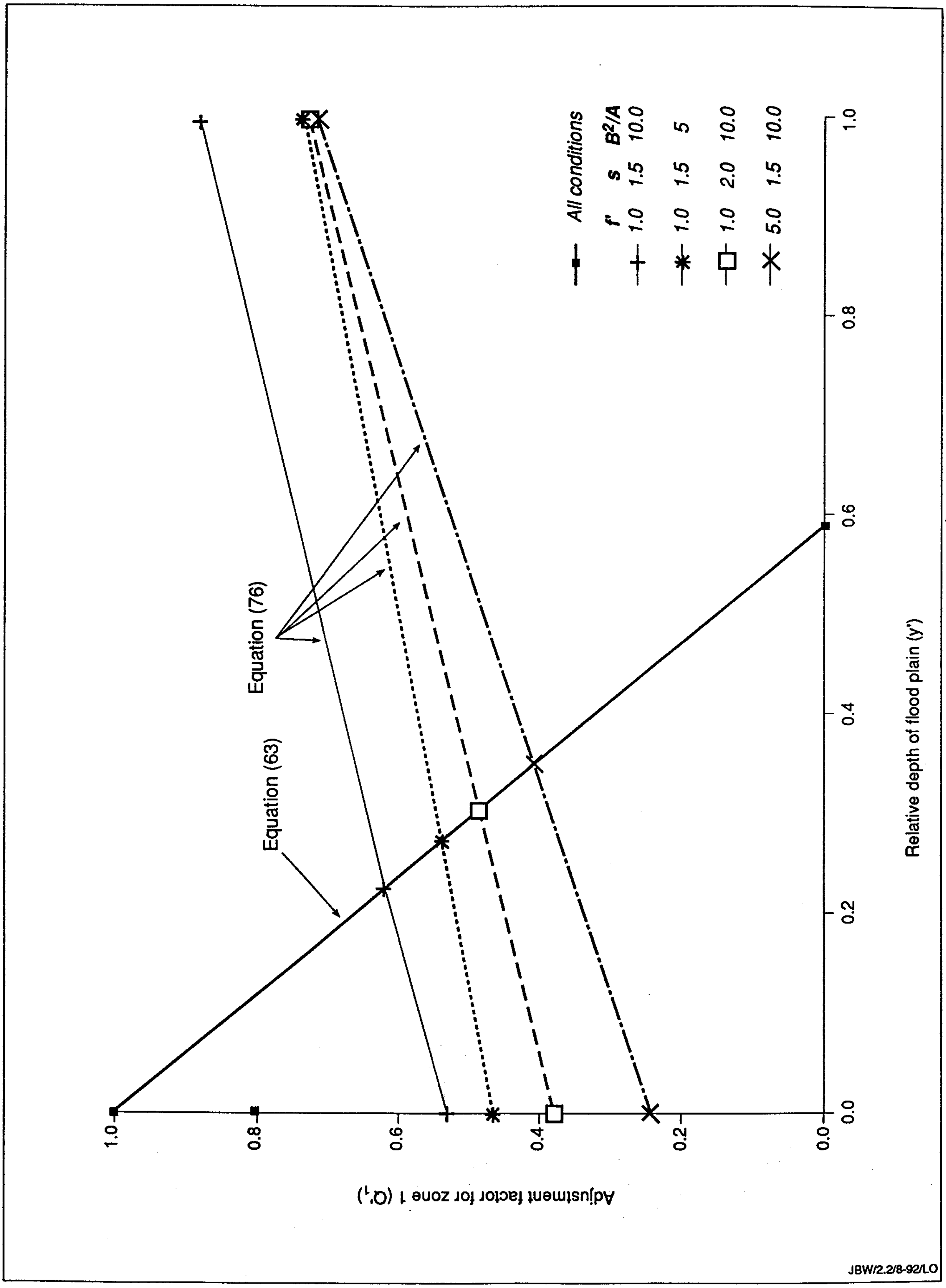

Figure 26b Adjustment factor for Zone 1 discharge

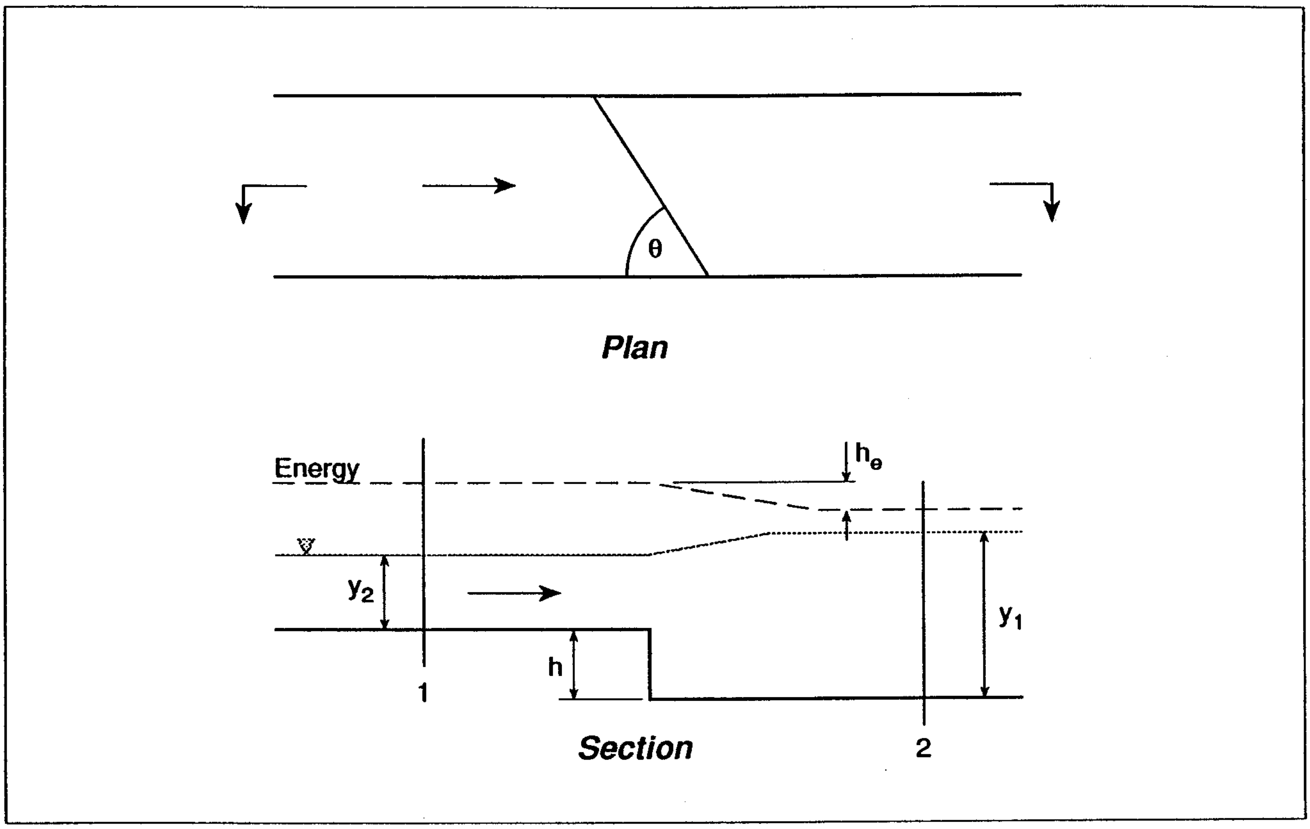

Figure 27 Flow expansion over a downward step

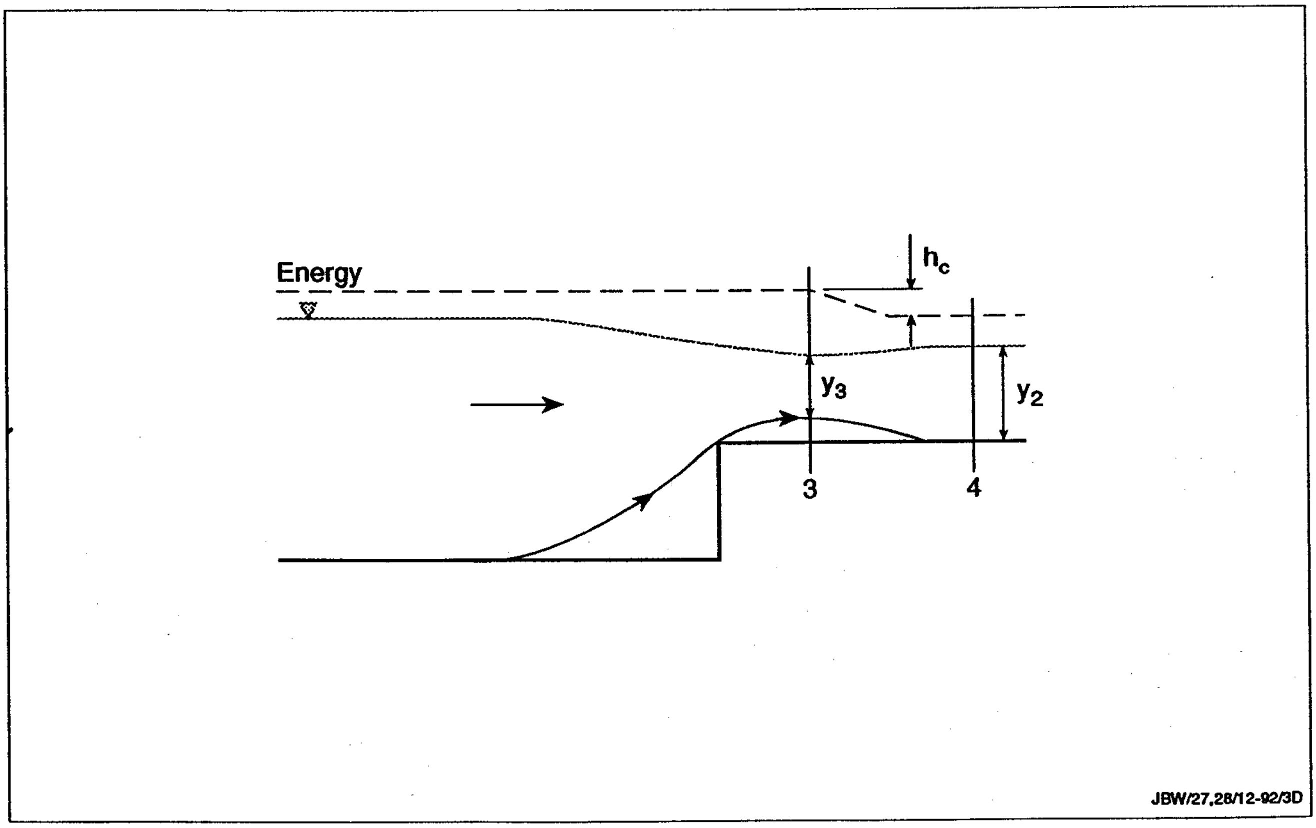

Figure 28 Flow contraction over an upward step

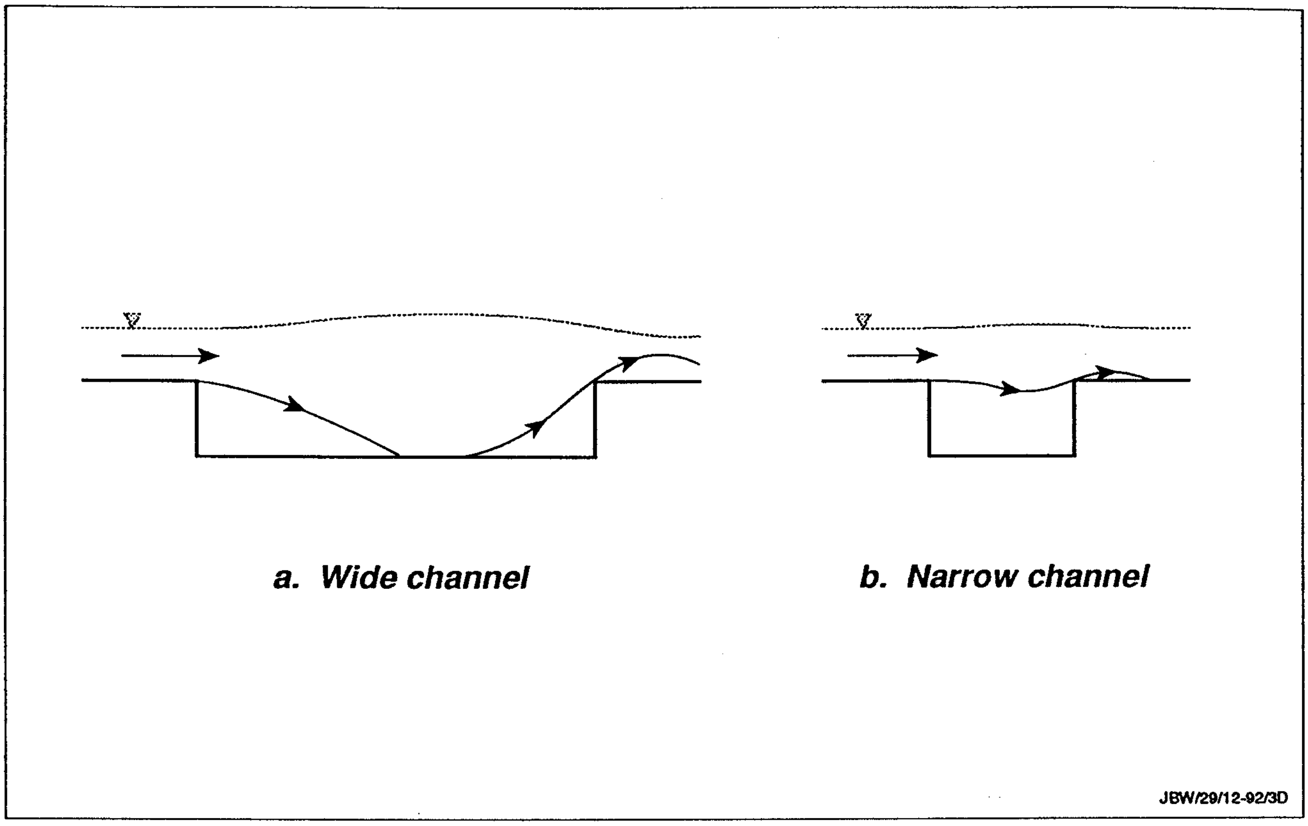

Figure 29 Expansion and contraction flow patterns

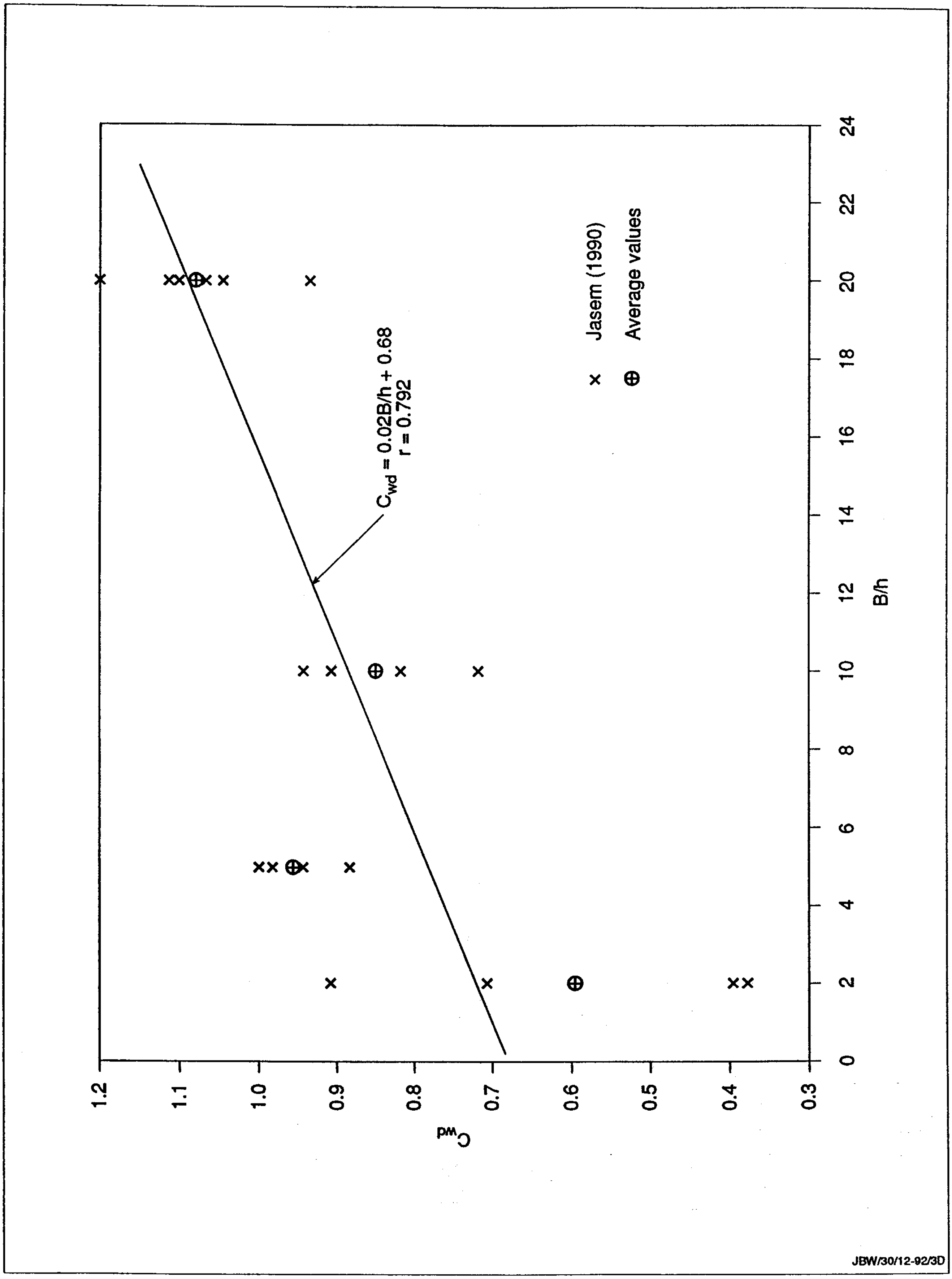

Figure 30 Width to depth ratio correction for expansion losses

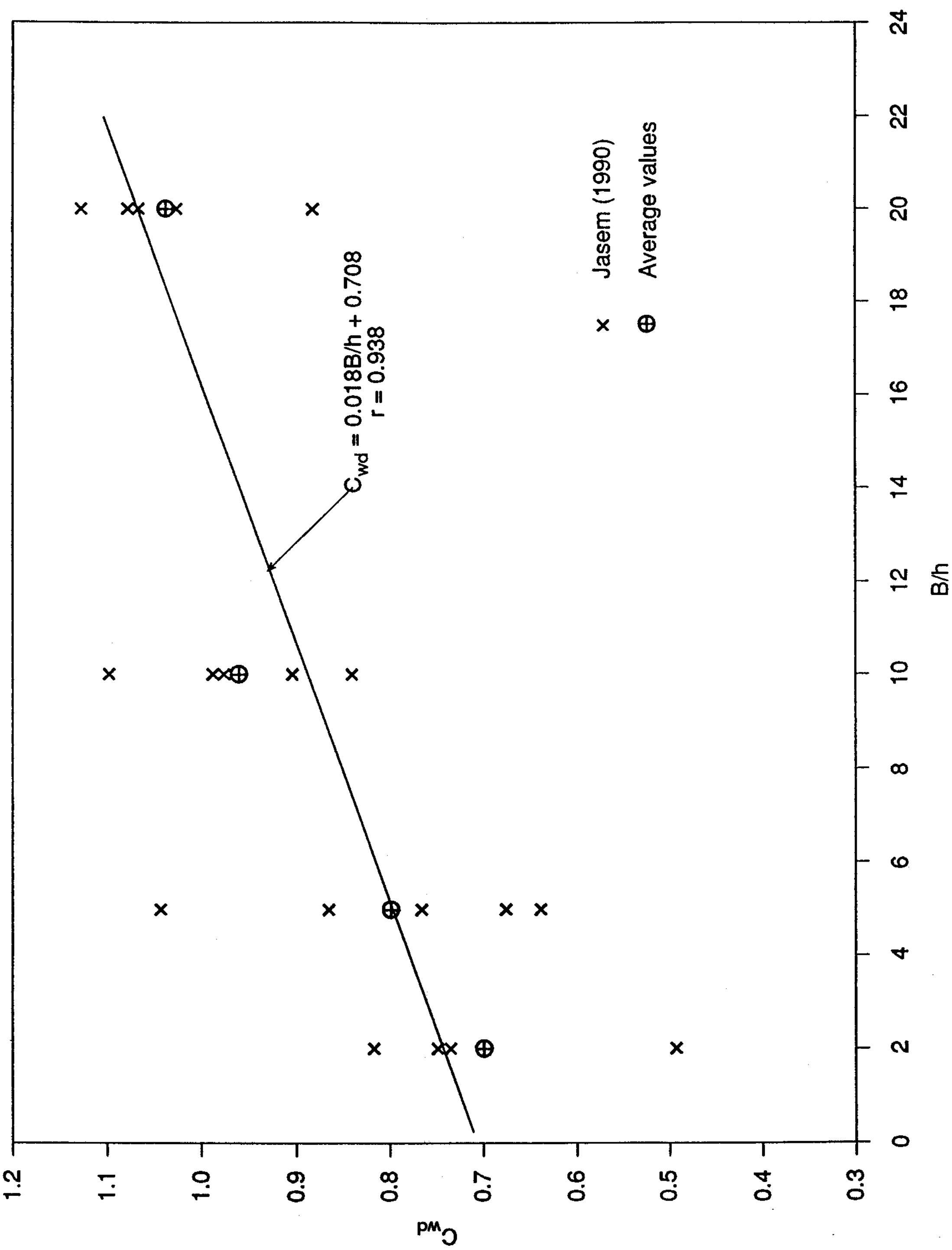

JBW/31/12-92/3D

Figure 31 Width to depth ratio correction for contraction losses

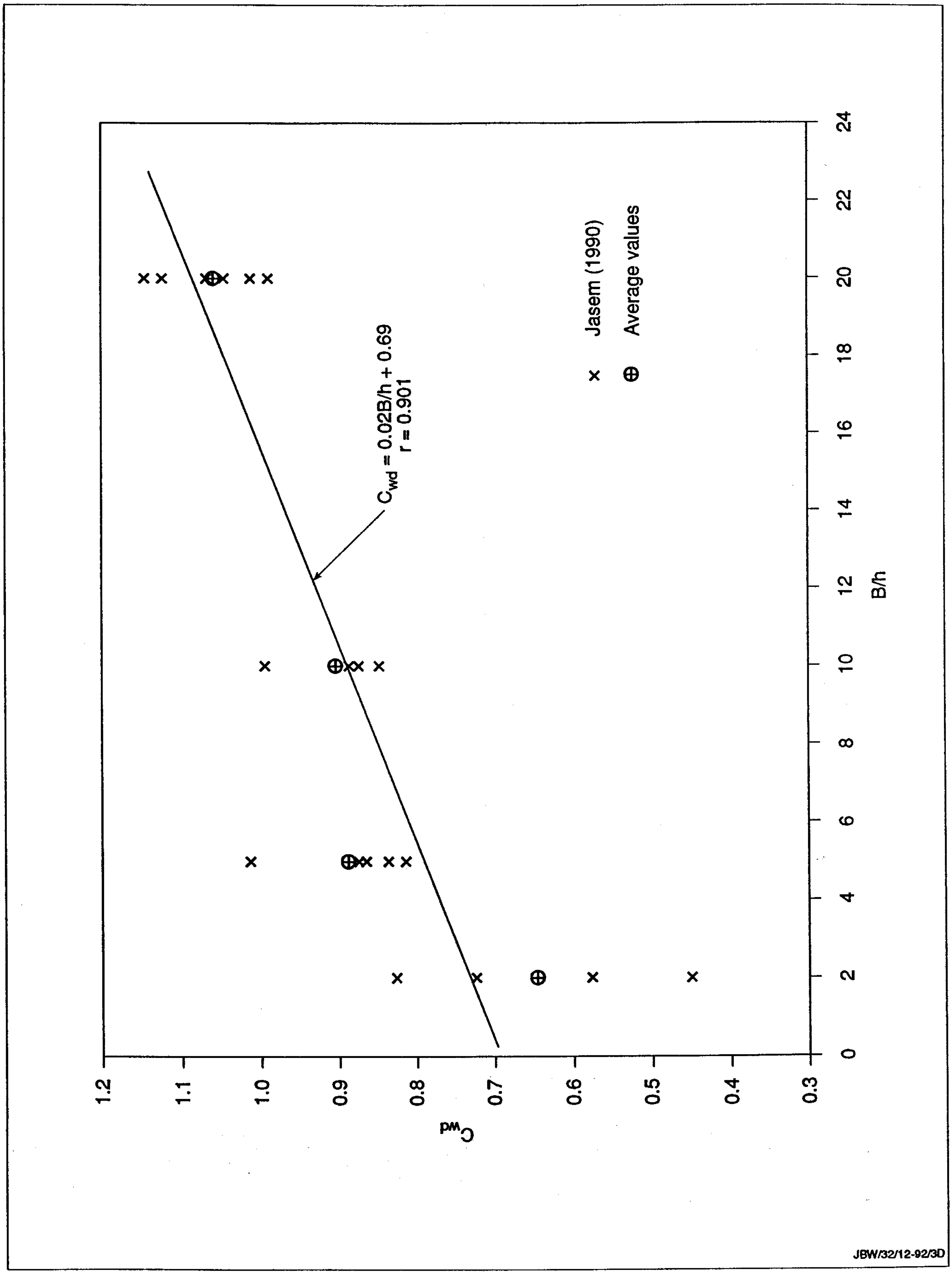

Figure 32 Width to depth ratio correction for combined expansion and contraction losses

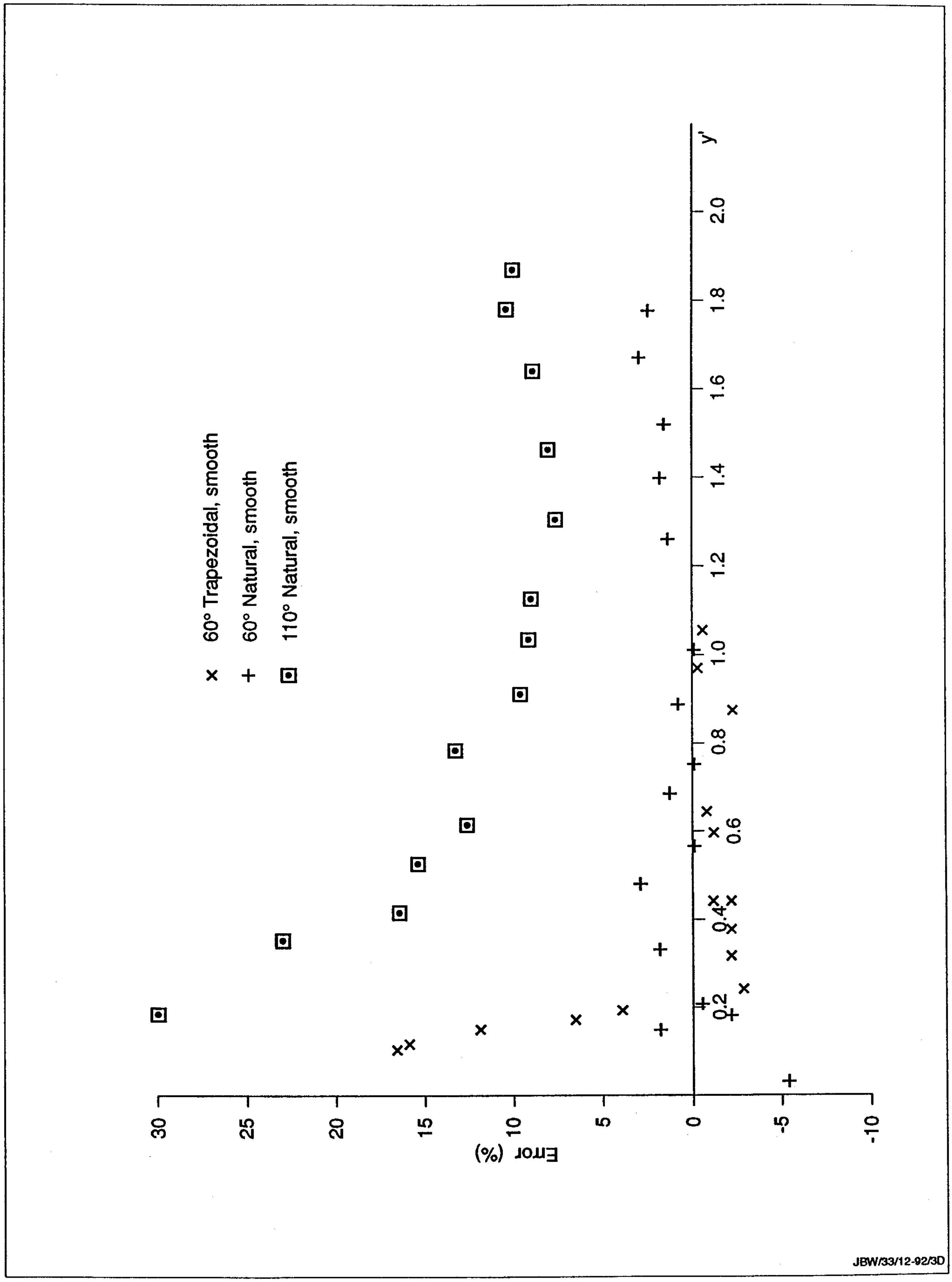

Figure 33 Errors for SERC predictions before sinuosity corrections

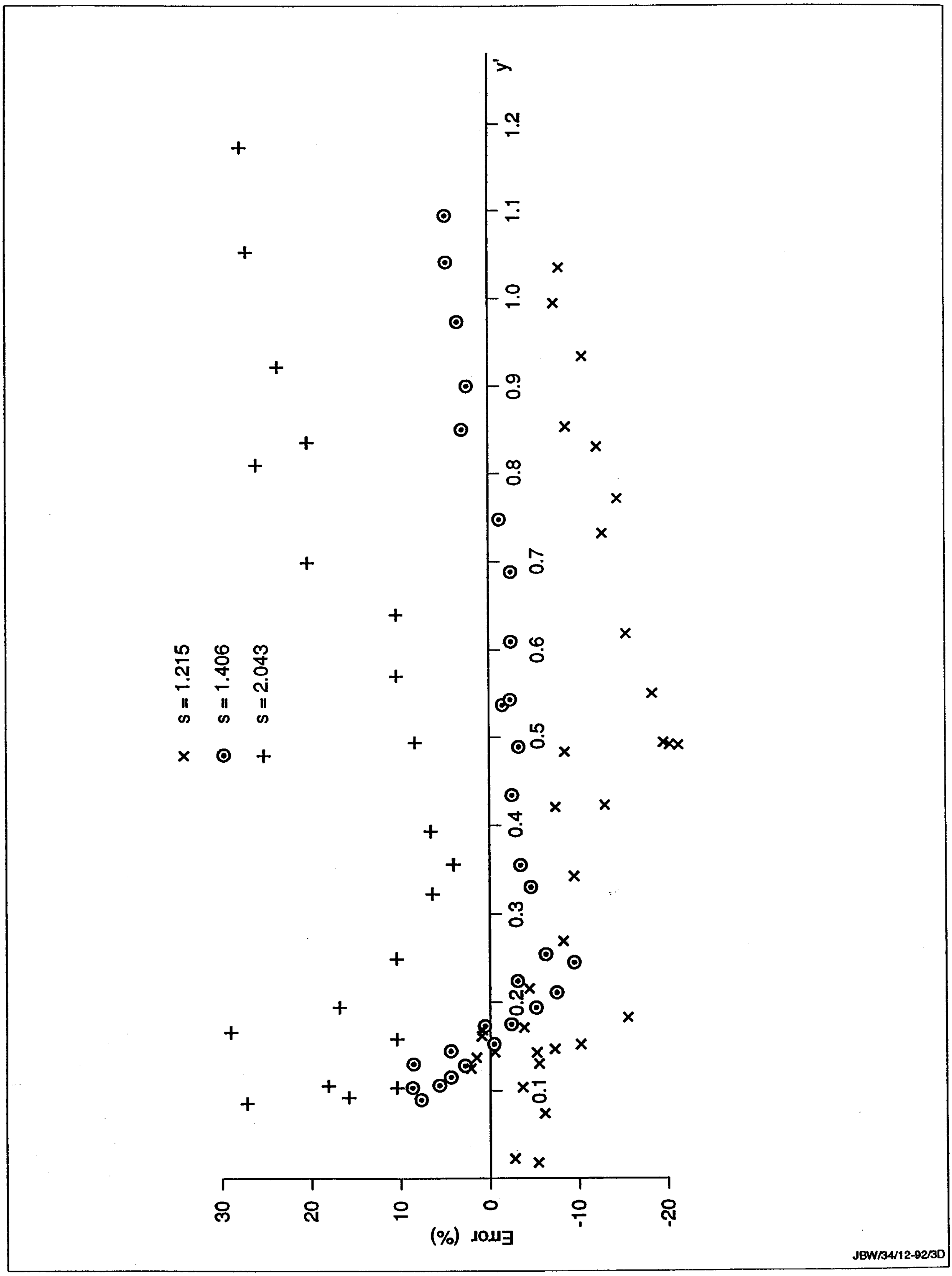

Figure 34 Errors for Aberdeen predictions before sinuosity corrections

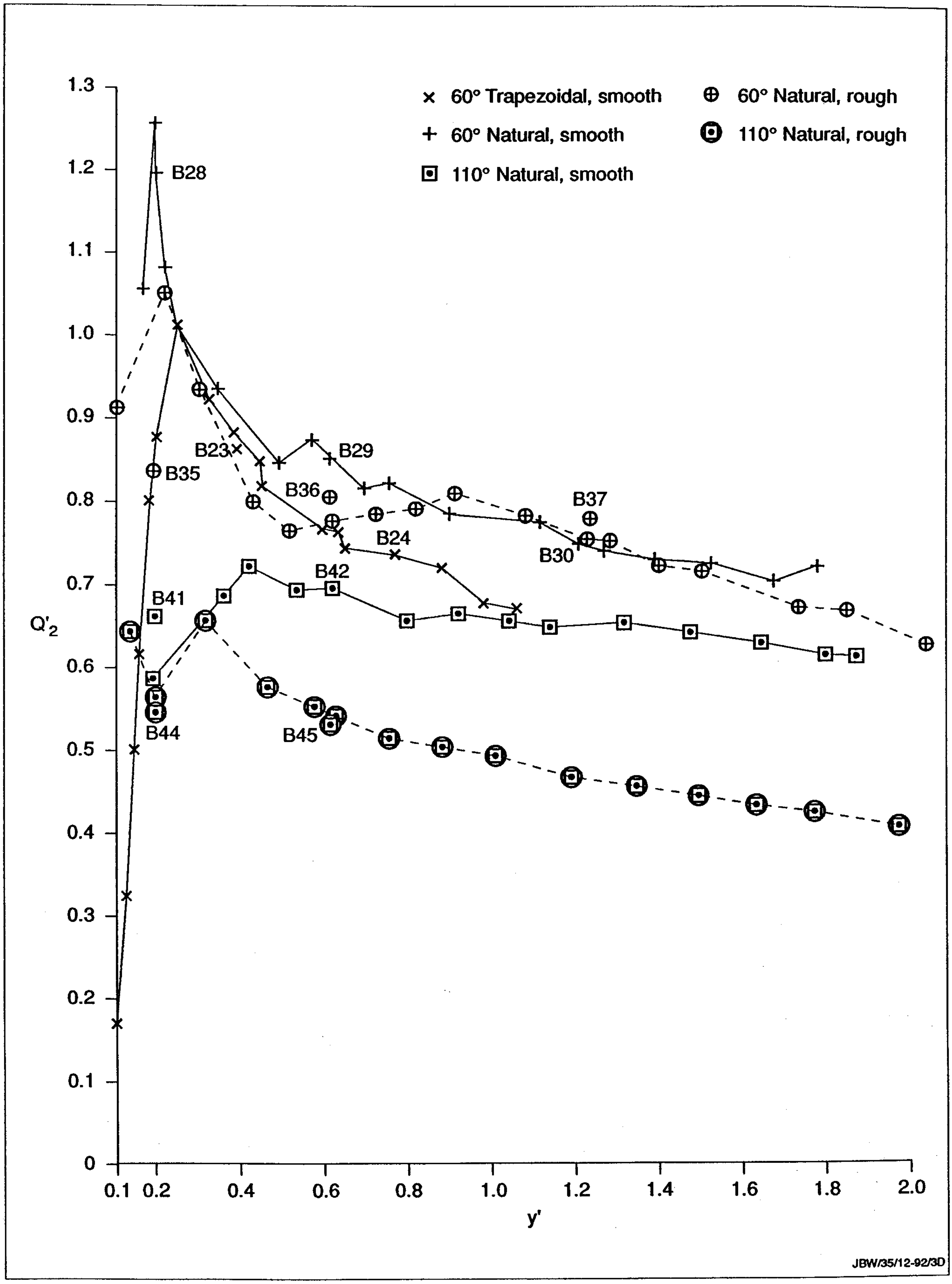

Figure 35 Adjustment factor for inner flood plain discharges for SERC Phase B experiments

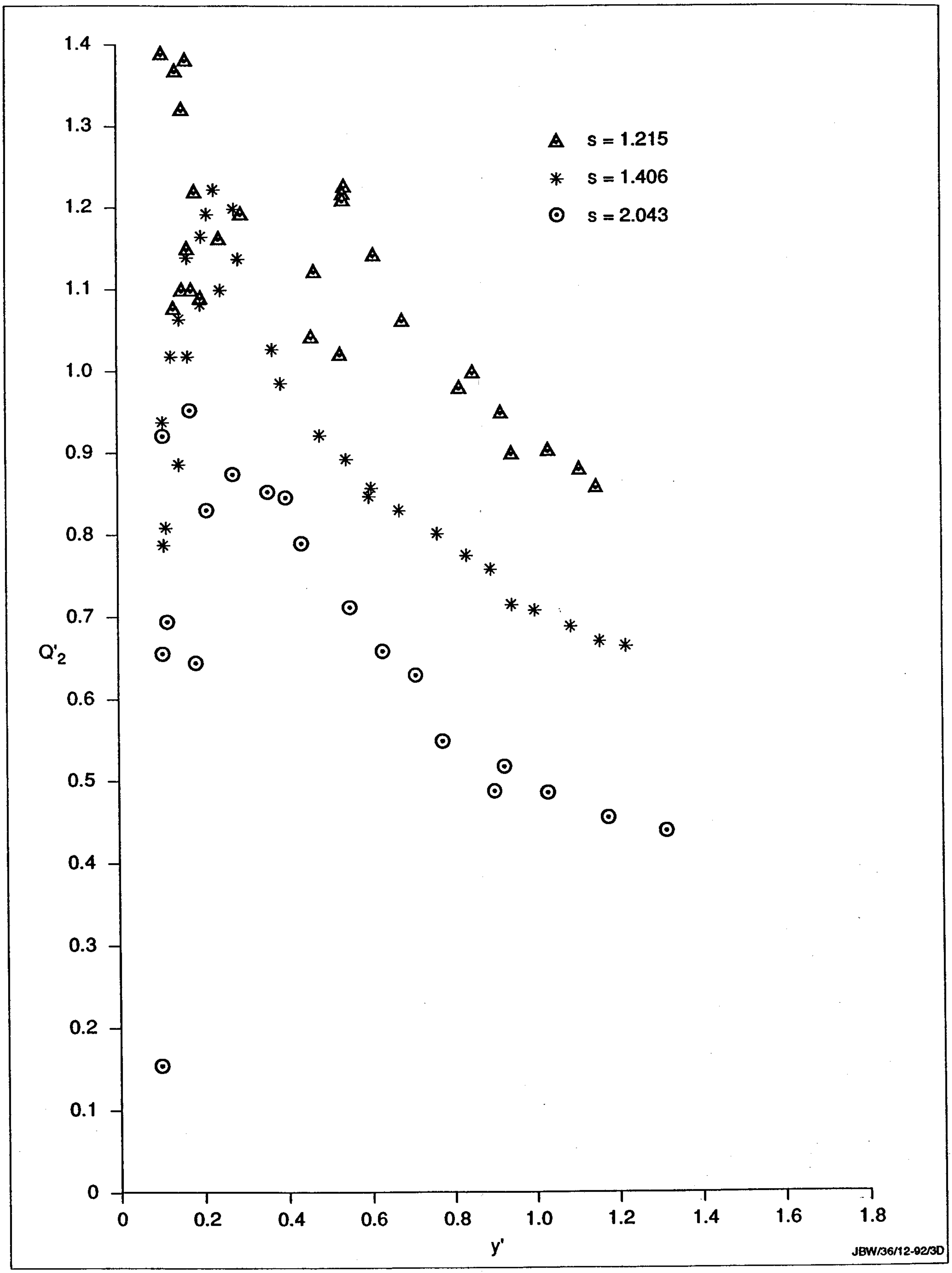

Figure 36 Adjustment factor for inner flood plain discharges for Aberdeen experiments

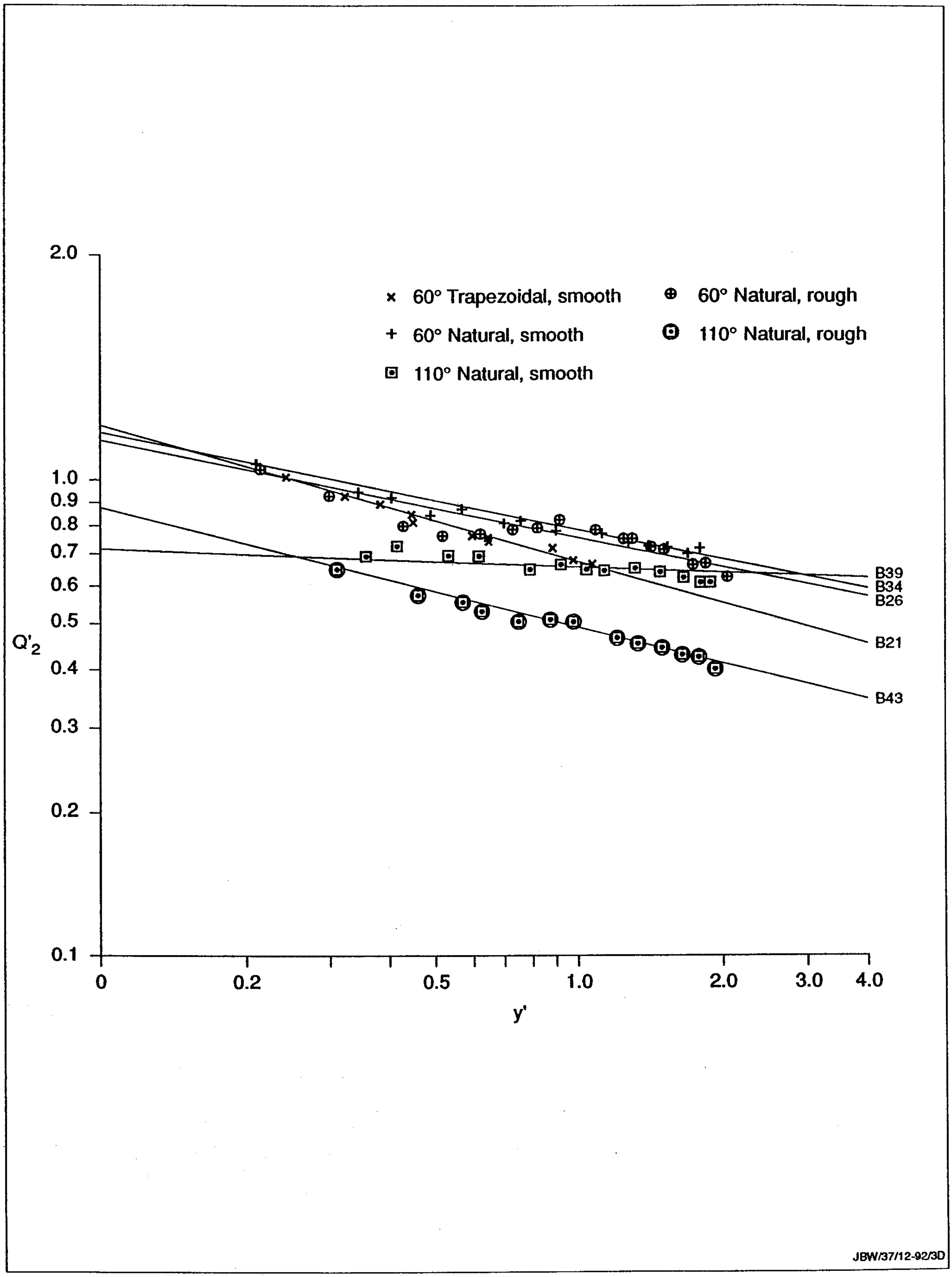

Figure 37 Adjustment factor for inner flood plain discharges for y' > 0.2 SERC Phase B data

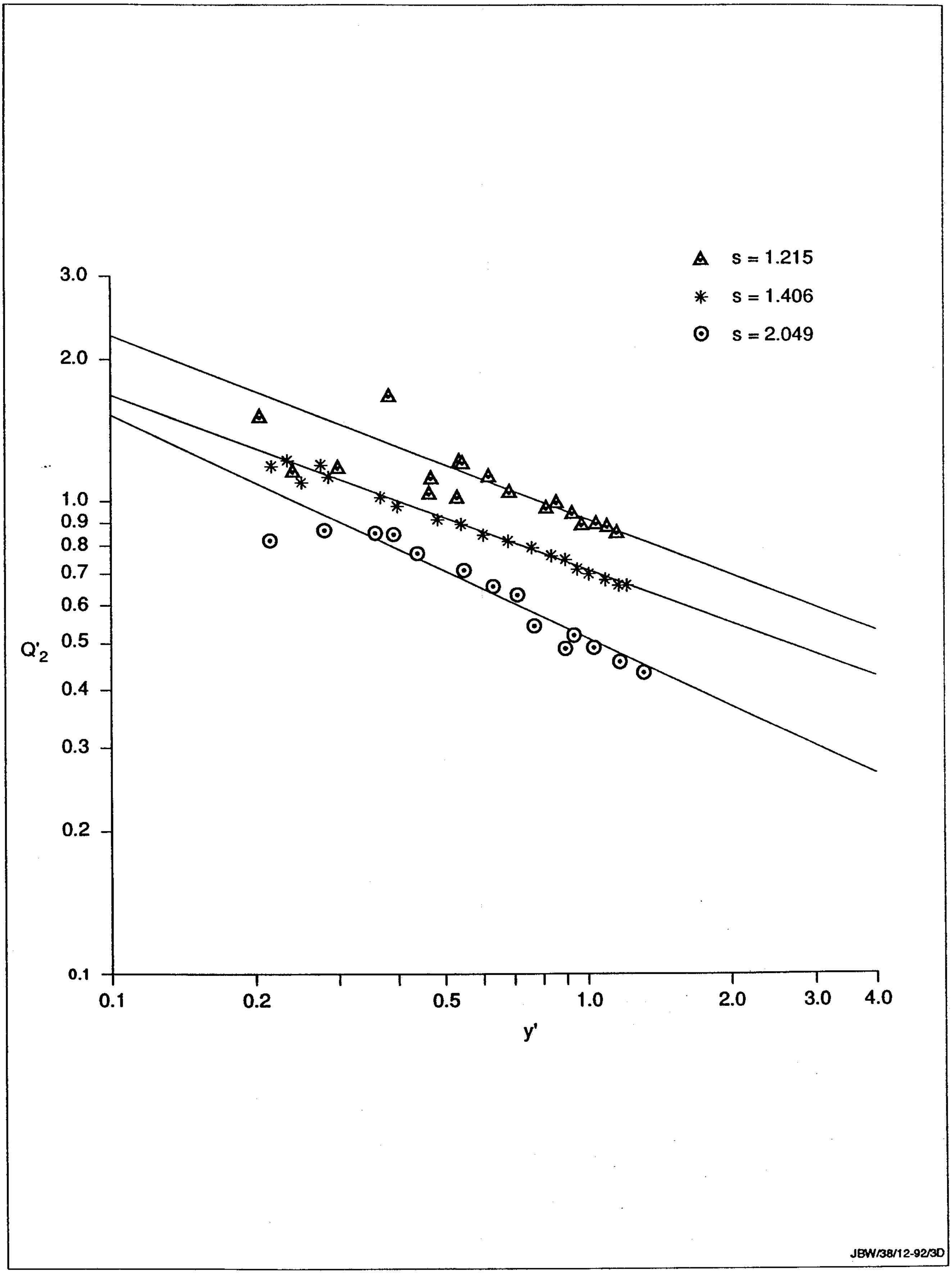

Figure 38 Adjustment factor for inner flood plain discharges for y' > 0.2, Aberdeen data

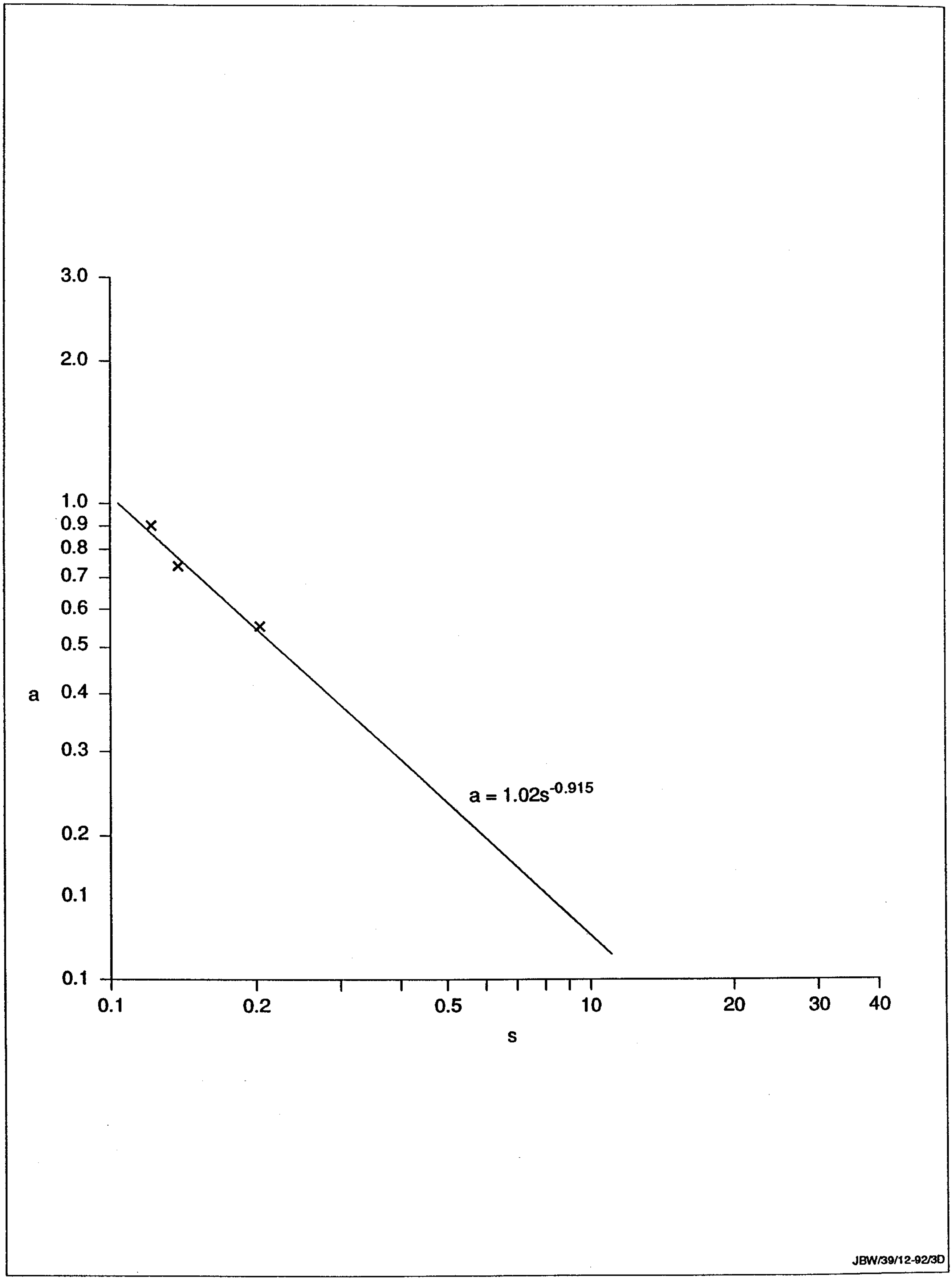

Figure 39 Variation of a with s

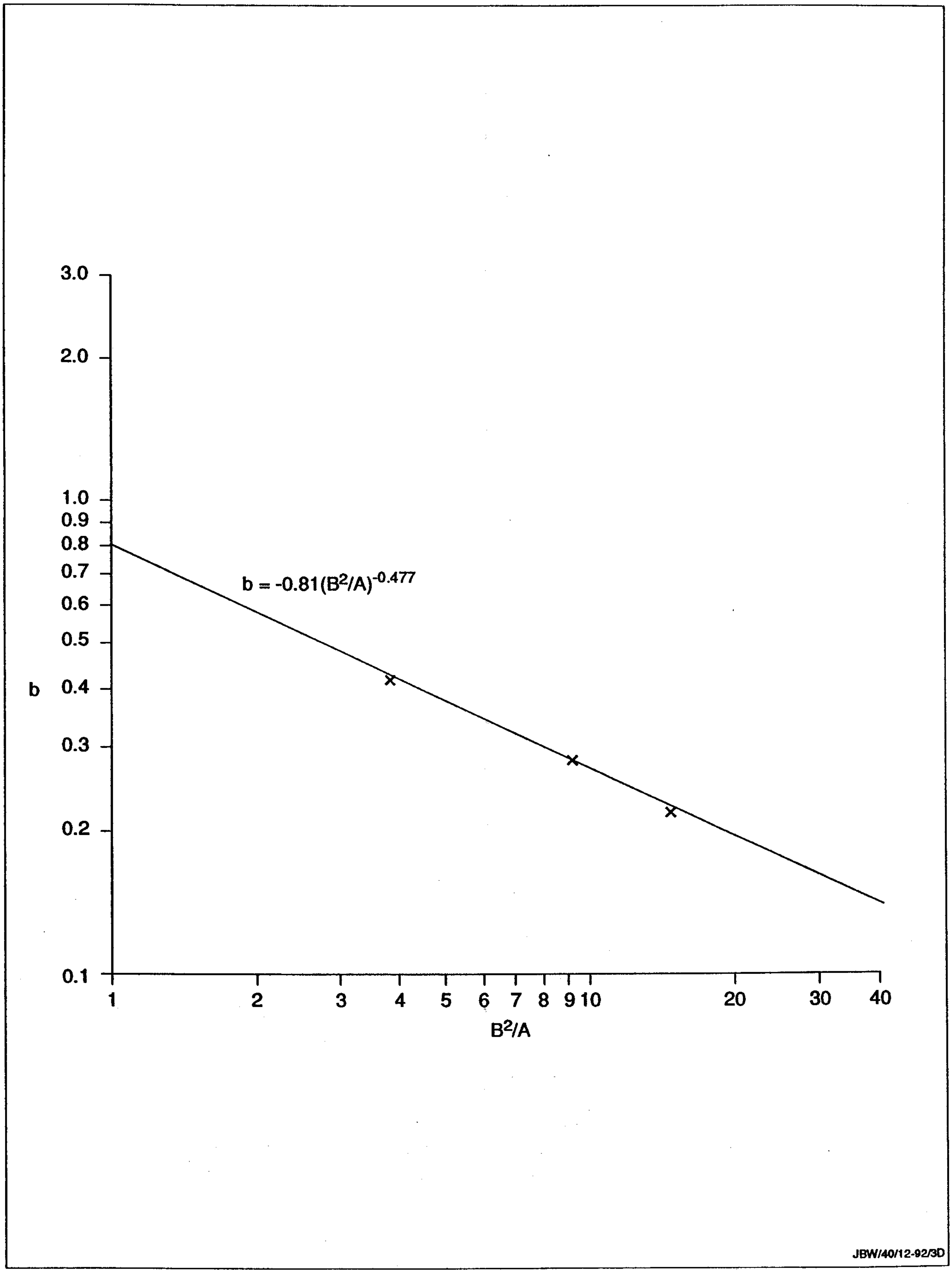

Figure 40 Variation of b with B^2/A

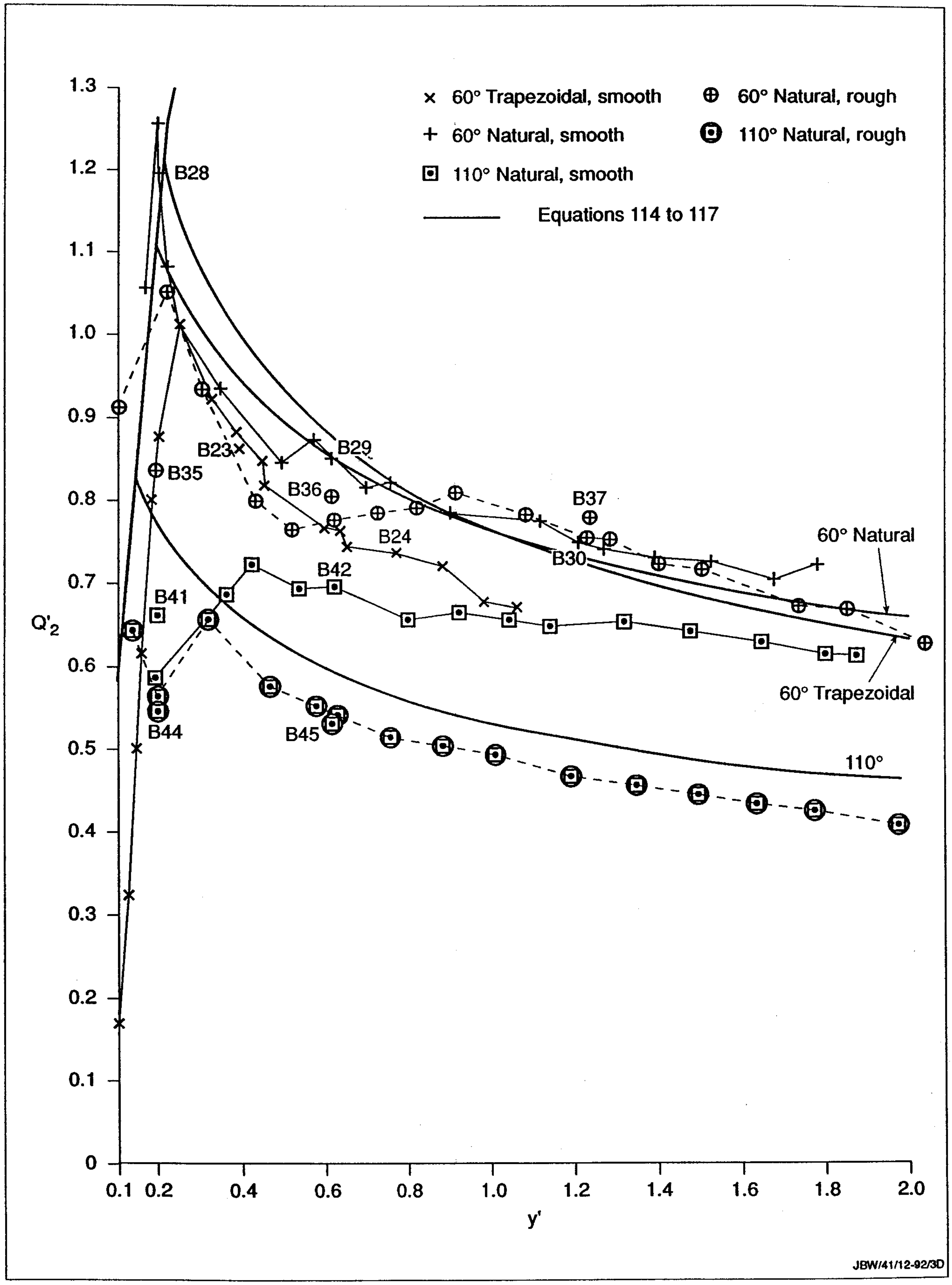

Figure 41 Comparison of predicted Zone 2 adjustment factor with SERC data

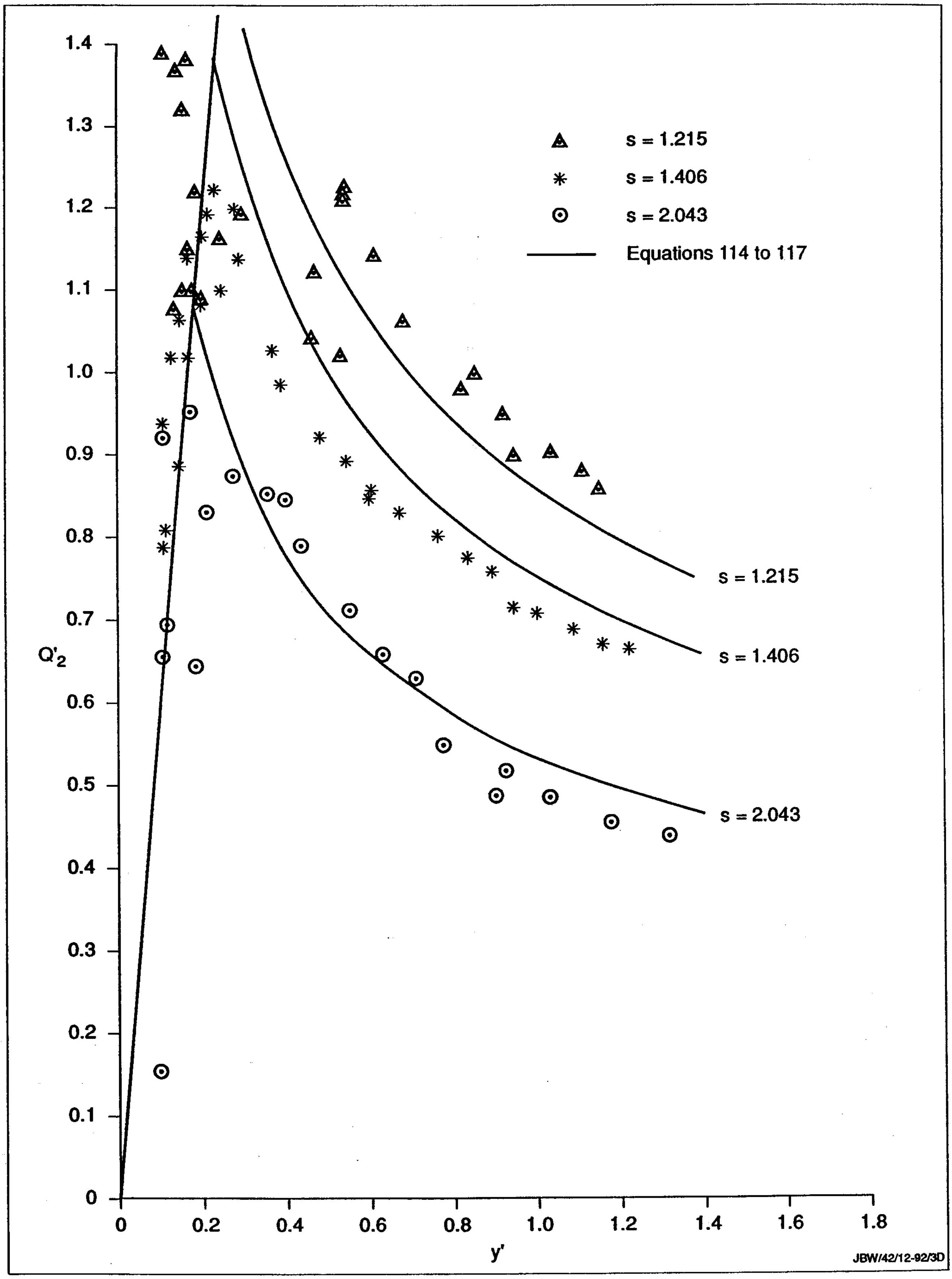

Figure 42 Comparison of predicted Zone 2 adjustment factor with Aberdeen data

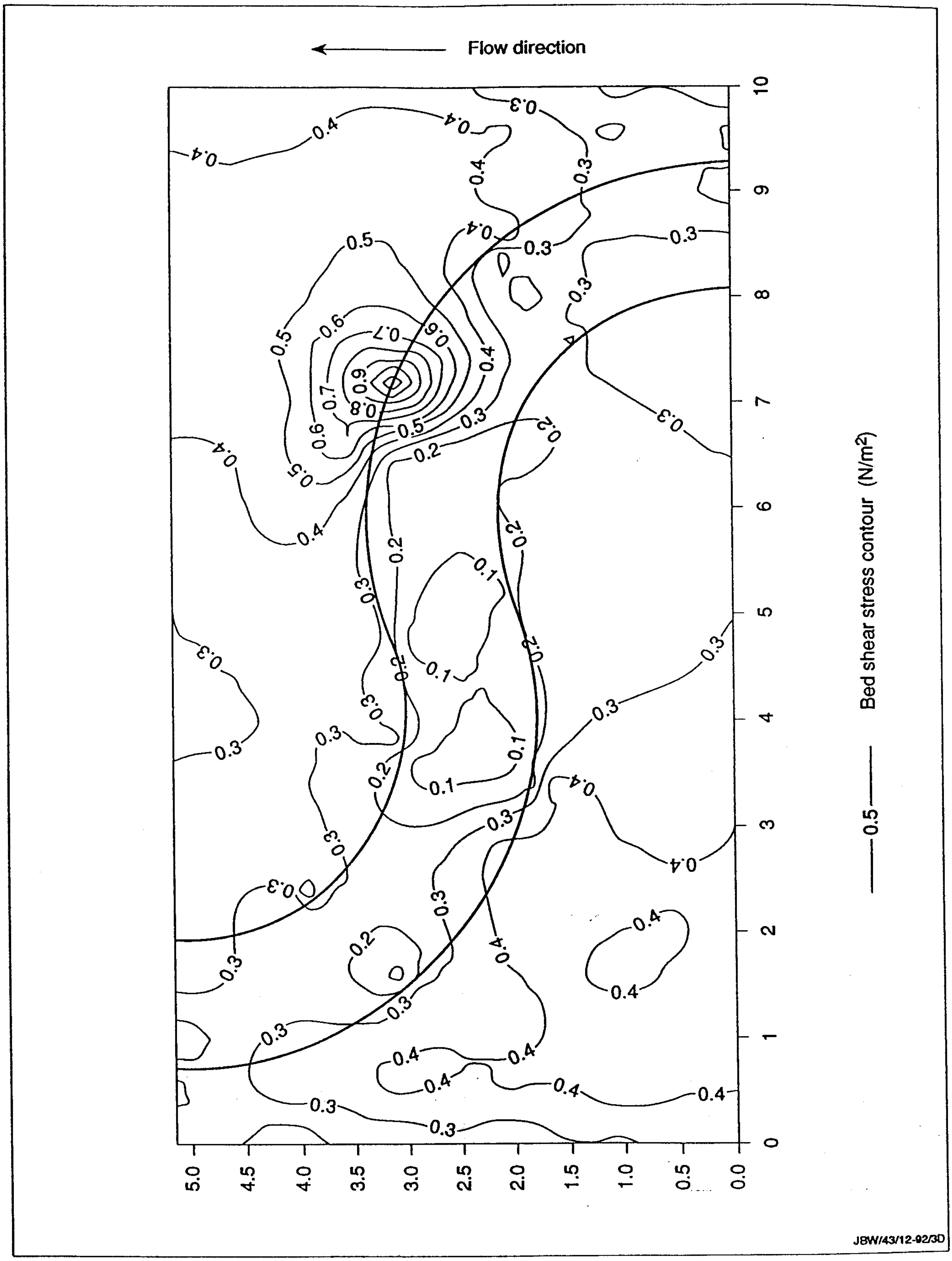

Figure 43 Example of boundary shear stress distribution in a meandering compound channel (after Lorena, 1991)

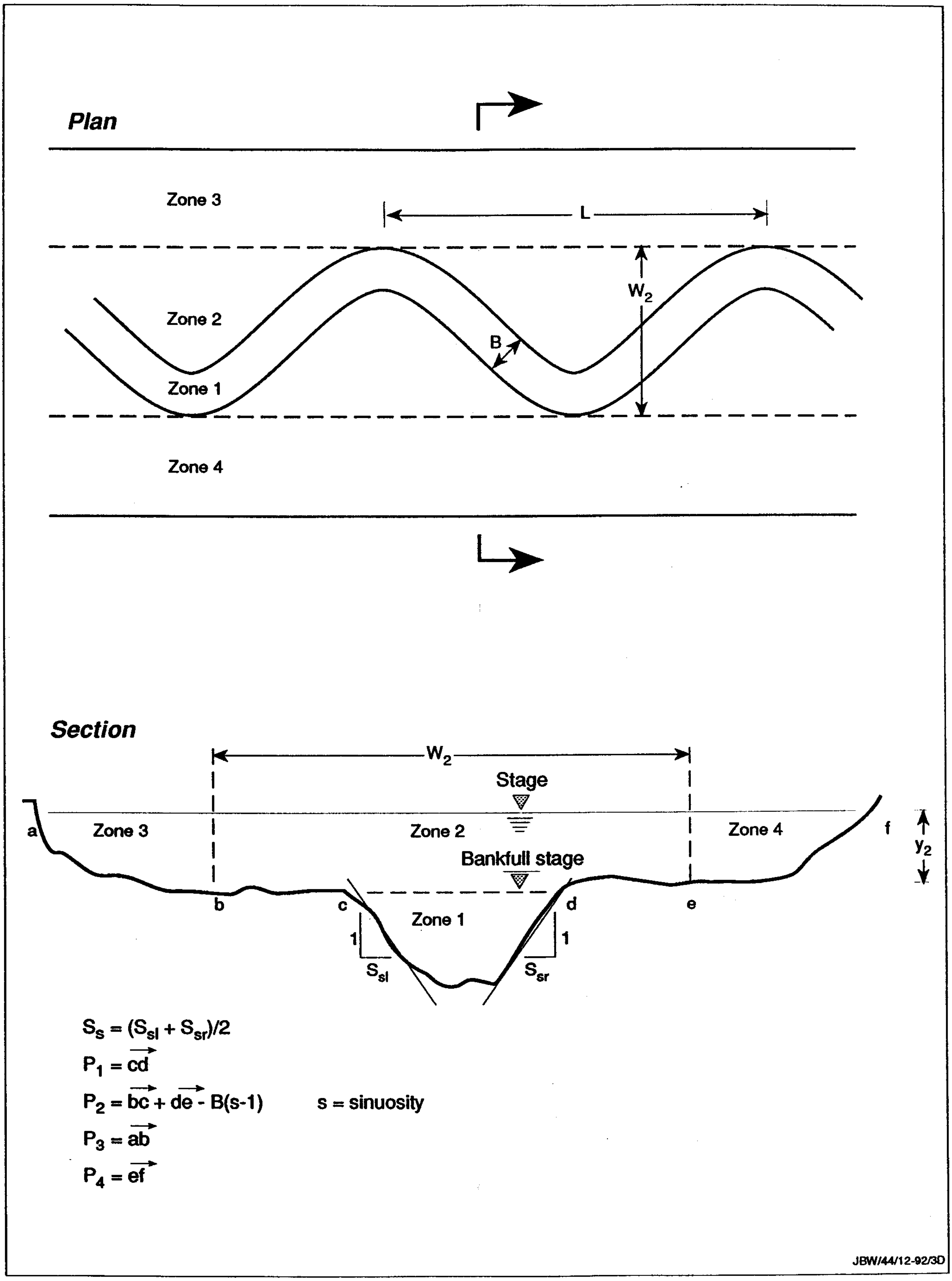

Figure 44 Cross-section subdivision of overbank flows, James and Wark

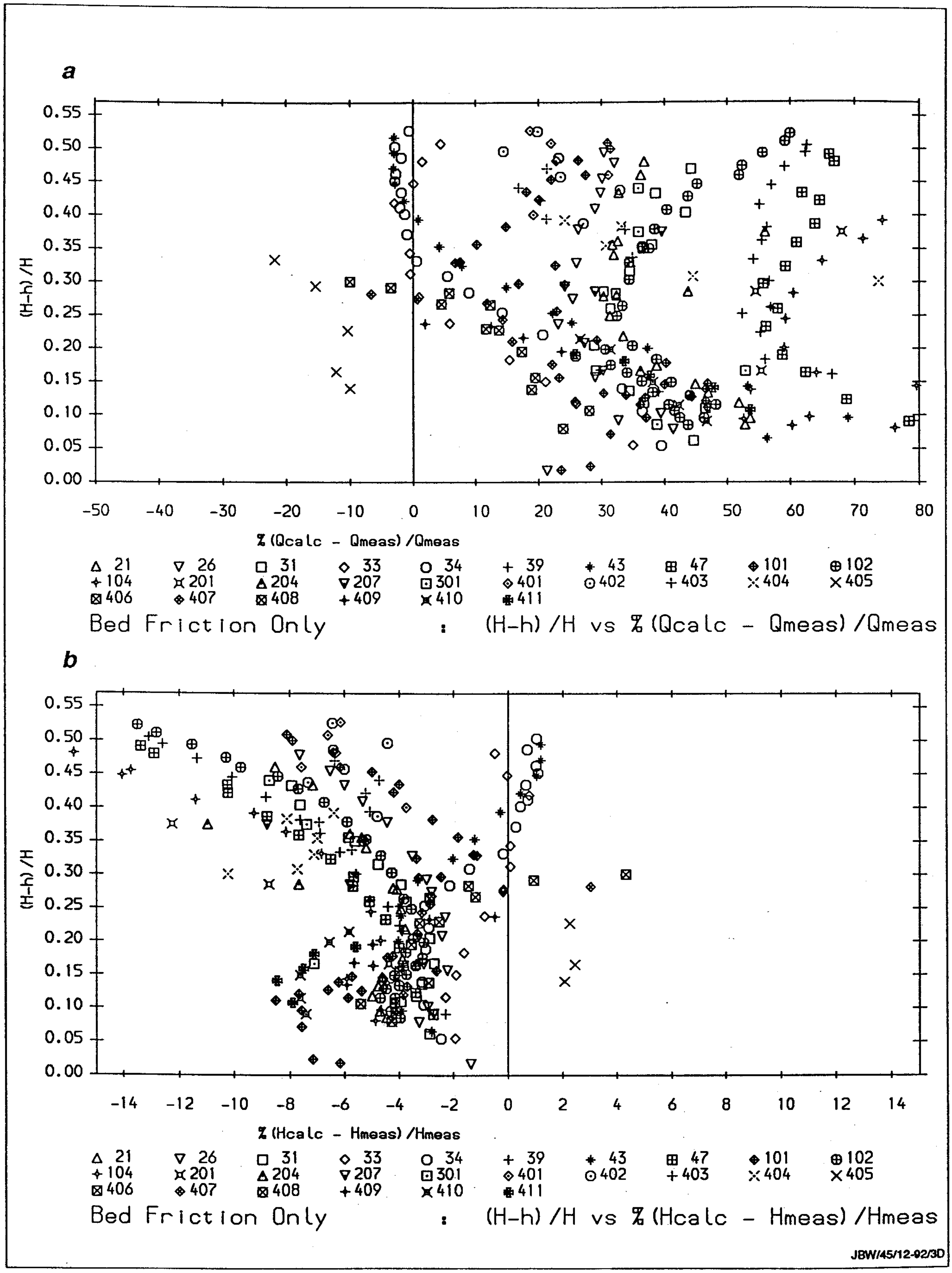

Figure 45 Errors in predicted discharge and depth: BFO

a

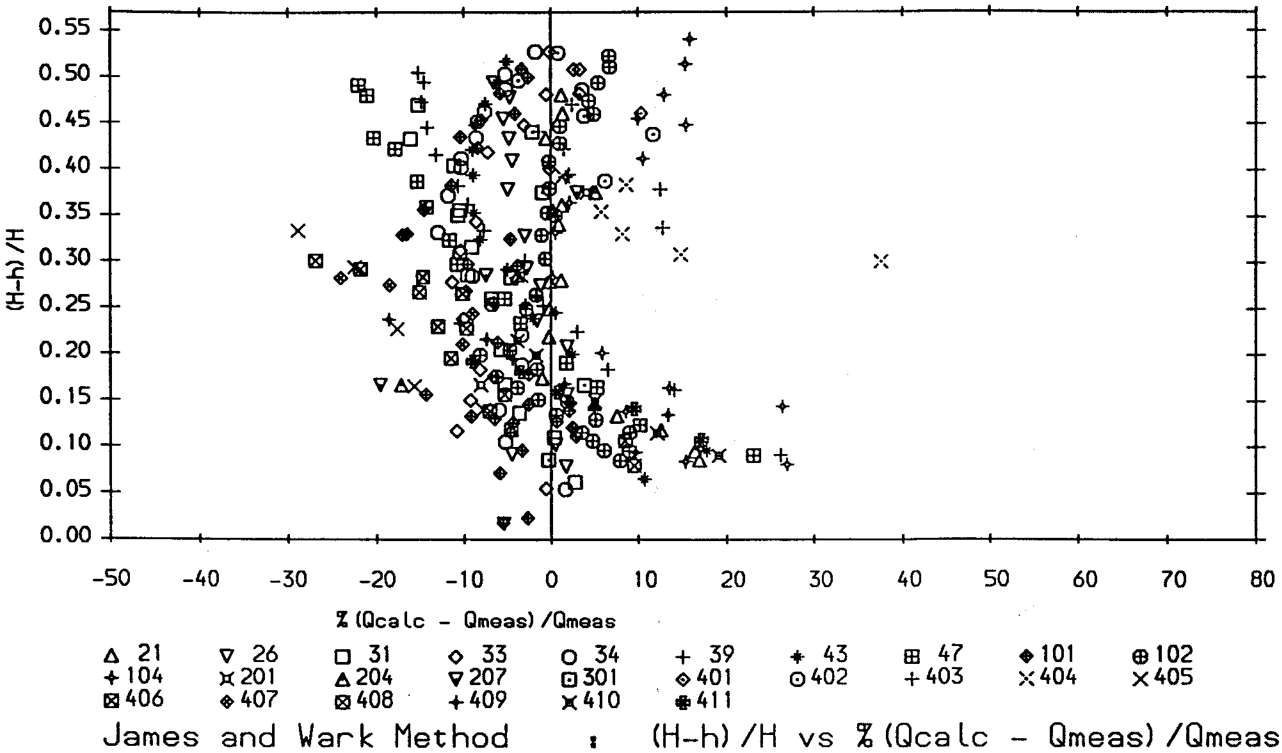

b

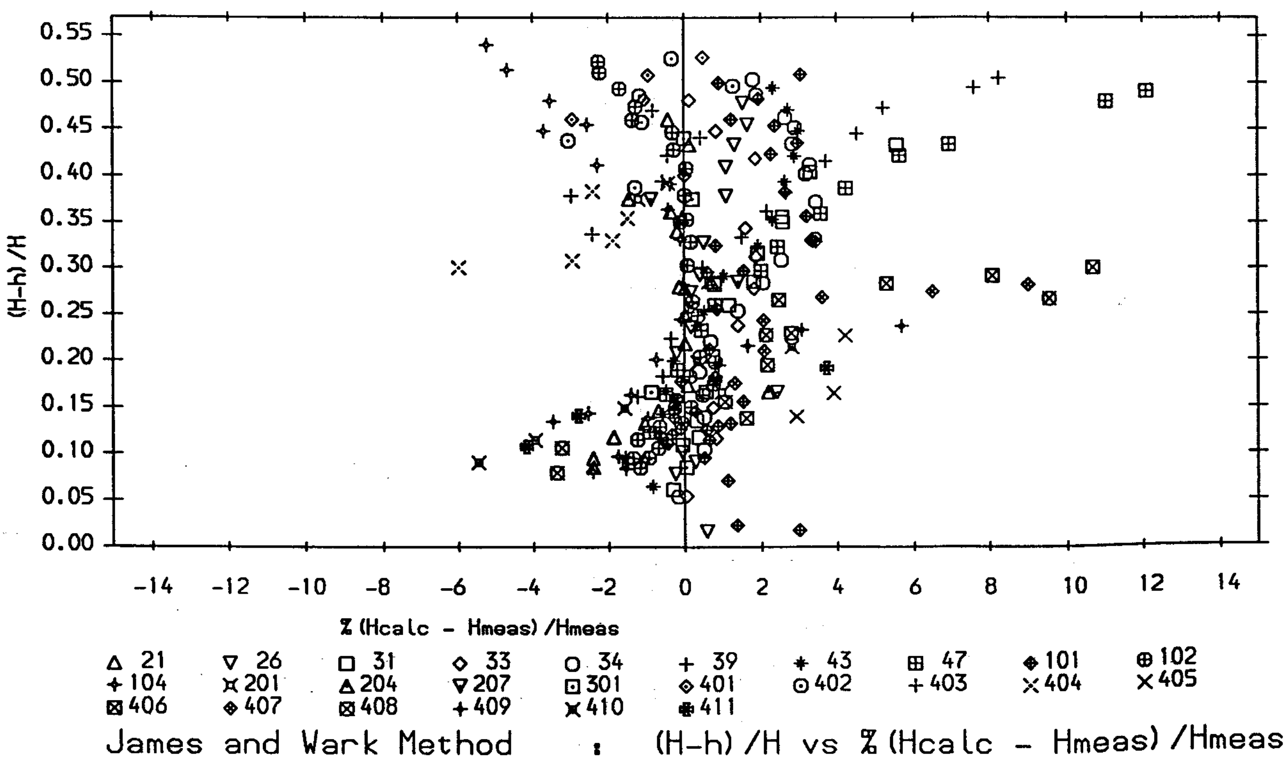

JBW/46/12-92/3D

Figure 46 Errors in predicted discharge and depth: JW

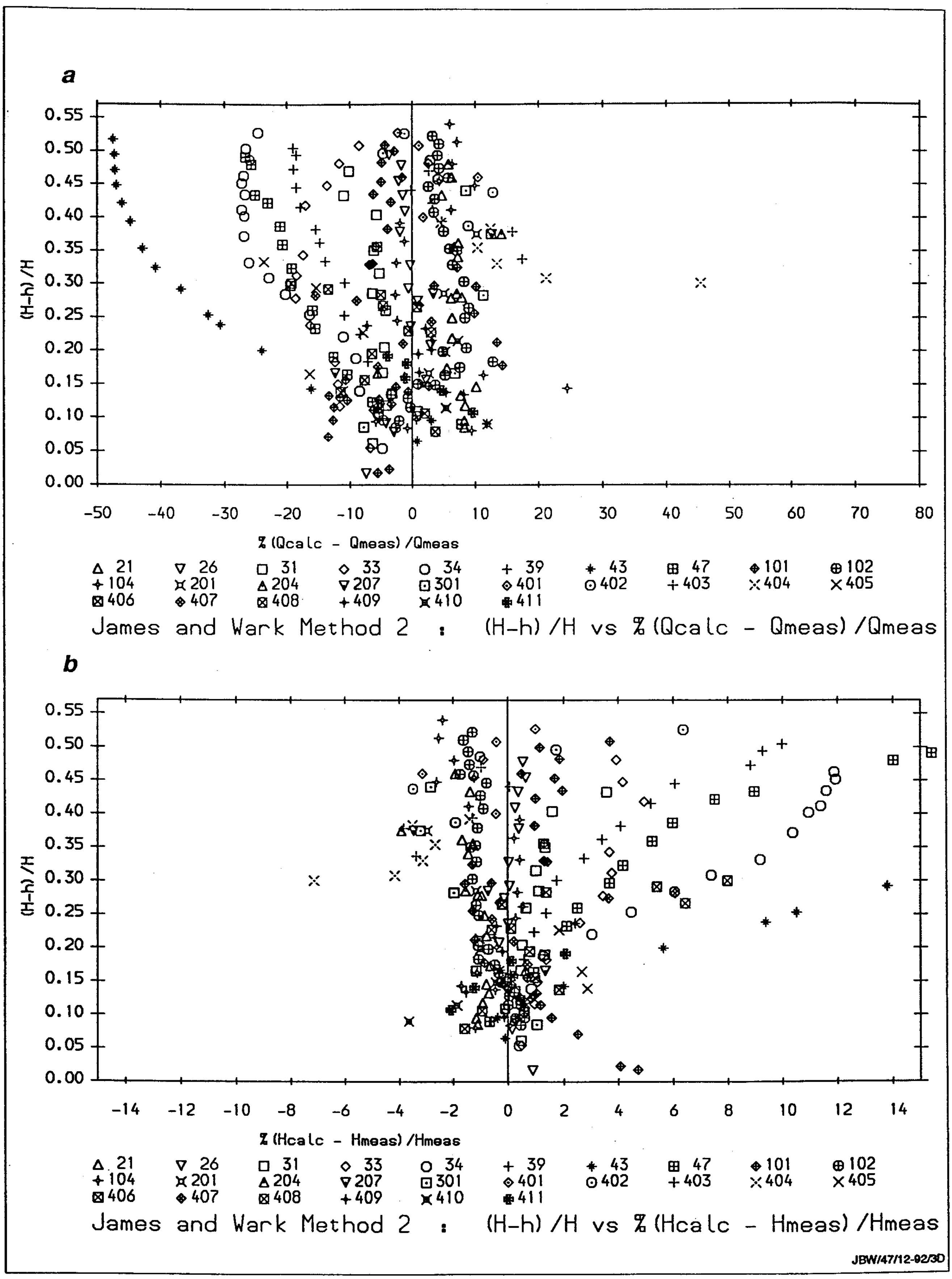

Figure 47 Errors in predicted discharge and depth: JW2

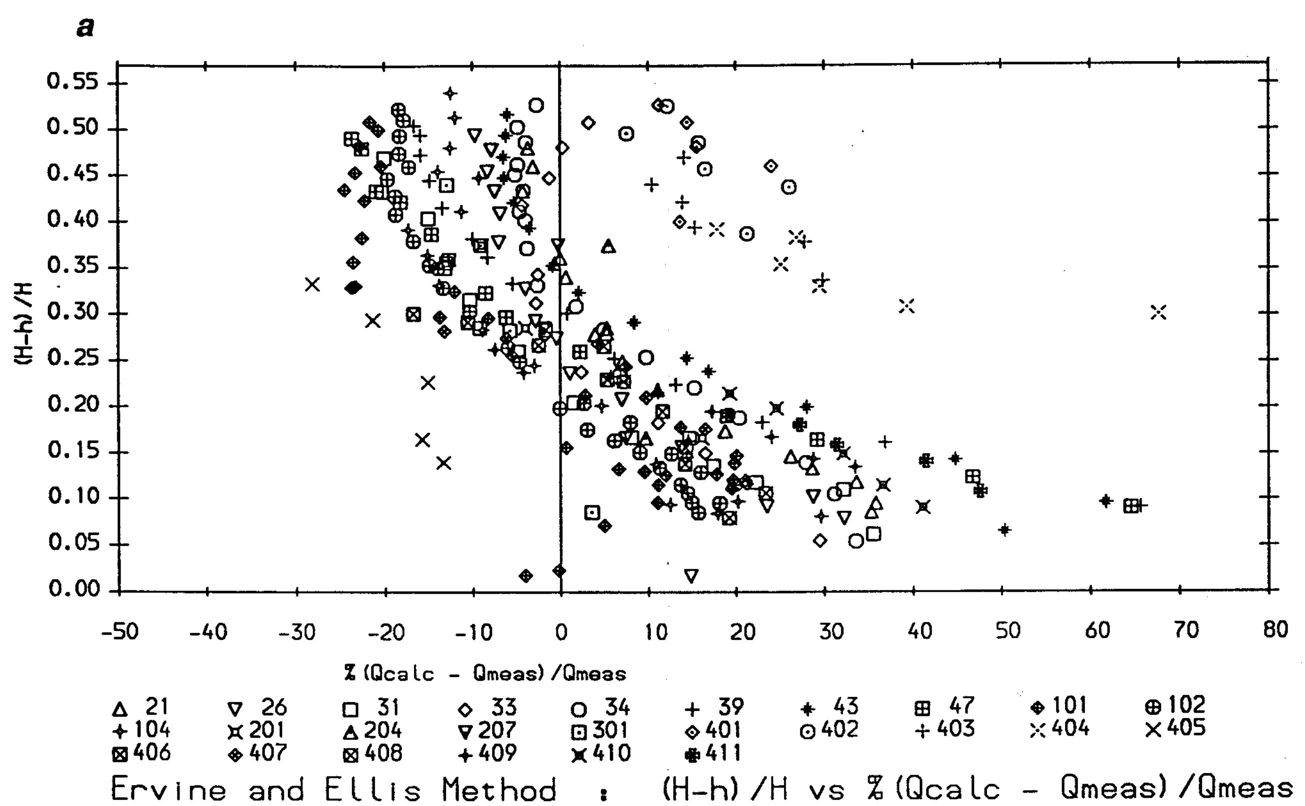

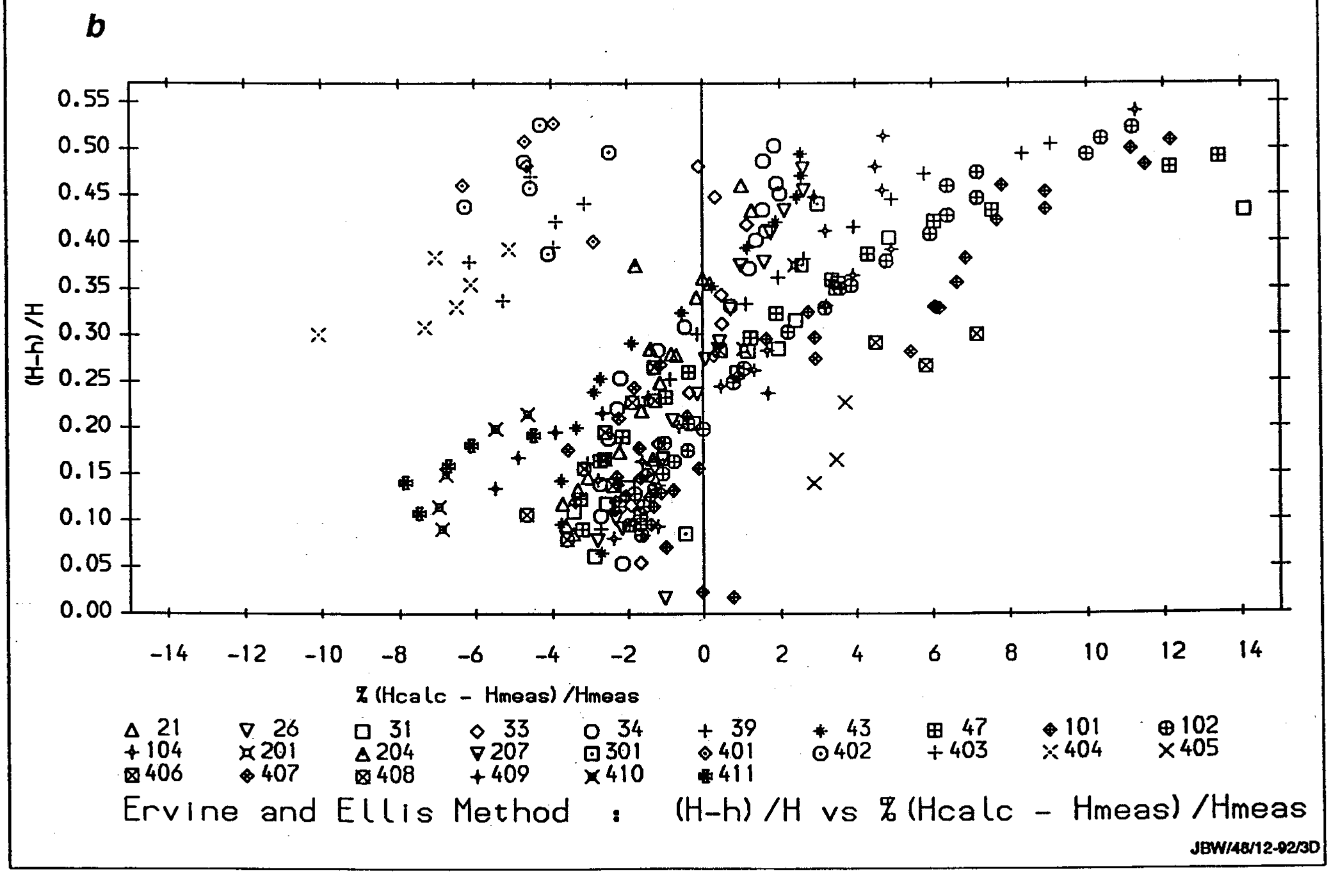

Figure 48 Errors in predicted discharge and depth: EE

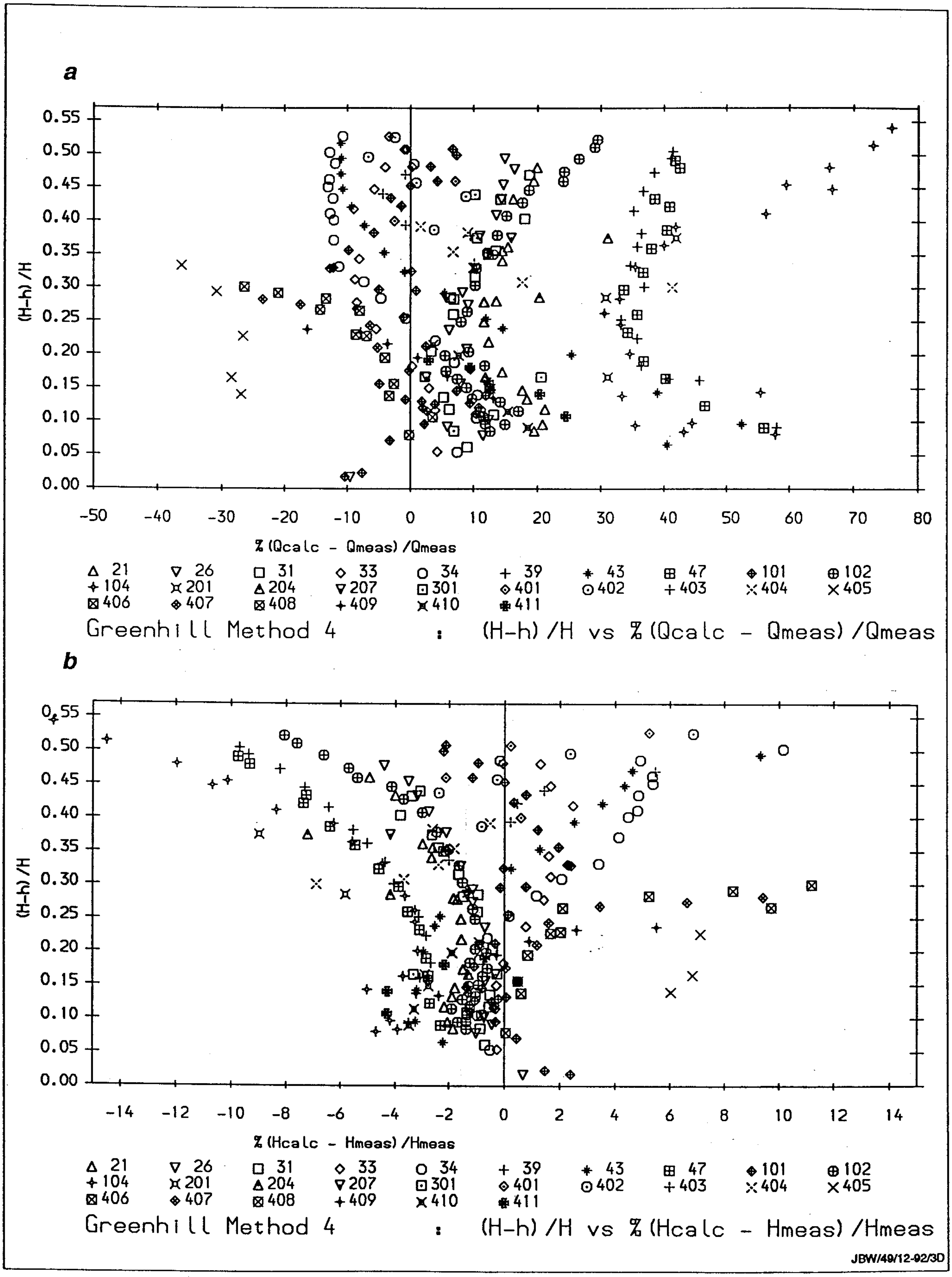

Figure 49 Errors in predicted discharge and depth: GH4

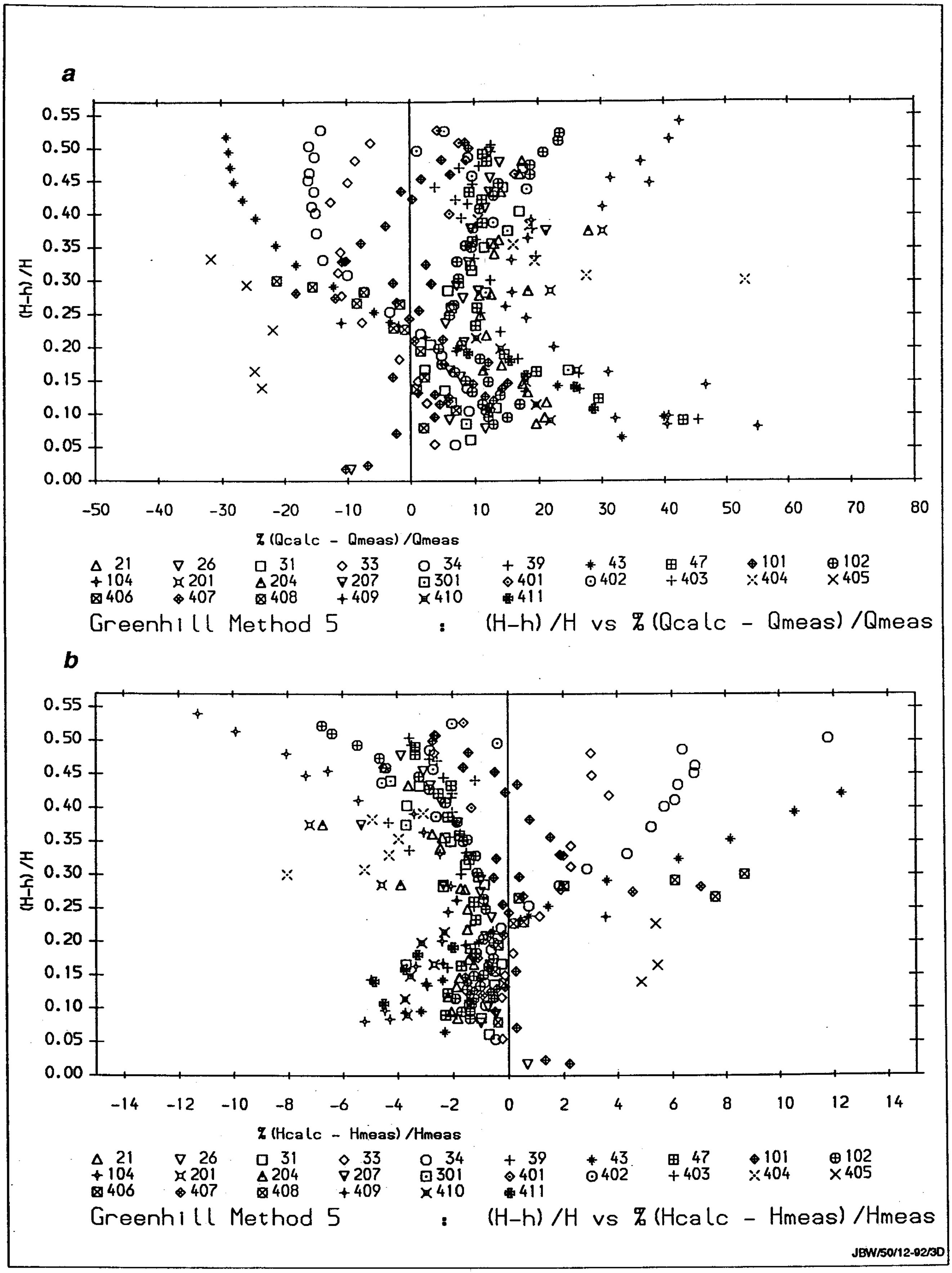

Figure 50 Errors in predicted discharge and depth: GH5

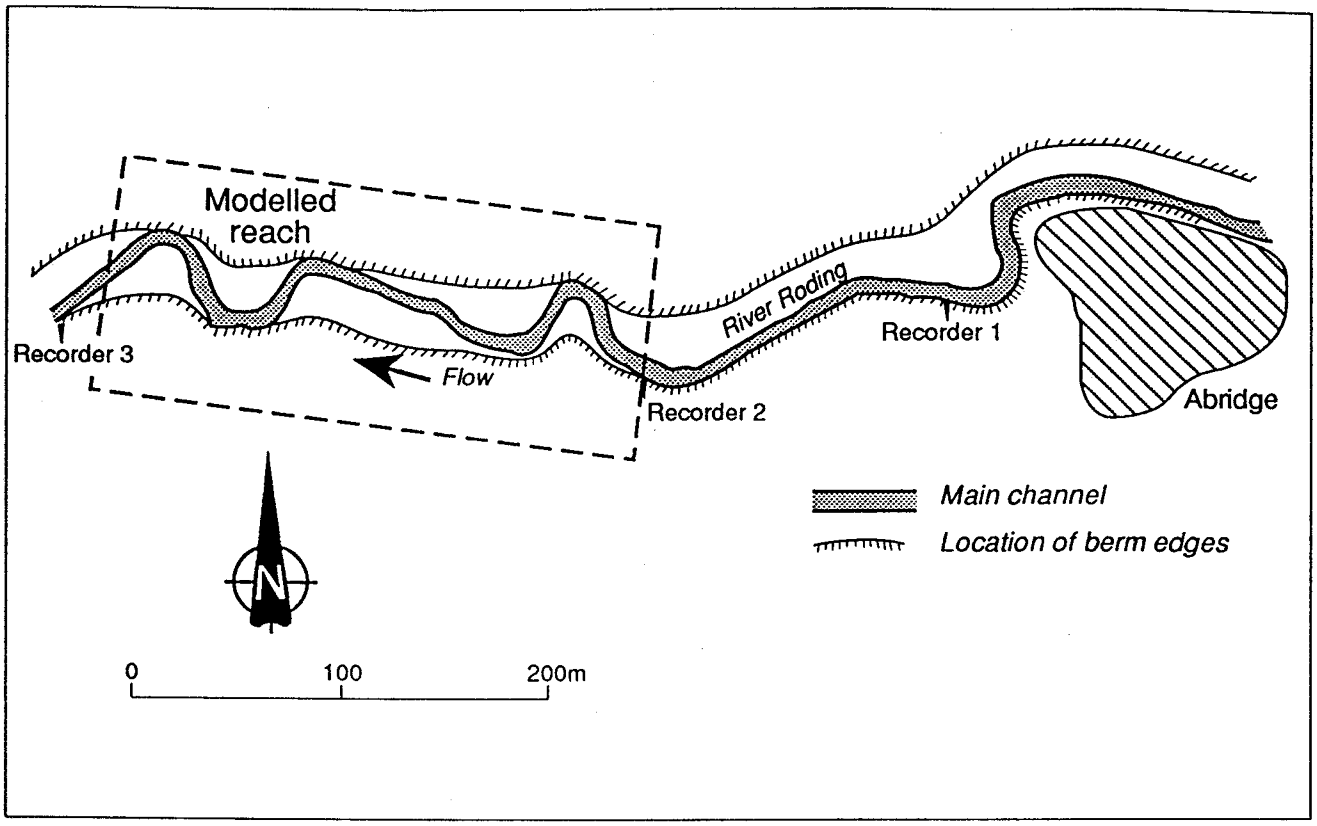

Figure 51 Location plan of study area on River Roding (after Sellin et al, 1990)

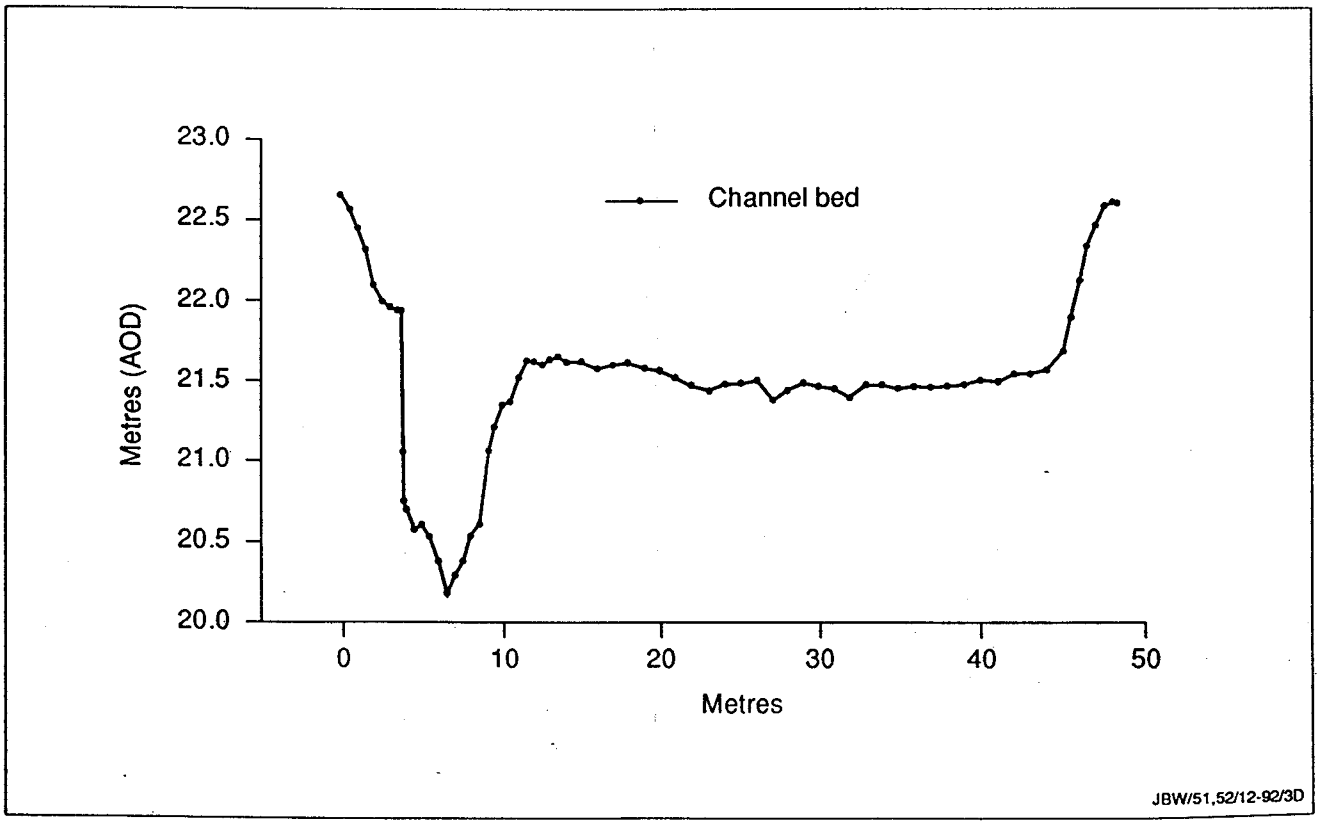

Figure 52 Roding at Abridge sample cross-section

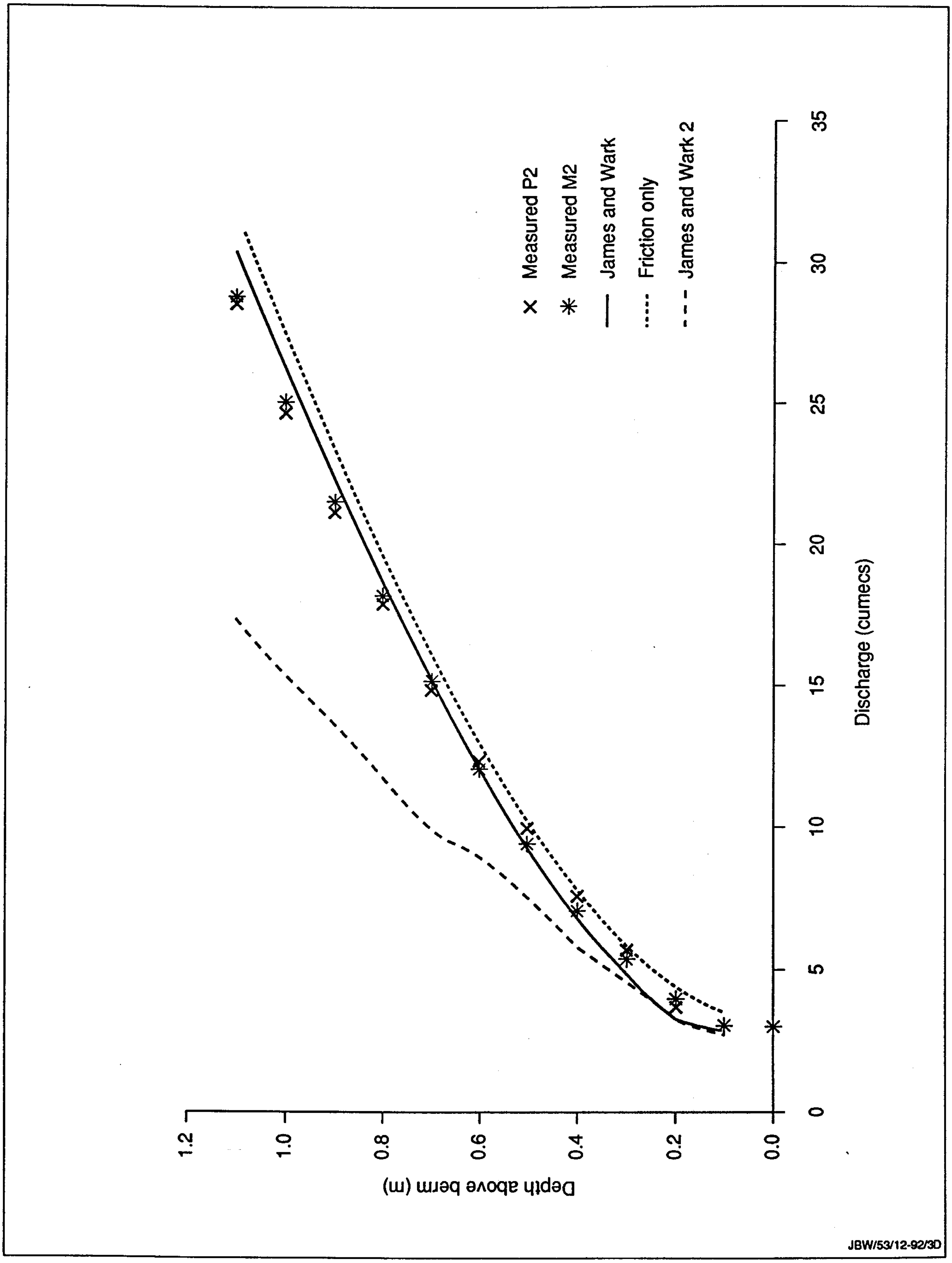

Figure 53 Roding at Abridge measured and calculated stage-discharges

Plates

Plate 1 FCF 60° channel geometry

JBW/Plate1,2/12-92/3D

Plate 2 FCF 110° channel geometry

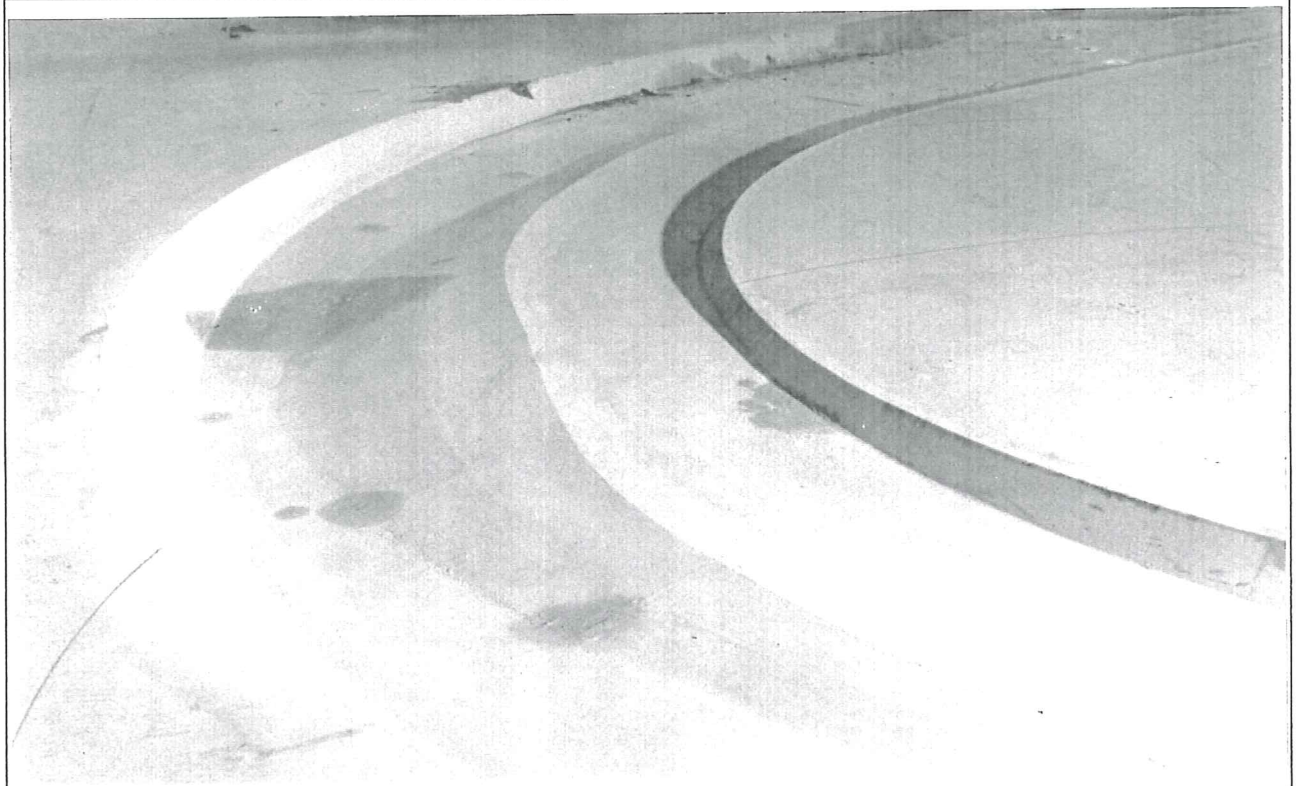

Plate 3 FCF natural cross-section

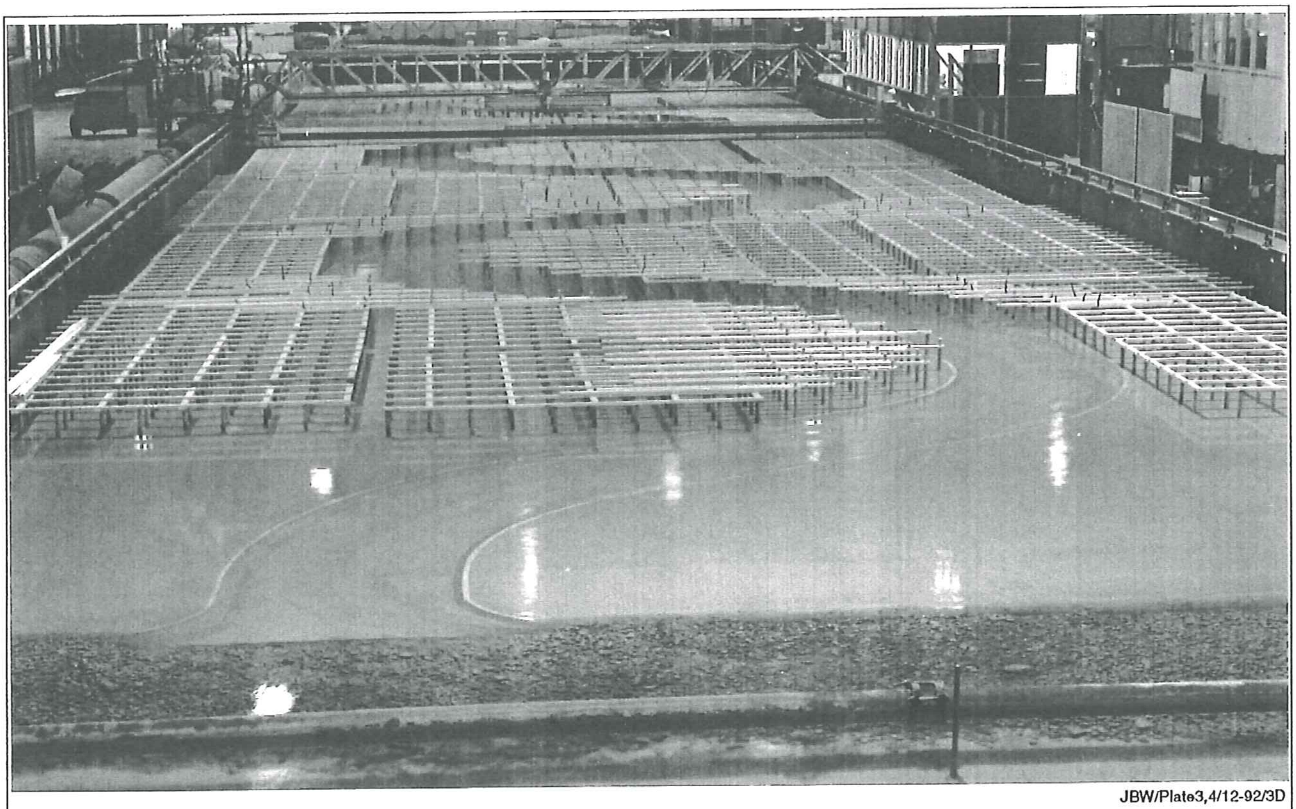

JBW/Plate3,4/12-92/3D

Plate 4 FCF rod roughened flood plain

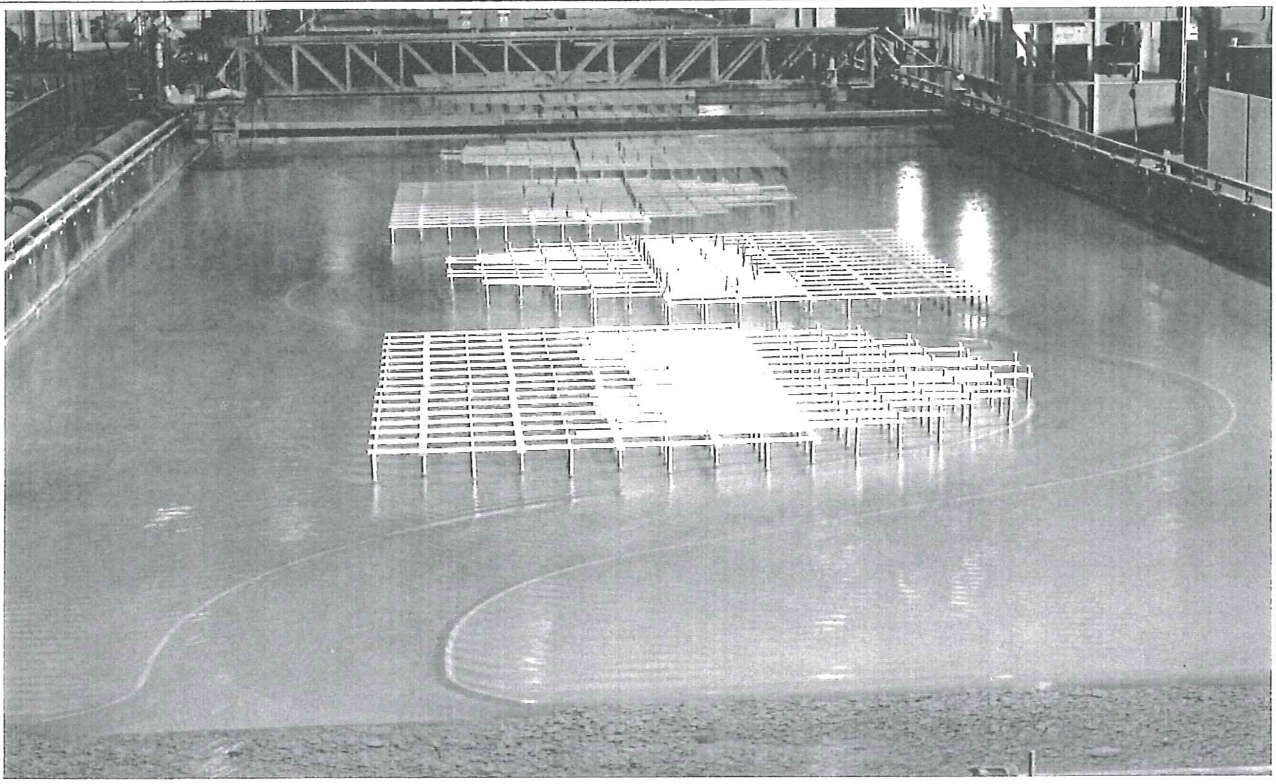

Plate 5 FCF partially rod roughened flood plain

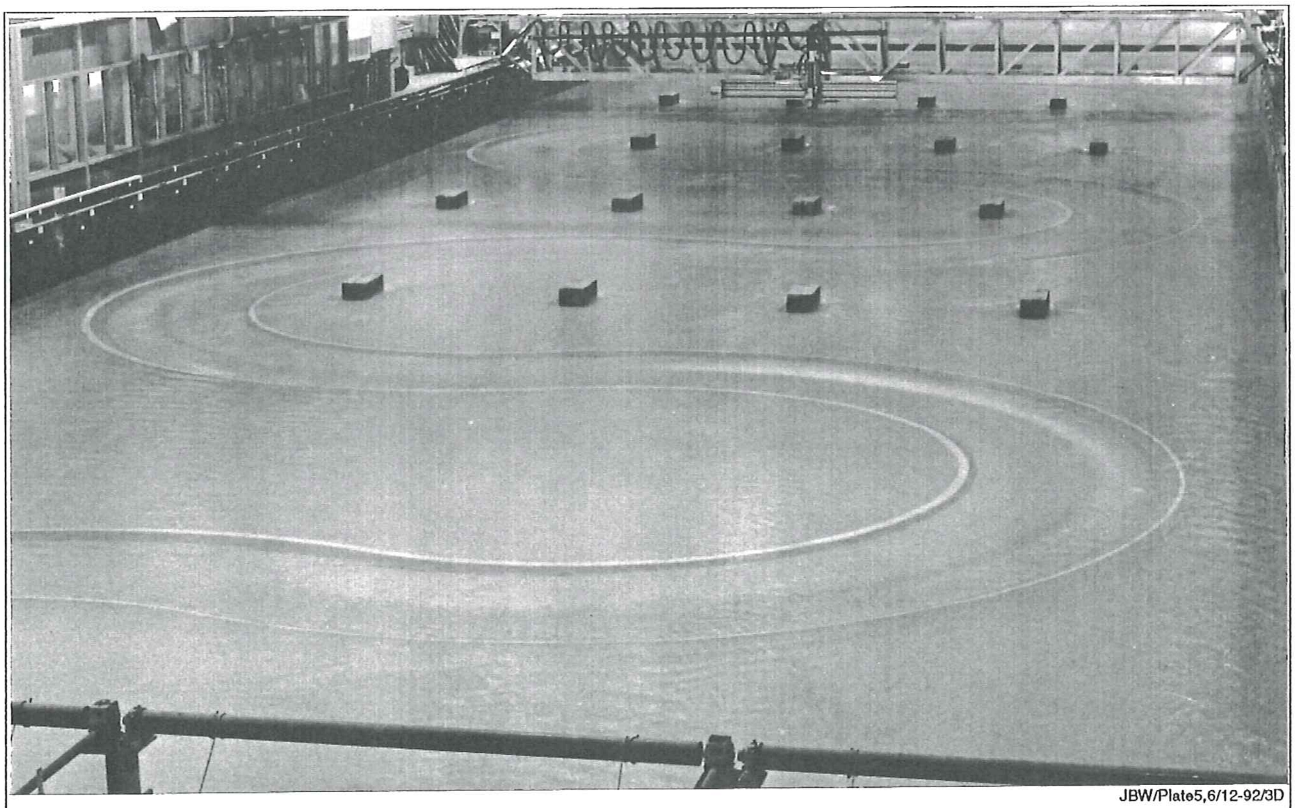

JBW/Plate5,6/12-92/3D

Plate 6 FCF breeze block roughened flood plain

Appendices

Appendix 1

Methods for determining equivalent roughness of channels with composite roughness

Appendix 1 Methods for determining equivalent roughness of channels with composite roughness.

In all the following cases, the channel section is divided into N parts. The hydraulic radius, wetted perimeter and Manning's roughness coefficient of an aribtrary Section i are R_i, P_i and n_i, respectively.

Horton, 1933

Horton assumed that each part of the cross-section has the same mean velocity, which at the same time is equal to the mean velocity of the whole section. On the basis of this assumption, the equivalent coefficient of roughness may be obtained by the following equation,

$$n = \left(\sum_{I}^{N} P_i (n_i^{3/2}) \right)^{2/3}$$

$$= \frac{(P_i n_i^{3/2} + \ldots + P_N n_N^{3/2})^{2/3}}{P^{2/3}}$$

The validity of the assumption which allows the derivation of this equation must be questioned. The velocity and thus the mean velocity are functions of roughness and depth, and so the mean velocity of parts with different roughnesses and depths must be different.

Lotter, 1933

By assuming that the total discharge is equal to the sum of the discharges in all the sub-sections, Lotter derived the following equation for the equivalent roughness coefficient,

$$n = \frac{P R^{5/3}}{\sum_{I}^{N} \frac{(P_i R_i^{5/3})}{n_i}}$$

ie

$$n = \frac{PR^{5/3}}{\frac{(P_i R_i^{5/3}}{n_i} + \frac{P_2 R_2^{5/3}}{n_2} + \ldots\ldots + \frac{P_N R_N^{5/3})}{n_N}}$$

In deriving this equation it is assumed that the bottom shear stress is constant along the wetted perimeter. It is well known that the shear stress acting on the sloping sides of the channel is less than the shear stress acting on the bed.

If the Colebrook-White equation is used instead of Manning's equation the equivalent roughness length is defined by:

$$K = 14.8\ R/10^{\left(\frac{1}{PR^{2/3}}\left[\sum_{i=1}^{N} P_i R_i^{3/2} \log_{10}\left(\frac{14.8\ R_i}{k_i}\right)\right]\right)}$$

Einstein and Banks, 1950

By assuming that the total force resisting the flow is equal to the sum of the forces resisting the flow developed in the individual areas, a formula for the equivalent roughness coefficient can be derived which is,

$$n = \frac{\left(\sum_{I}^{N} (P_i n_i^2)\right)^{1/2}}{p^{1/2}} = \frac{(P_i n_i^2 + P_2 n_2^2 + \ldots.. + Pn^2)^{1/2}}{p^{1/2}}$$

As with the method proposed by Lotter it has been explicitly assumed in deriving this formula that, in the channel with the constant equivalent roughness coefficient, the bottom shear stress is constant along the wetted perimeter. One more assumption made is that the hydraulic radius of each sub-divided section is equal to the hydraulic radius of the whole section; this need not be the case.

Einstein and Banks tested the above theory by carrying out a series of laboratory experiments. They used a 17ft flume, 12 inches wide and 18 inches deep with sides of painted sheet metal. The bed of the flume comprised concrete blocks into which pegs could be inserted. A series of experiments were carried out with the concrete blocks vertically offset relative to each other and with and without the pegs inserted. By measuring the water suface profile the total resistance was computed. The resistance due to each of the components of the bed was also calculated. It was found that the total resistance exerted by combined types of roughness is equal to the sum of the resistance forces exerted by each type individually.

Krishnamurthy and Christensen, 1972

Krishnamurthy and Christensen derived a method for calculating the equivalent roughness of a composite channel by making the following assumptions:

(a) the whole cross-section is assumed to be shallow.
(The secton is divided into smaller vertical sub-sections).

(b) the hydraulic radius, R_i, of each sub-section can be approximated by the vertical depth, d_i.

(c) the vertical velocity distribution in each sub-section follows a logarithmic law.

The formula developed by Krishnarmurthy and Christensen is,

$$\ln n = \frac{\sum_{I}^{N} p_i d_i^{3/2} \ln n_i}{\sum_{I}^{N} P_i d_i^{3/2}}$$

This formula is not applicable to rectangular channels because it does not take account of side wall effects. However, if the channel is wide and the influence of the side walls if negligible the method of Krishnamurthy and Christensen can be used. Under these conditions the above equation can be modified to give,

$$\ln n = \frac{\sum_{I}^{N} P_i \ln n_i}{P}$$

In order to verify their method Krishnamurthy and Christensen used data from the Lower Mississippi river. They showed that for this data their method gave closer agreement with the measured roughness coefficient than the methods of Horton, Lotter or Einstein and Banks.

Appendix 2

The lateral distribution method

Appendix 2 The lateral distribution method

In order to model all of the complex flow mechanisms that are known to occur in compound channels a complex three dimensional flow and turbulence model is required. Such models are extremely complex and require sophisticated numerical schemes and powerful computers. Inorder to obtain accurate representations of the turbulence and flow fields very small numerical grids are required. The cost of collecting such detailed survey data and the computational effort required is not justified in typical engineering applications. However it is possible to introduce some simplifying assumptions into the basic mathematics and so account for the effects of the small scale turbulence on the overall flow pattern.

This is the approach followed in developing the lateral distribution method. The basic equations of turbulent flow are known as the Reynolds' equations and are the mathematical description of all turbulent flows. By making the following assumptions it is possible to simplify these very general equations:

1) Flow is steady.
2) Flow is unidirectional.
3) Turbulent shear stresses are linear functions of local velocity gradients. This is the eddy viscosity concept and in simple unidirectional flow this may be expressed as equation 1. Where τ is the shear stress, ρ is the fluid density, υ_t is the eddy viscosity and U is the velocity.

$$\tau = \rho \, v_t \left[\frac{\partial U}{\partial y}\right] \tag{1}$$

The next simplification is introduced by depth integrating the resulting equation over the water column depth. it is necessary to assume that the water surface is horizontal across the channel width. This depth integration results in the following equation for the lateral distribution of depth integrated flow in a channel.

$$gDS - \frac{Bf|q|q}{8D^2} + \frac{\partial}{\partial y}\left[v_t \quad \frac{\partial q}{\partial y}\right] = 0 \tag{2}$$

Where B is a factor relating stress on an inclined surface to stress on a horizontal plane, D is the local flow depth, f is the Darcy friction factor, g is gravitational acceleration, q is the unit flow (ie the discharge per unit width = UD), S is the surface slope and U is the depth averaged velocity (refs 1,2).

The variable q must be continuous even across a vertical step in depth where as the depth averaged velocity will display large discontinuities in these situations. It is obviously preferable to base calculations on a variable which is known to vary smoothly across the domain.

Turbulence model for depth integrated flow : At this point some model must be assumed for the lateral eddy viscosity υ_t. It is possible to use a sophisticated turbulence model but a price must be paid in terms of computational effort. It has been found that the simple model (3) can give acceptable results in many situations.

$$\upsilon_t = \lambda \, U.D \tag{3}$$

The problem in applying this model is in choosing appropriate values of λ, the Non-dimensional Eddy Viscosity (NEV) and U_* is the local shear velocity. Knight et al (ref 2) have reported derived values of λ which vary strongly across channel and floodplain both in laboratory and natural channels. While not disagreeing with this conclusion the authors experience in applying a model based on equations 2 and 3 indicates that adequate precision can be achieved with a single value of λ applied to both channel and floodplain. However this is likely to be true only for the gross distribution of flow across the channel. The transport of pollutants or suspended sediments is far more sensitive to the local turbulent structure, secondary currents etc, which affects the value of λ. Hence if one is interested in the distribution of transported substances this simple one value model maybe inappropriate.

3 The numerical method

The sets of equations 2 and 3 which form the lateral distribution method may be solved analytically only in certain simple situations and in general a numerical solution must be sought. The authors use a finite difference technique with a staggered grid and Newtons' method to linearize the coupled non-linear equations. Iteration is required and the initial guess is provided by setting $\upsilon_t = 0$. Convergence is usually attained within 5 iterations. Typically over 100 points are used for the numerical integration across a section.

4 Limitations

The LDM is based on the assumption that the flow is relatively uniformly distributed with depth through the water column. Where strong secondary currents exist such as in tight bends then these simple models will not give good predictions. It is possible to modify the basic theory to account for mildly curved flow paths and differing slopes in the main channel and floodplains. These empirical adjustments are intended to widen application of a model which is theoretically only applicable to straight channels. The simple one parameter turbulence model (eqn 3) is attractive when considering river flows since it relates the turbulent shear stresses to the channel bed friction. In rivers bed friction is usually the dominant process but in situations where other effects become important this model is less appropriate. One difficulty in practice is that calibrated values of λ include the effects of secondary currents on the lateral transport of momentum and so it is difficult to give definitive guidance on appropriate values.

5 References

1 WARK J.B., SAMUELS P.G. and ERVINE D.A. (l990) - "A Practical Method of Estimating Velocity and Discharge in Compound Channels", Intl. Confr. on River Flood Hydraulics, Wallingford, Oxfordshire, Sept.

2 KNIGHT D.W., SHIONO K. and PIRT J. (1989) - "Prediction of Depth Mean Velocity and Discharge in Natural Rivers with Overbank Flow", Int'l. Conf. of Coastal, Estuarine and River Waters, Bradford, England, 19-21 Sept.

Appendix 3

The FCFAM design method for
straight compound channels

Appendix 3 The FCFAM design method for straight compound channels

1. Introduction

A "compound" channel consists of a main channel, which accommodates normal flows, flanked on one or both sides by a flood plain which is inundated during high flows. Figure 1.1 illustrates a typical compound cross-section and defines the geometric variables used in the procedures to follow.

For water levels above the flood plain, the flow is strongly influenced by the interaction between the fast-flowing water in the main channel and the relatively slow-flowing water over the plains. This significantly complicates the estimation of stage-discharge relationships. The extra turbulence generated by the flow interaction introduces energy loss over and above that associated with boundary resistance. This is not accounted for by the conventional resistance equations (such as Chézy, Manning and Darcy-Weisbach), and their direct application may result in considerable error. If the channel cross-section is treated as a unit with one of these equations, the discharge for any given stage will invariably be underestimated.

The usual approach presented in hydraulics text books is to divide the cross-section into distinct subsections corresponding to the main channel and flood plain flows. The discharge for each subsection is then calculated separately using the Manning (or other similar) equation, and the total discharge obtained by adding these together. This approach invariably overestimates the discharge for any given stage.

Various attempts have been made to improve the latter approach, usually by including subdivision interfaces in the wetted perimeters to account for the apparent shear stresses induced by the interaction, or by locating the subdivisions on planes of zero shear. To date, all of these methods have been based on the results of small scale laboratory experiments and are unreliable on natural river scales.

The procedure presented here was developed by P Ackers (1991) and follows the channel subdivision approach. Subsection discharges are calculated and added to obtain a "basic" discharge, which is then adjusted to account for the effects of the interaction between the subsection flows. The adjustment required depends on the characteristics of the channel and also varies with stage. Four regions of flow behaviour are identified, as shown in Figure 1.2. This diagram presents some typical experimental results, showing the ratio of actual to basic discharge (on the horizontal axis) for a range of dimensionless flow depths (on the vertical axis). The effect of flow interaction is complex, alternately increasing and decreasing with flow depth through the different regions. Also shown on this diagram is the curve of channel coherence. This is the ratio of the conveyance calculated as a single cross-section to that calculated by summing the conveyances of the separate flow zones. A different adjustment function is defined for each region, but as the limits of the regions vary with channel characteristics it is not possible to identify the appropriate region for a particular water level beforehand. A logical procedure is given, however, for selecting the correct discharge value from those calculated assuming each adjustment function in turn. An additional correction is provided to account for the effect of deviations of up to 10^0 between the alignments of the main channel and the flood plains.

The adjustment functions were derived from experimental results from the large scale SERC Flood Channel Facility at HR Wallingford. They have been validated by comparison of predictions with measured results from smaller scale laboratory studies and some full scale river data. These data cover a range of discharges from 5 l/s to over 500 m^3/s and a range of gradients from less than 0.0002 to more than 0.002. The comparisons suggest a computational accuracy for the method within two or three per cent, which is within the probable tolerances of the river data.

A procedure is also given for dividing the computed total discharge at any stage into main channel and flood plain components.

The interaction between main channel and flood plain flows also affects the magnitude and distribution of boundary shear stress, and will therefore influence scour patterns and requirements for scour protection. Local shear stresses on the flood plain close to the main channel may be five times greater than the value calculated from flow depth and channel gradient. The average boundary shear stress within the main channel is reduced, and a relationship for estimating the reduced value is given.

The effects of the flow interaction also have significant implications for sediment transport. Calculations for a hypothetical case have suggested that total bed material discharge could be reduced by a factor of two or three. Detailed assessment of these effects will be the subject of future research. Until new results are available, the effects should be provisionally accounted for by using conventional methods with the relevant hydraulic parameters, such as flow velocity and boundary shear stress, determined according to the procedures presented here.

The procedures for applying the methods are outlined below. Full details of their background and development are presented in the comprehensive reports by Ackers (1991).

2. Procedure for stage-discharge computation

The steps which follow outline the procedure for computing discharge values corresponding to specified water levels.

Steps 1 to 3 define the physical characteristics of the channel reach and cross-section in terms of the variables required for the subsequent calculations.

Steps 4 to 6 compute the basic discharges for the main channel, flood plains, and the whole cross-section for a specified water level.

Steps 7, 8, 10 and 12 adjust the basic total discharge to account for flow interaction between the main channel and flood plains, assuming the flow to be in Regions 1, 2, 3 and 4 respectively.

Steps 9, 11 and 13 apply the logical procedure for identifying the correct flow region and hence the correct adjusted discharge. The adjustment and selection steps are interspersed so that the correct region is identified at the earliest opportunity, to avoid unnecessary calculations.

Step 14 applies the additional correction to account for deviation between the main channel and flood plain alignments.

Preliminary investigations suggest that most UK rivers with compound sections will flow in Regions 1 or 2 for floods with recurrence intervals up to about 20 years. Calculations should be carefully checked if higher regions are indicated. Artificial or modified channels may operate over a wider range of regions than natural ones.

Step 1. Determine the longitudinal gradient of the channel reach, S_o, from survey information.

Step 2. Determine the geometric variables required to define the adjustment functions. The basic discharges for the main channel and flood plain zones can be computed using flow areas and wetted perimeters obtained directly from the appropriate surveyed cross-section. The discharge adjustment functions, however, include the geometric variables defined in Figure 1.1, and their estimation requires representation of the cross-section by a basic trapezoidal geometry. This is done using the following steps.

2.1 Plot the surveyed cross-section, as illustrated by Figure 2.1, for example.

2.2 Identify the points on the cross-section which most realistically mark the divisions between the main channel and the flood plains on both sides. Draw vertical lines through these points to define the bank lines separating the main channel and flood plain zones. The distance between the bank lines is $2w_C$. If there is a flood plain on one side of the main channel only, then just one bank line is defined and w_C is half the main channel width at the level of the division point.

2.3 Determine the river bank elevation. This is defined by the bank elevations at the locations of the bank lines - one value if there is only one flood plain, and the average of the two values for two flood plains.

2.4 By eye, fit a uniform slope to the main channel bank on each side. If the banks are irregular and the actual slopes vary, fit the straight lines to the upper two thirds of the bank profiles. The average of these slopes, expressed as ratios of horizontal to vertical distances, defines s_C.

2.5 Calculate the cross-sectional area of the main channel below the river bank elevation (as determined in step 2.3 above) and between the bank lines, A_{Csurv}, from the surveyed cross-section.

2.6 Determine the depth of the main channel, h. This is the distance below the river bank elevation of a horizontal channel bed located so that the area of the trapezium defined by the bed, the top width

(2w_C) at the river bank elevation, and the side slopes (s_C), is the same as A_{Csurv}. It can be calculated as

$$h = \frac{2w_c \pm \{((2w_c)^2 - 4\ s_c\ A_{Csurv})^{0.5}}{2s_c}$$

It will be obvious which of the two solutions of this equation is correct.

2.7 Determine the bottom width of the main channel,

$2b = 2w_C - 2\ h\ s_C$

2.8 Identify the positions of the backs of the flood plains. The distance between these defines the maximum total compound channel width, 2B, for two flood plains. For one flood plain the maximum value of B is the distance from the back of the flood plain to the bank line, plus w_C. Note that if the flood plains slope upwards and are not completely inundated, the total width (2B) is less than the maximum, with the dry part ignored (see Figure 2.1). The limits of the water surface can be determined from the surveyed cross-section.

Step 3. Estimate roughness coefficients for the main channel and flood plains. The resistance equation used is a matter of personal choice. Manning's equation (with corresponding n values) is probably the most widely accepted and will be used for describing the procedure, although this does not necessarily imply recommendation for its general use. If measured stage-discharge data are available, they should be used to estimate roughness coefficients. For the main channel, the value (n_C) adopted should correspond to near bank-full flows. It is not possible to infer the value for the flood plains (n_F) directly from measured data; a value must be assumed, which can be checked subsequently and refined. The slope used for calculating the n values should be the hydraulic gradient, but if reliable measurements of this are not available the surveyed channel gradient (S_o) can be used. If no measured data are available, n_C and n_F should be estimated in the usual way.

Step 4. Specify a value for H, the flow depth measured above the idealized bed of the main channel. The steps that follow lead to an estimate of the discharge for this water level. These steps should be repeated for the required range of H values to define the stage-discharge relationship.

Step 5. Calculate the basic discharges in the main channel and flood plain zones for the specified flow depth, using Manning's equation. In these calculations the bank lines between the zones should be excluded from the wetted perimeters. Areas and wetted perimeters should be measured from the surveyed cross-section, not the idealized trapezoidal section.

Step 6. Add the zonal basic discharges together to obtain Q_{basic}, the basic discharge for the whole cross-section. This must now be adjusted to account for flow interaction effects. The adjustment must be made using the adjustment function applicable in each of four possible flow regions; the correct value will be selected from these as calculations proceed.

Step 7. Adjust Q_{basic} assuming flow is in Region 1.

7.1 Calculate H_*, the ratio of flow depths on the flood plains and in the main channel,

$$H_* = \frac{(H-h)}{H}$$

7.2 Calculate the Darcy-Weisbach friction factors for the main channel, f_C, and the flood plains, f_F, using the relationship

$$f = \frac{8\ g\ R\ S}{V^2}$$

in which
- g is the gravitational acceleration = 9.81 m/s^2,
- R is the appropriate hydraulic radius (= A/P, excluding the bank lines from P) (m),
- S is the hydraulic gradient, equal to the channel gradient (S_o) for uniform flow, and
- V is the appropriate basic average flow velocity (m/s).

V_C and V_F can be calculated by dividing the basic zonal discharges (step 5) by the appropriate areas. If there are two flood plains a single value of f_F should be calculated by using the combined areas, wetted perimeters and basic discharges.

7.3 Calculate the dimensionless flood plain discharge deficit,

$$Q_{*2F} = -\ 1.0\ H_*\ \frac{f_c}{f_F}$$

7.4 Calculate the dimensionless main channel discharge deficit,

$$Q_{*2C} = -\ 1.240 + 0.395\ \frac{B}{w_c} + G\ H_*$$

for one flood plain, or

$$Q_*2C = -\ 1.240 + 0.395 \frac{2B}{2w_c} + G\ H_*$$

for two flood plains.

In these equations

$$G = 10.42 + 0.17\frac{f_F}{f_c} \qquad \text{for } S_C \geq 1.0$$

$$G = 10.42 + 0.17\frac{f_F}{f_c} + 0.34\,(1 - S_C) \qquad \text{for } S_C < 1.0$$

The value of Q_{*2C} should not be less than 0.5. If the calculated value is less than this, set it to 0.5 and set Q_{*2F} to zero.

7.5 Calculate the aspect ratio adjustment factor,

$$ARF = \frac{2b}{10h}$$

ARF should not exceed 2.0. If the calculated value is greater than this, set it to 2.0.

7.6 Calculate the total discharge deficit, the difference between Q_{basic} and the actual discharge,

$$DISDEF = (Q_{*2C} + N_F\, Q_{*2F})\,(V_C - V_F)\, H\, h\, ARF$$

in which N_F is the number of flood plains (1 or 2), and
V_c, V_F are the zonal main channel and flood plain average flow velocities respectively.

7.7 Calculate the Region 1 adjusted discharge for the specified water level,

$$Q_{R1} = Q_{basic} - DISDEF$$

Step 8. **Adjust Q_{basic} assuming flow is in Region 2.** The adjustment is defined by the channel coherence at a flow depth greater than that specified. (Channel coherence is the ratio of the conveyance calculated as a single cross-section to that calculated by summing the conveyances of the separate flow zones).

8.1 Calculate the "shift" to be applied to the specified flow depth,

$$\text{shift} = 0.05 + 0.05\, N_F \qquad \text{for } s_C \geq 1.0$$

$$\text{shift} = -0.01 + 0.05\, N_F + 0.06\, s_C \qquad \text{for } s_C < 1.0$$

8.2 Calculate the shifted flow depth,

$$H' = \frac{H\, h}{(h - \text{shift}\, H)}$$

8.3 Calculate the channel coherence for the shifted flow depth, H',

$$COH = \frac{(1 + A_*)\, \{((1 + A_*) / (1 + f_* P_*))\}^{0.5}}{1 + A_*\, \{(A_* / (f_* P_*))\}^{0.5}}$$

in which $A_* = A_F / A_C$,
A_F is the total flood plain flow area (i.e. for both sides if there are two flood plains),
A_C is the main channel flow area,
$f_* = f_F / f_C$,
f_F is the Darcy-Weisbach friction factor for the flood plains,
f_C is the Darcy-Weisbach friction factor for the main channel,
$P_* = P_F / P_C$,
P_F is the total flood plain wetted perimeter (i.e. for both sides if there are two flood plains), excluding the bank lines,
P_C is the main channel wetted perimeter, excluding the bank lines.

The areas and wetted perimeters should correspond to the required flow depth, i.e. H' for this calculation.

The friction factors should also be recalculated, as in Step 7.2, using H'. If the shifted flow depth is above the extreme lateral points of the surveyed cross-section, extend the cross-section vertically from these points to the required level to enable areas and wetted perimeters to be calculated.

8.4 Define the Region 2 discharge adjustment factor,

$$DISADF_2 = COH$$

8.5 Calculate the Region 2 adjusted discharge for the specified water level,

$$Q_{R2} = Q_{basic} \times DISADF_2$$

Step 9. Determine if Q_{R1} is the actual discharge, Q.

If $Q_{R1} \geq Q_{R2}$ then $Q = Q_{R1}$

If $Q = Q_{R1}$ the calculations are complete for the specified water level, unless a skew correction (step 14) is required. If $Q_{R1} < Q_{R2}$ the actual discharge is still unknown; in this case proceed with step 10.

Step 10. Adjust Q_{basic} assuming flow is in Region 3.

10.1 Calculate the channel coherence, COH, using the equation given for the Q_{R2} calculation, but for the specified flow depth, H, instead of H'.

10.2 Calculate the Region 3 discharge adjustment factor,

$$DISADF_3 = 1.567 - 0.667\ COH$$

10.3 Calculate the Region 3 adjusted discharge for the specified water level,

$$Q_{R3} = Q_{basic} \times DISADF_3$$

Step 11. Determine if Q_{R2} is the actual discharge.

If $Q_{R2} \leq Q_{R3}$ then $Q = Q_{R2}$

If $Q = Q_{R2}$ the calculations are complete for the specified water level, unless a skew correction (step 14) is required. If $Q_{R2} > Q_{R3}$ the actual discharge is still unknown; in this case proceed with step 12.

Step 12. Adjust Q_{basic} assuming flow is in Region 4.

12.1 Define the Region 4 discharge adjustment factor. This is equal to the channel coherence for the specified flow depth, H, as calculated above for Region 3, i.e.

$$DISADF_4 = COH$$

12.2 Calculate the Region 4 adjusted discharge for the specified water level,

$$Q_{R4} = Q_{basic} \times DISADF_4$$

Step 13. Determine which of Q_{R3} and Q_{R4} is the actual discharge.

If $Q_{R3} > Q_{R4}$ then $Q = Q_{R3}$

If $Q_{R3} < Q_{R4}$ then $Q = Q_{R4}$

Discharge calculations are now complete for the specified water level, unless a skew correction is required. If so, proceed with step 14.

Step 14. Apply the skew correction if the main channel is not aligned with the flood plains. This is done as follows and applies for angles of skew up to 10°.

14.1 Measure the angle of skew (in degrees) between the main channel and the flood plain (Φ) on a suitable map.

14.2 Calculate the discharge deficiency from the results already obtained,

$$DISDEF = Q_{basic} - Q$$

14.3 Correct the discharge deficiency to account for skewness,

$$DISDEF_{skew} = DISDEF \times (1.03 + 0.074\ \Phi)$$

14.4 Recalculate the actual discharge,

$$Q = Q_{basic} - DISDEF_{skew}$$

Q is the actual discharge for the specified flow depth, H.

3. Procedure for separation of main channel and flood plain discharges

If discharges for the main channel and flood plains are required separately, they can be estimated as follows. This will be necessary if f_F is to be estimated from measured data. The procedure has not been verified for skewed main channels and should be applied with caution for such cases.

Step 1. Determine the actual, adjusted, total discharge for the required water level, as described in Section 2.

Step 2. Identify the flow region and calculate the separate discharges.

2.1 If the actual discharge is in Region 1, i.e. $Q = Q_{R1}$, determine the separate discharges using the results from the predictive method described in the section 2, i.e.

$$Q_C = Q_{Cbasic} - Q_{*2C} (V_C - V_F) H h ARF$$

for the main channel, and

$$Q_F = Q_{Fbasic} - Q_{*2F} (V_C - V_F) H h ARF$$

for each flood plain.

2.2 If the actual discharge is in one of Regions 2, 3 or 4, assume that the flood plain discharges are unaffected by the interaction, and allocate all the adjustment to the main channel discharge, i.e.

$$Q_C = Q_{Cbasic} - DISDEF$$

$$Q_F = Q_{Fbasic}$$

4. Procedure for estimation of boundary shear stress

Boundary shear stresses are required for predicting locations of scour, designing scour protection, and estimating sediment transport rates. These issues will be addressed by future research. The following steps can be used for obtaining provisional estimates of the average shear stress on the main channel bed and the average and maximum shear stresses on the flood plains.

Step 1. Calculate the average shear stress on the bed in the main channel.

1.1 Calculate the average boundary shear stress, ignoring the interaction effects,

$$\tau_{oC} = \rho g R_C S$$

in which ρ is the density of water (1000 kg/m^3), and

R_C is the hydraulic radius of the main channel, excluding the bank lines from the wetted perimeter.

1.2 Calculate the discharge adjustment factor for the main channel,

$$DISADF_C = Q_C / Q_{Cbasic}$$

in which Q_C is the actual main channel discharge, as calculated in Section 3, and
Q_{Cbasic} is the basic main channel discharge, as calculated in Section 2, step 5.

1.3 Calculate the corrected average boundary shear stress, accounting for the interaction effect,

$$\tau_{oC}' = \tau_{oC} (DISADF_C)^2$$

Step 2. Calculate the average shear stress on the surface of the flood plain, ignoring the interaction effects,

$$\tau_{oF} = \rho\, g\, (H - h)\, S$$

This will apply on the flood plain surface beyond the zone of interaction with the main channel flow. Allow for a maximum local value of 5 τ_{oF} within a distance of 3 h from the bank line.

5. Reference

Ackers, P. (1991) The hydraulic design of straight compound channels, Report SR 281, HR Wallingford, December.

6. Notation

A	cross-sectional area
A_{Csurv}	area of main channel below bank elevation, from surveyed cross-section
A_*	ratio A_F/A_C
B	half the total compound channel width for two flood plains; width of flood plain plus half main channel width for one flood plain
b	half the bottom width of the main channel
COH	channel coherence
DISADF	adjustment factor applied to basic discharge to account for interaction effects; subscript will indicate appropriate region
DISDEF	discharge deficit, i.e. difference between actual and basic discharges
$DISDEF_{skew}$	discharge deficit, accounting for main channel skew
f	Darcy-Weisbach friction factor, $= 8gRS/V^2$
f_*	ratio f_F/f_C
G	parameter in Region 1 discharge deficit prediction
g	gravitational acceleration
H	depth of flow in main channel
H_*	ratio of flow depths on flood plain and main channel, i.e. $(H-h)/H$
H'	shifted flow depth in main channel (for Region 2 prediction)
h	depth of main channel bed below river bank elevation
N_F	number of flood plains, 1 or 2
n	Manning's roughness coefficient
P	wetted perimeter
P_*	ratio P_F/P_C
Q	actual discharge, unsubscripted for whole compound channel
Q_{basic}	zonal discharge ignoring bank lines from wetted perimeter, unsubscripted for sum of main channel and flood plain values
Q_R	discharge as adjusted to account for interaction effects in region indicated by numerical subscript
Q_{*2}	discharge deficit normalized by $(V_C-V_F)Hh$
R	hydraulic radius, $= A/P$
S	hydraulic gradient of channel
S_o	surveyed channel gradient
s_C	side slope of main channel bank, horizontal/vertical
shift	addition to main channel flow depth in Region 2 adjustment prediction
V	average flow velocity
w_C	half width of main channel between bank lines
ρ	density of water
τ_o	average bed shear stress
τ_{oC}'	average main channel bed shear stress adjusted for interaction effect
Φ	angle of skew between main channel and flood plains

subscripts :

C	main channel
F	flood plain
L	left bank

R	right bank
1,2,3,4	region of flow behaviour

Appendix 4

Data from laboratory studies into meandering flow

Appendix 4 Data from laboratory studies into meandering flow

The stage discharge data available from the various laboratory studies are listed below. The data includes:

SERC FCF	B20, B21, B25, B26, B31, B32, B33, B34, B38, B39, B43, B46, B47, B48, B49, B50.
Aberdeen	AB100, AB100A, AB101, AB102, AB103, AB104, AB105.
Vicksburg	VB201, VB202, VB203, VB204, VB205, VB206, VB207, VB208, VB209, VB210, VB211.
Kiely	KI300, 301
Sooky	SK401, SK402, SK403, SK404, SK405, SK406, SK407, SK408, SK409, SK410, SK411.

The file format is as follows:

The first ten lines at the top of each file are comment lines. Information about the data is listed here.

The first two numbers after this are:

1 The test series number
2 The number of data points

The stage discharge data for each discharge point follows. An Example data line is shown below.

Date	discharge	depth1	depth2	slope	tailgate	temp
29 11 89	0.01975	59.34	59.32	0.996	667.84	11.4

Date is given as three integers: day, month and year.

Discharge is given in cubic metres per second.

Depth1 is the depth in millimetres as recorded in the original data files.

Depth2 is the depth in millimetres as corrected to the channel bed slope. This value of depth should be used in any analysis. It is worth noting that only the SERC FCF data was adjusted in this way. Depth1 and Depth2 for the other data sets are identical.

Slope is the longitudinal valley slope of the flume. These values should be multiplied by 1/1000.

Tailgate is the tailgate setting for the SERC FCF. This data was retained in the files but should not be used.

Temp is the temperature in degrees centigrade of the water in the flume as recorded by the investigators. Where the temperature was not recorded a default value of 15 °C has been assumed.

1 SERC FCF Stage Discharge Data Phase B Meandering case
2
3 File name (ASSIGNED FOR MEANDR) : SDB20
4 Plan geometry (angle of cross over) : 60
5 Main Channel X-sn : Trapezoidal
6 Floodplain width : Standard
7 Floodplain roughness : Smooth
8

9 DATE	DISCHARGE m3 sec.	DEPTH AS RECORDED mm	DEPTH AS PLOTTED mm	SLOPE	TAILGATE	TEMP c.
10						
20 17						
29 11 89	0.01975	59.34	59.32	0.996	667.84	11.4
27 11 89	0.02512	67.16	67.26	0.996	663.84	11.0
17 11 89	0.02654	71.89	71.98	0.996	661.81	12.4
27 11 89	0.03056	77.56	77.14	0.996	658.72	10.8
17 11 89	0.03308	82.43	82.63	0.996	656.68	12.4
29 11 89	0.03630	86.06	86.08	0.996	653.81	11.6
30 11 89	0.04015	91.56	91.70	0.996	650.83	11.5
01 12 89	0.04425	97.79	97.65	0.996	648.15	11.6
07 12 89	0.04708	101.92	101.92	1.001	646.00	12.7
30 11 89	0.04782	102.99	103.02	0.996	644.92	11.5
29 11 89	0.05015	105.29	105.93	0.996	643.39	11.7
27 11 89	0.04974	105.68	105.96	0.996	643.49	10.9
20 11 89	0.04953	106.92	106.80	0.996	643.22	12.4
16 11 89	0.05467	111.57	111.50	0.996	641.12	13.7
16 11 89	0.05702	113.94	113.94	0.9969	640.00	12.7
15 11 89	0.06035	118.84	119.00	0.996	636.81	13.6
16 11 89	0.07073	131.24	131.50	0.996	629.67	12.9

1 SERC FCF Stage Discharge Data Phase B Meandering case
2
3 File name (ASSIGNED FOR MEANDR) : SDB21
4 Plan geometry (angle of cross over) : 60
5 Main Channel X-sn : Trapezoidal
6 Floodplain width : Standard
7 Floodplain roughness : Smooth
8

9 DATE	DISCHARGE m3/sec.	DEPTH AS RECORDED mm	DEPTH AS PLOTTED mm	SLOPE	TAILGATE	TEMP C
10						
21 16						
28 11 89	0.08240	163.93	164.13	0.9960	562.37	11.5
28 11 89	0.08576	165.56	165.84	0.9960	561.56	11.5
28 11 89	0.09753	169.85	170.11	0.9660	560.13	11.4
24 11 89	0.10960	172.73	173.05	0.9660	559.72	11.6
24 11 89	0.11980	175.48	175.70	0.9660	559.42	11.6
02 11 89	0.14940	181.49	181.66	0.9660	559.00	14.6
01 11 89	0.20390	191.98	191.98	0.9986	557.00	14.0
06 11 89	0.24960	199.61	199.73	0.9960	556.00	12.8
23 11 89	0.30228	207.65	207.95	0.9960	556.90	12.2
01 11 89	0.30300	208.46	208.46	0.9903	555.00	14.5
16 11 89	0.44020	227.59	227.63	0.9960	552.00	13.2
16 11 89	0.48501	232.90	232.90	1.0069	551.41	14.4
28 11 89	0.49360	235.02	235.00	0.9960	551.74	11.0
10 02 90	0.76670	264.84	264.84	0.9978	546.00	12.3
10 02 90	0.87861	277.48	277.95	0.9960	543.40	12.3
10 02 90	0.98939	289.11	288.73	0.9960	541.40	12.3

1 SERC FCF Stage Discharge Data Phase B Meandering case
2
3 File name (ASSIGNED FOR MEANDR) : SDB25
4 Plan geometry (angle of cross over) : 60
5 Main Channel X-sn : Natural inbank
6 Floodplain width : Standard
7 Floodplain roughness : Smooth
8

9 DATE	DISCHARGE m3 sec.	DEPTH AS RECORDED mm	DEPTH AS PLOTTED mm	SLOPE	TAILGATE	TEMP c.
10						
25 10						
17 7 90	0.01019	99.57	99.57	0.9960	610.00	16.1
17 7 90	0.01207	103.59	103.59	0.9954	610.03	16.1
16 7 90	0.01442	108.40	108.60	0.9660	606.67	16.1
16 7 90	0.01612	112.36	112.25	0.9960	605.31	16.0
16 7 90	0.01806	116.50	116.48	0.9960	603.21	16.1
16 7 90	0.02150	123.20	123.16	0.9960	600.20	16.0
19 7 90	0.02288	125.73	125.66	0.9960	599.10	16.0
17 7 90	0.02498	129.09	129.23	0.9960	597.59	16.2
18 7 90	0.02646	131.04	131.65	0.9960	596.53	16.0
06 8 90	0.03341	142.34	132.34	0.9977	592.00	17.1

SERC FCF Stage Discharge Data Phase B Meandering case

File name (ASSIGNED FOR MEANDR) : SDB26
Plan geometry (angle of cross over) : 60
Main Channel X-sn : Natural Over bank
Floodplain width : Standard
Floodplain roughness : Smooth

DATE	DISCHARGE m3 /sec.	DEPTH AS RECORDED mm	DEPTH AS PLOTTED mm	SLOPE	TAILGATE	TEMP c.
26	16					
12 07 90	0.03993	152.75	152.64	0.9960	562.06	16.2
06 08 90	0.04965	162.89	162.89	0.9942	557.00	17.1
10 10 90	0.05791	165.23	165.23	1.0030	557.00	13.5
13 07 90	0.06051	166.93	167.11	0.9960	555.53	15.9
10 07 90	0.10310	177.91	177.89	0.9960	555.10	14.7
12 07 90	0.16018	189.58	189.58	0.9962	555.00	15.9
10 07 90	0.20447	196.64	196.53	0.9960	554.87	14.4
13 07 90	0.26744	206.84	206.84	0.9980	553.88	16.0
10 07 90	0.30725	212.06	212.26	0.9960	553.56	14.7
12 07 90	0.38733	222.92	223.35	0.9960	552.31	15.5
11 07 90	0.53963	241.21	241.38	0.9960	549.70	14.9
11 07 90	0.64651	253.42	253.94	0.9960	547.39	15.5
11 07 90	0.75203	264.59	264.96	0.9960	545.60	15.6
11 07 90	0.85873	274.82	275.23	0.9960	544.47	15.7
27 10 90	0.97758	287.76	287.69	0.9960	542.59	13.9
27 10 90	1.09296	296.46	296.46	1.0167	541.33	14.2

SERC FCF Stage Discharge Data Phase B Meandering case

File name (ASSIGNED FOR MEANDR) : SDB31
Plan geometry (angle of cross over) : 60
Main Channel X-sn : Natural
Floodplain width : Narrow
Floodplain roughness : Smooth

DATE	DISCHARGE m3/sec.	DEPTH AS RECORDED mm	DEPTH AS PLOTTED mm	SLOPE	TAILGATE	TEMP c.
31	14					
22 9 90	0.03871	159.80	159.83	0.9960	562.57	14.0
22 9 90	0.05079	168.51	168.51	0.9973	559.88	13.9
19 9 90	0.05766	170.21	170.15	0.9960	559.68	14.4
21 9 90	0.06616	173.64	173.64	0.9948	560.0	14.4
18 9 90	0.08538	180.03	180.05	0.9960	559.13	14.0
18 9 90	0.11231	188.91	188.75	0.9960	558.81	14.1
21 9 90	0.16120	202.76	202.76	0.9951	559.07	14.4
21 9 90	0.19296	209.76	209.94	0.9960	558.21	14.4
18 9 90	0.22834	218.89	219.18	0.9960	556.68	14.3
19 9 90	0.28208	230.53	230.85	0.9960	554.39	14.7
21 9 90	0.29029	232.86	232.86	0.9968	555.00	15.4
20 9 90	0.38009	251.55	251.58	0.9960	552.93	15.6
20 9 90	0.47314	264.45	264.68	0.9960	550.69	15.3
20 9 90	0.57135	282.52	282.78	0.9960	547.47	15.0

SERC FCF Stage Discharge Data Phase B Meandering case

File name (ASSIGNED FOR MEANDR) : SDB32
Plan geometry (angle of cross over) : 60
Main Channel X-sn : Natural
Floodplain width : Standard
Floodplain roughness : Breeze blocks simulating piers

DATE	DISCHARGE m3/sec.	DEPTH AS RECORDED mm	DEPTH AS PLOTTED mm	SLOPE	TAILGATE	TEMP c.
32	13					
10 01 91	0.04333	159.91	158.85	0.9960	558.62	12.3
10 01 91	0.05430	165.26	165.37	0.9960	556.60	12.2
10 01 91	0.09961	178.41	178.54	0.9960	554.55	13.4
10 01 91	0.13331	185.85	186.00	0.9960	553.62	13.3
11 01 91	0.19814	198.68	198.50	0.9960	533.37	13.4
10 01 91	0.26714	210.92	210.92	0.9973	550.00	13.3
11 01 91	0.33568	221.92	221.87	0.9960	547.56	13.0
11 01 91	0.39576	231.31	231.88	0.9960	545.49	13.4
26 10 90	0.45946	238.23	238.23	0.9959	543.00	15.2
26 10 90	0.57207	254.93	254.77	0.9960	539.20	15.0
26 10 90	0.68564	269.36	269.52	0.9960	535.29	14.5
26 10 90	0.80040	284.61	284.43	0.9960	531.22	14.2
26 10 90	0.91832	297.51	298.55	0.9960	527.53	13.9

SERC FCF Stage Discharge Data Phase B Meandering case

File name (ASSIGNED FOR MEANDR) : SDB33
Plan geometry (angle of cross over) : 60
Main Channel X-sn : Natural
Floodplain width : Standard
Floodplain roughness : Partially roughened dowel rods

DATE	DISCHARGE m3/sec.	DEPTH AS RECORDED mm	DEPTH AS PLOTTED mm	SLOPE	TAILGATE	TEMP c.
33 12						
05 11 90	0.04161	158.77	158.68	0.9960	558.15	12.2
05 11 90	0.06651	169.86	169.83	0.9960	553.06	12.2
01 11 90	0.08653	176.51	176.51	1.0012	551.72	12.8
01 11 90	0.11244	183.67	183.60	0.9960	550.17	13.0
01 11 90	0.16988	196.35	196.83	0.9960	546.61	13.0
05 11 90	0.22181	207.55	207.80	0.9660	543.63	12.1
05 11 90	0.27174	218.23	218.23	0.9966	540.00	11.8
05 11 90	0.32182	228.39	228.50	0.9960	535.81	11.6
31 10 90	0.49790	258.89	257.87	0.9960	524.22	13.4
31 10 90	0.56938	271.79	271.95	0.9960	517.76	13.0
31 10 90	0.67561	289.11	289.22	0.9960	509.89	13.3
31 10 90	0.76534	305.01	305.01	0.9975	503.00	13.3

SERC FCF Stage Discharge Data Phase B Meandering case

File name (ASSIGNED FOR MEANDR) : SDB34
Plan geometry (angle of cross over) : 60
Main Channel X-sn : Natural
Floodplain width : Standard
Floodplain roughness : Roughened with Dowel Rods

DATE	DISCHARGE m3/sec.	DEPTH AS RECORDED mm	DEPTH AS PLOTTED mm	SLOPE	TAILGATE	TEMP c.
34 18						
16 11 90	0.04015	158.61	158.58	0.9960	557.03	15.0
16 11 90	0.05445	167.64	167.64	0.9957	552.01	14.5
16 11 90	0.06742	174.00	174.32	0.9960	549.24	14.4
15 11 90	0.09209	184.90	184.80	0.9960	544.63	15.0
15 11 90	0.11197	192.13	192.50	0.9960	541.24	14.7
15 11 90	0.13203	200.79	201.01	0.9960	537.18	15.0
15 11 90	0.15440	209.36	209.60	0.9960	532.63	14.8
14 11 90	0.17485	217.21	217.17	0.9960	529.05	15.4
12 11 90	0.19857	224.48	224.45	0.9960	525.09	13.8
12 11 90	0.23395	238.71	238.65	0.9960	517.06	14.2
14 11 90	0.26401	250.38	250.83	0.9960	510.00	15.0
12 11 90	0.27588	255.26	254.83	0.9960	507.97	14.8
14 11 90	0.30182	265.00	265.35	0.9960	501.62	15.0
12 11 90	0.32655	272.95	273.40	0.9960	497.12	14.6
13 11 90	0.34158	278.44	279.08	0.9960	493.31	14.8
14 11 90	0.37602	292.09	292.25	0.9960	485.36	14.6
13 11 90	0.41000	301.68	301.96	0.9960	479.64	15.4
13 11 90	0.45527	317.31	317.55	0.9960	469.64	15.0

SERC FCF Stage Discharge Data Phase B Meandering case

File name (ASSIGNED FOR MEANDR) : SDB38
Plan geometry (angle of cross over) : 110
Main Channel X-sn : Natural Inbank
Floodplain width : Standard
Floodplain roughness : Smooth

DATE	DISCHARGE m3/sec.	DEPTH AS RECORDED mm	DEPTH AS PLOTTED mm	SLOPE	TAILGATE	TEMP c.	
38 11							
23 4 91	0.01135	109.80	110.06	1.0210	604.17	10.4	
31 7 91	0.01322	115.16	115.16	1.0144	601.00	15.0	
24 4 91	0.01533	120.30	120.30	1.0218	598.95	10.5	
31 7 91	0.01560	120.73	120.73	1.0217	597.92	14.4	
01 8 91	0.01699	124.20	124.20	1.0161	596.00	14.1	*
23 4 91	0.01873	127.91	127.91	1.0205	595.00	10.3	
30 7 91	0.02006	130.72	130.72	1.0161	594.22	15.9	*
01 8 91	0.02206	135.66	135.66	1.0262	590.50	14.9	*
23 4 91	0.02342	138.82	138.54	1.0210	588.59	10.3	
24 4 91	0.02432	140.08	140.27	1.0210	587.69	10.5	
23 4 91	0.02778	146.72	146.72	1.0210	584.46	10.4	

* DEPTHS SET FOR DR I GUYMER FOR DISPERSION TESTS

SERC FCF Stage Discharge Data Phase B Meandering case

File name (ASSIGNED FOR MEANDR) : SDB39
Plan geometry (angle of cross over) : 110
Main Channel X-sn : Natural
Floodplain width : Standard
Floodplain roughness : Smooth

DATE	DISCHARGE m3/sec.	DEPTH AS RECORDED mm	DEPTH AS PLOTTED mm	SLOPE	TAILGATE	TEMP c.
39	14					
05 7 91	0.03815	165.14	165.14	1.0177	557.00	15.5
22 4 91	0.07693	178.92	178.92	1.0210	553.50	10.3
22 4 91	0.09972	183.58	183.76	1.0210	553.35	10.3
23 5 91	0.14208	193.65	193.43	1.0210	552.56	12.7
08 5 91	0.17925	200.61	200.61	1.0221	552.00	11.4
23 5 91	0.25282	214.07	214.75	1.0210	549.63	12.9
03 7 91	0.32467	225.21	225.20	1.0210	548.26	14.5
03 7 91	0.39138	235.01	235.13	1.0210	546.61	15.4
03 7 91	0.44517	242.66	242.77	1.0210	545.20	15.3
07 5 91	0.55351	256.86	256.86	1.0201	541.07	11.2
07 5 91	0.66137	270.05	270.33	1.0210	538.6	11.6
07 5 91	0.77988	284.50	284.48	1.0210	535.60	12.0
24 5 91	0.88127	296.88	296.71	1.0210	532.73	13.2
24 5 91	0.94356	302.82	302.88	1.0210	532.43	14.5

SERC FCF Stage Discharge Data Phase B Meandering case

File name (ASSIGNED FOR MEANDR) : SDB43
Plan geometry (angle of cross over) : 110
Main Channel X-sn : Natural
Floodplain width : Standard
Floodplain roughness : Roughened with dowel rods

DATE	DISCHARGE m3/sec.	DEPTH AS RECORDED mm	DEPTH AS PLOTTED mm	SLOPE	TAILGATE	TEMP c.
43	15					
02 9 91	0.03252	160.54	160.47	1.0210	558.13	16.6
23 8 91	0.03688	165.98	165.98	1.0124	556.00	16.7
16 8 91	0.05451	175.02	175.06	1.0210	550.42	16.3
16 8 91	0.08361	187.39	187.60	1.0210	544.68	16.3
15 8 91	0.10803	197.19	197.08	1.0210	540.27	16.1
29 8 91	0.11685	200.85	200.85	1.0205	539.00	16.7
21 8 91	0.14392	211.73	211.75	1.0210	533.30	16.9
21 8 91	0.17375	221.75	221.93	1.0210	527.26	16.7
19 8 91	0.20112	231.55	231.93	1.0210	523.13	16.3
21 8 91	0.24342	247.40	247.35	1.0210	514.40	16.4
19 8 91	0.27848	259.26	259.27	1.0210	507.51	16.5
19 8 91	0.31616	272.21	271.89	1.0210	500.31	16.3
20 8 91	0.34940	283.40	283.42	1.0210	493.42	16.5
20 8 91	0.38851	296.31	296.60	1.0210	486.25	17.0
20 8 91	0.43331	311.19	310.53	1.0210	477.62	16.4

SERC FCF Stage Discharge Data Phase B Meandering case

File name (ASSIGNED FOR MEANDR) : SDB46
Plan geometry (angle of cross over) : 110
Main Channel X-sn : Natural
Floodplain width : Standard
Floodplain roughness : Roughened with breeze blocks

DATE	DISCHARGE m3/sec.	DEPTH AS RECORDED mm	DEPTH AS PLOTTED mm	SLOPE	TAILGATE	TEMP c.	
46	14						
17 9 91	0.03525	162.88	162.83	1.0210	559.07	15.7	
17 9 91	0.05185	171.30	171.30	1.0224	555.00	15.7	*
16 9 91	0.10064	184.99	185.18	1.0210	552.82	15.7	
19 9 91	0.12617	190.98	190.89	1.0209	552.00	15.4	*
19 9 91	0.15775	197.96	197.96	1.0203	555.00	15.3	*
17 9 91	0.16817	200.65	200.64	1.0210	549.54	15.8	
19 9 91	0.21985	210.96	210.77	1.0210	547.34	15.4	
19 9 91	0.25247	216.84	217.15	1.0210	545.67	15.7	
17 9 91	0.31685	229.81	229.45	1.0210	542.83	16.0	
20 9 91	0.36295	237.38	237.55	1.0210	539.78	14.7	
20 9 91	0.46613	254.90	254.95	1.0210	533.93	15.0	
18 9 91	0.53525	263.78	263.60	1.0210	531.27	15.8	
18 9 91	0.64489	280.09	280.15	1.0210	526.63	16.6	
18 9 91	0.75729	296.26	296.35	1.0210	520.87	16.3	

SERC FCF Stage Discharge Data Phase B Meandering case

File name (ASSIGNED FOR MEANDR) : SDB47
Plan geometry (angle of cross over) : 110
Main Channel X-sn : Natural
Floodplain width : Narrow
Floodplain roughness : Smooth

DATE	DISCHARGE m3/sec.	DEPTH AS RECORDED mm	DEPTH AS PLOTTED mm	SLOPE	TAILGATE	TEMP c.
47	14					
03 10 91	0.03559	164.84	164.94	1.0210	556.44	13.9
01 10 91	0.05023	171.12	171.12	1.0206	555.02	14.3
30 09 91	0.07456	179.60	179.50	1.0210	553.62	14.2
30 09 91	0.09496	185.23	185.30	1.0210	553.60	13.8
07 10 91	0.13586	195.66	195.63	1.0210	551.44	13.2
30 09 91	0.16491	202.48	202.65	1.0210	549.50	14.0
01 10 91	0.22050	213.55	213.54	1.0210	547.00	13.6
03 10 91	0.25933	221.65	221.65	1.0210	544.78	14.7
01 10 91	0.32792	234.20	234.12	1.0210	540.65	14.1
03 10 91	0.38649	244.55	244.52	1.0210	538.20	14.0
07 10 91	0.48556	259.96	259.63	1.0210	534.10	13.3
04 10 91	0.53429	264.95	264.93	1.0210	532.85	14.5
08 10 91	0.69847	288.42	288.46	1.0210	526.23	14.3
08 10 91	0.75055	294.75	294.60	1.0210	524.70	13.4

SERC FCF Stage Discharge Data Phase B Meandering case

File name (ASSIGNED FOR MEANDR) : SDB48
Plan geometry (angle of cross over) : 110
Main Channel X-sn : Natural
Floodplain width : Standard
Floodplain roughness : Smooth with walls

DATE	DISCHARGE m3/sec.	DEPTH AS RECORDED mm	DEPTH AS PLOTTED mm	SLOPE	TAILGATE	TEMP c.
48	8					
15 10 91	0.03353	170.30	169.85	1.0210	560.46	13.5
14 10 91	0.03499	174.95	175.05	1.0210	555.90	14.0
14 10 91	0.04065	189.95	189.95	1.0210	544.80	14.0
11 10 91	0.04540	202.60	202.60	1.0210	534.12	13.9
14 10 91	0.04945	212.68	212.68	1.0210	525.50	13.7
15 10 91	0.05538	232.44	232.44	1.0223	510.00	13.4
11 10 91	0.05659	233.15	233.25	1.0210	509.45	13.6
15 10 91	0.06312	242.35	242.05	1.0210	502.40	13.2

SERC FCF Stage Discharge Data Phase B Meandering case

File name : SDB49

Main Channel X-sn : trapezoidal

Floodplain roughness : rod roughness Phase A orientation

DATE	DISCHARGE m3/sec.	DEPTH AS RECORDED mm	DEPTH AS PLOTTED mm	SLOPE	TAILGATE	TEMP c.
49 7						
03 01 92	0.02252	29.586	29.64	1.0224	540.0	11.1
03 01 92	0.04432	50.644	50.57	1.0130	527.0	10.9
02 01 92	0.06183	65.082	65.08	1.0210	518.0	10.5
05 01 92	0.07971	84.130	83.78	1.0152	505.0	11.6
02 01 92	0.10305	110.895	109.25	0.9897	485.0	10.8
05 01 92	0.13002	134.722	135.52	1.0284	470.0	12.1
03 01 92	0.16352	162.180	163.43	1.0363	453.0	11.4

SERC FCF Stage Discharge Data Phase B Meandering case

File name : SDB50

Main Channel X-sn : trapezoidal

Floodplain roughness : rod roughness Phase B orientation

DATE	DISCHARGE m3/sec.	DEPTH AS RECORDED mm	DEPTH AS PLOTTED mm	SLOPE	TAILGATE	TEMP c.
50 7						
10 01 92	0.02225	28.241	28.24	1.0210	542	12.3
09 01 92	0.04134	45.233	45.42	1.0277	533	13.1
08 01 92	0.06159	62.602	62.00	1.0038	522	12.9
08 01 92	0.07982	84.135	83.40	1.0060	505	13.1
08 01 92	0.10015	101.256	101.98	1.0439	495	13.3
09 01 92	0.13394	132.168	132.11	1.0190	475	13.3
09 01 92	0.16028	153.969	154.10	1.0238	460	13.1

```
1    VICKSBURG DATA SET   2ft WIDE MAIN CHANNEL
2
3    File name (ASSIGNED FOR MEANDR)       :  SDVB201
4    Plan geometry         (SINUOSITY)     :  1.571
5    Main Channel X-sn                     :  Trapezoidal
6    Floodplain width                      :  4.877
7    Floodplain roughness                  :  0.012
8
9    DATE    DISCHARGE     DEPTH AS       DEPTH AS      SLOPE     TAILGATE    TEMP
10             m3/sec.     RECORDED mm    PLOTTED mm                             C

201    3

01 01 01     0.0702     182.88     182.88       1.0000       0.00    15.0
01 01 01     0.1424     213.36     213.36       1.0000       0.00    15.0
01 01 01     0.2231     243.84     243.84       1.0000       0.00    15.0


1    VICKSBURG DATA SET   2ft WIDE MAIN CHANNEL
2
3    File name (ASSIGNED FOR MEANDR)       :  SDVB202
4    Plan geometry         (SINUOSITY)     :  1.571
5    Main Channel X-sn                     :  Trapezoidal
6    Floodplain width                      :  4.877
7    Floodplain roughness                  :  0.025
8
9    DATE    DISCHARGE     DEPTH AS       DEPTH AS      SLOPE     TAILGATE    TEMP
10             m3/sec.     RECORDED mm    PLOTTED mm                             C

202    3

01 01 01     0.0430     182.88     182.88       1.0000       0.00    15.0
01 01 01     0.0875     213.36     213.36       1.0000       0.00    15.0
01 01 01     0.1546     243.84     243.84       1.0000       0.00    15.0


1    VICKSBURG DATA SET   2ft WIDE MAIN CHANNEL
2
3    File name (ASSIGNED FOR MEANDR)       :  SDVB203
4    Plan geometry         (SINUOSITY)     :  1.571
5    Main Channel X-sn                     :  Trapezoidal
6    Floodplain width                      :  4.877
7    Floodplain roughness                  :  0.035
8
9    DATE    DISCHARGE     DEPTH AS       DEPTH AS      SLOPE     TAILGATE    TEMP
10             m3/sec.     RECORDED mm    PLOTTED mm                             C

203    3

01 01 01     0.0396     182.88     182.88       1.0000       0.00    15.0
01 01 01     0.0733     213.36     213.36       1.0000       0.00    15.0
01 01 01     0.1283     243.84     243.84       1.0000       0.00    15.0


1    VICKSBURG DATA SET   2ft WIDE MAIN CHANNEL
2
3    File name (ASSIGNED FOR MEANDR)       :  SDVB204
4    Plan geometry         (SINUOSITY)     :  1.400
5    Main Channel X-sn                     :  Trapezoidal
6    Floodplain width                      :  4.877
7    Floodplain roughness                  :  0.012
8
9    DATE    DISCHARGE     DEPTH AS       DEPTH AS      SLOPE     TAILGATE    TEMP
10             m3/sec.     RECORDED mm    PLOTTED mm                             C

204    3

01 01 01     0.0830     182.88     182.88       1.0000       0.00    15.0
01 01 01     0.1560     213.36     213.36       1.0000       0.00    15.0
01 01 01     0.2430     243.84     243.84       1.0000       0.00    15.0


1    VICKSBURG DATA SET   2ft WIDE MAIN CHANNEL
2
3    File name (ASSIGNED FOR MEANDR)       :  SDVB205
4    Plan geometry         (SINUOSITY)     :  1.400
5    Main Channel X-sn                     :  Trapezoidal
6    Floodplain width                      :  4.877
7    Floodplain roughness                  :  0.025
8
9    DATE    DISCHARGE     DEPTH AS       DEPTH AS      SLOPE     TAILGATE    TEMP
10             m3/sec.     RECORDED mm    PLOTTED mm                             C

205   3

01 01 01     0.0490     182.88     182.88       1.0000       0.00    15.0
01 01 01     0.0985     213.36     213.36       1.0000       0.00    15.0
01 01 01     0.1679     243.84     243.84       1.0000       0.00    15.0
```

```
1    VICKSBURG DATA SET  2ft WIDE MAIN CHANNEL
2
3    File name (ASSIGNED FOR MEANDR)      :  SDVB206
4    Plan geometry        (SINUOSITY)     :  1.400
5    Main Channel X-sn                    :  Trapezoidal
6    Floodplain width                     :  4.877
7    Floodplain roughness                 :  0.035
8
9    DATE   DISCHARGE    DEPTH AS      DEPTH AS      SLOPE      TAILGATE     TEMP
10            m3/sec.    RECORDED mm   PLOTTED mm                               C

206   3

01 01 01     0.0439    182.88     182.88       1.0000        0.00    15.0
01 01 01     0.0832    213.36     213.36       1.0000        0.00    15.0
01 01 01     0.1373    243.84     243.84       1.0000        0.00    15.0


1    VICKSBURG DATA SET  2ft WIDE MAIN CHANNEL
2
3    File name (ASSIGNED FOR MEANDR)      :  SDVB207
4    Plan geometry        (SINUOSITY)     :  1.200
5    Main Channel X-sn                    :  Trapezoidal
6    Floodplain width                     :  4.877
7    Floodplain roughness                 :  0.012
8
9    DATE   DISCHARGE    DEPTH AS      DEPTH AS      SLOPE      TAILGATE     TEMP
10            m3/sec.    RECORDED mm   PLOTTED mm                               C

207  3

01 01 01     0.0915    182.88     182.88       1.0000        0.00    15.0
01 01 01     0.1792    213.36     213.36       1.0000        0.00    15.0
01 01 01     0.2772    243.84     243.84       1.0000        0.00    15.0


1    VICKSBURG DATA SET  2ft WIDE MAIN CHANNEL
2
3    File name (ASSIGNED FOR MEANDR)      :  SDVB208
4    Plan geometry        (SINUOSITY)     :  1.200
5    Main Channel X-sn                    :  Trapezoidal
6    Floodplain width                     :  4.877
7    Floodplain roughness                 :  0.025
8
9    DATE   DISCHARGE    DEPTH AS      DEPTH AS      SLOPE      TAILGATE     TEMP
10            m3/sec.    RECORDED mm   PLOTTED mm                               C

208   3

01 01 01     0.0550    182.88     182.88       1.0000        0.00    15.0
01 01 01     0.1090    213.36     213.36       1.0000        0.00    15.0
01 01 01     0.1798    243.84     243.84       1.0000        0.00    15.0


1    VICKSBURG DATA SET  2ft WIDE MAIN CHANNEL
2
3    File name (ASSIGNED FOR MEANDR)      :  SDVB209
4    Plan geometry        (SINUOSITY)     :  1.200
5    Main Channel X-sn                    :  Trapezoidal
6    Floodplain width                     :  4.877
7    Floodplain roughness                 :  0.035
8
9    DATE   DISCHARGE    DEPTH AS      DEPTH AS      SLOPE      TAILGATE     TEMP
10            m3/sec.    RECORDED mm   PLOTTED mm                               C

209   3

01 01 01     0.0484    182.88     182.88       1.0000        0.00    15.0
01 01 01     0.0864    213.36     213.36       1.0000        0.00    15.0
01 01 01     0.1437    243.84     243.84       1.0000        0.00    15.0


1    VICKSBURG DATA SET  2ft WIDE MAIN CHANNEL
2
3    File name (ASSIGNED FOR MEANDR)      :  SDVB210
4    Plan geometry        (SINUOSITY)     :  1.200
5    Main Channel X-sn                    :  Trapezoidal
6    Floodplain width                     :  9.144
7    Floodplain roughness                 :  0.035
8
9    DATE   DISCHARGE    DEPTH AS      DEPTH AS      SLOPE      TAILGATE     TEMP
10            m3/sec.    RECORDED mm   PLOTTED mm                               C

210   3

01 01 01     0.0674    182.88     182.88       1.0000        0.00    15.0
01 01 01     0.1399    213.36     213.36       1.0000        0.00    15.0
01 01 01     0.2449    243.84     243.84       1.0000        0.00    15.0
```

```
1    VICKSBURG DATA SET  2ft WIDE MAIN CHANNEL
2
3    File name (ASSIGNED FOR MEANDR)        :  SDVB211
4    Plan geometry        (SINUOSITY)       :  1.571
5    Main Channel X-sn                      :  Trapezoidal
6    Floodplain width                       :  9.144
7    Floodplain roughness                   :  0.035
8
9    DATE    DISCHARGE    DEPTH AS     DEPTH AS     SLOPE     TAILGATE     TEMP
10             m3/sec.    RECORDED mm  PLOTTED mm                             C

211   3

01 01 01    0.0507    182.88    182.88      1.0000       0.00   15.0
01 01 01    0.1178    213.36    213.36      1.0000       0.00   15.0
01 01 01    0.2226    243.84    243.84      1.0000       0.00   15.0
```

```
1    KIELY (UNIV COLLEGE CORK)  DATA SET
2
3    File name (ASSIGNED FOR MEANDR)        :  SDKI301
4    Plan geometry        (SINUOSITY)       :  1.224
5    Main Channel X-sn                      :  RECTANGULAR
6    Floodplain width                       :  1.200
7    Floodplain roughness.                  :  Smooth
8
9    DATE    DISCHARGE    DEPTH AS     DEPTH AS     SLOPE     TAILGATE     TEMP
10             m3/sec.    RECORDED mm  PLOTTED mm                             C

301   5

01 01 01    2.43E-3     54.7       54.7   1.0000      0.00   15.0
01 01 01    3.10E-3     60.0       60.0   1.0000      0.00   15.0
01 01 01    6.70E-3     69.7       69.7   1.0000      0.00   15.0
01 01 01    11.1E-3     80.0       80.0   1.0000      0.00   15.0
01 01 01    16.3E-3     89.4       89.4   1.0000      0.00   15.0

POINTS BELOW ARE THREE INBANK  RESULTS AND THE BANKFULL POINT FROM THE
RATING CURVE

01 01 01    0.669E-3       20.0        20.0       1.0000       0.00   15.0
01 01 01    1.303E-3       28.4        28.4       1.0000       0.00   15.0
01 01 01    2.042E-3       40.0        40.0       1.0000       0.00   15.0

01 01 01    2.324E-3       50.0        50.0       1.0000       0.00   15.0

NOTE THESE DATA HAVE BEEN SCALED OFF OF A PLOT
```

```
1    TOEBES+SOOKY (SOOKY'S THESIS) DATA SET
2
3    File name (ASSIGNED FOR MEANDR)      :  SDSK401
4    Plan geometry          (SINUOSITY)   :  1.1 (GIVEN BY SOOKY)
5    Main Channel X-sn                    :  RECT  1.5" DEEP
6    Floodplain width                     :  3.886' 1.1845m  SL = 0.675E-3
7    Floodplain roughness                 :  Smooth
8
9    DATE    DISCHARGE    DEPTH AS       DEPTH AS      SLOPE     TAILGATE    TEMP
10             m3/sec.    RECORDED mm    PLOTTED mm                          C

401   5

01 01 01     6.309E-3       63.6          63.6      0.675       0.00    15.0
01 01 01     7.886E-3       70.6          70.6      0.675       0.00    15.0
01 01 01     9.463E-3       73.5          73.5      0.675       0.00    15.0
01 01 01    11.041E-3       77.5          77.5      0.675       0.00    15.0
01 01 01    12.618E-3       80.6          80.6      0.675       0.00    15.0
```

```
1    TOEBES+SOOKY (SOOKY'S THESIS) DATA SET
2
3    File name (ASSIGNED FOR MEANDR)      :  SDSK402
4    Plan geometry          (SINUOSITY)   :  1.1 (GIVEN BY SOOKY)
5    Main Channel X-sn                    :  RECT  1.5" DEEP
6    Floodplain width                     :  3.886' 1.1845m SL = 0.87E-3

7    Floodplain roughness                 :  Smooth
8
9    DATE    DISCHARGE    DEPTH AS       DEPTH AS      SLOPE     TAILGATE    TEMP
10             m3/sec.    RECORDED mm    PLOTTED mm                          C

402   6

01 01 01     6.309E-3       62.2         62.2       0.87       0.00    15.0
01 01 01     7.886E-3       67.8         67.8       0.87       0.00    15.0
01 01 01     9.463E-3       70.3         70.3       0.87       0.00    15.0
01 01 01    11.041E-3       74.1         74.1       0.87       0.00    15.0
01 01 01    12.618E-3       75.7         75.7       0.87       0.00    15.0

01 01 01    14.195E-3       80.4         80.4       0.87       0.00    15.0
```

```
1    TOEBES+SOOKY (SOOKY'S THESIS) DATA SET
2
3    File name (ASSIGNED FOR MEANDR)      :  SDSK403
4    Plan geometry          (SINUOSITY)   :  1.1 (GIVEN BY SOOKY)
5    Main Channel X-sn                    :  RECT  1.5" DEEP
6    Floodplain width                     :  3.886' 1.1845m SL = 1.6E-3
7    Floodplain roughness                 :  Smooth
8
9    DATE    DISCHARGE    DEPTH AS       DEPTH AS      SLOPE     TAILGATE    TEMP
10             m3/sec.    RECORDED mm    PLOTTED mm                          C

403   6

01 01 01     6.309E-3      57.5       57.5         1.60       0.00    15.0
01 01 01     7.886E-3      61.3       61.3         1.60       0.00    15.0
01 01 01     9.463E-3      62.9       62.9         1.60       0.00    15.0
01 01 01    11.041E-3      65.9       65.9         1.60       0.00    15.0
01 01 01    12.618E-3      68.2       68.2         1.60       0.00    15.0

01 01 01    14.195E-3      71.9       71.9         1.60       0.00    15.0
```

```
1    TOEBES+SOOKY (SOOKY'S THESIS) DATA SET
2
3    File name (ASSIGNED FOR MEANDR)      :  SDSK404
4    Plan geometry          (SINUOSITY)   :  1.1 (GIVEN BY SOOKY)
5    Main Channel X-sn                    :  RECT  1.5" DEEP
6    Floodplain width                     :  3.886' 1.1845m  SL = 3.67E-3
7    Floodplain roughness                 :  Smooth
8
9    DATE    DISCHARGE    DEPTH AS       DEPTH AS      SLOPE     TAILGATE    TEMP
10             m3/sec.    RECORDED mm    PLOTTED mm                          C

404   6

01 01 01     6.309E-3      54.5       54.5        3.67      0.00    15.0
01 01 01     7.886E-3      55.1       55.1        3.67      0.00    15.0
01 01 01     9.463E-3      56.9       56.9        3.67      0.00    15.0
01 01 01    11.041E-3      59.0       59.0        3.67      0.00    15.0
01 01 01    12.618E-3      61.8       61.8        3.67      0.00    15.0

01 01 01    14.195E-3      62.7       62.7        3.67      0.00    15.0
```

1 TOEBES+SOOKY (SOOKY'S THESIS) DATA SET
2
3 File name (ASSIGNED FOR MEANDR) : SDSK405
4 Plan geometry (SINUOSITY) : 1.1 (GIVEN BY SOOKY)
5 Main Channel X-sn : RECT 3.0" DEEP
6 Floodplain width : 3.886' 1.1845m SL = 0.3E-3

7 Floodplain roughness : Smooth
8

9 DATE	DISCHARGE	DEPTH AS	DEPTH AS	SLOPE	TAILGATE	TEMP
10	m3/sec.	RECORDED mm	PLOTTED mm			C
405 5						
01 01 01	4.100E-3	88.6	88.6	0.30	0.00	15.0
01 01 01	4.732E-3	91.3	91.3	0.30	0.00	15.0
01 01 01	6.309E-3	98.6	98.6	0.30	0.00	15.0
01 01 01	9.463E-3	107.9	107.9	0.30	0.00	15.0
01 01 01	12.618E-3	114.3	114.3	0.30	0.00	15.0

1 TOEBES+SOOKY (SOOKY'S THESIS) DATA SET
2
3 File name (ASSIGNED FOR MEANDR) : SDSK406
4 Plan geometry (SINUOSITY) : 1.1 (GIVEN BY SOOKY)
5 Main Channel X-sn : RECT 3.0" DEEP
6 Floodplain width : 3.886' 1.1845m SL = 0.675E-3

7 Floodplain roughness : Smooth
8

9 DATE	DISCHARGE	DEPTH AS	DEPTH AS	SLOPE	TAILGATE	TEMP
10	m3/sec.	RECORDED mm	PLOTTED mm			C
406 7						
01 01 01	4.732E-3	88.4	88.4	0.675	0.00	15.0
01 01 01	6.309E-3	94.7	94.7	0.675	0.00	15.0
01 01 01	7.886E-3	98.9	98.9	0.675	0.00	15.0
01 01 01	9.463E-3	103.8	103.8	0.675	0.00	15.0
01 01 01	11.041E-3	106.4	106.4	0.675	0.00	15.0
01 01 01	12.618E-3	107.6	107.6	0.675	0.00	15.0
01 01 01	14.195E-3	109.0	109.0	0.675	0.00	15.0

1 TOEBES+SOOKY (SOOKY'S THESIS) DATA SET
2
3 File name (ASSIGNED FOR MEANDR) : SDSK407
4 Plan geometry (SINUOSITY) : 1.1 (GIVEN BY SOOKY)
5 Main Channel X-sn : RECT 3.0" DEEP
6 Floodplain width : 3.886' 1.1845m SL = 0.87E-3
7 Floodplain roughness : Smooth
8

9 DATE	DISCHARGE	DEPTH AS	DEPTH AS	SLOPE	TAILGATE	TEMP
10	m3/sec.	RECORDED mm	PLOTTED mm			C
407 7						
01 01 01	4.732E-3	86.6	86.6	0.87	0.00	15.0
01 01 01	6.309E-3	92.5	92.5	0.87	0.00	15.0
01 01 01	7.886E-3	96.5	96.5	0.87	0.00	15.0
01 01 01	9.463E-3	100.7	100.7	0.87	0.00	15.0
01 01 01	11.041E-3	104.2	104.2	0.87	0.00	15.0
01 01 01	12.618E-3	105.0	105.0	0.87	0.00	15.0
01 01 01	14.195E-3	106.2	106.2	0.87	0.00	15.0

1 TOEBES+SOOKY (SOOKY'S THESIS) DATA SET
2
3 File name (ASSIGNED FOR MEANDR) : SDSK408
4 Plan geometry (SINUOSITY) : 1.1 (GIVEN BY SOOKY)
5 Main Channel X-sn : RECT 3.0" DEEP
6 Floodplain width : 3.886' 1.1845m SL = 1.0E-3
7 Floodplain roughness : Smooth
8

9 DATE	DISCHARGE	DEPTH AS	DEPTH AS	SLOPE	TAILGATE	TEMP
10	m3/sec.	RECORDED mm	PLOTTED mm			C
408 5						
01 01 01	4.416E-3	82.8	82.8	1.00	0.00	15.0
01 01 01	4.732E-3	85.3	85.3	1.00	0.00	15.0
01 01 01	6.309E-3	90.3	90.3	1.00	0.00	15.0
01 01 01	9.463E-3	98.7	98.7	1.00	0.00	15.0
01 01 01	12.618E-3	104.0	104.0	1.00	0.00	15.0

1 TOEBES+SOOKY (SOOKY'S THESIS) DATA SET
2
3 File name (ASSIGNED FOR MEANDR) : SDSK409
4 Plan geometry (SINUOSITY) : 1.1 (GIVEN BY SOOKY)
5 Main Channel X-sn : RECT 3.0" DEEP
6 Floodplain width : 3.886' 1.1845m SL = 1.6E-3
7 Floodplain roughness : Smooth
8

9 DATE	DISCHARGE	DEPTH AS	DEPTH AS	SLOPE	TAILGATE	TEMP
10	m3/sec.	RECORDED mm	PLOTTED mm			C
409 6						
01 01 01	6.309E-3	88.1	88.1	1.60	0.00	15.0
01 01 01	7.886E-3	91.6	91.6	1.60	0.00	15.0
01 01 01	9.463E-3	94.7	94.7	1.60	0.00	15.0
01 01 01	11.041E-3	97.2	97.2	1.60	0.00	15.0
01 01 01	12.618E-3	99.4	99.4	1.60	0.00	15.0
01 01 01	14.195E-3	99.9	99.9	1.60	0.00	15.0

1 TOEBES+SOOKY (SOOKY'S THESIS) DATA SET
2
3 File name (ASSIGNED FOR MEANDR) : SDSK410
4 Plan geometry (SINUOSITY) : 1.1 (GIVEN BY SOOKY)
5 Main Channel X-sn : RECT 3.0" DEEP
6 Floodplain width : 3.886' 1.1845m SL = 3.0E-3
7 Floodplain roughness : Smooth
8

9 DATE	DISCHARGE	DEPTH AS	DEPTH AS	SLOPE	TAILGATE	TEMP
10	m3/sec.	RECORDED mm	PLOTTED mm			C
410 5						
01 01 01	6.940E-3	83.8	83.8	3.00	0.00	15.0
01 01 01	7.886E-3	86.1	86.1	3.00	0.00	15.0
01 01 01	9.463E-3	89.6	89.6	3.00	0.00	15.0
01 01 01	12.618E-3	95.1	95.1	3.00	0.00	15.0
01 01 01	14.195E-3	97.0	97.0	3.00	0.00	15.0

1 TOEBES+SOOKY (SOOKY'S THESIS) DATA SET
2
3 File name (ASSIGNED FOR MEANDR) : SDSK411
4 Plan geometry (SINUOSITY) : 1.1 (GIVEN BY SOOKY)
5 Main Channel X-sn : RECT 3.0" DEEP
6 Floodplain width : 3.886' 1.1845m SL = 3.67E-3
7 Floodplain roughness : Smooth
8

9 DATE	DISCHARGE	DEPTH AS	DEPTH AS	SLOPE	TAILGATE	TEMP
10	m3/sec.	RECORDED mm	PLOTTED mm			C
411 5						
01 01 01	7.886E-3	85.4	85.4	3.67	0.00	15.0
01 01 01	9.463E-3	88.7	88.7	3.67	0.00	15.0
01 01 01	11.041E-3	90.6	90.6	3.67	0.00	15.0
01 01 01	12.618E-3	93.0	93.0	3.67	0.00	15.0
01 01 01	14.195E-3	94.3	94.3	3.67	0.00	15.0

Appendix 5

Summary of the Ackers Rod Roughness method

Appendix 5 Summary of the Ackers Rod Roughness method

Basic resistance calculations for rod roughness as in the Wallingford tests may be based upon the following set of formulae, which allow for different numbers of rods in alternate rows:

$\beta_1 \quad = (1-n_1 z\ d/A)^{-2}$

$\beta_2 \quad = (1-n_2 z\ d/A)^{-2}$

For $1.75 < Z_* < 6.6$:

$\alpha C_D \quad = 1.184 - 0.277\ Z_* + \sqrt{(0.529\ Z_* - 0.843)}$

else $\alpha C_D \quad = 0.95$

$1/\sqrt{f_S} \quad = 2.02 \log(Re\sqrt{f_S}) - 1.38$

$f_{TOT} \quad = 8gRS/V^2 = 4\alpha C_D(\beta_1 N_1 + \beta_2 N_2)\ d\ z/P + (\beta_1 + \beta_2)f_S/2$

where

Re	= Reynolds number of blocked channel = $2\ V\ R\ (\sqrt{\beta_1}+\sqrt{\beta_2})/\nu$
$\beta_{1,2}$	= blockage effect, i.e. square of area ratios for alternate rows
$n_{1,2}$	= number of rods of dia d across zone rows 1 and 2
$N_{1,2}$	= number of rods per unit length of zone, rows 1 and 2
z	= depth of flow
A	= cross sectional area of zone under consideration
f_S	= friction factor due to smooth boundary
f_{TOT}	= overall friction factor
V	= nominal velocity given by component discharge/A
αC_D	= effective drag coefficient of rods
Z_*	= z/d
R	= hydraulic mean depth A/P, for zone under consideration
S	= hydraulic gradient (water surface slope)

The vertical rods were mounted in wooden frames (2.46m by 2.33m) to allow them to be lifted in and out of the flume. During Phase A the frames were placed in the flume with their short dimension perpendicular to the flow and during phase B the frames were used with the long dimension perpendicular to the flow direction, Figure A5.1.

Thus the appropriate values of n and N etc are slightly different for Phase A and B.

Phase A

Zone width	= 2.33m
Length of frame	= 2.46m
lateral rod spacing	= 0.315m
longitudinal rod spacing	= 0.537m

$n_{1,2}$ = 8, 7

$N_{1,2}$ = $n_{1,2}$ / longitudinal rod spacing

rod diameter = 0.025m

Phase B

Zone width	= 2.46m
Length of frame	= 2.33m
lateral rod spacing	= 0.537m
longitudinal rod spacing	= 0.315m

$n_{1,2}$ = 5, 5
$N_{1,2}$ = $n_{1,2}$ / longitudinal rod spacing
rod diameter = 0.025m

Thus the Ackers procedure was applied to a single frame when computing rod roughness friction factors. The method was developed based on calibration data collected during phase A and it was considered necessary to carry out an independent check on the method for the phase B orientation of the frames.

In order to carry out an independent assessment of the Ackers rod roughness method two extra sets of stage discharge tests were carried out as part of HR's internal research programme. The FCF had already been infilled and effectively turned in to a rectangular channel with width 10m. The portable side walls were used to narrow the flume and the extra tests were carried out in a trapezoidal channel with bottom width 4.6078m and side slopes of 1:1. The longitudinal bed slope was assumed to be the Phase B 110 flood plain slope of 1.021×10^{-3}.

Two sets of stage discharge results were measured and the important aspects of each are listed below:

B49 Stage Discharge results in trapezoidal channel with the roughness frames oriented as during Phase A.

B50 Stage Discharge results in trapezoidal channel with the roughness frames oriented as during Phase B.

Seven individual values of stage and discharge were measured for each roughness configuration. These two sets of data are listed in Table A5.1.

The stage discharge data were analyzed in two ways:

1 Values of friction factor were back calculated from the measured flows and the known channel geometry and compared with the values obtained from the Ackers rod roughness method. The results of this analysis are shown in Table A5.2

2 The Ackers rod roughness method was used to calculate the flow in the channel and this was compared with the measured flows. The results of this analysis are shown in Table A5.3.

The calculated Darcy friction factors are in error by between -9.47% and 23.80%. The data point which gave this large error was judged to be suspect and the mean error was calculated for Phase B case both including this point and omitting it. The mean errors in the calculated friction factors were 2.9% for the phase A case and 4.5% for the phase B case. As can be seen the Ackers method gave mean errors in discharge of 0.7% and -2.0% for the Phase A and B roughness patterns respectively. The standard deviations for these results are 4.8% and 2.9%. The fairly wide range of errors is probably due to the fact that a wider tolerance was allowed on the measured water surface slopes in these measurements than during either Phase A or B.

The Ackers rod roughness method has been tested against two independent sets of stage discharge data and reproduced the measured discharges and total friction factors to an acceptable level of accuracy. Hence the Ackers rod roughness method may be used in all future analysis of rod roughened SERC FCF data.

Table A5.1 Stage Discharge Measurements

Date	Discharge cumecs	Depth mm	Temp °C
B49 Phase A Roughness			
030192	0.02252	29.64	11.1
030192	0.04432	50.57	10.9
020192	0.06183	65.08	10.5
050192	0.07971	83.78	11.6
020192	0.10315	109.25	10.8
050192	0.13002	135.52	12.1
030192	0.16352	163.43	11.4
B50 Phase B Roughness			
100192	0.02225	28.24	12.3
090192	0.04134	45.42	13.1
080192	0.06159	62.00	12.9
080192	0.07982	83.40	13.1
080192	0.10015	101.98	13.3
090192	0.13394	132.11	13.3
090192	0.16028	154.10	13.1

Notes

1 Depths are adjusted for flood plain slope 1.021×10^{-3}

Table A5.2 Friction Factor Analysis

Discharge cumecs	Depth mm	Actual Value Darcy f	Calculated Darcy f	% Error in Darcy f
Phase A Roughness				
0.02252	29.64	0.0874	0.0767	13.95
0.04432	50.57	0.1121	0.1105	-1.43
0.06183	65.08	0.1230	0.1400	13.82
0.07971	83.78	0.1579	0.1729	9.50
0.10315	109.25	0.2100	0.2101	0.05
0.13002	135.52	0.2523	0.2373	-5.95
0.16352	163.43	0.2798	0.2533	-9.47
MEAN % ERROR				2.92
Phase B Roughness				
0.02225	28.24	0.0774	0.0732	-5.43
0.04134	45.42	0.0934	0.0964	3.21
0.06159[2]	62.00	0.1074	0.1326	23.80
0.07982	83.40	0.1554	0.1713	10.23
0.10015	101.98	0.1808	0.1996	10.40
0.13394	132.11	0.2200	0.2341	6.41
0.16028	154.10	0.2442	0.2494	2.13
MEAN % ERROR				7.25[3]
MEAN % ERROR				4.49[4]

Notes

1 % Error = 100*(Calc - Meas)/Meas
2 This data point is out of sequence and is suspect
3 Mean Error including suspect point
4 Mean Error with suspect point omitted

Table A5.3 Flow Analysis

Discharge cumecs	Depth mm	Calculated flow	% Error in Calc Flow
Phase A Roughness			
0.02252	29.64	0.02405	6.78
0.04432	50.57	0.04467	0.80
0.06183	65.08	0.05795	-6.27
0.07971	83.78	0.07622	-4.38
0.10315	109.25	0.10304	-0.01
0.13002	135.52	0.13002	3.10
0.16352	163.43	0.16352	5.18
MEAN % ERROR			0.74
Phase B Roughness			
0.02225	28.24	0.02289	2.88
0.04134	45.42	0.04070	-1.55
0.07982	83.40	0.07604	4.73
0.10015	101.98	0.09530	-4.84
0.13394	132.11	0.12989	-3.02
0.16028	154.10	0.15867	-1.00
MEAN % ERROR			-2.05[2]

Notes

1 % Error = 100*(Calc - Meas)/Meas
2 Mean Error with suspect point omitted

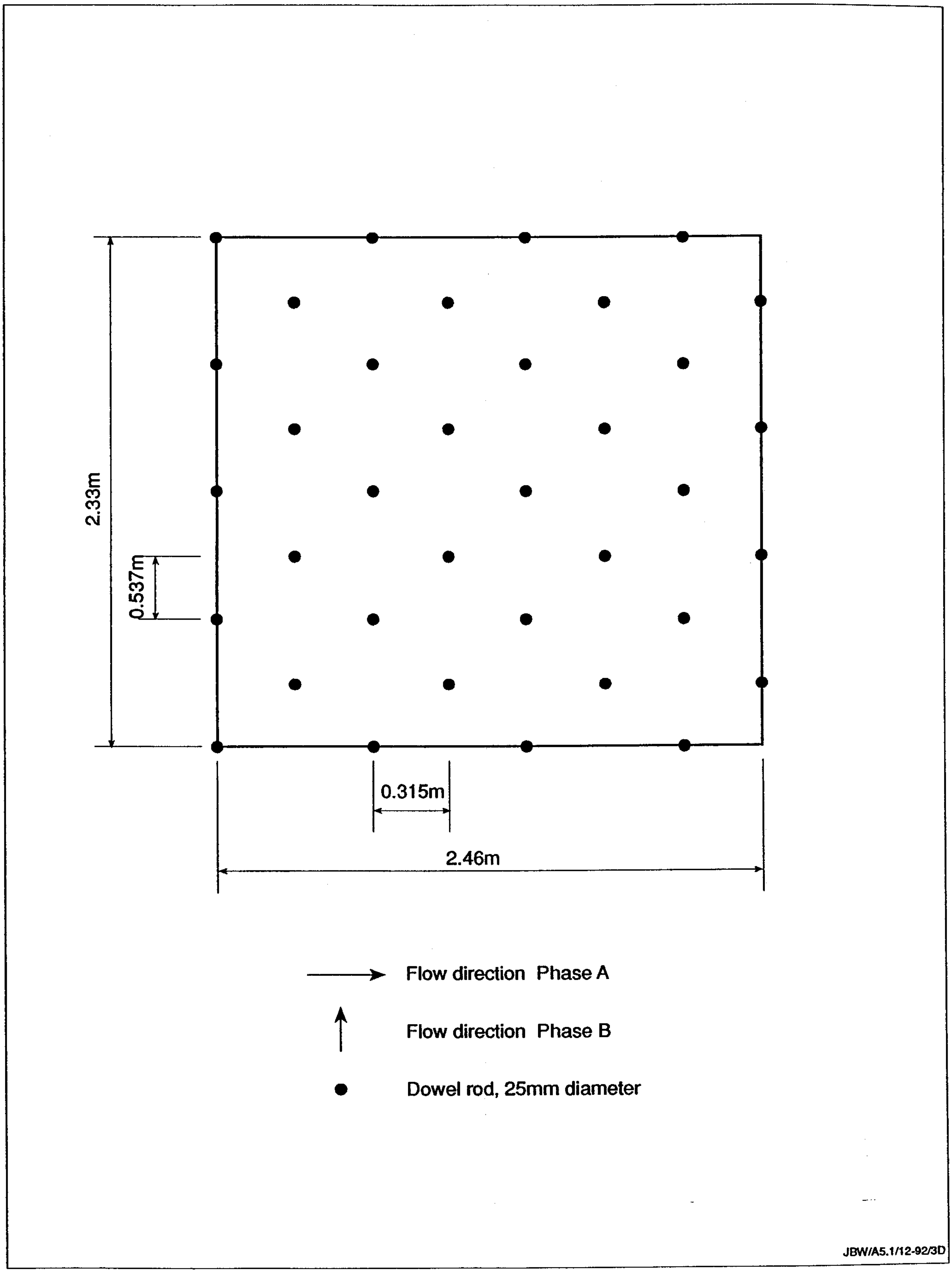

Figure A5.1 Schematic of rod roughness frame